



LYNX MISSION DESIGN

6 Lynx Design Reference Mission

The *Lynx* X-ray Observatory will inspire extraordinary new science investigations that are not possible through existing or planned missions. The Design Reference Mission will deliver revolutionary scientific returns across all three science pillars driving *Lynx* mission requirements. The approach detailed here leverages extensive spacecraft and mission operations heritage, all while requiring only four key technologies to be advanced to Technology Readiness Level 6. This approach will greatly reduce risk posture while maximizing mission success.

6.1 Lynx Design Rationale

The *Lynx* science pillars address some of the most profound science questions facing the astronomy community today. These science pillars set the mission goals and observatory requirements for the notional Design Reference Mission (DRM) (Figure 6.1), defined here as the science program, observatory architecture and telescope design, and the notional mission profile. The DRM is designed to achieve transformational science with low risk by (1) prioritizing a General Observer (GO) program with a long mission lifetime and high observing efficiency, (2) capitalizing on advanced payload technologies with clear development paths, (3) embracing heritage architecture and operations paradigms, and (4) incorporating proven spacecraft technologies.

A team of dedicated engineers, technologists, and scientists from NASA Centers, government institutions, universities, and industry has generated a mission concept and preliminary observatory design. The *Lynx* team started with a broad trade space, including key technology, mission profile, and spacecraft options. Exhaustive trades were carried out at the component, system, and mission levels (§9 and Appendix B), resulting in a streamlined, highly capable DRM that will perform science befitting a flagship mission for a cost and schedule that permits a balanced astrophysics portfolio.

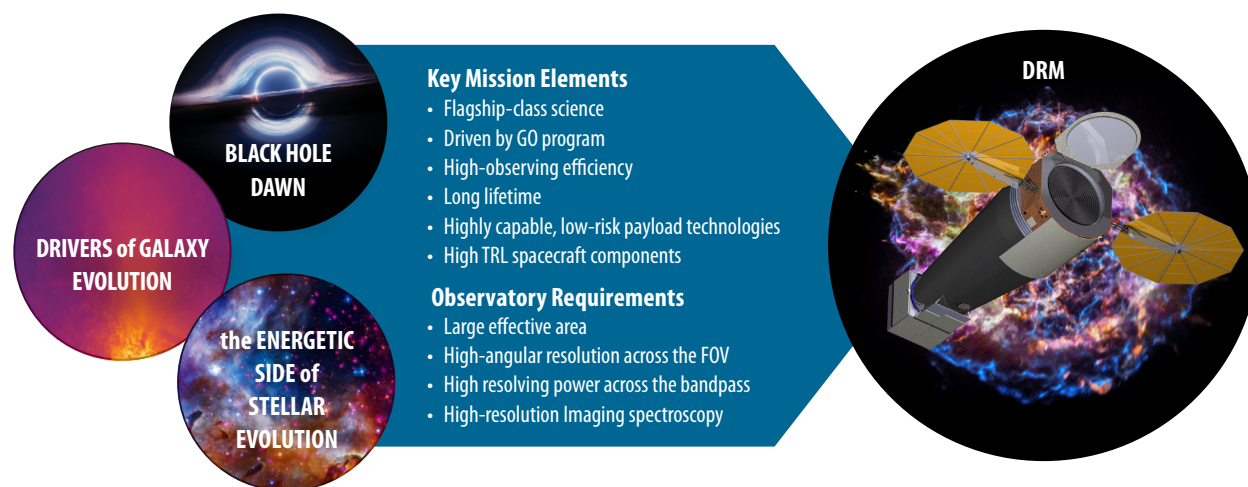


Figure 6.1. The *Lynx* DRM stems from the challenging science drivers defined by the science pillars. At a high level, these requirements present a need for an extremely sensitive X-ray telescope with a large collecting area coupled with high angular resolution across the field of view and unprecedented spectral resolution. The resulting architecture enables a broad range of science across the field and serves as an Observatory for the astrophysics community.

6.1.1 Mission Architecture

Lynx will provide the worldwide astronomical community with a flexible and efficient observing platform: an X-ray observatory with a large effective area coupled with high angular resolution across a large Field of View (FOV) and unparalleled spectral resolution. *Lynx* will operate at a halo orbit at Sun-Earth-L2 (SE-L2), an orbit that allows high viewing efficiency (>85%), an extended mission duration, a benign thermal environment, and easily managed communications. *Chandra*-proven mission operations and infrastructure will be implemented to ensure efficient, queued observation scheduling; *Chandra*-like pointing attitude control, stability, and knowledge consistent with sub-arcsecond imaging; and robust communication infrastructure to rapidly acquire and distribute processed data to observers (Figure 6.2).

Like all NASA flagships, *Lynx* will be a mission of high national priority. The *Lynx* mission architecture and spacecraft design therefore adopt a Risk Class A profile, which allows no credible single-point failures to prevent mission success. This means following strict implementation of risk management and mission assurance practices with redundancies on credible critical single-point failures. This also means that the *Lynx* design will use flight-proven hardware and operational procedures where feasible

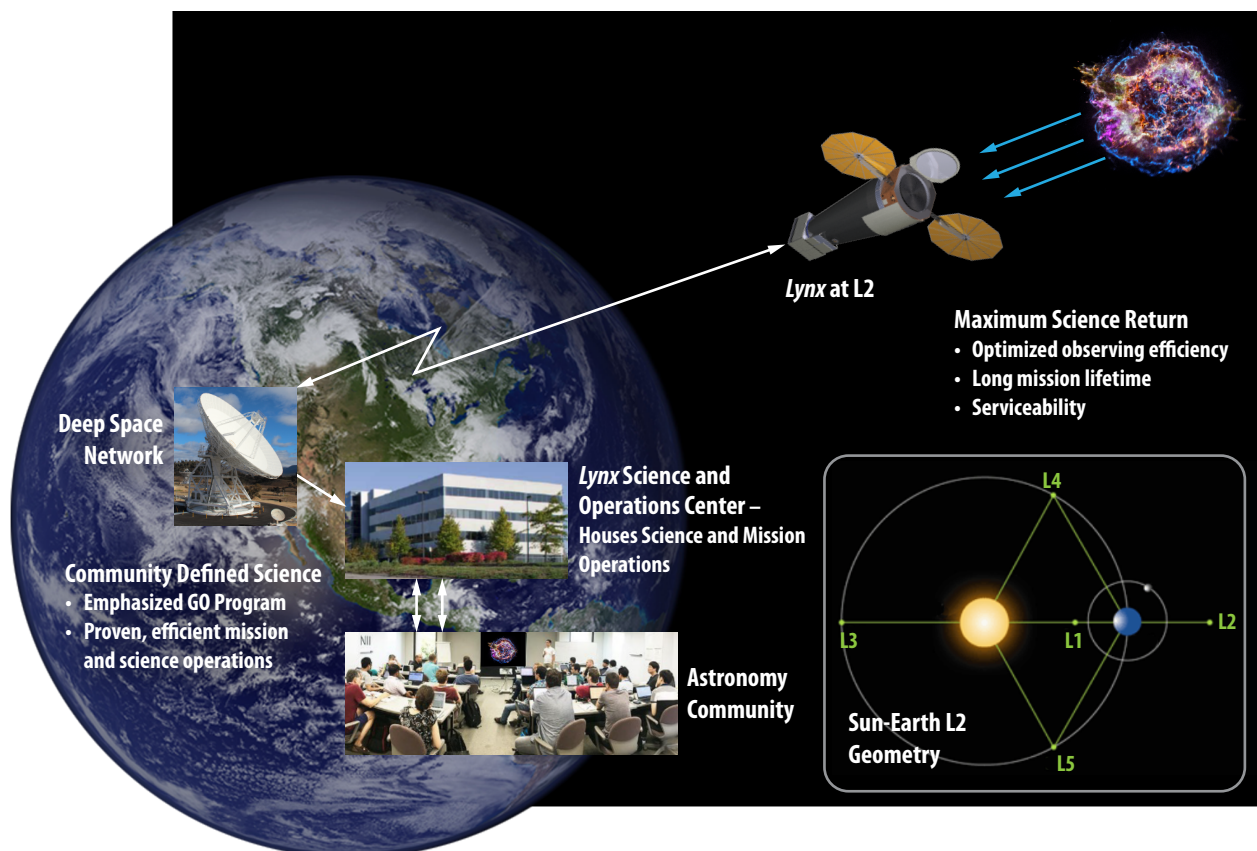


Figure 6.2. Depiction of *Lynx* at SE-L2 (not to scale). *Lynx* operation goals and leveraging of previous mission heritage processes are highlighted.

and will aim for mission longevity in a relatively benign operating environment. Key *Lynx* mission parameters are summarized in Table 6.1.

Lynx will operate as a GO facility, allowing for a broad range of community-driven observing programs that include the both the science detailed in the pillars outlined in §1 – §3 and the Observatory/Discovery science (§4). In keeping with the GO program philosophy, all *Lynx* observations will be subject to peer review, including those related to the three science pillars. Time pre-allocation can be considered only for a small number of multi-purpose key programs, such as surveys in pre-selected regions of the sky.

Although *Lynx* will be a large observatory, estimates of its mass and volume have ensured its compatibility with multiple future heavy-class launch vehicles anticipated to be available in the 2030 timeframe, including the Space Launch System (SLS). This flexibility significantly reduces *Lynx*'s mission risk and cost by eliminating the historical single-source constraint. The success of new launch vehicle systems such as the Falcon Heavy has greatly changed the landscape, and *Lynx* is designed to take full advantage of the likely 2030 launch market.

Table 6.1. Defining *Lynx* Mission Parameters. High-observing efficiency, long lifetime, dedicated GO program, and launch vehicle flexibility are among the high-priority *Lynx* mission attributes.

Mission Parameter	Value
Mission Risk Class	A
Orbit	SE-L2
Observing Efficiency	>85%
Mission Lifetime	
Baseline	5 years operation
Provisioned	20 years operation
Science Program	GO driven
Launch Vehicle Class	Heavy

6.1.2 Observatory Architecture

The *Lynx* science program requires an observatory that is significantly more capable than any other X-ray mission, previous or planned. Capabilities include high sensitivity for sub-arcsecond imaging over a wide FOV and milli-Angstrom resolution spectroscopy. On-axis angular resolution of 0.5-arcsecond Half-Power Diameter (HPD) is required to avoid source confusion (i.e., the noise generated by the numerous sources that are too faint to be detected individually (Appendix A)) and background limitations at the faintest fluxes, and to uniquely associate X-ray sources with counterparts at other wavelengths. A mirror effective area of 2 m² at 1 keV and an FOV with arcsecond or better imaging extending to ~10 arcminutes off-axis are needed to adequately sample the population of supermassive black hole seeds at high redshift in a reasonable amount of time. The combination of arcsecond or better angular resolution with up to $R = 2,000$ spectral resolution is needed to map the thermodynamic state of hot gas flows in nearby stellar nurseries, extragalactic winds, Active Galactic Nuclei (AGN) outflows, and the cores of clusters of galaxies. An even higher resolving power ($R = 5,000$) is needed to probe low-density circumgalactic and intergalactic gas in absorption against background AGNs and to resolve all major emission line diagnostics of plasma physics in the soft X-ray band (§6.3.3).

The *Lynx* Observatory meets the requirements necessary to achieve these science goals due to the careful integration of the spacecraft and telescope and through the use of advanced technologies. The spacecraft and telescope elements must be designed in unison and guided by trades that maximize system capability. Understanding the impact of the spacecraft elements (e.g., thermal regulation, vibration, and dynamic operation) on the telescope is essential to achieving the necessary performance. The error budgets necessary to achieve the required imaging and spectroscopic performance are exacting, and are shown in §6.6.1.

The *Lynx* spacecraft is designed to meet the telescope demands with a low-risk design posture. While recent advances in propulsion systems, power systems, avionics, Command and Data Handling (C&DH), and many other areas will be implemented, all spacecraft systems will be high Technology Readiness Levels (TRLs), i.e. 7–9. Minimizing on-orbit operational risk is also a mission priority. The *Lynx* mission has been specifically designed to avoid unique orbital or pointing maneuvers and complicated deployments. Onboard mechanisms needed for standard deployments such as solar array panels and instrument and mirror contamination doors will all have strong spaceflight heritage (high TRL), and flight-heritage mechanisms will be employed for focal plane instrument translation and focusing as well as for grating array insertion and retraction.

The underlying *Lynx* architecture is dictated by the nature of X-ray light from astronomical sources (Figure 6.3). Though the paths of X-rays are not easily altered, X-rays can be reflected and focused by grazing incidence mirrors at incident angles that are less than the critical angle of total external reflection. At X-ray energies, this angle is on the order of arcminutes to a few degrees from parallel to the reflecting surface. Therefore, for practical focal ratios, focal lengths are measured in meters, the effective collecting area for a single mirror is modest, and the resulting paucity of focused X-rays puts every photon at a premium. Meeting the *Lynx* effective collecting area requirement requires nesting large numbers of thin, lightweight, co-aligned, co-axial mirrors in order to optimize the available aperture and to achieve acceptably low mass.

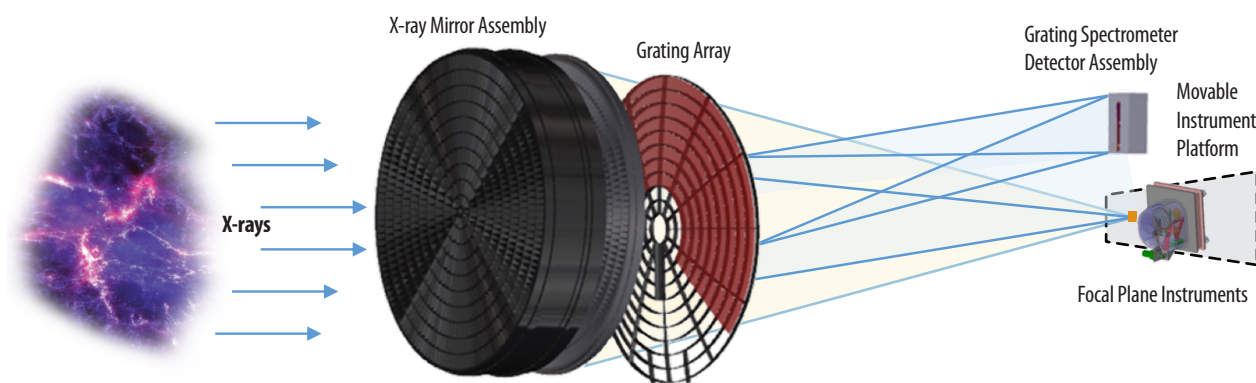


Figure 6.3. Diagram tracing X-ray photons through a generic X-ray mirror assembly and onto a detector located at the focal plane. A translation stage can be used to translate different instruments into the focal point. X-ray gratings can be deployed to intercept the X-rays leaving the mirror assembly, diffracting them onto a detector assembly at a fixed location on the focal plane.

X-ray detectors measure each photon's arrival time, energy, and location in the focal plane. A given detector can only be optimized for a subset of these capabilities. Since different science objectives require different instrumentation, the *Lynx* design envisions a single X-ray mirror assembly and a suite of science instruments that can be individually placed within the optical path when requested for an observation. Accordingly, *Lynx* requires a high-angular resolution, large-effective-area mirror assembly and a science instrument suite that collectively is capable of fine imaging, high-resolution dispersive grating spectroscopy at low energies, and high-resolution imaging spectroscopy across the *Lynx* waveband in order to meet all *Lynx* science goals.

This architecture is similar to most past and present X-ray observatories. The *Lynx* team has leveraged the demonstrated *Chandra* legacy elements, including placing a retractable grating array for dispersive spectroscopy; adopting an updated, State-of-the-Art (SOA) pointing and aspect determination system conceptually identical to *Chandra*'s Pointing Control and Aspect Determination (PCAD) system; and implementing the *Chandra* operations and mission planning paradigm, among others.

Achieving leaps in capability requires improvements beyond the current SOA in X-ray mirrors and science instrumentation. The *Lynx* team recognizes that the path to achieving flagship-class science while also maintaining an acceptable cost and risk posture requires the *Lynx* telescope elements to be well defined, have relatively mature candidate technologies at the present time, and well-defined maturation paths over the next several years. Technology development paths, schedules, and cost estimates to reach TRL 6 by mission Preliminary Design Review (PDR) are summarized in §7 and in comprehensive technology development plans. Further risk reduction for the *Lynx* concept may be attributed to the multiple candidate technology alternatives for payload elements and science instrument components, and due to the fact that all instrument technologies baselined for the *Lynx* DRM have evolved from either flight-proven heritage or from designs destined for near-term, space-based missions. A special section of the *Journal of Astronomical Telescopes, Instruments, and Systems (JATIS)* details ongoing efforts to develop these technologies specifically for the *Lynx* mission [533].

6.2 Observatory Configuration

The *Lynx* Observatory consists of the telescope and the spacecraft. The telescope includes all elements related to the *Lynx* Mirror Assembly (LMA), science instruments, and Optical Bench Assembly (OBA), while the spacecraft provides all basic systems to support the telescope and operations, including propulsion; Guidance, Navigation, and Control (GN&C); power; thermal; avionics and flight software; and C&DH. The GN&C also provides the data necessary to compute a highly accurate aspect solution on the ground, modeled after the *Chandra* PCAD system. As *Lynx* is a Class A mission, the Observatory has been designed with redundancies for all credible single-point failures (summarized in Table 6.14).

The *Lynx* Observatory configuration is defined primarily by the science requirements for effective area, FOV, and angular and spectral resolution over a 0.2- to 10-keV energy range. To meet these requirements, *Lynx* has baselined its telescope to have a 3-m-diameter mirror assembly with a 10-m focal length, coupled to a suite of science instruments with a fixed optical bench structure. These three science instruments are known as the High-Definition X-ray Imager (HDXI), the X-ray Grating Spectrometer (XGS), and the *Lynx* X-ray Microcalorimeter (LXM).

Additional configurations (§9) were considered, and a trade study on the achievable science as a function of cost was carried out. Baselining the 3-m diameter mirror assembly with 10-m focal length was determined to provide the most science per dollar and will allow the science outlined in the *Lynx* science pillars (§1 – §3) to be completed within ~50% of the 5-year baseline mission, reserved for Observatory/Discovery science (§4). This configuration will also allow for an observatory architecture with a realizable, near-term implementation plan and is optimized for a x5-m heavy-class launch vehicle fairing. Primary *Lynx* Observatory resources are summarized in Table 6.2.

The *Lynx* Observatory configuration (expanded in Figure 6.4) illustrates a straightforward design with a stable platform capable of maintaining the alignment between the mirror assembly and the focal plane instruments (via a fixed optical bench) within tolerances needed to maintain the exacting imaging performance. This design allows for stable pointing over time-scales needed for typical observations, and for either focal plane instrument to be easily translated into and out of the focal point (§6.3.5).

The *Lynx* spacecraft will provide the structure and environment needed to support the telescope, as well as all the necessary mechanisms to ensure the spacecraft can meet the science requirements. Key mechanisms include

Table 6.2. LXO resources.

Observatory Resource	Parameter
Overall dimensions (solar panels stowed)	4.5-m diameter × 12.7-m long
Predicted total mass (includes 23% Mass Growth Allowance (MGA))	7,713 kg
Predicted Power (includes 34% margin)	7,421 W
Data Volume	240 Gbits/day (500 Gbits data storage)
Pointing accuracy	10 arcsec (3 σ)
Ground aspect knowledge (Post-facto)	1 arcsec RMS absolute to sky
Image reconstruction	0.2 arcsec HPD within 10 arcmin radius
Stability (between LMA & focal plane)	±1/6 arcsec per s, per axis (3 σ)
LMA	3-m outer diameter and 10-m focal length
Science instrument suite	<ul style="list-style-type: none"> • HDXI • XGS • LXM

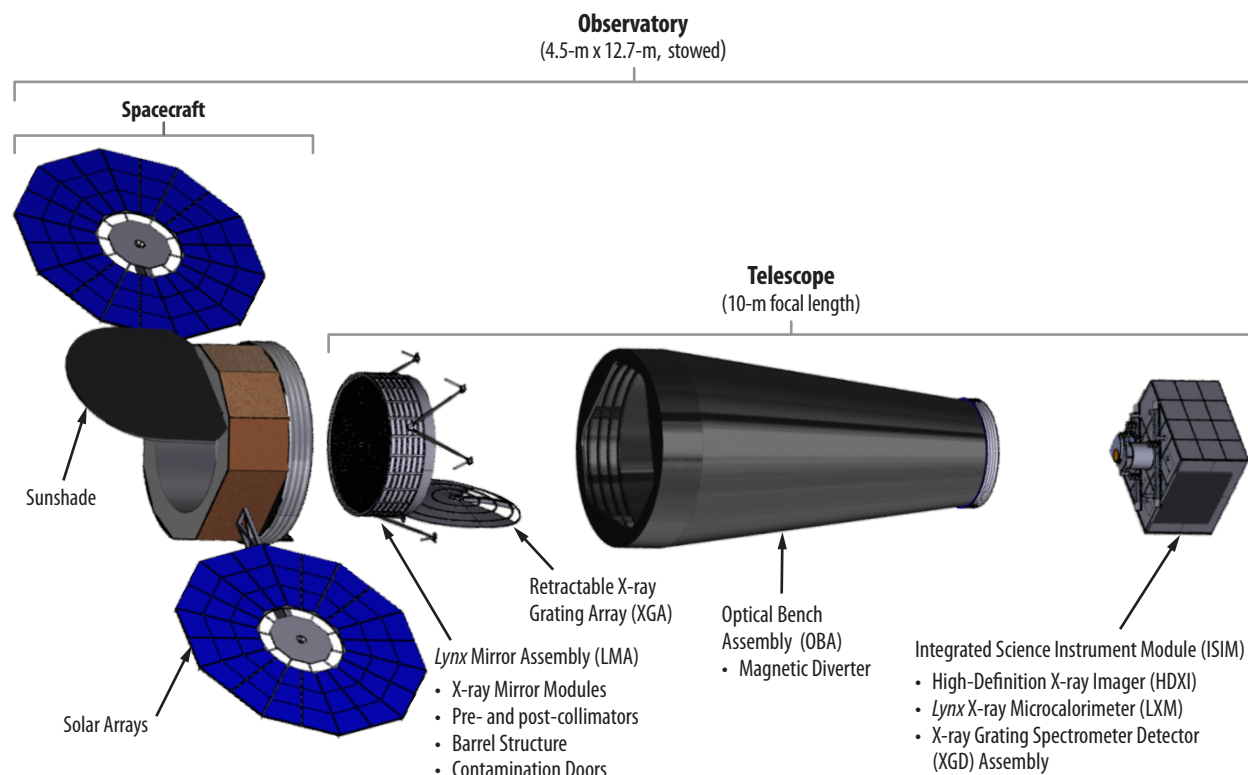


Figure 6.4. *Lynx* configuration expanded to show the telescope and spacecraft portions of the Observatory. The LMA is surrounded by the spacecraft and consists of a high-resolution, large-area mirror assembly with pre- and post-collimators and contamination doors. A retractable X-ray Grating Array (XGA) is attached just after the LMA. A fixed OBA ties the LMA to the science instruments that include HDXI, LXM, and XGS, where the XGS is comprised of the XGA and X-ray Grating Detector (XGD) assembly. [Credit: NASA/M. Baysinger]

those used to deploy the sunshade door to prevent sunlight from illuminating the telescope entrance aperture, insert and retract the X-ray Grating Array (XGA), and to translate the science instruments into and out of the focal point. A summary of primary mechanisms is provided in §6.4.7 (Table 6.20). All of these mechanisms are at TRL 6 or higher (most are at TRL 9) and require little to no maturation.

Equally vital to achieving the *Lynx* science requirements is the overall system integration and interface design (§6.6). This includes the impact on the Observatory from the SE-L2 natural environment (e.g., global deformations due to system-wide thermal gradients), as well as the impact on the telescope performance from the telescope system interfaces and spacecraft elements (e.g., the thermal and mechanical interfaces between the LMA and the OBA and those between the OBA and the spacecraft). Error budget allocations have been generated to identify requirements on system elements and to allocate performance budgets to each element; these are detailed in §6.6.1, and provide allocations for the on-axis imaging performance, spectroscopic performance, and LMA effective area. Elements within these error budget allocations are examples of key driving science requirements that will be tracked as Technical Performance Measures (TPMs) as the *Lynx* design matures. Tracking these TPMs using the *Lynx* Model-Based Systems Engineering (MBSE) tool (Appendix C) will allow monitoring of reserve usage and trends of margin changes. This allows rapid, proactive design assessment and reduces technical risk.

6.3 Design of the Telescope Elements

Given that the spacecraft design is relatively straightforward and that minimal to no development is required, *Lynx*'s success lies primarily in the design and implementation of the telescope. The primary elements requiring some degree of development in order to meet *Lynx* science requirements are the X-ray mirrors and the three science instruments.

The LMA is a fixed structure attached to the OBA. Figure 6.5 shows the attachment of the LMA to the OBA and of the OBA to the spacecraft using bipods. Forward and aft contamination doors are used to control contamination on the X-ray mirrors while on the ground, and en route to SE-L2. Once on-orbit, these doors and a sunshade attached to the spacecraft will be opened and will remain open throughout the mission. A single retractable grating array, the XGA, has the ability to move into and out of the optical

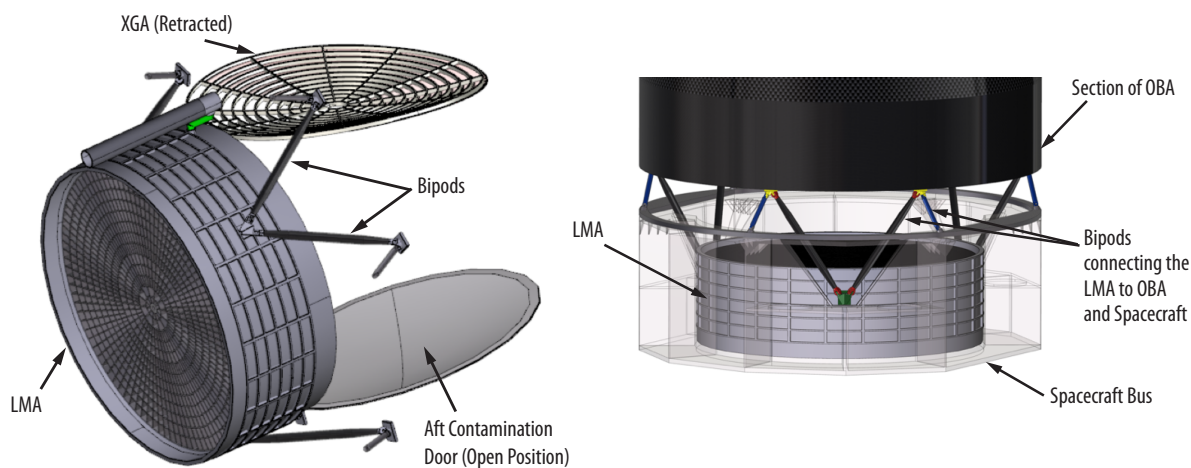


Figure 6.5. Drawing of the LMA with the XGA in the retracted position and aft-contamination door open. Bipods are used to attach the LMA to the OBA and from the OBA to the spacecraft bus.

path as required. The XGA will launch in the retracted position and will have a failsafe mechanism that automatically retracts if the controlling mechanism fails.

The Integrated Science Instrument Module (ISIM) provides an interface to the OBA and houses the focal plane instruments (HDXI, the X-ray Grating Detector (XGD) assembly, and LXM), their electronics, radiators, and supporting structure (Figure 6.6). Two of the science instruments—HDXI and LXM—along with their electronics and radiators are mounted on a moveable platform that is part of the ISIM, while the XGD assembly is located on a fixed platform. The ISIM also provides interfaces for thermal, power, and data for these instruments. More detail is found in (§6.3.5).

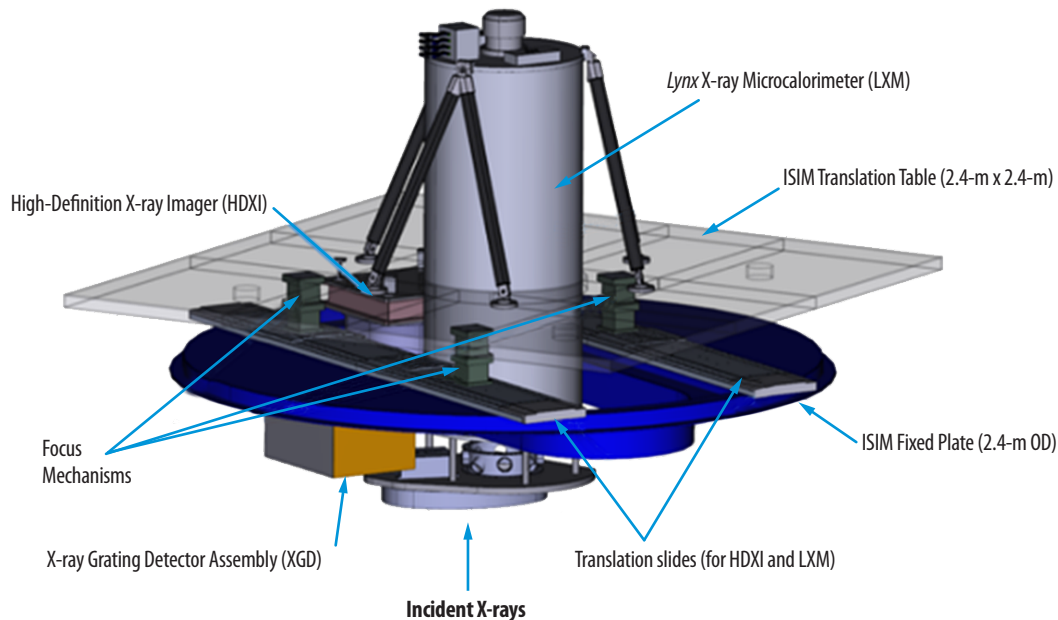


Figure 6.6. ISIM with the translation table shown in translucent-gray, to which HDXI and LXM are attached. The HDXI and LXM can be translated on-axis, depending on the desired science measurement. Three focusing mechanisms allow for fine focus of the HDXI and LXM. The XGD assembly is mounted to the ISIM fixed plate, and has a focus mechanism built into its housing. The electronics boxes for the instruments and the radiators are not shown in this view.

6.3.1 Lynx Mirror Assembly

The *Lynx* Mirror Assembly design incorporates fine angular resolution across the full field of view with large effective area. These capabilities empower synergistic observations with 30-m-class, ground-based telescopes planned for operation in the 2030s.

The LMA will be the most advanced of its kind, designed to preserve the sharp vision of *Chandra* on-axis but extended over the entire FOV while increasing the collecting power with significantly larger effective area.

These requirements flow directly from the *Lynx* science goal of observing the first supermassive black hole seeds and unambiguously associating them with the first galaxies observed by the *James Webb Space Telescope (JWST)*. *Lynx*'s on-axis angular resolution of 0.5 arcseconds (HPD) is required

to avoid source confusion at the faintest fluxes and to uniquely associate X-ray sources with high-redshift optical and near-infrared (IR) galaxies. A mirror effective area of 2 m^2 at 1 keV and an FOV with arcsecond or better imaging extending to ~ 10 arcminutes off-axis will allow for the population of supermassive black hole seeds at high redshift to be adequately sampled in a reasonable amount of time (§1).

LMA requirements (Table 6.3) will enable the next generation of X-ray astronomy and will deliver synergistic observations with ground- and space-based observatories with high angular resolutions.

6.3.1.1 LMA Design Overview

The LMA gain in performance over existing and planned missions is acquired through the use of advanced silicon X-ray mirror technology combined with a precise mirror prescription and modular assembly. *Chandra* achieved on-axis sub-arcsecond angular resolution with four nested pairs of full-shell mirrors that were directly fabricated out of Zerodur® glass, cut and polished to thicknesses ranging from 16- to 24-mm and coated with iridium [534]. *Lynx* will achieve the same angular resolution with much thinner (0.5 mm) mirrors that allow for greater nesting of mirror pairs and larger effective area while simultaneously reducing mass per collecting area.

Lynx's large FOV and off-axis angular resolution are enabled through the use of shorter mirror segments and by changing the telescope geometry from a Wolter Type I (used by *Chandra*) to a Wolter-Schwarzschild configuration. The Wolter-Schwarzschild configuration provides a much flatter best-focus surface because it does not suffer from comatic aberration [535]. The *Lynx* Point Spread Function (PSF) for the low-energy end of the band-pass (0.2 to ~ 2 keV) is expected to be better than 1 arcsecond HPD at 1 keV to a field radius of at least 10 arcminutes. The flatter *Lynx* response is required for wide-field surveys and efficient imaging of extended sources at high-angular resolution. Figure 6.7 illustrates how the PSF varies as a function of off-axis

Table 6.3. LMA primary requirements.

LMA Parameter	Requirement
Energy range	0.2–10 keV
Angular Resolution: On-Axis Across the FOV	0.5 arcsecond HPD < 1 arcsecond HPD
Grasp at 1 keV (effective area \times FOV for <1 arcsec HPD)	$\sim 600 \text{ m}^2 \text{ arcminutes}^2$
Field of View (FOV)	20 arcminutes diameter
Effective area at 1 keV	2 m^2
Effective area at 6 keV	0.1 m^2

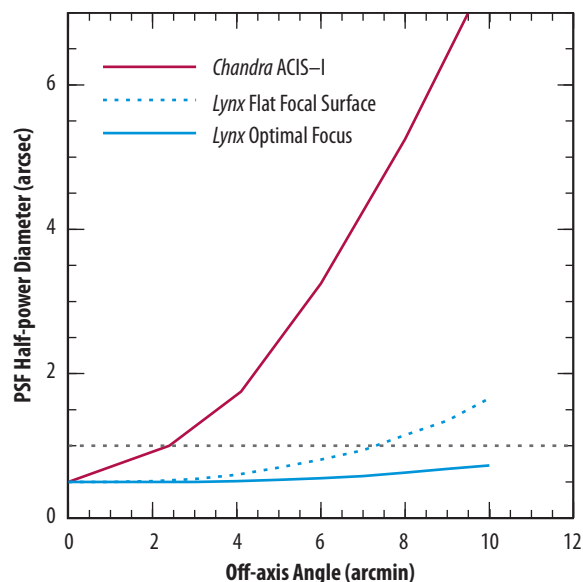


Figure 6.7. The *Chandra* PSF (HPD) resulting from the use of Wolter Type I mirror prescription and the focal surface of ACIS-I, compared to the predicted *Lynx* PSF that will use a Wolter-Schwarzschild prescription coupled to a curved “optimal” focal plane detector assembly. *Lynx* will achieve sub-arcsecond angular resolution across the required FOV.

angle and includes the effect of the detector focal plane geometry for both *Chandra* (coupled with the Advanced CCD Imaging Spectrometer (ACIS-I) [536]) and *Lynx* (coupled with HDXI; §6.3.2.1).

The achievable angular resolution is highly dependent on the mirror technology—fabrication, coating, alignment, and mounting processes. During this concept study, the *Lynx* team focused on three mirror technologies that have a long history of development and are currently being funded: Silicon Meta-shell Optics [537], Full Shell Optics [538, 539], and Adjustable Segmented Optics [540, 541]. A trade study considered each technology’s ability to meet *Lynx* science requirements as well as their capacity for overcoming technical challenges and meeting programmatic constraints. Members of the *Lynx* Science and Technology Definition Team (STDT), NASA program and technology experts, industry partners, independent consultants, and members from the Silicon Meta-shell Optics, Full Shell Optics, and Adjustable Segmented Optics technology teams carried out this assessment. Over 5,000 manhours over 6 months were spent on this study, with over 100 documents produced. All three technologies met the *Lynx* requirements and were deemed viable options. The recommendation, then, was to use the most mature technology, the Silicon Meta-shell Optics, to focus the design (see Appendix B.2.1 for more detail on this trade study). The availability of alternative feasible technologies, however, reduces the risk to development and enhances the *Lynx*’s ability to meet its requirements with a design that meets cost and schedule constraints.

The *Lynx* Silicon Meta-shell Optics are mature, and their modular design is highly amenable to mass production. Multiple parallel production lines at multiple locations will optimize mirror segment fabrication and assembly.

The Silicon Meta-shell Optics technology combines advanced polishing technology with monocrystalline silicon, whose near-zero internal stress enables the fabrication of extremely thin (lightweight) optics using advanced deterministic polishing technology, and is actively being developed by a team at NASA Goddard Space Flight Center (GSFC). Silicon also has other highly desirable properties, including a low Coefficient of Thermal Expansion (CTE), high elastic modulus, high thermal conductivity, and low density, making it the best material choice for the *Lynx* mirrors.

Silicon Meta-shell Optics use a modular design in which modules are built by layering mirror segment pairs of nearly identical size on top of one another. The first mirror pair is kinematically supported for alignment and then permanently bonded at eight locations onto a silicon plate, which serves as the structural backbone of a mirror module. Subsequent layers are built up in the same manner. A baffle is included to reduce stray X-ray photons (i.e., unwanted photons that originate from the diffuse cosmic X-ray background that scatter onto the mirror aperture). Multiple modules are mounted into a meta-shell ring-like structure of a given diameter. Multiple meta-shells are nested together to attain the required

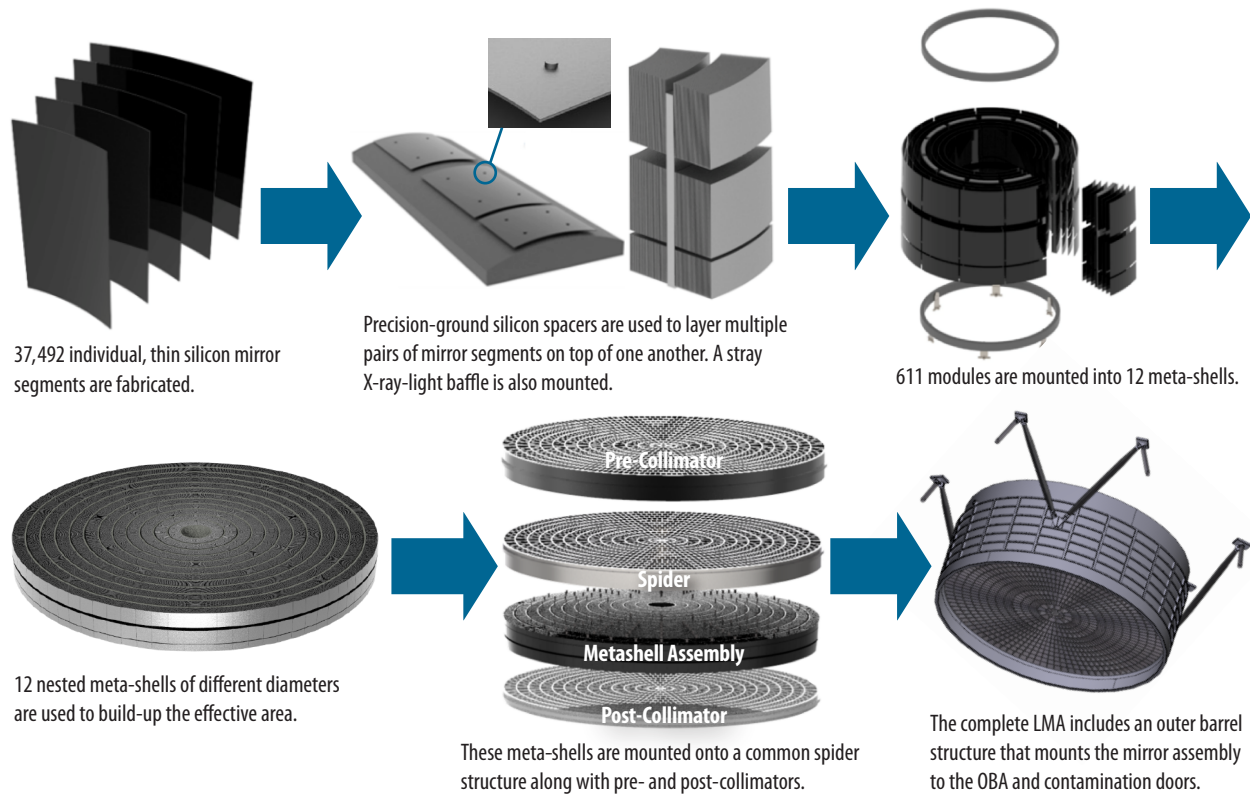


Figure 6.8. The LMA mirror segments are mounted into modules along with baffles that reduce the amount of scattered X-ray light onto the focal plane. These modules are mounted into multiple meta-shells of different diameters to build-up effective area. These meta-shells are mounted onto a common support structure called the ‘spider,’ along with pre- and post- collimators for thermal control. The entire assembly is mounted inside a barrel that interfaces to the OBA.

effective area (Figure 6.8). A significant advantage of this modular design is that it is highly amenable to mass production. Multiple, parallel production lines will be used to optimize mirror segment fabrication and assembly. As part of this study, a manufacturing optimization algorithm has been developed and is being refined to assess the trade between production time and the cost of the LMA [542].

The LMA will include pre- and post-collimators to help regulate the thermal response of the mirror on-orbit and a barrel structure that mounts the mirror assembly to the OBA using flight-proven (TRL 9) flexures and forward and aft contamination doors for ground operations. LMA design characteristics are summarized in Table 6.4.

Table 6.4. Key LMA design characteristics. The Silicon Meta-shell Optics use a modular design that uses many mirror segments that mount into meta-shells, which are nested into the mirror assembly.

Mirror Assembly Parameter	Value
Optical Assembly Geometry	Wolter-Schwarzschild
Mirror Segment Material	Mono-crystalline Silicon
Segment Size	100-mm x 100-mm
Segment Thickness	0.5 mm
Number of Mirror Segments	37,492
Number of Modules	611
Number of Meta-shells	12
Meta-shell Radius Range	120-mm (inner) – 1,500-mm (outer)
Total Length (pre- to post- collimator)	0.85 m
Predicted LMA Mass (includes collimators, support structure, and contamination doors)	2,035 kg
Steady-State Temperature	293 K \pm 0.25 K
Contamination Limit (based on <i>Chandra</i>) Molecular Particulate	~40 Å < 10 ⁻⁵ surface coverage

This design exceeds the *Lynx* LMA requirements for effective area and FOV and is made possible using thin (0.5-mm) mirror segments that are also relatively short. The effective area for this geometry at 1 keV is 2.1 m^2 (Figure 6.9); the ghost-free FOV, which accounts for structure blockage, is 22 arcminutes in diameter.

A description of the current performance for Silicon Meta-shell Optics and an overview of the development path to TRL 6 are provided in §7.2.1. A comprehensive technology development plan is provided in the *Silicon Meta-shell Optics Technology Roadmap*.

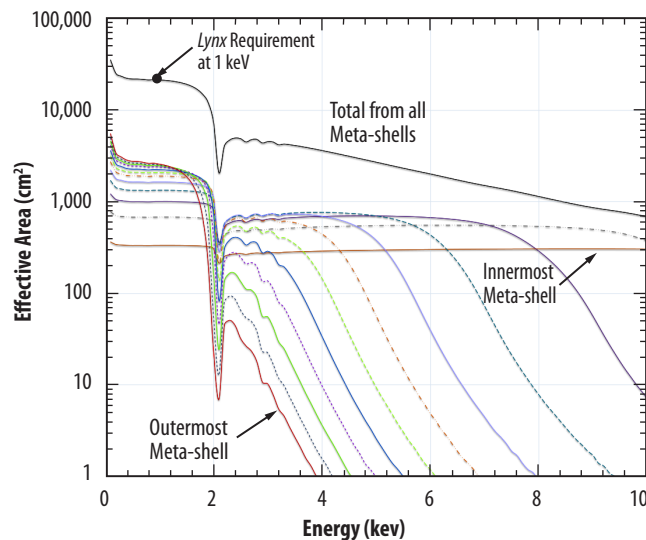


Figure 6.9. The total LMA effective area as a function of energy and the effective area for each of the 12 meta-shells are shown.

6.3.1.2 *Lynx* Mirror Assembly Performance Considerations

The baseline design for the LMA is a product of multiple engineering studies that included detailed structural, dynamics, and thermal designs. The results of these studies have been compiled into the *DRM Supplemental Design Package*. Critical design features include mitigating contamination on the mirror assembly (both on the ground and on-orbit), thermal control, and launch survivability.

Contamination Control— Contamination control on the mirrors is needed on the ground and on-orbit, as molecular and particulate contaminants on X-ray optical surfaces can degrade performance, and changes in contamination levels can compromise calibration stability. To control contamination, doors have been incorporated into the LMA that allow for a dry nitrogen purge on the ground, with the covers remaining closed post-calibration through the completion of a post-launch outgassing phase. In operation, the *Lynx* thermal control subsystem maintains the LMA at approximately room temperature—higher than the surrounding subsystem structure by around 10°C —to minimize particulate and molecular adhesion to mirror surfaces over time.

Thermal Analysis— The LMA thermal operation on-orbit is $293 \text{ K} \pm 0.25 \text{ K}$, necessary to maintain the fine angular resolution required by the *Lynx* science goals. A detailed thermal analysis on the optics spider and pre-collimator was conducted to optimize their geometries and to improve thermal performance and minimize power requirements for the optical system. The design uses the mirror support element (or spider) to double as the active, heated portion of a thermal pre-collimator to radiatively

heat the LMA, plus a passive portion forward of the spider to minimize the heat lost to space (Figure 6.10). Similar pre-collimator designs have been used previously on multiple X-ray telescopes, including the *Einstein* Observatory and *Chandra*. In addition, the LMA will have a post-collimator (with similar geometry to the spider) to thermally control the exit aperture of the telescope and the grating array. The results of this analysis were used to size the heater controllers and power system (§6.4.3).

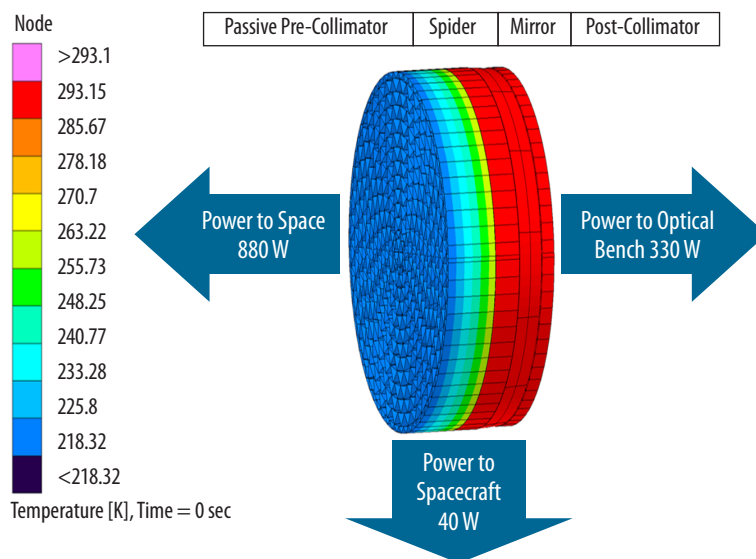


Figure 6.10. Results of LMA thermal analysis.

Launch Survivability and Structural Considerations — Factors that impact analyses related to LMA launch survivability require knowledge of the specific launch vehicle environment, as well as a more detailed design than is practical for this design concept phase. However, initial high-level assessments have been made based on the current design and assumed launch vehicle loads provided by the NASA Launch Services Program (LSP) Office (§6.5). Analyses indicate that the LMA would survive launch assuming standard engineering design practices are followed. All safety factors are per NASA-STD-5001B W [543].

Two specific areas were investigated for this analysis: (1) quasi-static strength of LMA subcomponents and (2) individual mirror strength and relative motion. These areas were assessed via linear static stress analyses and frequency response analyses.

Quasi-static Strength — Structural details and analysis of the LMA are presented in the *Lynx DRM Supplemental Design Package*. Analyses performed to assess LMA launch survivability included linear static stress analyses based on Mass Acceleration Curve (MAC) load factors that were developed by the Silicon Meta-shell Optics design team at GSFC as shown in Table 6.5. The loads are reflective of the Atlas V and Delta IV launch vehicles. These MAC load factors are intended to include transients, quasi-static ascent, and random vibrations. These are first-cut estimates and are expected to be conservative. As the project evolves and detailed structural dynamic analyses are performed, these loads will be tailored for the more detailed design.

Table 6.5. LMA MAC load factors for the 12 meta-shells.

Meta-shell	Mass (kg)	MAC Curve Load Factor (G's) Atlas V/ Delta IV
1	31.3	19.8
2	44.5	18.1
3	54.8	16.4
4	63.7	15.9
5	72.0	15.3
6	79.6	14.8
7	85.3	14.3
8	91.2	13.8
9	97.9	13.3
10	103.7	13.3
11	108.7	12.9
12	115.5	12.9

Post Bonds between Mirror Segments — As shown in Figure 6.8 (middle of the top row), precision ground spacers (or posts) are used to layer multiple segment mirror pairs on top of one another for assembly into a module. The applicable MAC quasi-static load factors were applied to each meta-shell in a static stress analysis to optimize the size of the posts and to calculate the adhesion shear/tension interaction margin of safety in the post bonds. Each meta-shell was analyzed as an independent “component” to the supporting spider. The minimum predicted margin of safety was +0.002 in the post bonds. The positive margin was indicative of an acceptable design, indicating that the posts meet the strength requirements.

Spider and Flexures — Static strength analyses were performed for the LMA spider and flexures, which are used to attach the meta-shells to the spider. This was done using International X-ray Observatory (IXO) Coupled Loads Analysis (CLA) results with a 2.0 modeling uncertainty factor, resulting in 12.3 G axially and 3.4 G laterally that were applied simultaneously. The predicted margin of safety for the spider was +6.55, and that of the flexures ranged from +0.53 to +2.25.

Mirror Segments — Due to the uncertainties related to structural analysis of brittle materials such as silicon, the LMA development plan will include steps to proof-test each mirror segment as it is fabricated. Only qualified mirror segments that pass flight-level stresses will be integrated into the assembly.

Mirror Segment Strength and Relative Motion — The mirror segments have a radial spacing of 5 mm within each of the mirror module assemblies. A high-level frequency response analysis of mirror segment vibration during launch was performed to estimate motion of these segments relative to one another. Using conservative estimates of the dynamic environment and a rigid input to the LMA barrel, it was determined that there were no issues regarding relative motion between mirror components or assemblies. A detailed analysis during Phase A will incorporate more realistic damping as well as a fully coupled loads analysis that will provide more realistic inputs to the launch locks.

6.3.2 High-Definition X-ray Imager

Together with the LMA, the HDXI will enable the high-angular resolution across the *Lynx* FOV required for the deepest surveys to detect the seeds of supermassive black holes, carry out the wider medium-depth surveys needed to study the evolution of black holes and galaxies, and mapping of the diffuse extended structures ranging from massive clusters of galaxies and galaxy halos to large star-forming clouds. The HDXI requires a FOV of 20×20 arcminutes² and a small pixel size that adequately oversamples the mirror 0.5-arcsecond PSF. The HDXI will also provide the necessary spectral resolution at soft energies to enable measurement of the thermodynamic properties of hot gas in galactic halos and other extended objects. High time resolution is needed to maintain single-photon counting when observing bright X-ray binaries and compact sources, avoiding event pileup. Like the LMA, the *Lynx* HDXI will combine the best heritage technology (specifically X-ray Charge-Coupled Device (CCD) technology) with ongoing sensor technology development efforts, which will provide the lowest risk/lowest cost path to the required measurement capabilities.

6.3.2.1 HDXI Design Overview

The *Lynx* High-Definition X-ray Imager's advanced megapixel X-ray sensors are natural extensions of legacy CCDs but with higher readout rates, improved spectroscopic performance, lower noise, and are intrinsically radiation hard.

Silicon-based X-ray imaging spectrometers are standard for nearly every recent X-ray observatory. Examples include *Chandra's* ACIS [544], *XMM-Newton's* EPIC MOS [545] and PN Cameras [546], and *Suzaku's* X-ray Imaging Spectrometer (XIS) [547]. All of these instruments use traditional X-ray CCDs with acceptable spectroscopic performance and imaging capability but relatively low readout rates. For X-ray observations with next-generation telescopes such as *Lynx* and *Athena*, the current generation of pixelated silicon sensors offer high readout rates, high-broadband quantum efficiencies, and minimal crosstalk compared to traditional CCDs, and have thus been baselined for the *Lynx* DRM.

The *Lynx* HDXI requires a detector array with small-pixel sensors that can appropriately oversample the telescope's PSF with low noise, large FOV, and high-count rate capability (Table 6.6). Based on the SOA and maturation path, the natural choice is to use an array of monolithic or hybrid pixelated Complementary Metal-Oxide Semiconductor- (CMOS-) based active sensors or advanced CCDs with CMOS readout. For purposes of costing and schedule, the hybrid CMOS sensor and associated Application-Specific Integrated Circuit (ASIC) has been adopted for the DRM. This choice was made simply because engineering interface information on the visible-band version of this technology is in the public domain and readily available. The HDXI detector candidate technologies are described in §7.3.1 and are detailed in the *HDXI Technology Roadmap* and elsewhere in the literature [548, 549, 550, 551]. All three of these technologies require similar resources from the spacecraft, are at the same

Table 6.6. HDXI meets the *Lynx* requirements as outlined in the STM.

HDXI Parameter	Capability
Energy Range	0.2–10 keV
Quantum Efficiency (excl. optical blocking filter)	≥ 0.85 0.5–7 keV
Field of view	22-arcmin diameter
Pixel size	$\leq 16 \mu\text{m} \times 16 \mu\text{m}$ (0.33 arcsec)
Read noise	$< 4e^-$ (RMS)
Energy resolution at 0.3 keV at 5.9 keV	< 70 eV (FWHM) < 150 eV (FWHM)
Full-field event rate	$> 8,000$ ct/s
Time resolution (20 \times 20-arcsec window)	$\leq 100 \mu\text{s}$
Framerate: Full-field mode Window mode (20 \times 20 arcsec)	> 100 frames/s $> 10,000$ windows/s
Filling factor/ chip gap	$> 95\%$
Radiation tolerance	5 yrs at L2 (baseline) 20 yrs at L2 (goal)
Optical/UV Blocking	10^{-6} in U- and V-bands
Filter(s)	Open aperture, optical blocking filter, closed position and calibration

level of maturity, and are currently funded for development. Having three technologies available for consideration for the HDXI significantly reduces the risk to development, ensuring that *Lynx* requirements will be met.

The design reference HDXI focal plane features 21 abutted advanced silicon sensors tiled to approximate the mean curved focal surface of the telescope (Figure 6.11) [548]. The 22-arcminute-diameter FOV is set by the FOV of the LMA. The HDXI focal plane sensor array and readout electronics are housed inside a vacuum enclosure with a circular aperture entrance window.

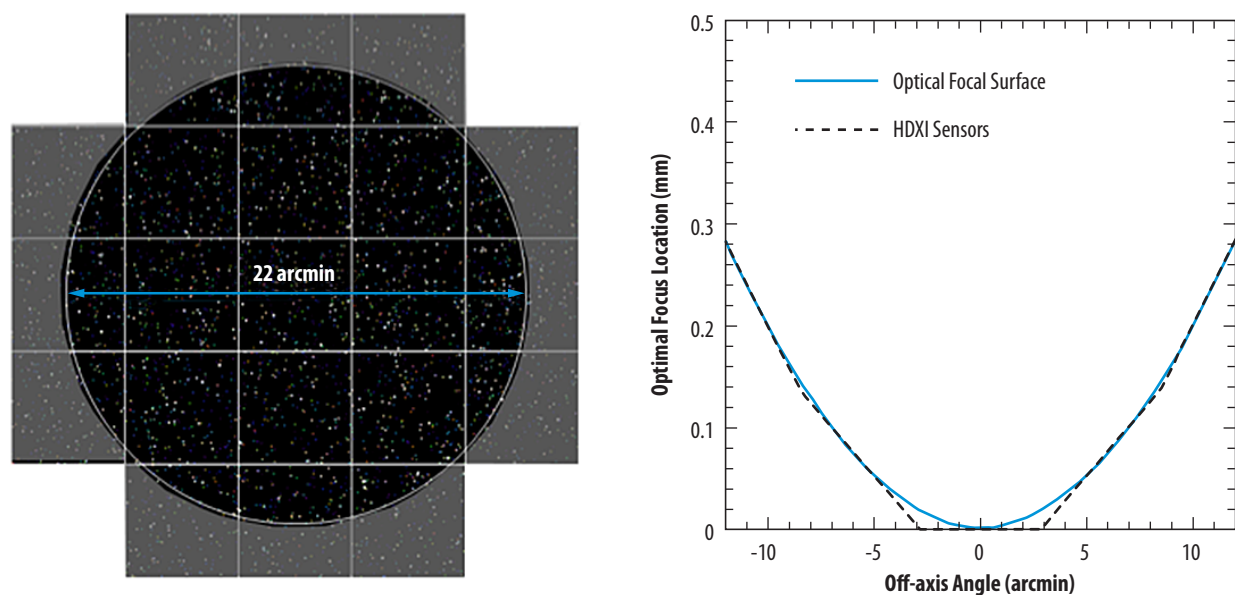


Figure 6.11. (Left) Simulation of a 4 Msec deep field with HDXI array of 21 sensors superimposed. The sensors have a pixel size that is well matched to the telescope PSF of 0.5 arcsec HPD. (Right) The sensors are tilted to approximate a curved focal plane, needed to optimize the angular resolution across the entire 22-arcminutes diameter FOV.

A schematic block diagram of the reference HDXI design is shown in Figure 6.12. The sensors are connected to the Front-End Mother Board (FEMB) via flexprint interconnections. Digitized sensor data from the FEMB are sent to Event Recognition Processors (ERPs) that filter non-X-ray events and empty pixels, reducing the telemetered data volume by 3 to 4 orders of magnitude. Processing is under the control of Detector Electronics Units (DEUs) commanded from the spacecraft and incorporating dedicated firmware and software. The HDXI has a high-speed windowing capability in which a 20×20 -arcsec region of a sensor can be read out in $<100 \mu\text{s}$, which will eliminate pileup from bright sources and allow high-resolution timing measurements of pulsars and magnetars. This windowing capability can be run simultaneously with the full-field readout so that events from the bright source are processed rapidly, but the entire FOV is also read out at the nominal ~ 100 -frames/s cadence. The HDXI system is capable of sustained throughput up to 8,000 cts/s, allowing continuous, pileup-free observations of any extended X-ray source in the sky. Finally, the system will be capable of transferring full sensor frames to the ground for diagnostic purposes. X-ray event data and auxiliary and diagnostic metadata will be formatted into Consultative Committee for Space Data Systems- (CCSDS-) compliant packets for transfer to the spacecraft onboard memory.

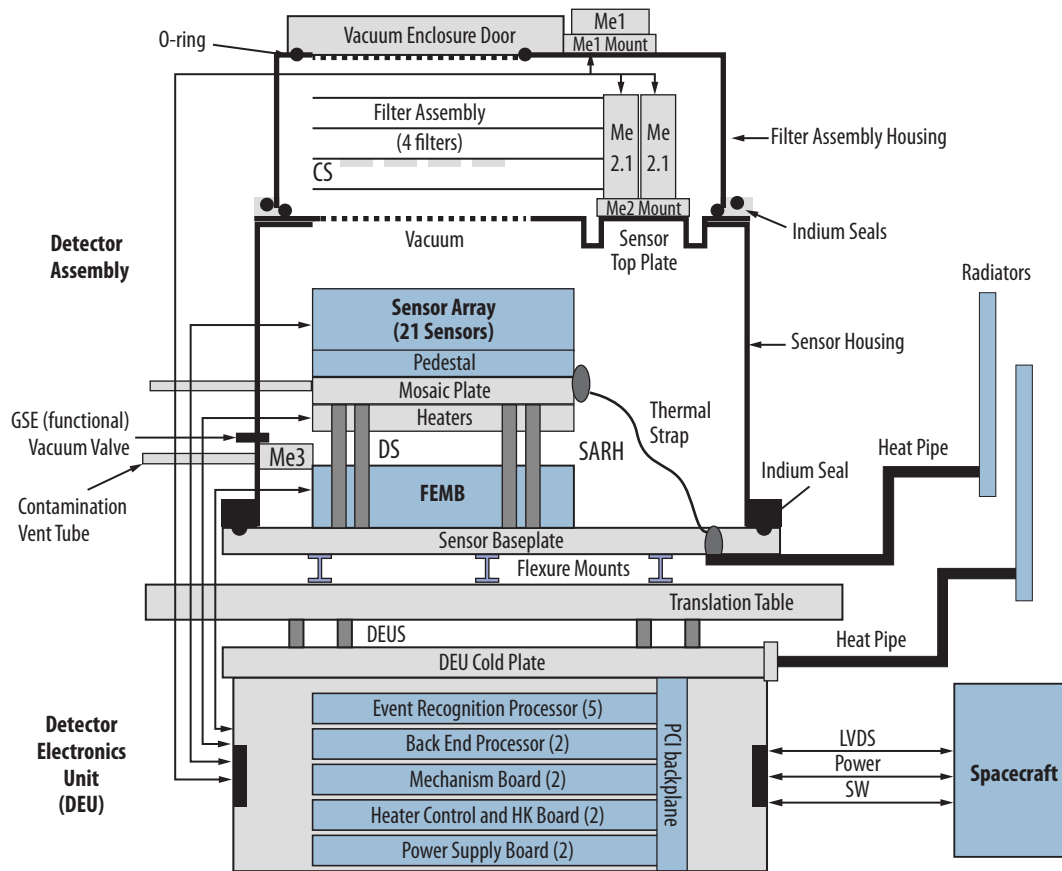


Figure 6.12. Block diagram of the *Lynx* HDXI system. The HDXI DEU and all radiators are attached to the ISIM translation table. Flex cables between the translation table and spacecraft provide power, control, and data. The filter mechanism allows for individual filters or a calibration source to be inserted in front of the sensor array.

The HDXI sensor array and FEMB are located inside an aluminum vacuum enclosure that also contains a filter mechanism (Figure 6.13). Cooling is provided through a cold strap connection between the sensor array which is conductively coupled to a silicon-carbide mosaic plate and the enclosure.

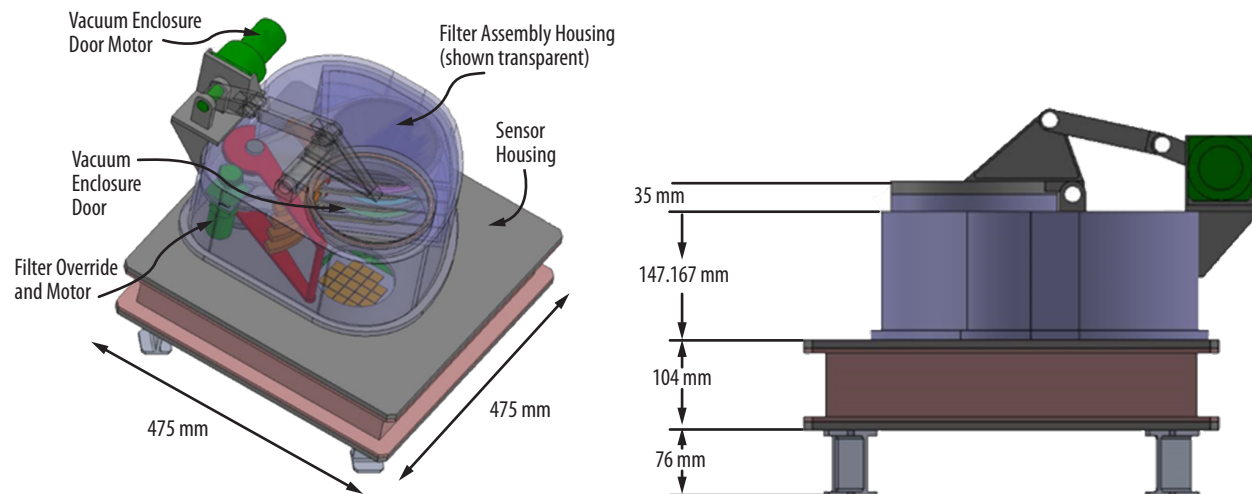


Figure 6.13. The HDXI showing the filter mechanism and vacuum housing. The DEU is not shown, as it is located on ISIM.

This enclosure, along with its thermal load from the rest of the instrument, is passively cooled via external radiators that are connected to the instrument through heat pipes that move along with the translation table. This scheme allows the sensors to be cooled to their nominal operating temperature of -90°C .

The filter mechanism is a unique design capable of supporting multiple filters that can be used in combination with one another. Though the DRM design includes an open aperture, an optical blocking filter, a ^{55}Fe calibration source, and a closed position, additional filter types will be studied during Phase A to maximize the science value.

The ISIM's translation table enables the HDXI (along with its support electronics and radiators) to be moved on- and off-axis as needed. A focus mechanism on the ISIM allows for axial translation of ± 1 cm, more than enough to establish the telescope focus and correct unpredicted variations that may arise due to thermal and structural displacements on-orbit. HDXI instrument features and spacecraft resources are detailed in Table 6.7.

Table 6.7. Reference HDXI design includes an array of 21 advanced silicon X-ray imaging sensors. Required spacecraft resources are listed.

HDXI Resource	Value
Sensor configuration	Back-illuminated, fully-depleted, CMOS-compatible
Detector material	Silicon
Number sensors in array	21 (curved focal plane)
Pixel elements per sensor	$1,024 \times 1,024$
Size	$\sim 48 \times 48 \times 36$ cm
Mass (includes sensors, structures, filter mechanism, DEU, and harnesses)	80 kg (104 kg with margin)
Power (with margin): Nominal Safe hold Survival	 249 W 7 W 7 W
Focal plane operating temperature	-90°C
Data rates: Nominal Peak	 600 kbps 6 Mbps
Contamination limit Molecular Particulate	 ~ 100 Å < Level 600

6.3.2.2 HDXI Performance Considerations

The HDXI design uses standard elements for active pixel sensors. Detailed studies that include thermal, mechanical, electrical, flight software, and instrument reliability are provided in the *DRM Supplemental Design Package*. HDXI longevity to 20 years without loss of performance is crucial. Primary considerations that may affect performance over time are radiation damage (which can result in degraded imaging and spectral resolution) and contamination on the sensor surface (which can degrade the low-energy response). With proper design and lessons learned from *Chandra*, however, both of these potential risks will be mitigated.

Radiation Considerations — At SE-L2, there is an appreciable flux of charged particles, primarily in the form of moderate-energy protons (§6.6.2.1). These charged particles exist as an omnidirectional flux, a portion of which can be concentrated through the LMA directly onto the focal plane. Relatively low (-90°C) sensor operating temperature and shielding on the HDXI enclosure will be used to mitigate the ambient particle flux, and a magnetic diverter (§6.3.6) will be used to “sweep” the charged particle flux away from the focal plane. This technique has been successfully implemented on nearly every focusing X-ray observatory (e.g., *Chandra* [552] primarily for electron flux). The magnetic diverter design for *Lynx* will be similar to what will be used for *Athena*, with a focus on diverting the low-energy proton flux to reduce background on the focal plane instruments [553]. In addition, the HDXI will use CMOS-based sensor technology that is inherently radiation hard, primarily because charge is not transferred across these devices but is instead read out directly from each pixel. The advanced

CCDs are in principle also sensitive to the effects of displacement damage on charge transfer efficiency. This is mitigated through a number of radiation-hardening features, as described in detail in [550]. Radiation tolerance testing is an integral part of the technology development path detailed in the *HDXI Technology Roadmap*. It is expected that the charged particle environment will be similar to that seen by *Chandra*, and therefore is not expected to be an issue, even over the extended 20-year lifetime. However, detailed designs of the HDXI and surrounding structure are required to accurately model the impact of the charged particle population on the sensor array over time. These studies will be performed during Phase A.

Contamination Considerations — A contamination control engineering study for HDXI was carried out as part of an Instrument Design Lab (IDL). Detailed results may be found in the *DRM Supplemental Design Package*. Contamination on the sensor array throughout mission lifetime will be minimized by venting of the HDXI filter and detector assemblies; careful temperature control of the sensor array, FEMB, and surrounding structure; and by the ability to bake out the sensor assembly to remove contamination buildup over time. Keeping the sensor array warmer than the rest of the surrounding structure during cruise will prevent outgassing materials from contaminating the detector. An early on-orbit bakeout in this configuration will drive off any water or other contaminants accumulated during launch processing. On-orbit, the filters, which are in close proximity to the sensor array, will be held at room temperature to mitigate contamination from the rest of the Observatory. The filters and mechanisms will be kept clean, and the filter housing interior will be coated with a molecular absorber coating. The HDXI has been designed with filter and detector bakeout capabilities, further mitigating contamination. During bakeout, when the instrument temperature is raised to evaporate contaminants, the instrument will be translated to one side of the translation table assembly, where the detectors will view a plate coated with a molecular absorber coating affixed to the stationary part of the ISIM. This plate will be in direct line-of-sight of the detector, minimizing contamination accumulation. During normal operation, the FEMB will be kept at a temperature that is $\sim 10^\circ\text{C}$ warmer than the sensor array. A more detailed temperature analysis and contamination study will be carried out during Phase A.

6.3.3 X-ray Grating Spectrometer

The *Lynx* X-ray Grating Spectrometer will be the most advanced of its kind, with $R > 5,000$ and a large effective area of $4,000\text{ cm}^2$ at 0.6 keV .

The *Lynx* XGS will characterize the warm gas in galactic halos out beyond their virial radius through absorption line studies of background AGNs — which require high spectral resolution of $R > 5,000$ — and sensitivity (effective area of $4,000\text{ cm}^2$ at 0.6 keV) in the $0.2\text{--}2.0\text{ keV}$ band, capable of 1-mÅ sensitivity in key absorption lines of OVII and OVIII. The XGS will carry out transformational science that includes these studies on the Warm Hot Intergalactic Medium (WHIM) and will expand our knowledge on active star-forming regions, stellar coronae, and the impact of X-ray and extreme ultraviolet flux and winds on planet habitability.

6.3.3.1 X-ray Grating Spectrometer Design Overview

The *Lynx* XGS will provide the highest-throughput, highest-resolution spectra at soft energies of any X-ray spectrometer ever flown to date (Figure 6.14). For comparison, the Reflection Grating Spectrometer (RGS) on *XMM-Newton* has a resolving power from $R = 150$ to 800 over the 0.33- to 2.5-keV band with an effective area of $\sim 150 \text{ cm}^2$ at 0.83 keV [554]. The High-Energy Transmission Grating (HETG) on *Chandra* provides spectral resolving power up to $R = \sim 65$ to 1,070 over the 0.4- to 10-keV range with an effective area of 59 cm^2 at 1 keV [536].

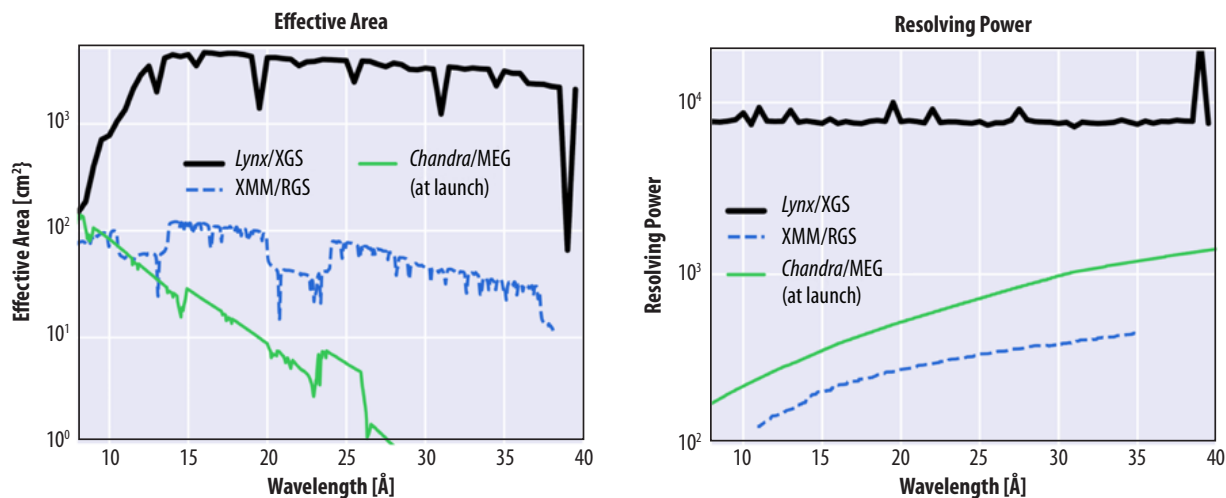


Figure 6.14. Plots comparing (Left) the CAT-XGS effective area summed over all detected diffraction orders, and (Right) resolving power averaged over all detected diffraction orders to that of *Chandra* and *XMM*. The XGS has orders of magnitude more effective area and unprecedented resolving power.

These increases in performance are made possible through recent developments in transmission [555] and reflection [556] grating technologies, both of which are able to meet *Lynx* requirements. Critical-Angle Transmission (CAT) gratings, currently being developed at the Massachusetts Institute of Technology (MIT), have been selected for the *Lynx* DRM for project costing and scheduling purposes (see Appendix B.5.1 for trade study details). Reflection gratings that operate in an Off-Plane (OP) geometry, currently being developed at Pennsylvania State University (PSU), offer equally high performance. Having two technologies that are similarly mature provides a low risk posture related to the development of this instrument.

A comprehensive CAT-XGS *Technology Roadmap* and an OP-XGS *Technology Roadmap* are summarized in §7.3.2 and §7.3.3. Much like the *Lynx* mirrors, the XGS technology will be competed once *Lynx* has been selected for funding.

The XGS consists of two major elements: (1) a large XGA located immediately after the LMA on a retractable structure and (2) the XGD assembly that is located on a fixed location on the ISIM. Defining characteristics are given in Table 6.8.

Table 6.8. Key CAT-XGS characteristics. XGS will meet the *Lynx* requirements as outlined in the STM.

XGS Parameter	Capability
Energy range	0.2 – 2 keV
Resolving power	$R > 5,000$ ($R = 7,500$ goal)
Effective area @ .6 keV	$\sim 4,400 \text{ cm}^2$ (4,000 cm^2 required)
XGD Parameter	Capability
Sensor Pixel size	$\leq 16 \mu\text{m} \times 16 \mu\text{m}$ (0.33 arcsec)
Read noise	$< 4e^-$ (rms)
Energy resolution for resolving spectral orders	$\leq 80 \text{ eV}$ (FWHM) @ 0.3 keV
Radiation tolerance	5 yrs at L2 (baseline) 20 yrs at L2 (goal)

X-rays that are focused by the LMA pass through the XGA, which diffracts the X-rays according to wavelength. The diffracted spectrum is observed by an array of sensors located on the focal surface (Figure 6.15). The gratings in the XGA are blazed such that most photons are diffracted into high-diffraction orders at large distances from the focal point, increasing the spectral resolving power. The line spread function of the diffracted orders determines the grating performance. Spatially overlapping diffraction orders with different wavelengths are “order-sorted” using the energy resolution of the sensors [555].

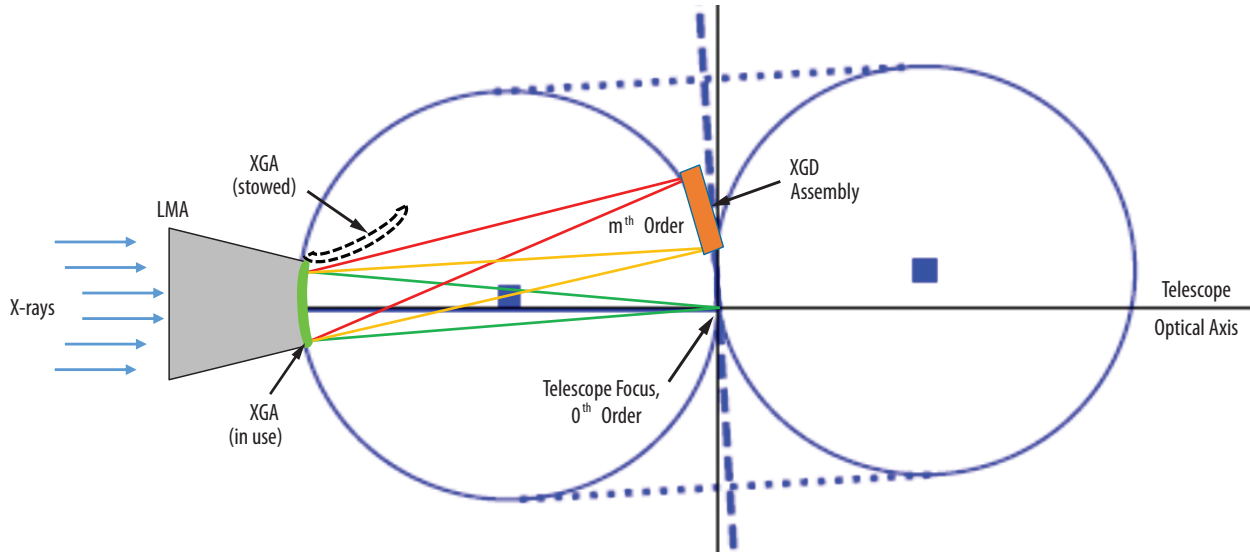


Figure 6.15. Conceptual sketch of the XGS “tilted Rowland torus” design optimized for blazed transmission gratings. The telescope focus is located at the origin of the coordinate system. The dotted lines represent the position of the torus. This design minimizes aberrations by bringing the torus surface close to tangential to the blazed grating facets.

The XGS design is based on the *Chandra* HETG spectrometer [557], which is a Rowland torus design but optimized for blazed transmission gratings (i.e., “tilted Rowland torus”). The Rowland torus is a three-dimensional extension of the Rowland circle geometry, which is necessary to avoid aberrations related to the incoming focused X-rays. In this configuration, the gratings are mounted on one side of the torus, while the detectors are located on the other side (for detailed descriptions see [558, 559]). The gratings, telescope imaging focus, and readout array share the same torus surface. The transmission geometry is comparatively insensitive to grating misalignment and grating non-flatness, leading to relaxed alignment and figure tolerances.

When deployed, the gratings cover roughly 73% of the LMA area (covering 264° in azimuth), leaving areas with the largest aberrations uncovered. The gratings are placed close to the mirrors because a longer distance between the gratings and the detector improves the spectral resolving power. Since individual grating facets are flat and the torus is curved, most points on the grating array do not match the Rowland torus exactly. Using a geometry with a tilted torus reduces this error.

The *Lynx* X-ray Grating Array (XGA) uses state-of-the-art grating technology that exceeds *Lynx* requirements. The X-ray Grating Array deployment heavily leverages heritage from *Chandra*, resulting in a simple, elegant design that provides repeatable deployment and relaxed alignment tolerances between the gratings and optics.

The *Lynx* XGA consists of ~2,100 individual grating facets (50×50 mm in size are baselined) mounted into a large grating array structure (or grating array door). Smaller gratings could be arranged to follow the surface of the Rowland torus better, which would reduce optical aberrations but increase the area blocked by support structures. Ray-traces for the XGS indicate that larger sized gratings can be used to achieve a resolving power of up to $R = 7,500$, which could reduce photon loss due to mounting structures and reduce fabrication cost [555]. A more detailed study involving a more detailed design of the LMA and XGD will be carried out during Phase A.

The single retractable grating array is attached to the LMA structure (Figure 6.16). Effort has been made to keep the mechanism simple while maintaining precise positioning each time the gratings are deployed. The actuator used to deploy the grating array allows for 1.2- μ m-level positioning for high repeatability. A second actuator has been added for redundancy. CAT gratings have an alignment tolerance of roughly 100–200 μ m along the optical axis, well within the capability of these actuators. Table 6.9 lists key spacecraft requirements for the XGA.

Mechanical stops at the deployed position ensure that the gratings are held stably at the precise axial spacing relative to the mirrors. The XGA insertion mechanism includes a spring-loaded feature that allows the stepper motor to overdrive and provide a constant preload force against the stops. Lateral position control of the grating array is handled passively with design constraints in the hinge-line, as well as the selection of grating metering path structures that match the thermal expansion or contraction of the LMA. Active features such as thermal control heaters may be added to the grating support structure to provide additional stability.

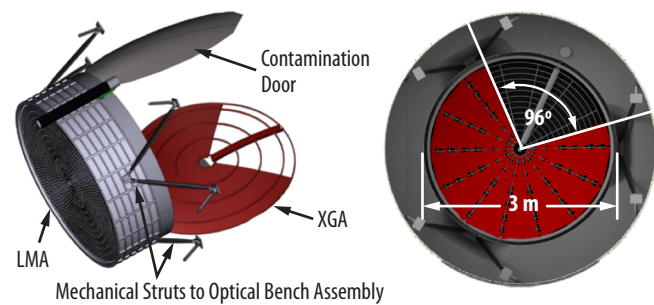


Figure 6.16. (Left) Conceptual drawing of the LMA with the XGS grating array shown. The XGA will be stored outside of the contamination door and launched in the open position. (Right) The grating array covers ~73% of the mirror area to provide the required effective area and can be retracted when not in use. [Credit: NASA MSFC/M. Baysinger/J. Rowe].

Table 6.9. *Lynx* spacecraft resources required by the CAT grating array. CAT gratings have relatively relaxed alignment tolerances and operational temperatures.

XGA Characteristic	Value
Number of gratings (with facets)	~2,100
Grating size	50×50 mm
Grating array inner/outer radius	~0.13 m/~1.5 m
Azimuthal LMA coverage	265°
Alignment stability (along optical axis)	200 μ m
Alignment tolerance to optics (along optical axis)	10 mm
Deployment repeatability	100 μ m
Grating door operational cycles	10,000 cycles (5,000 on ground, 5,000 on-orbit)
Grating door Fail Safe	Non-deployed (or "open") position
Operational temperature	$20 \pm 4^\circ\text{C}$
Survival temperature	-18 to 55°C
Grating array mass (with door structure)	69 kg (87 kg with margin)

The grating array will be launched out of the FOV in the retracted position and held in place for launch with pin-puller mechanisms that will be released once on-orbit. The insertion method is through a drive mechanism at the hinge-line once unlocked. The grating array door will also include a failsafe device to remove it from the FOV should both the primary and redundant mechanisms fail.

Chandra and *XMM-Newton* serve as excellent examples of X-ray missions that have successfully flown and operated large-scale grating spectrometers, demonstrating that scaling individual gratings to large arrays is a surmountable challenge. Scaling to the large areas required by the *Lynx* XGS is addressed by both CAT and OP technologies in §7.3.2 and §7.3.3, respectively, and in their respective technology development plans. The same manufacturing algorithm to be applied to the *Lynx* mirror segments will also be applied to the XGS gratings to optimize cost and schedule and to reduce risk [542].

The *Lynx* XGS will have a dedicated detector assembly with an array of active pixel sensors enclosed in a vacuum housing on a fixed platform on the ISIM. An optical blocking filter will be deposited directly onto the X-ray sensors to block stray light that could adversely affect the background level. The detector array will also have an independent focus adjustment mechanism that is sufficient to establish the telescope focus on-orbit and for overcoming unpredicted thermal and mechanical deviations.

The detector will use the same sensor technology as that of the HDXI to save cost and schedule. As such, the *HDXI Technology Roadmap* serves as the development plan for the XGD. The HDXI pixel size of $16 \times 16 \mu\text{m}$ is such that it oversamples the 100- μm (Full Width at Half Maximum (FWHM)) line spread function required for $R = 5,000$ by more than a factor of 6, making it much more capable than required by *Lynx* [555]. The XGD detector type will be revisited during Phase A when a detailed trade study can be conducted to determine the most optimal technology type for a given cost and schedule.

The XGD mechanical layout is consistent with the Rowland torus defined by the gratings. The zeroth-order for the CAT gratings will be detected using HDXI or LXM, while blazed higher orders are dispersed onto a detector array located as close as possible to the zeroth-order without occulting the HDXI or LXM (Figure 6.17). Since the gratings mostly disperse soft x-rays and become highly transparent for shorter wavelengths, the zeroth-order contains most of the incident flux at higher energies and can be used for simultaneous spectroscopy, in addition to the flux from the mirror area not covered by the XGA.

The XGD assembly is similar to that of HDXI, with the primary differences being the reduced number of sensors (i.e., from 21 for HDXI to 18 for XGD). The XGD does not have a filter wheel, but does have a built-in focus mechanism. The sensor array is electrically connected to a front-end motherboard (FEMB) that contains the readout electronics. Heaters, heat pipes, and radiators regulate the sensor array temperature.

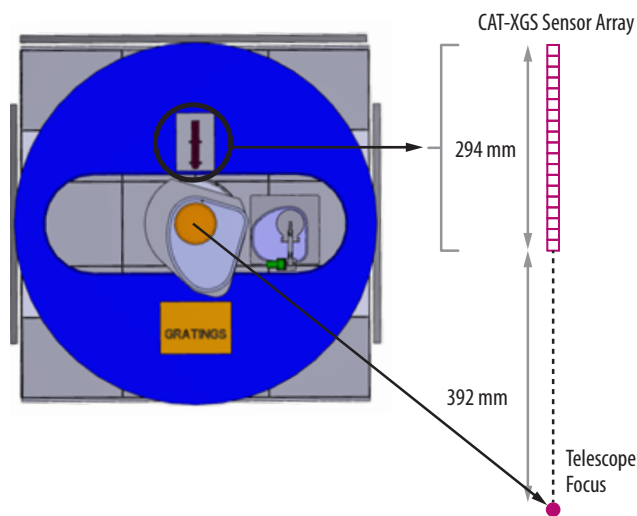


Figure 6.17. Drawing of the layout for the XGD, located on the fixed plate of the ISIM (in blue). The zeroth-order is located at the telescope focus and is detected by the LXM or HDXI. Higher orders are dispersed into the linear array offset from the focal point.

The DEU containing ERPs, backend processors, VERSA-Module Europe card (VME) -based controllers, detector controllers, and power supplies receives power from the spacecraft and allows for command and data flow (Figure 6.18). A more detailed design is found in the *DRM Supplemental Design Package*.

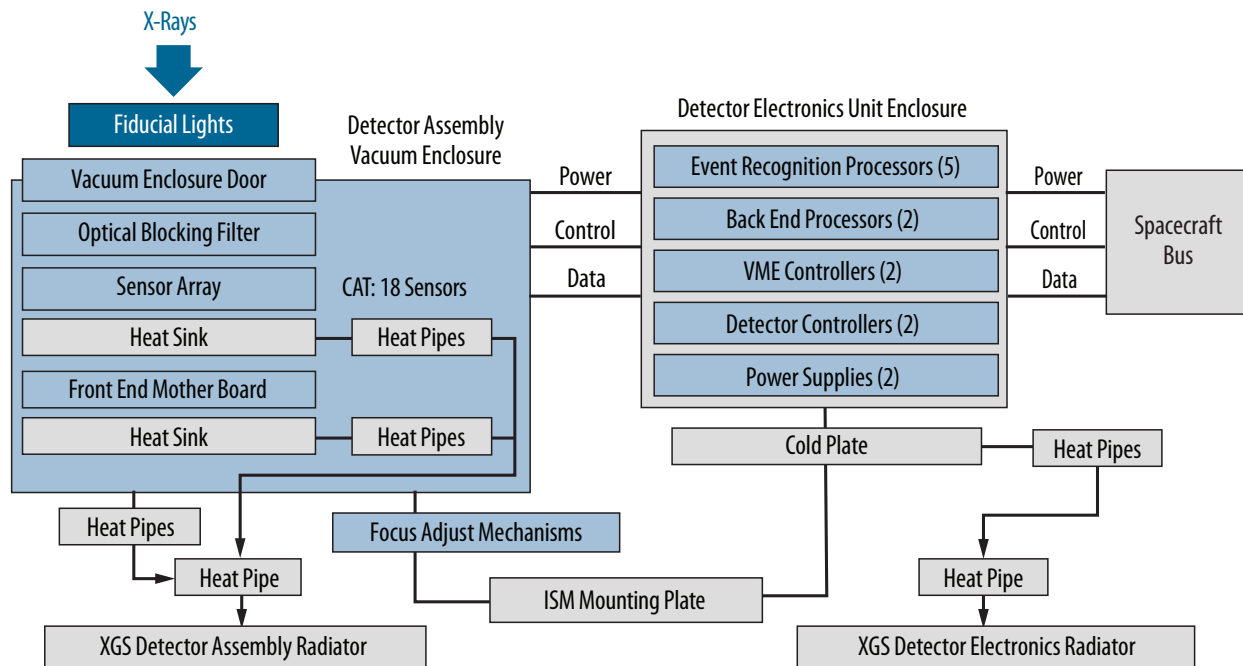


Figure 6.18. CAT-XGS detector assembly block diagram. This architecture is similar to that of HDXI, the main differences being fewer sensors than the HDXI, the lack of a filter wheel, and the inclusion of a focusing mechanism.

Spacecraft resources required for the XGD are similar to those for the HDXI (Table 6.10). Maximum data rates are conservatively set to be the same as that of HDXI, given that the gratings will be always be less efficient than direct detection. A more detailed study to refine these rates will be conducted during Phase A.

6.3.3.2 XGS Performance Considerations

XGS is designed for high performance (large effective area coupled with high resolving power) and longevity (20-year extended mission). Three key considerations have been factored into the XGS performance: (1) launch survivability, (2) ability to maintain alignment between the LMA and XGA on-orbit, and (3) ability to mitigate contamination sufficient to maintain the required performance throughout the mission lifetime.

Table 6.10. XGD spacecraft requirements are listed. Required temperatures and expected data rates are consistent with those of HDXI.

XGD Resource	Value
Number of sensors	18 (with 0.5-mm gaps in between)
Power (with margin):	
Nominal	190 W
Safehold	7 W
Survival	7 W
Operating Temperature	−90°C
Data rates:	
Nominal	600 kbps
Peak	6 Mbps
Detector Focus Range	± 1 cm
Focus Stability	3 μm
Assembly enclosure size (L×W×H)	40 × 27 × 15 cm
Mass (sensors, structures, DEU, fine focusing motor, and harnesses)	65 kg (80.4 kg with margin)

Launch Survivability — The XGA is made up of many relatively small, thin gratings mounted to a larger structure. The concept leverages the grating design used on *Chandra*, which grants confidence in its feasibility. As the XGA concept matures, static strength analyses will be performed to size the hardware per MAC load factors, and random vibration analyses will be performed to ensure that any potential unique dynamics are identified and considered. MAC load factors are intended to be a combined design load covering transients, quasi-static ascent, and random vibrations. As the project evolves and detailed structural dynamic analyses are performed, loads will be tailored for the evolving design. Random vibration environments known to envelope potential launch vehicle environments will be utilized until *Lynx*-specific environments are defined.

Alignment to Mirrors — The gratings are arranged on the surface of a torus. Shifts of the entire XGS grating structure of 1 cm along the optical axis or several millimeters perpendicular to it do not significantly affect the line spectra function keeping the resolving power of the spectrograph within requirements. The acceptable translation of several millimeters corresponds to an angular precision of a few arcminutes' rotation with respect to the mirrors given the size of the XGA [555]. Additionally, misalignment along the optical axis can be corrected with the focusing mechanism in flight, making this a very robust design that reduces cost and scheduling risk by minimizing the steps required for relative alignment of mirrors and the XGA.

Radiation Considerations — The natural radiation environment at SE-L2 is the primary consideration regarding the XGD. As these sensors are the same as those used for the HDXI, the same mitigation applies (§6.3.2.2).

Contamination — On-orbit, the grating arrays will be kept at higher temperatures than the surrounding subsystems to minimize particulate and molecular adhesion to mirror and grating surfaces. A detailed thermal analysis will be carried out during Phase A to optimize the thermal control system. Additionally, the XGA has an effective area of 4,400 cm², which is more than the 4,000 cm² required to meet *Lynx* science goals. If a fraction of the XGA does become contaminated over time, the remaining effective area should still meet the requirement. Contamination on the XGD will be minimized using the same considerations as those for the HDXI, that is, through proper venting and careful thermal control of the assembly and surrounding structure (§6.3.2.2).

6.3.4 *Lynx* X-ray Microcalorimeter

The *Lynx* X-ray Microcalorimeter will be the most advanced X-ray microcalorimeter ever flown. With over 100,000 pixel elements arranged into three separate arrays, the *Lynx* X-ray Microcalorimeter will provide an extensive range of imaging and spectroscopic capabilities. Due to recent advances in technology and heavy leveraging of previous and present day microcalorimeter design elements, this design is highly feasible.

The *Lynx* science pillars require a range of angular and energy resolution capabilities and rely heavily on the LXM's performance. The LXM will be capable of: spatially resolving AGN feedback signatures from surrounding hot gas and jets in galaxies, groups, and clusters on 1-arcsecond or finer scales with

2-eV energy resolution; resolving starburst-driven winds in low-redshift galaxies at a high spectral resolution of ~ 0.3 eV over ~ 1 -arcminute FOVs (at 1-arcsecond imaging resolution); mapping metallicity gradients (3 eV resolution over a 5-arcminute FOV) in circumgalactic, group, and galaxy cluster fields; and surveying young Supernova Remnants (SNRs) in local group galaxies.

The *Lynx* team has performed multiple simulations showing the feasibility of spectroscopic observations on arcsecond and sub-arcsecond resolution scales, which have been highlighted in the text (e.g., in §2.2 and §3.3).

6.3.4.1 LXM Design Overview

A feasible LXM design has been developed for the *Lynx* DRM that meets the combinations of spectral, spatial, and FOV required to enable this transformational science. Though unique, this design borrows heavily from flight heritage and design elements for other X-ray microcalorimeters currently in development, and uses high-TRL elements whenever possible [560].

The most important LXM element required to meet the *Lynx* science goals is its focal plane. The LXM focal plane is composed of a large array of pixels (or absorbers) with sensors attached that determine the energy of individual incident photons by precisely measuring the temperature rise from the heat deposited. As the thickness of the absorber decreases, so does its heat capacity and usable energy range. Thus, there is a tradeoff between energy resolution and energy range in order to achieve the best possible energy resolution for a given energy.

The LXM Focal Plane Assembly (FPA) has three sensor arrays, each designed to meet particular *Lynx* science requirements. The Main Array (MA) is designed to provide a large FOV with good angular resolution and energy resolution across the *Lynx* bandpass. The Enhanced Main Array (EMA) has a narrower FOV, but an angular resolution that is precisely matched to that of the *Lynx* telescope. The Ultra-High-Resolution Array (UHRA) has the same reduced FOV as the EMA, but with much higher energy resolution at lower energies (Figure 6.19).

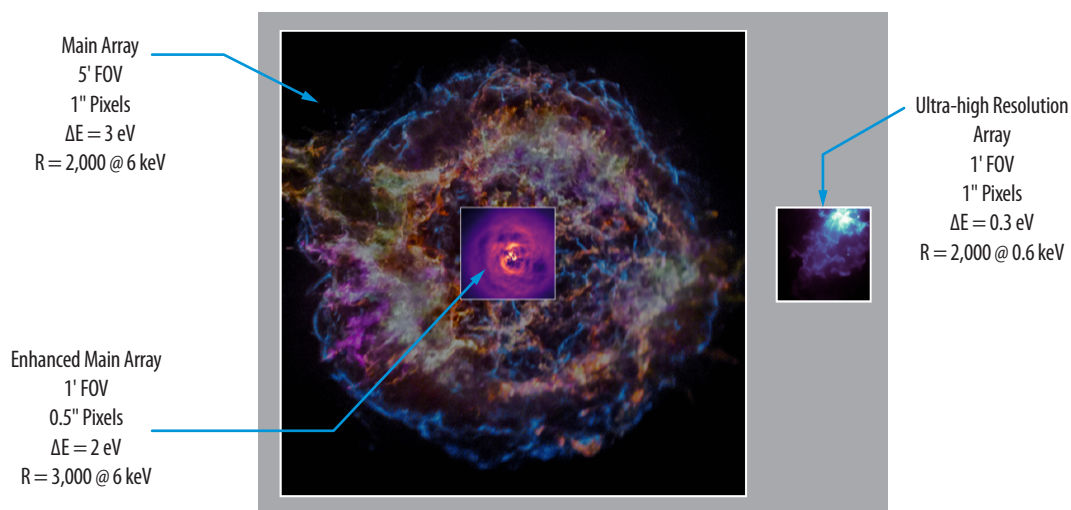


Figure 6.19. LXM will have three sensor arrays that share the focal plane. The Main Array will provide a large FOV with good angular resolution and energy resolution across the *Lynx* bandpass. The Enhanced Main Array has a narrower FOV but an angular resolution that is precisely matched to that of the *Lynx* telescope. The Ultra-High-Resolution Array has the same reduced FOV as the Enhanced Main Array but with much higher energy resolution at lower energies.

The count rate capability is much higher for the UHRA than for the MA and EMA, and is a derived value based on the intrinsic design of the arrays. The design of the UHRA pixels is inherently a few times faster than the MA and EMA hydra designs due to the lower heat capacity of the UHRA absorbers and also due to the small size of the UHRA Transition Edge Sensors (TESs). The UHRA count rate capability ranges from 80 cts/s to 1,000 cts/s per 1-arcsecond pixel, depending on the required energy resolution. The UHRA is useful up to ~ 2 keV based upon the Quantum Efficiency (QE) and energy resolution, with the energy resolution degrading slowly with energy to ~ 3 eV. For all three arrays, a lower energy resolution requirement would allow for a higher count rate capability.

Using three arrays for the LXM design not only meets the *Lynx* science goals, but also provides a feasible design that can be fabricated in the relative near-term. By contrast, if one were to design an X-ray microcalorimeter capable of achieving 0.3-eV resolution up to 7 keV across the full LXM FOV, it would require 360,000 pixels and 360,000 TESs, which is currently not practical. Additionally, many of the LXM-expected science observations would result in photon-starved pixels, effectively negating any benefit from the higher angular resolution; this was not considered an acceptable design trade.

A trade study examined the potential benefits of extending the LXM response to higher energies of ~ 15 to 20 keV. The science case for this is broad and includes improving black hole spin measurements [561], expanding our understanding of the X-ray-emitting corona associated with accreting black holes [562], improved feedback measurements [563], studies of obscured AGN [564, 565], X-ray reverberation mapping to uncover the geometry of the central engine [566], and studies of ultraluminous X-ray sources [567]. A higher energy response can be achieved without modifying the current instrument design (and by operating the microcalorimeters at a slightly higher heatsink temperature); however, modifying the LMA via additional mirrors or multilayer coatings would be required. This trade is documented in Appendix B.2.2.1.

The true power of the X-ray microcalorimeter was first realized by the Soft X-ray Spectrometer (SXS) on the JAXA *Hitomi* (Astro-H) mission, when it revealed the high-resolution (4.9 eV FWHM at 6 keV) spectrum of the core of the Perseus cluster, tightly constraining the velocity dispersion of the cluster gas [568]. Building on the successful implementation of *Hitomi's* SXS, the European Space Agency's (ESA's) planned *Athena* Observatory will include an X-ray microcalorimeter (the X-ray Integral Field Unit (X-IFU)) in its payload that is well matched to *Athena's* large FOV and higher angular resolution [569]. The X-IFU focal plane has a different design than the SXS, with many more pixel elements to read out and requiring an even higher energy resolution. The LXM will be the most capable yet, as the *Lynx* science case requires an FOV comparable to the X-IFU, but matched to the order of magnitude higher angular resolution expected for the *Lynx* telescope. The LXM will also deliver an even higher energy resolution, which will be necessary to address some of the most compelling and unanswered science questions regarding the fundamental drivers of galaxy and large-scale structure formation and evolution. However, a finer angular resolution combined with a relatively large FOV translates into an increased number of pixel elements over that of the X-IFU. Due to innovative thermal multiplexing, the number of sensors (TESs) read out in the LXM will be twice that of the X-IFU [560].

Thermal multiplexing will be performed using hydras in the form of TESs [570, 571] (Figure 6.20). These have been baselined due to their relatively high maturity levels compared to other thermometer technologies. Multi-pixel TESs, or hydras, reduce the number of TESs that need to be read out. This multiplexing allows for wider focal plane coverage (or finer sampling of the FOV for the same coverage) without a commensurate increase in the number of wires or readout components.

Superconducting Quantum Interference Devices (SQUIDs) in resonators allow the multiplexed readout of hundreds of sensors on a single electronics chain. In a microwave SQUID multiplexed readout, the current signals from sensors biased with DC voltage stimulate Radio Frequency- (RF-) SQUIDs that change the resonant frequency of the microwave resonators coupled to a common feedline [572, 573].

A comb of microwave tones probe the resonators, and a shared semiconductor amplifier (e.g., a High-Electron Mobility Transistor (HEMT) or a Silicon-Germanium Heterojunction Bipolar Transistor (SiGe HBT)) measures the summed tones. The maximum assumed number of HEMTs powered on at a single time is 16. Minimal to no energy resolution degradation from the readout is expected for this design [572].

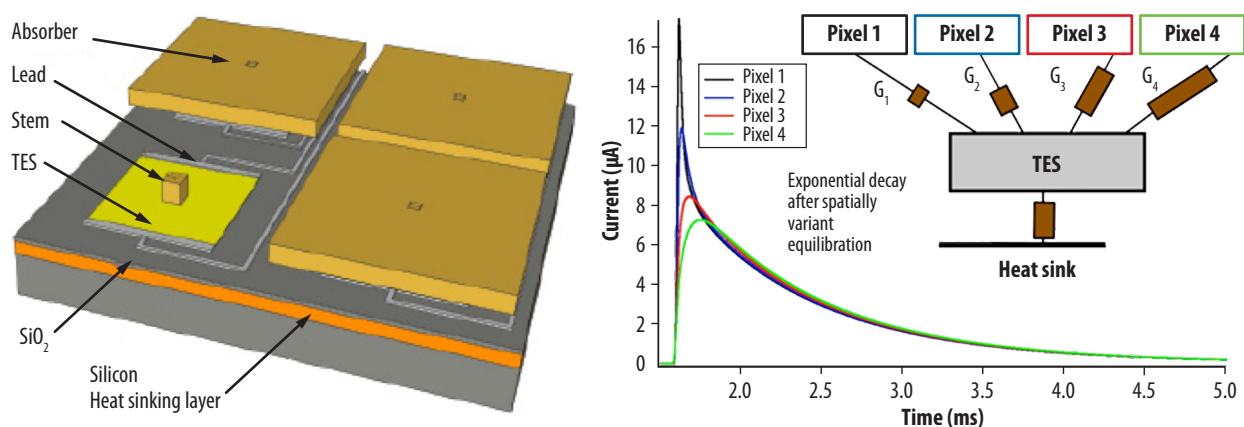


Figure 6.20. (Left) Schematic showing components of a TES calorimeter that uses the thermal boundary between the TES film and the substrate to decouple the TES from the substrate. (Right) Schematic representation of the TES hydra. (Inset Top-Right) Thermal model of a multipixel TES consisting of four X-ray absorbers connected to a single TES via varied thermal conductance $G_i = 1 \dots 4$. The TES is weakly thermally coupled to a heatsink via conductance. The measured average X-ray pulse shapes for a 4-pixel hydra at 6 keV is shown. The differences in pulse shapes before equilibration are used to determine the pixel that absorbed the X-ray photon. *Lynx* will use 25 hydras for the MA and EMA, and no hydras for the UHRA.

The combined capability of the three LXM sensor arrays (Table 6.11) highlights the LXM's full potential to achieve the *Lynx* science pillars and to make new discoveries. The design's technical feasibility has been established through numerous recent breakthrough technologies, not only for the sensor, but also for the supporting elements. The technology development path is described in detail in §7.3.4 and in the *LXM Technology Roadmap*.

Table 6.11. Key characteristics for LXM for the three arrays. The energy resolution and count rate capability are inversely related. A lower energy resolution allows for a higher count rate. The range of this trade space is indicated by the terms ‘high-res’, ‘mid-res,’ and ‘low-res’. The design of the UHRA pixels are inherently a few times faster than the MA and EMA hydra designs due to the lower heat capacity of the UHRA absorbers and also due to the small size of the UHRA TESs.

Characteristic	Main Array (MA)	Enhanced Main Array (EMA)	Ultra-high Resolution (UHR) Array
Energy range (keV)	0.2 – 7 keV	0.2 – 7 keV	0.2 – 0.75
Quantum efficiency: Area fill factor Vertical QE	> 90% > 80% at 6 keV	> 80% > 80% at 6 keV	> 90% > 99% at 0.75 keV
Field of view	5 × 5 arcmin [1.5 cm × 1.5 cm]	1 × 1 arcmin [3 mm × 3 mm]	1 × 1 arcmin [3 mm × 3 mm]
Pixel size (arcsec)	1 × 1 [50 μm × 50 μm]	0.5 × 0.5 [25 μm × 25 μm]	1 × 1 [50 μm × 50 μm]
Energy resolution: High-res Mid-res Low-res	3 eV (FWHM) at 6 keV 5 eV (FWHM) at 6 keV 10 eV (FWHM) at 6 keV	2 eV (FWHM) at 6 keV 4 eV (FWHM) at 6 keV 10 eV (FWHM) at 6 keV	0.3eV (FWHM) at 0.75 keV 0.8 eV (FWHM) at 0.75 keV 2 eV (FWHM) at 0.75 keV
Number of pixel elements (number of TES readouts)	86,400 (3,456)	14,400 (576)	3,600 (3,600)
Number of hydras per pixel	25	25	N/A
Count-rate capability: High-res Mid-res Low-res	10 cts/hydra (0.1 mC) 40 cts/hydra (0.4 mC) 150 cts/hydra (1.5 mC)	10–20 cts/hydra (0.1–0.2 mC) 40–80 cts/hydra (0.4–0.8 mC) 150–300 cts/hydra (1.5–3.0 mC)	80 cts/s/pixels (0.8 mC) 320 cts/s/pixel (3.2 mC) 1,000 cts/s/pixel (10 mC)
Absolute energy calibration	1 eV	1 eV	0.25 eV
Timing resolution	2 μs		
Timing accuracy	50 μs		
Instrument background	<5 × 10 ⁻³ cts cm ⁻² s ⁻¹ keV ⁻¹		

Achieving high energy resolution across the *Lynx* bandpass requires that the LXM focal plane array be cooled to 50 mK. The LXM FPA is housed within a cryostat designed to minimize the LXM’s overall footprint on the ISIM. The architecture has roots in previous X-ray missions such as *Hitomi*, but has a cryogen-free operation (i.e., there are no expendable cryogenics that limit mission lifetime).

The key components in the cooling system, shown in Figure 6.21, are the cryocooler, which cools from room temperature (~283 K) down to 4.5 K, and then a multi-stage Adiabatic Demagnetization Refrigerator (ADR), which provides continuous cooling down to 50 mK [574].

A thrust tube design provides mechanical support to the various temperature stages to minimize the diameter of the LXM (Figure 6.22), which allows the XGD to be placed closer to the telescope optical axis. The use of these canonical thrust tubes (and verification of the thermal and structural performance) will be confirmed in pre-Phase A and Phase A. The Advanced Cryocooler Development Program (ACTDP) four-stage (Mega4-1) pulse tube cryocooler developed by Lockheed Martin is already at a relatively high TRL and has been baselined for providing 4.5-K cooling. As there are a number of different options for providing this cooling—such as the Turbo-Brayton Cryocooler developed by Creare—a trade study will be conducted during Phase A to assess the state of these technologies and the advantages and disadvantages of each. The dominant heat loads from the detection chain at 4.5 K come from the HEMTs (estimated to dissipate 16 mW) and the harnesses (estimated to conduct 3 mW) [574].

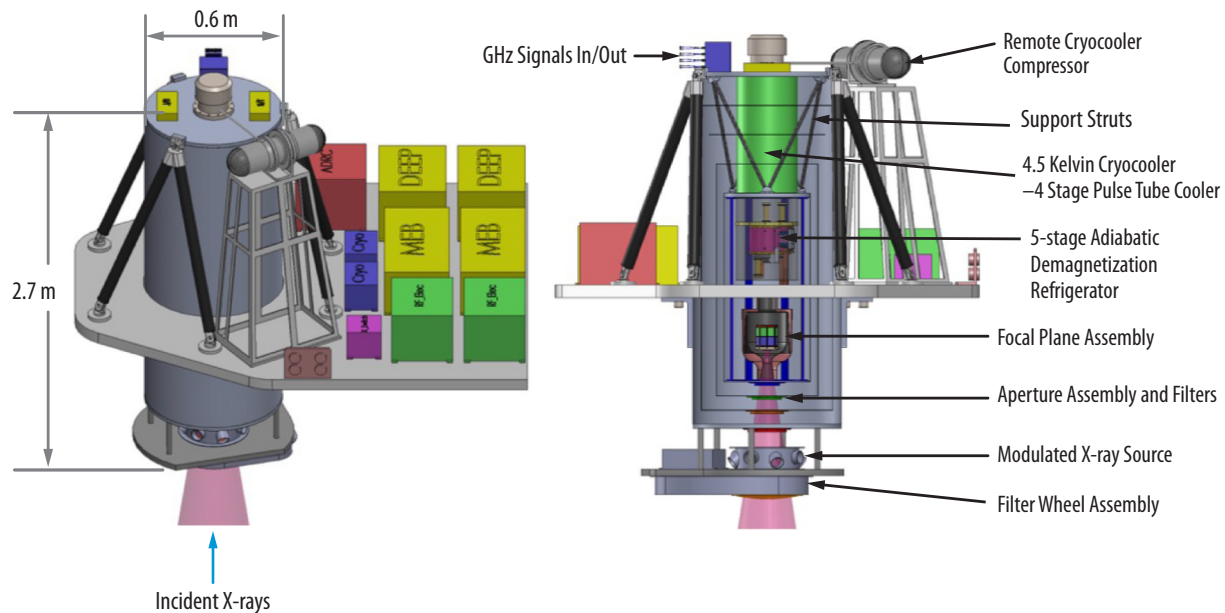


Figure 6.21. (Left) Overview of the LXM cryostat and readout electronics. (Right) Side-on view of the LXM, including a cross-sectional view of the cryostat. The X-rays enter the cryostat from the bottom. The filter wheel and modulated X-ray source (with its electronics) are located a small distance below the bottom of the main cryostat on a separate mounting plate, which is attached to the main cryostat.

At one end of the cryostat are a gate valve and an aperture assembly that incorporates thin-film filters similar to those on *Hitomi* to block IR and optical photons. An engineering study was conducted to determine the optimum IR-blocking filter design to provide a high system (filter + detector) QE across the *Lynx* bandpass [575]. Outside of the gate valve, the LXM will include an external filter wheel and a modulated X-ray source capable of providing pulsed X-ray lines at multiple energies similar to that used on *Athena*'s X-IFU [569] and *Hitomi*'s SXS [576] for in-flight calibration.

The LXM detector assembly, cryostat, and the full complement of readout electronics are located on the translation table on the ISIM. When the LXM is translated into the optical axis, its electronics and radiators move along with it, minimizing the overall complexity of the ISIM. A block diagram for the

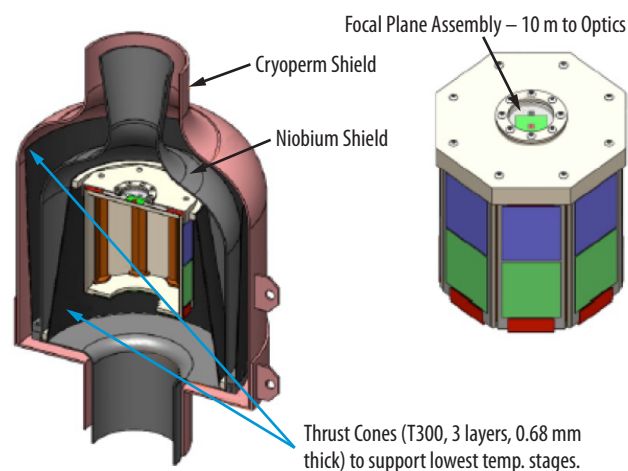


Figure 6.22. (Left) LXM FPA cross section. The high-magnetic-permeability Cryoperm shield is at 4.5 K, and the superconducting niobium shield is at 0.6 K. (Right) View of the FPA 50-mK stage. The MA, EMA, and UHRA are visible on the top surface through an IR-blocking filter that is transparent in this figure. The multiplexer readout components are on each of the eight side panels shown in blue and green.

entire LXM is shown in Figure 6.23. The block diagram shows the FPA design for housing the detector array also includes the cold readout and an anticoincidence detector utilized to reduce the background X-ray events [577]. Two redundant electronics boxes for controlling the cryocooler and the redundant Main Electronics Boxes (MEBs) are also shown. Most of the electronics boxes consist of standard circuits and components used frequently for space, such as control microprocessors, conditioned power sources, and control signals for all of the various components and mechanisms. The Digital Electronics and Event Processor (DEEP) and the analog RF electronics boxes are the only ones that are technically demanding, and thus in need of technology development, as described in the *LXM Technology Roadmap*.

The primary resources required for the spacecraft to support the LXM are listed in Table 6.12. The largest mass contributions for the LXM come from the cryostat and the electronics boxes. Power estimates are dominated by the DEEP boxes (615 W) and the cryocooler (653 W), followed by the RF electronics boxes (141 W), other electronics boxes, and operational heaters. The choice for the Field Programmable Gate Arrays (FPGAs) — a main part of the DEEP electronics — was conservative. Future processors are likely to become available that could reduce the power needed. Similarly, it is very possible that future cryocoolers will require less power. A reduction in power leads

Table 6.12. LXM spacecraft resources.

LXM Resource	Value
Total mass (with margin)	468 kg (585 kg)
Cryostat	164 kg
Electronics Boxes	146 kg
Thermal (heat pipes, etc.)	72 kg
Misc. (harnesses, structures, filters)	86 kg
Power (with margin)	
Nominal	1,575 W (2,205 W)
Safehold	310 W (434 W)
Survival	10W (14 W)
Operating temperature:	
Cryocooler	Cools from 283 K to 4.5K
Multistage ADR	Cools from 4.5 K to 50 mK
Data Rates	
Nominal	20 kbps
Peak	8 Mbps
Detector Focus Range	± 1 cm
Focus Stability	3 μ m
Cryostat Size (length x diameter)	1.43 m x 0.6 m

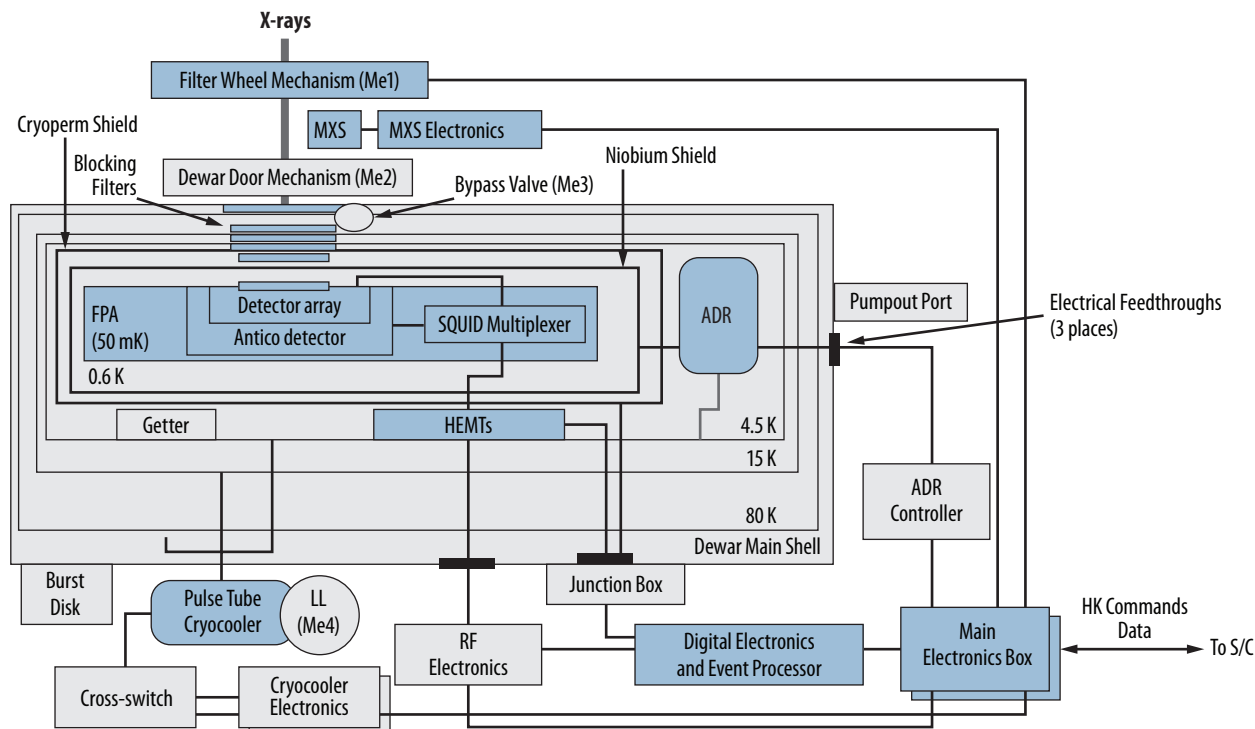


Figure 6.23. LXM block diagram.

to a reduction in the mass of the radiators, which have a margin of 40% and are part of the ISIM. The LXM is assumed to launch warm and only needs about 10 W of housekeeping power until the Observatory is en route to SE-L2.

The assumed maximum data rate for the LXM is based upon a total maximum count rate for the whole array of 100,000 cts/s and an assumption that 80 bits are needed to describe each event. Therefore, the LXM has a maximum data rate of 8 Mbps. When looking at the brightest sources such as Sco X-1, the instantaneous data rate may be higher. In these instances, it is assumed that the other instruments are turned off and that there is a limit on exposure such that the total volume of data collected is <240 Gbps per day, which matches *Lynx*'s telemetry limit.

The LXM design is a natural progression from *Hitomi*'s SXS, the *X-ray Imaging and Spectroscopy Mission*'s (XRISM's) Resolve, and *Athena*'s X-IFU. One example of how *Lynx* will leverage technology development from these other payload is through the use of the Modulated X-ray Source (MXS), which will be included on the LXM FPA for in-flight calibration by providing pulsed X-ray lines at multiple energies. The LXM will also leverage the X-IFU readout layout (similar wire density and flex cable technologies) due to the similar focal plane size. This also allows for the mechanical, thermal, magnetic shielding, anticoincidence detector, and IR filter designs from the X-IFU to be leveraged. Cooling the LXM focal plane will be met with a cryostat that uses heritage from SXS and Resolve, and design details from the X-IFU. Other cooling system elements will be achieved via a thrust-tube-type design mounted in a fashion similar to that used for *Spitzer*.

6.3.4.2 LXM Performance Considerations

The LXM performance relies not only on the performance of the instrument itself, but also on how the LXM interfaces to the Observatory. The LXM must survive launch and must have adequate vibration and thermal isolation from the ISIM.

Launch Vibration — The cryocooler will use the same staging configuration as the ACTDP four-stage cooler. This configuration is robust and straightforward to design, assemble, and test. The LXM cryocooler may be required to support significant masses during launch vibration, so design iterations during Phase A are expected in order to meet minimum resonant frequency requirements.

Vibration and Thermal Isolation — Vibration and thermal isolation between LXM and the ISIM are necessary to ensure that Observatory performance is not affected by vibrations from the LXM cryocooler. Isolation is addressed in the design through the use of three bipods to connect the cryostat to the ISIM and by locating the cryocooler compressor, rotating valve, and all moving parts onto a separate stand from the cryostat. The cryocooler is only coupled to the cryostat through a flexible tube, allowing the cryostat to remain vibrationally isolated. As an alternate option, the turbo-Brayton cryocooler by Creare is also being considered for the 4.5-K cooling. There is an inherent lack of vibration generated by the cryocooler, as it is based upon the use of extremely low-mass parts generating extremely small vibrations at frequencies in excess of 1 kHz, and the use of gas bearings and clearance seals that prevent mechanical contact and thus eliminate wear. This is a slightly lower TRL than the ACTDP; however, Creare is currently funded to mature this technology.

The cryostat design utilizes heritage from *Hitomi*'s SXS regarding the design of the vibration and thermal isolation. However, detailed analyses will need to be conducted in Phase A to optimize this scheme for *Lynx*. The TES sensor technology used by the X-IFU and the LXM is based upon a first-stage SQUID amplifier with a low impedance input, which is inherently less sensitive to vibrations of the sensor and its wiring.

Contamination — The LXM contamination control requirements are based upon those previously set by *Hitomi*. These requirements are driven primarily by the sensitivity of the detector system and the optical blocking filters. The detector is subject to degradation if the filter or calorimeter surfaces are contaminated with particles or residue.

Surface contamination requirements for the thin film optical filters, associated carriers, and the aperture assembly will be designed to minimize filter obscuration, prevent particles from physically damaging the filters, and limit end-of-life film thickness for non-volatile residue and ice to 500 Å. To meet these limits, the filters will be kept visibly clean. For the particulate contamination requirement, no particles larger than 50 µm will be allowed. For the molecular contamination requirement, the molecular limit will be determined by analysis and X-ray transmission tests. The FPA and carrier surfaces will be cleaned and verified upon final assembly and will subsequently be maintained at that level through filter integration. The detector system must meet the surface contamination requirements similar to that of the thin film filters. Therefore, upon assembly, detector system surfaces will be visibly clean with no particles larger than 10 µm. Detector system surface cleanliness will be maintained by keeping the assembly in controlled environments and periodically cleaning surfaces where feasible.

The ADR contamination control requirements will be designed to minimize contaminant redistribution to sensitive filter or detector surfaces. To minimize such contaminant redistribution, internal dewar surface contamination and outgassing levels will be limited. Vent paths for dewar pump-down will be designed such that the flow of outgassed molecules and particulate contamination across thin film filter surfaces is minimized. Proper venting of helium gas will be designed to avoid thermal conduction caused by vented gaseous molecules. The LXM cryostat outgassing levels will be limited by selecting low-outgassing materials and by baking out assemblies that contain significant quantities of nonmetallic materials. For materials selection, the criteria that should be applied are a maximum of 1% total mass loss and 0.1% collected volatile mass. Vacuum bakeout tests will be conducted for harnessing and Multilayer Insulation (MLI).

Radiation Considerations — Superconducting detectors and electronics are generally considered more resistant to radiation than semiconducting electronics because they do not depend on the mobility of individual electrons and holes and because the material properties of a superconductor are averaged over spatial scales of the coherence length, which greatly exceeds the small size of damage features created by ionizing radiation. Research on radiation effects has focused on superconducting tunnel junctions because their nanometer-scale barriers are the only features whose size approaches the scale of radiation damage. Irradiation tests have been performed on tunnel junctions by a number of researchers, including by those on the *Lynx* team. These results are summarized below:

- A Japanese research team exposed two Nation Institute of Standards and Technology- (NIST-) series SQUID arrays to 160 MeV protons, delivering a 10-krad dose. Their performance before and after irradiation was statistically consistent. More tests of this type are planned for the *Athena* project.

- The Gravity Probe B team exposed three cold DC SQUIDS to 105 to 107 protons/s/cm² with proton energies of 50–280 MeV. They concluded, “No changes of the type to be expected from critical current variations were observed, nor was any permanent damage noted in the SQUIDS.” [578]
- For Herschel, “More than 100 junctions have been irradiated with [10 MeV proton] doses between 109 and 1,013 protons/cm. According to the analysis, a 2×1,010 protons/cm dose would correspond to ... 4 years mission with a 1-mm thick Al shielding. After the tests, only small and not significant changes (about 1%) were observed on the junctions I-V curves.” [579]
- Frunzio et al. 1998 summarized irradiation experiments. Two proton-irradiation experiments on niobium-based tunnel junctions (as are planned for *Athena*) delivered doses of 77 and 500 Mrad without causing damage. A third experiment that delivered 5,000 Mrad resulted in damage [580].

One estimate [581] for the radiation dose from four years at L2 with 1-mm-thick aluminum shielding is about 50 krad (given for silicon, but assumed applicable here, too). Frunzio determined the damage threshold for niobium junctions to between 500 and 5,000 Mrad. Hence, the damage threshold is at least a factor of 104 greater than the expected mission dose [580].

In regard to radiation effects, the LXM’s main potential sensitivity is to the effects of radiation damage in the room temperature electronics. All LXM electronics will meet the radiation tolerance requirements necessary for the flight electronics to operate over the lifetime of the *Lynx* mission at SE-L2. The processors, Analog-to-Digital Converters (ADCs), and Digital-to-Analog Converters (DACs) needed for microwave SQUID readouts are the critical electronics components that require high performance and must be radiation-tolerant. A detailed discussion of the flight-compatible components identified as an initial baseline are described in [582].

The HEMTs are the main remaining components that are potentially sensitive to the radiation environment. Based upon the known radiation sensitivity properties of semiconducting devices similar to the HEMTs currently baselined for LXM, space-qualifying the SOA HEMTs is not expected to be a problem. However, this still needs to be verified, and this verification process has been included as an important component of the *LXM Technology Roadmap*.

6.3.5 Integrated Science Instrument Module

The ISIM is the support structure for the focal plane instruments that interfaces to the OBA and places the required focal plane camera in the proper position for each observation.

The HDXI and LXM are mounted on a translating table, while the XGD assembly is mounted on a fixed platform. Both the translation table and the XGS platform will be capable of focus adjustment to establish the best focus on-orbit and to allow for offsets of the focal planes for those three cameras. ISIM resources are summarized in Table 6.13.

Table 6.13. ISIM resources are summarized. The ISIM mass of 1,460 kg interfaces to the optical bench. The total number of moves and distances for translation and focus include ground testing and 20 years on-orbit.

ISIM Resource	Value
Total mass (with margin)	1,460 kg
Translation table and interfaces	108 kg
Fixed table	73 kg
Housing	123 kg
Radiators, and thermal hardware	194 kg
Mechanisms	193 kg
Instruments (total)	769 kg
Average operating temperature	283 K
Focus range	± 1-cm
Focus stability	3 μm
Focus accuracy	0.01 mm
Focus total number of moves	20,000
Focus total distance	200 m
Translation range	75 cm
Translation stability	3 μm
Translation accuracy	5 μm
Translation total number of moves	20,000
Translation total distance	15,000 m

This translation table assembly allows any point along a line to be chosen as the celestial target aim point. This allows, for example, selection of the desired LXM subarray, or optimizing the focus over the FOV of the tilted HDXI chips. The XGD is mounted in a fixed location on the ISIM offset from the optical axis to intercept the dispersed spectrum regardless of whether the HDXI or LXM is at the primary focus. The XGD has an independent focus mechanism built into its housing. The positioning requirements and lifetimes are easily met with standard design practices and high-TRL mechanisms. The placement of the instrument electronics boxes was optimized to minimize the distance between each of the instruments and their electronics (shown in Figure 6.24). A more detailed design will be carried out during Phase A and will also include the heat pipe placement. Mechanisms for translating and focusing the instruments have dual-redundant motors (§6.4.7).

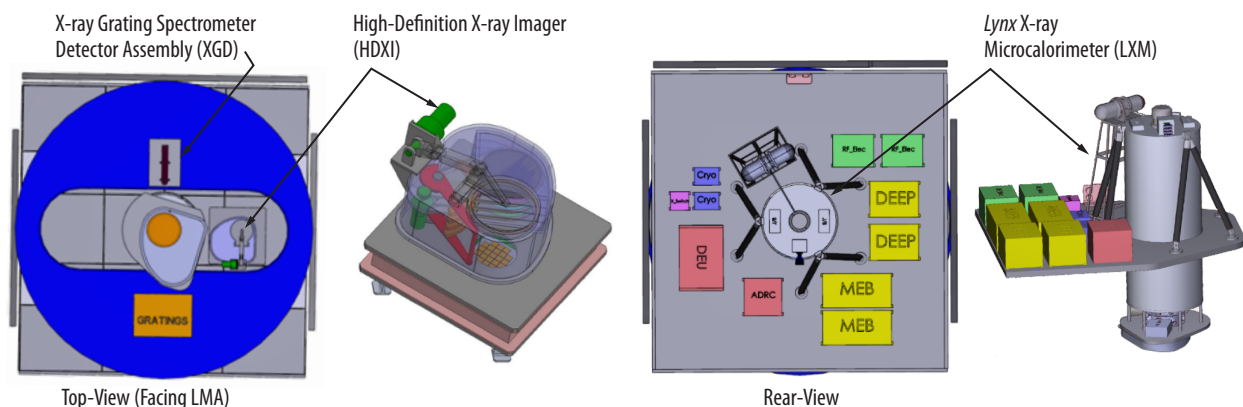


Figure 6.24. Views of the ISIM with HDXI, XGD, and LXM mounted, along with a view of their electronics boxes. An elliptical opening, seen in the top-view in the ISIM fixed plate allows for the HDXI and LXM to translate across the focal plane.

The ISIM also provides a protective, light-tight cover for the instruments, as well as mounting surfaces for the radiators required by the cold LXM focal plane detectors and the cryocooler. Radiators will be placed on the three coldest sides of the ISIM based on the temperature requirements and proximity to the instruments they serve. For those requiring significant heat transfer from instrument to radiator panel (e.g., the LXM DEEP boxes), heat pipes will be employed as both the primary path and for spreading heat over a large radiator panel. The size of the radiators sets the size of the ISIM translatable platform, resulting in ample real estate for supporting electronics and thermal management.

The Sun-exposed surfaces of the ISIM will be treated with low-absorptance, high-emittance external treatments such as Optical Solar Reflectors (OSRs) or zinc-oxide-filled painted coatings (e.g., Z-93). Overall, the ISIM's temperature will be cold-biased to support colder focal plane detectors as well as reduce the overall heat load of the instruments to the radiators.

6.3.6 Optical Bench Assembly

The OBA's function (depicted in Figure 6.25) is to maintain precise control of the geometric alignment between the optical elements of the LMA and the science instruments within the ISIM. To perform this function, the OBA design uses a near-zero CTE, lightweight, high-tensile, compressive strength carbon fiber composite (M46J) structure additionally supported by ring stiffeners. To provide stability against vibration and high-frequency jitter while maintaining the required rigidity, the LMA is optimally anchored to the OBA by three pairs of bipods, while the ISIM is attached directly to the OBA. To minimize thermal gradients and rapid localized temperature excursions due to Observatory reorientation, the OBA is cold-biased and uses passive thermal insulation and active, autonomous thermal control via resistive heaters. The OBA is opaque to stray light.

The OBA presents the largest outward surface area toward both hot and cold (Sun and anti-Sun) sides of the Observatory. It therefore potentially suffers the largest amplitude deformations due to induced thermal gradients and other disturbances that affect the alignment of the optical elements along and perpendicular to the optical axis.

Thermal effects are minimized by placing MLI blankets on top of the low-CTE OBA composite structure. In addition, to maintain positive thermal control within the OBA over a longer lifetime of 20 years, the MLI is augmented with a one-time-deployed siliconized Kapton® sunshade (§6.4.4). The sunshade deployment uses a simple series of spring ribs along the length of the OBA, with the ribs and sunshade held just above the MLI with single-shot actuators during launch, which then release the sunshade to its flat shape upon deployment. This arrangement keeps the outer layer of the MLI blanket under 10 °C so that the net heat flow is from the OBA to the exterior for all allowable Observatory orientations. The sunshade extends as needed to allow the full field of regard adopted for the mission, including the $\pm 15^\circ$ roll capability.

Thermoelastic analysis of the Observatory indicates that maximum deformations do not exceed 2.4 μm along any principle axis due to changes in orientation relative to the Sun. Critically, along the optical axis, these maximum deformations are much less than the telescope depth of focus and will not compromise the *Lynx* PSF. *Lynx* is more tolerant of deformations perpendicular to the optical axis because lateral placement is monitored by the Fiducial Transfer System (FTS).

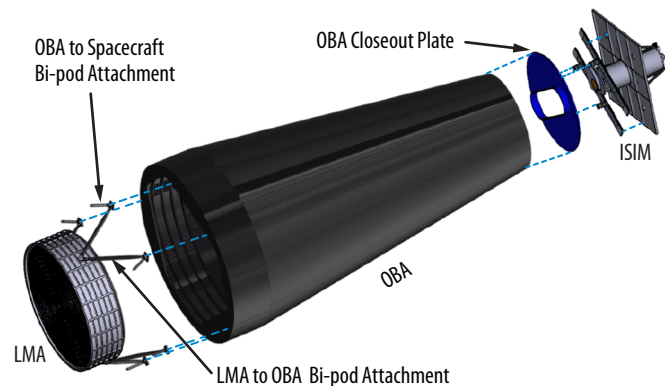


Figure 6.25. OBA provides geometric alignment between the optics and science instruments.

Chandra and *XMM-Newton* experience beyond Earth's radiation belts shows that charged particle flux through the open aperture of telescope optics can be substantial. *Chandra* utilizes a magnetic diverter located within the OBA between the mirror assembly and the focal plane instruments to deflect electrons from paths toward the on-axis science instrument. A similar magnetic diverter for soft protons is planned for *Athena* [553]. *Lynx* can accommodate a similar magnetic diverter within the OBA cavity. Though no specific design has yet been considered, a mass with ample mass growth allowance based on *Chandra*'s magnetic diverter as a first-order approximation has been assumed and incorporated into the Master Equipment List and cost estimate.

As described in §6.4.2, to monitor the alignment of the optical system, the *Lynx* GN&C system has adopted the *Chandra*-heritage PCAD system. The PCAD system includes an FTS, as depicted in Figure 6.26. The FTS places images of Light Emitting Diodes (LEDs) located near each science instrument in the FOV of the star-tracking camera. These diodes serve as points of reference of the instrument's lateral position with respect to the star camera boresight.

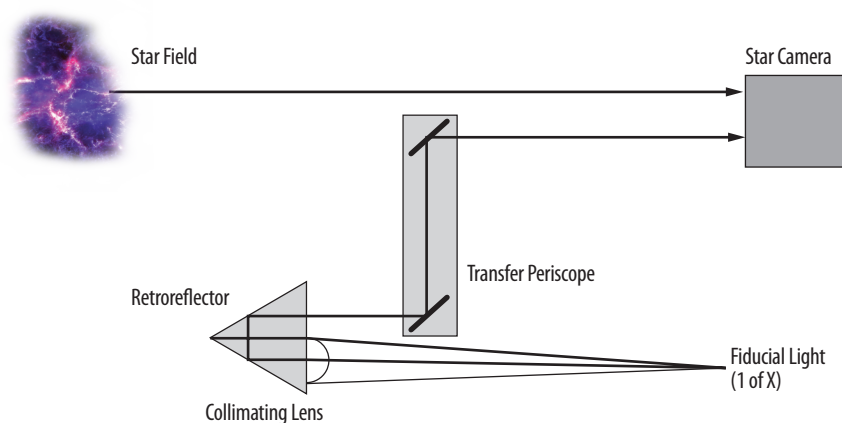


Figure 6.26. Schematic demonstrating the principle of the *Lynx* FTS. In addition to imaging the tracking starfield, the star camera images light from LEDs located near each science instrument. The fiducial light passes through a collimating lens and retroreflector mounted at the node of the LMA before being transferred via a highly stable periscope to the star camera.

6.4 Design of Spacecraft and Subsystems

The Spacecraft will meet *Lynx* requirements with high TRL, low risk design solutions. *Lynx* will take advantage of emerging subsystem technologies to enhance performance and reduce risk without expensive architecture changes. Subsystem elements have been designed to provide 20 years of on-orbit operation and to maximize launch flexibility.

The spacecraft includes all necessary subsystems to enable the scientific and operational functionality of the Observatory, as shown in Figure 6.27. The *Lynx* system block diagram is shown in FO2, illustrating the system dependencies.

Following a trade study on configuration architecture, a *Chandra*-like spacecraft was selected (Appendix B.1.1). This layout is straightforward, with no complicated deployments and provides for standard thermal management of the LMA. The design of the spacecraft and individual subsystems is robust, with extensive use of low-risk, high-TRL, heritage, and commercially available components. However, the architecture itself is not dependent on obsolescent technologies, and newer technologies can be incorporated as available during detailed design. The application of Risk Class A design requirements and industry-standard margins have been used throughout, and credible single-point failures have dual-redundant systems (summarized in Table 6.14).

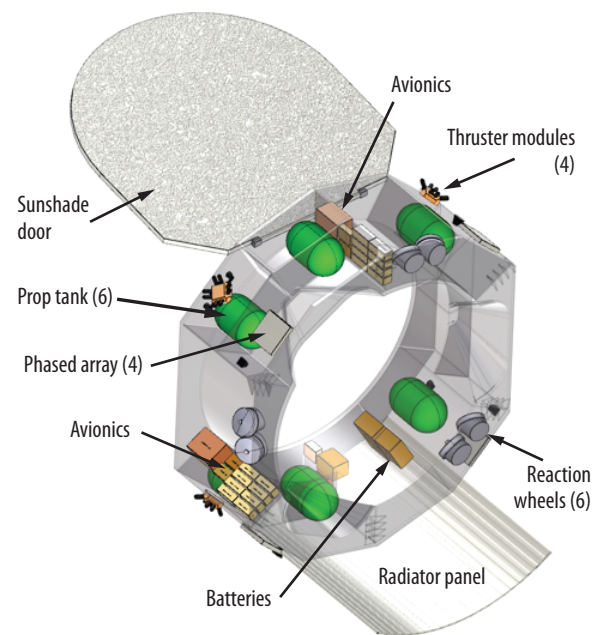


Figure 6.27. *Lynx* spacecraft schematic. All spacecraft subsystems are at high maturity levels or modified heritage.

6.4.1 Propulsion

The propulsion subsystem is a monopropellant blowdown system utilizing hydrazine as fuel and gaseous nitrogen as the pressurant, and can be realized through existing high-TRL and/or modified heritage components. The current design utilizes six modified ATK 80274 propellant tanks, two (plus two redundant) Northrop Grumman MRE-15 main engines, and eight (plus eight redundant) MRE-1.0 Reaction Control System (RCS)/Attitude Control System (ACS) thruster modules. The ATK 80274 standard model tank is flight-proven, but *Lynx* will utilize a modified version to extend the height to allow for the 489-kg load of propellant. The propulsion system is sized to meet the delta-V required to reach the SE-L2 orbit and perform an initial de-spin (also called de-tumble, the negation of unwanted motion after separation from the launch vehicle), with sufficient residual propellant to perform station-keeping and momentum unloading maneuvers for a minimum of 20 years on-orbit.

Table 6.14. Redundant systems have been developed for every credible single point failure on *Lynx*.

Subsystem	Provisions for Fault Tolerance
Mechanisms	<ul style="list-style-type: none"> • Forward Door Assembly (FDA): Dual-redundant motors • Aft Door Assembly (ADA): Dual-redundant motors • Grating Arrays: Dual-redundant motors • Horizontal translation table mechanisms: Redundant horizontal drive motors in series • Drive screw itself considered non-credible failure • Vertical translation table mechanisms: Dual-redundant vertically stacked actuators • Instrument fine focusing motor: Dual-redundant motors
CD&H	<ul style="list-style-type: none"> • Flight Computer: Dual-redundant Spacecraft Flight Computers + Redundant Safe Mode Backup Controllers • Solid-state Recorder: Internally redundant with redundant power, control, and data I/O connections Redundancy provided by blocks of independently addressable memory • Data Acquisition Units: Dual-redundant for spacecraft + aft DAU • Main Propulsion System Controller: Dual-redundant • Reaction Control System Controller: Dual-redundant • Reaction Wheel Controller: Dual-redundant • LMA Heater Controller: Internally redundant • SC/OB/ISIM Heater Controller: Internally redundant • Avionics/Propulsion Heater Controller: Internally redundant • Translation Table Mechanisms Controller: Dual-redundant • Solar Panel Array Drive: Dual-redundant • Remote Command and Telemetry Units: Internally redundant
Communication	<ul style="list-style-type: none"> • X-Band Transponder: Dual-redundant • Ka-Band Transceiver: Dual-redundant • Ka-Band Diplexer: Dual-redundant • X-Band traveling-wave tube amplifier: Dual-redundant • X-Band traveling-wave tube: Dual-redundant • Ka-Band traveling-wave tube: Dual-redundant • Ka-Band traveling-wave tube amplifier: Dual-redundant • Ka-Band PAA: With 4 antennas, a loss of one reduces available FOV. Operational maneuvers may be required to establish Earth link with remaining antennas • X-Band antennas: Passive components, failures are not expected
Power	<ul style="list-style-type: none"> • Solar Array Drive Actuators: Dual-redundant actuators • Power distribution: Separate distribution to spacecraft and science instruments • Batteries: One additional battery added for fault-tolerance
Propulsion	<ul style="list-style-type: none"> • Main Engines: Dual-redundant set of 2 thrusters • Thrusters: Dual-redundant set of 8 thrusters; allows momentum unloading after worst-case 3 failures
GN&C	<ul style="list-style-type: none"> • Control Actuators: Six-wheel reaction wheel pyramid allows for single wheel failure; Any 3 wheels can control vehicle, with reduced momentum envelope and increased slew times. • Coarse Sun Sensors: One additional sensor for fault tolerance • Ultra-fine Sun Sensor: Dual-redundant • Inertial Measurement Unit: Any 2 of 6 gyro channels allow for 3-axis rate measurement • Aspect Star Camera: Redundant Focal Planes and Electronics.
Thermal	<ul style="list-style-type: none"> • Foil resistance heaters and heater controllers are internally redundant. Redundant temperature sensors provided for each heater zone. Fault detection and switching functions performed within the heater controllers or by command • Heat pipe radiators are inherently fault tolerant. Transport and header heat pipes are shielded. Heat rejection hardware failures are non-credible

Mission analyses used to determine delta-V are based on the *JWST* and the *IXO*, while estimates of de-spin and momentum unloading propellant mass are provided by analysis of the *Lynx* insertion scenario. Figure 6.28 shows the *Lynx* mission profile with all maneuvers and delta-V budget.

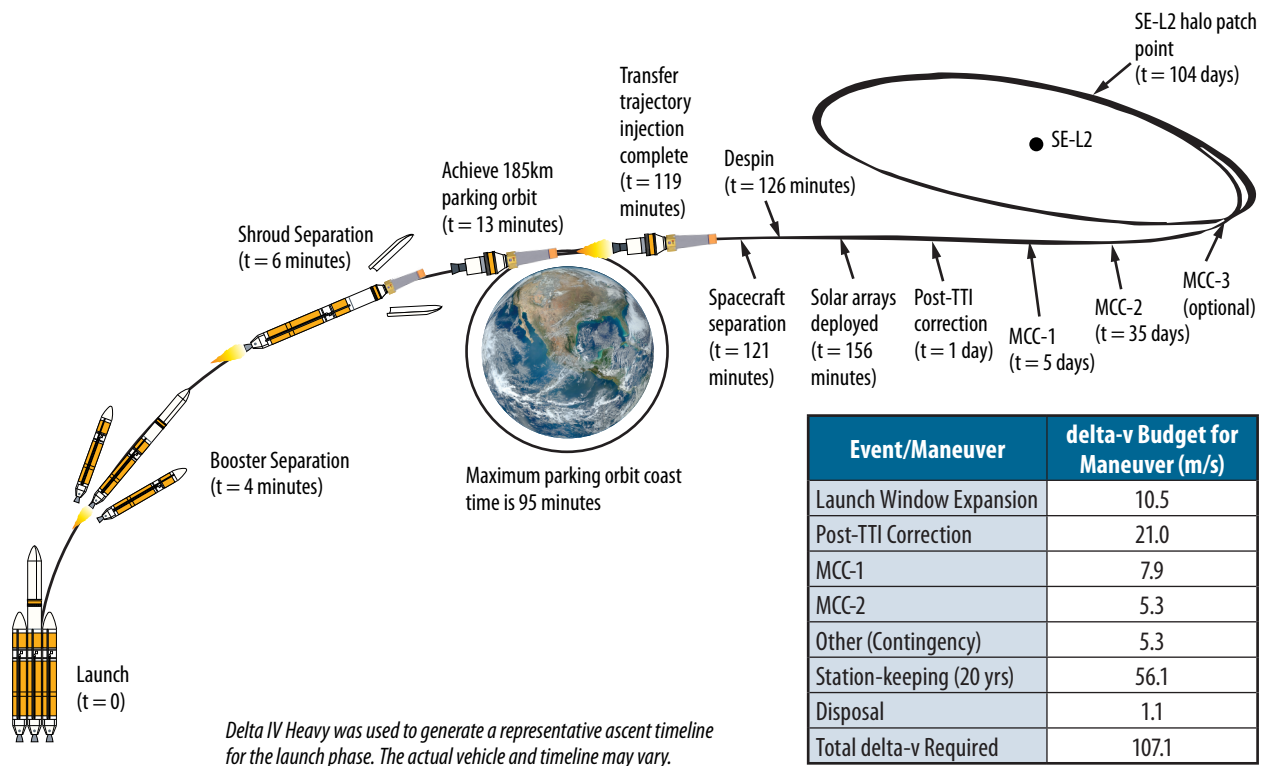


Figure 6.28. Launch to orbit timeline and delta-v budget.

6.4.2 Guidance, Navigation, and Control

The GN&C system maintains knowledge of the spacecraft orientation, controls the maneuvers required to orient desired celestial targets within the telescope FOV, and holds each target attitude for the commanded duration. Table 6.15 highlights key parameters of this system. The *Lynx* system achieves the required 10-arcsecond absolute pointing accuracy and stability of ± 0.17 arcsecond per second per axis after target acquisition and allows the Observatory to carry out a 90° slew maneuver in ~ 50 minutes. The minimum continuous observation time-on-target is 105 seconds, with longer observation times possible with appropriate momentum management. In addition, the GN&C system provides sufficient data for post-facto calculation of an absolute location on the sky to within a 1-arcsecond RMS radius and to reconstruct X-ray images within a 0.2-arcsecond RMS diameter.

Table 6.15. The GN&C subsystem meets derived science and mission requirements with low risk design solutions.

GN&C Subsystem Key Parameters	Value
Observations	1–20 targets per day, 1,000–100,000 s per observation
Orbit determination accuracy	30 km
Pointing accuracy	10 arcsec (3 σ)
Onboard knowledge	4 arcsec
Ground aspect knowledge	1 arcsec absolute to sky
Stability	± 0.17 arcsec per sec per axis
Slew performance	90° degree slew in 50 min

The *Lynx* GN&C system architecture is based on *Chandra*'s PCAD design heritage. The *Lynx* design includes an SOA Ball Aerospace High-Accuracy Star Tracker (HAST) camera capable of simultaneously tracking 8 to 10 object images with 1- to 4-second readouts, three 3-axis strapdown Honeywell Miniature Inertial Measurement Units (MIMUs), two Adcole Coarse Sun Sensors, two Adcole Ultra-Fine Sun Sensors, and six Rockwell Collins TELDIX® RDR 68-3 reaction wheels sized to counteract environmental disturbance torques. To hold the target attitude, the star camera acquires and tracks known guide stars in the target vicinity, the MIMUs monitor rotational rates, and reaction wheels are commanded to spin as needed to compensate for disturbance torques (due primarily to solar wind and radiation pressure). The MIMUs and reaction wheels are used to maneuver to science targets.

Unloading of reaction wheel momentum due to environmental disturbance torques (primarily due to solar pressure) is assumed to occur once the reaction wheels reach a total momentum capacity of ~50%. The determination of disturbance torques is based on worst-case geometric offset of Observatory center of mass and center of pressure for a conservative estimate of propellant needed (Figure 6.29). This offset will be optimized (i.e., minimized) during detail design to grant an opportunity for higher propellant margin.

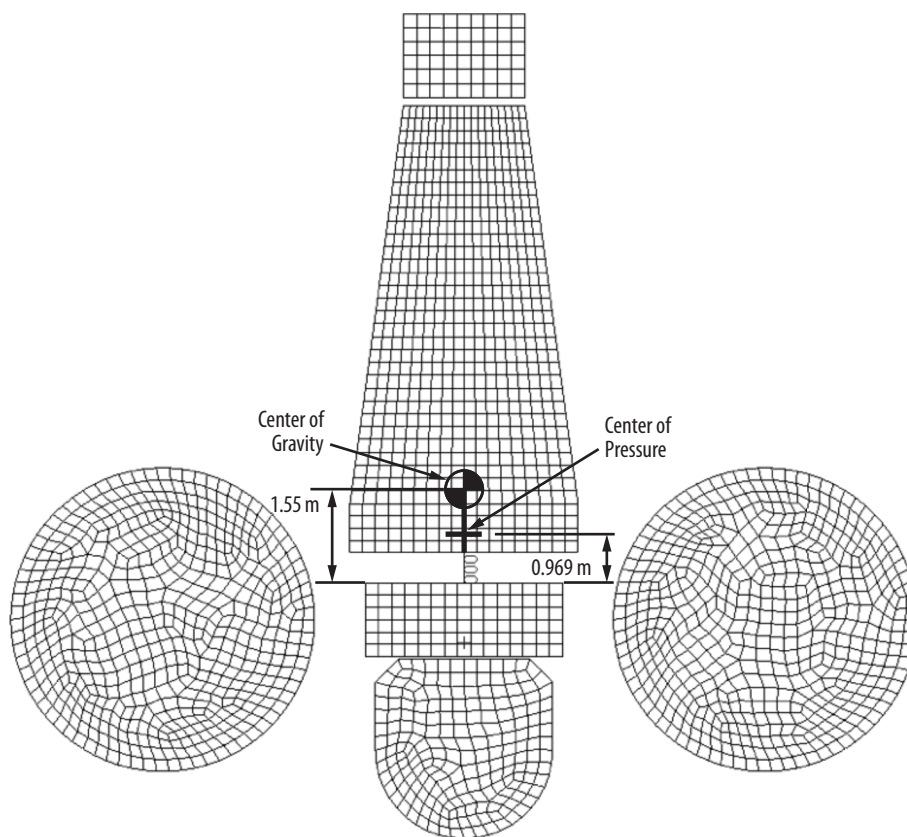


Figure 6.29. The *Lynx* center of gravity and center of solar pressure were included in the GN&C analysis and are sufficient. The design will be further optimized to improve propellant efficiency during preliminary design.

The *Lynx* SE-L2 orbit is free from Earth and Moon shadowing, allowing for uninterrupted observation of any target. However, no *Lynx* science instrument can tolerate direct solar radiation, so viewing is restricted to angles larger than 45° from the direction toward the Sun (Figure 6.30). This restriction makes about 15% of the sky inaccessible at any given moment, but no part of the sky remains inaccessible for more than three months of each year. In addition, the spacecraft and instrument designs take advantage of the hot and cold sides of the Observatory to locate radiators, fuel lines, etc., which imposes a constraint on the Observatory roll angle (rotation about bore-sight) of approximately $\pm 15^\circ$ to prevent impingement of direct sunlight on these surfaces.

The post-facto aspect solution makes use of the guide star positions, the fiducial light positions, and the integrated MIMU rate data to compute the solution for the pointing direction, roll, and gyroscope biases. It then interpolates the solution to the precise arrival time of each registered X-ray photon event, allowing each photon to be registered to its point of origin on the sky.

Ranging and Doppler velocity data are sufficient for station-keeping a satellite at a linear Lagrange point, such as the SE-L2 in the case of *Lynx* [583]. Deep Space Network (DSN) ranging and Doppler measurement data will be obtained during the three one-hour daily communication passes. Detailed simulations performed for the *JWST* mission showed that two 30-minute (alternately, two 3-hour) passes per day will measure the velocity to 6.5 (5.9) mm/s versus a requirement of 2 cm/s accuracy to maintain a halo-type orbit [584]. The simulation assumes that both northern and southern hemisphere DSN stations are used, and that the solar radiation pressure force can be modeled to 5%. Station-keeping maneuvers will be done approximately every three weeks. Approximately 2.5 m/s per year is the expected correction. Unloading angular momentum is not done with a perfect torque couples by thrusters. An unloading efficiency of 87% is expected, and thus 13% of the force produces orbital perturbation. In principle, ideal momentum unloading could contribute to the station-keeping. However, random orientations relative to the orbit will be assumed. Thus, for the 49 momentum dumps expected per year, a random walk delta-V of 1.6 cm/s per year is imparted, a small impact to the total 2.5 m/s adjustment.

The *Lynx* propellant budget is sized for the 2.5 m/s per year for a 20-year mission. A future study will determine if significant propellant can be saved via improved orbit determination. Candidates for the improved determination are use of the DSN delta-Doppler one-way ranging, or incorporating onboard cameras dedicated to tracking solar system objects including the Earth, Moon, and asteroids.

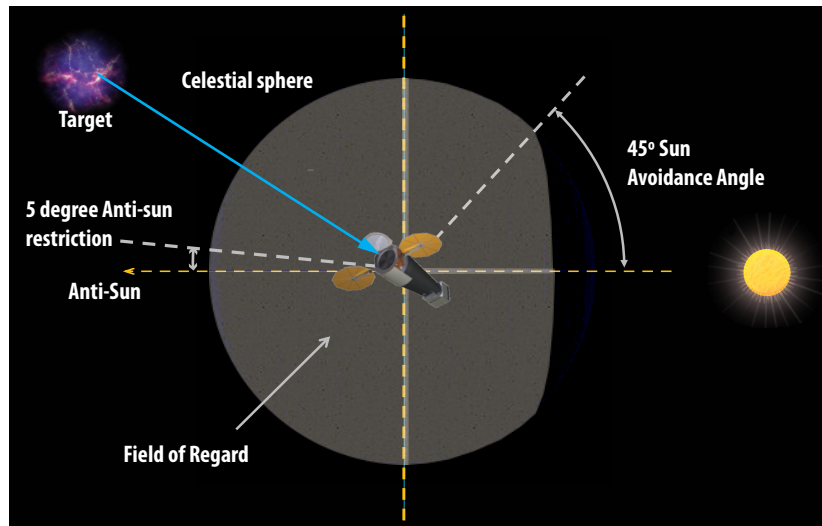


Figure 6.30. *Lynx* Field of Regard. *Lynx* can view the entirety of the celestial sphere less the 45° Sun avoidance cone imposed by the sunshield that is in place to protect the sensors from solar impingement.

6.4.3 Power

As summarized in Table 6.16, the electrical power system is designed using all high-heritage components to generate, store, manage, and distribute required power to the Observatory throughout all phases of operation via a combination of deployable solar panels and onboard energy storage. Energy storage is supplied via five 28-V batteries, with one additional battery to ensure single-fault tolerance. The batteries are sized to provide launch power (743 W) for 156 minutes from launch to the completion of initial checkout and solar array deployment. Initial thermal analyses suggest that the LMA, OBA, HDXI, and XGS can be powered down during the launch phase. Survival heaters following the launch phase but prior to solar array deployment will be powered by onboard batteries until the solar arrays are deployed. A more detailed analysis will be conducted during Phase A that will contain the possible inclusion of additional batteries or a small body-mounted solar array panel, to provide additional survival power in the event of an anomaly before full solar array deployment.

Two UltraFlex™ deployable solar arrays with a total area of 51 m² are utilized to provide sufficient total power and are articulated to allow for full Sun illumination at any boresight pitch angle with respect to the Sun. The arrays are sized to meet the 7.4-kW peak operational power requirement (XGA inserted and LXM at the primary focus) with ~40% margin. The power system design accounts for expected degradation over a 20-year mission lifetime.

Table 6.16. The *Lynx* power system is designed to provide power throughout all phases of operation. All power values are in Watts.

Source	Launch (0 – 156 min)	Survival Mode (5 min) Battery Power Only	Normal Mode (LXM, XGS on, Downlink)
Avionics	551	546	1,812
GN&C	0	283	283
Propulsion	0	510	510
Mechanisms	0	0	210
Thermal	178	154	178
Total SCE Subsystems	729	1,493	2,993
LXM	14	14	2,205
HDXI	0	7	248
XGS	0	7	190
LMA Heater	0	593	1,346
OBA Heaters	0	438	438
Total Telescope	14	1,059	4,427
Total Observatory	743	2,552	7,420

6.4.4 Thermal

Thermal control and regulation of the LMA and OBA are critical to meeting Observatory performance requirements. The spacecraft thermal subsystem is designed to maintain the spacecraft and OBA at an average temperature of 283 K and the LMA at a warmer temperature than the spacecraft (293 K \pm 0.25 K) (Table 6.17). The temperature of the mirrors will be controlled throughout assembly and alignment as well as in flight to minimize contamination. The Observatory-level thermal system design includes the use of a high-TRL thermal control approach with the use of conventional MLI, a siliconized Kapton sunshade, OSRs where appropriate, and redundant heaters and radiators.

Table 6.17. The Thermal subsystem uses active and passive design to maintain the required temperature envelope for all allowable sun angles, to meet science requirements, and to control possible contamination of the mirrors over the mission lifetime.

Thermal Subsystem Key Parameters	Value
LMA temperature	293 K \pm 0.25K
SCE maximum average temperature	283 K
OBA maximum average temperature	
ISIM maximum average temperature	
Translation table maximum average temperature	
OBA average zone Temperature for full range of allowable sun angles	283 \pm 2 K

The current DRM conceptual design uses advanced high-performance radiators to reduce mass. This technology has a clear path to TRL advancement; however, current flight-heritage radiator technology can meet the *Lynx* thermal performance requirements with a nominal mass increase.

A trade study of the OBA thermal control comparing passive and active control options concluded that a purely passive system of heat pipes and MLI could not maintain the required limit on temperature gradients at all pitch angles due to variation in heat pipe inputs on the bench. See Appendix B.6.6 for more details.

Another study was conducted to determine an alternative to the use of *Chandra*-heritage silverized Teflon MLI on the optical bench. This study was prompted by the more-rapid-than-predicted degradation of the *Chandra* MLI due to Ultraviolet (UV) exposure. Analysis of the *JWST*-heritage siliconized Kapton revealed poor thermal control in using this material as simply the outer MLI layer for the *Lynx* geometry. OSRs were also studied, and although the OSR solution provided the desired thermal performance, the support structure required to mount them to the optical bench was determined to have an unacceptably large mass impact. Following this study, an additional option was analyzed that included the use of a lightweight, flat, simple deployable sunshade of siliconized Kapton. Through a modest study of pitch and roll combinations, the preliminary analysis showed that this design produced similar performance to the OSR solution without significant additional mass (see Figure 6.31 and the *Lynx DRM Supplemental Design Package* for more details).

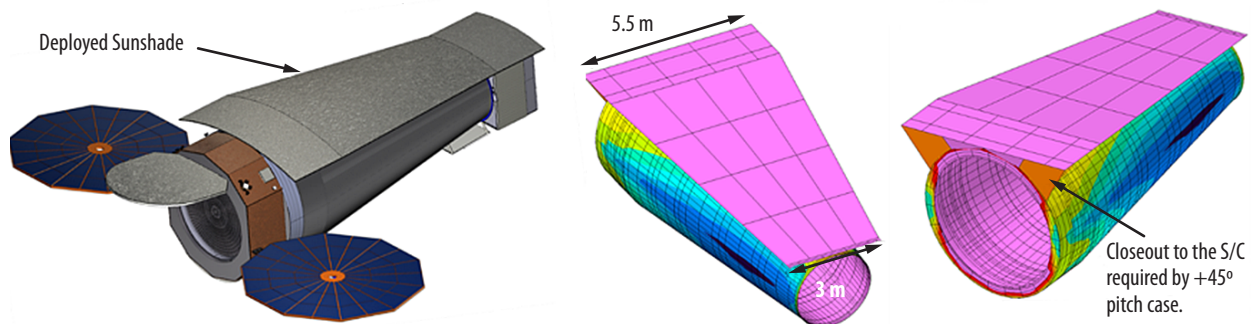


Figure 6.31. Schematic depiction of single-deployment Si-Kapton sunshade mounted on sun-facing side of OBA.

6.4.5 Avionics and Flight Software

The avionics equipment in the *Lynx* spacecraft is designed to perform the functions of GN&C, power switching, data storage, command management, uplink and downlink communications, and thermal control. These systems will draw heavily from heritage (e.g., *Mars Orbiter*, *Chandra*, *Spitzer*, and *JWST* designs). *Lynx* requirements allow the use of technologies that are readily available. Table 6.18 summarizes key parameters for this system.

Table 6.18. The Avionics and Flight Software (S/W) subsystem meets requirements with heritage design solutions.

Avionics and Flight Software Subsystem Key Parameters	Value
Total science data collection rate	240 Gbit/day (2.78 Mbps)
Total science memory storage	48 hours (~500 Gbit)
Total SCE memory storage	1 Tbit (1.4 Gbps capacity)
Flight software lines of code	100,000
Flight software reuse (%)	68%

A temperature-controlled, ultra-stable oscillator (1 part in 10^9 per day) synchronizes all spacecraft control and data and command functions. A heritage flight computer system will be baselined, similar to that used for the Jet Propulsion Laboratory's (JPL's) *Mars Orbiter*, which is designed for long life in the SE-L2 environment. Based on analysis of the science instrument designs, the maximum science data rate is 240 Gbits per day. The spacecraft design assumes up to 48 hours of science data storage, with a total data storage capacity of 1 TB and spacecraft capacity of 1.4 Gbps. The *Lynx* flight software includes software for the spacecraft and science instruments. The spacecraft software will reside on the redundant spacecraft flight computers. Remote command and telemetry units interface between the spacecraft computer and the functional subsystems, including the focal plane instruments.

Flight software will control communications and data handling, attitude control, recorder management for housekeeping and science data, spacecraft health and safety monitoring, PCAD, electrical power, thermal control, and will be responsible for recognizing fault conditions and managing safe modes. Safe mode control will include a separate set of control processing electronics that operate with different software. The science instruments will include software that will reside on the electronics units developed by each science instrument provider. The flight software will incorporate new development only for mission-specific components and as needed for obsolescence. Examples of reuse of software algorithms include power management, C&DH, health and safety, executive services, and memory loads and dumps. Examples of *Lynx*-specific software components include instrument support, mission-specific operations concept support, power switching services, and mechanism control. Based on system design and Class A requirements, $\sim 10^5$ software lines of code are estimated for the *Lynx* flight software system, at $\sim 68\%$ reuse. All *Lynx* flight software development will comply with NASA Software Engineering Requirements per NASA Procedural Requirement (NPR) 7150.2, and NASA software safety standard 8719.13 as Class A Safety Critical software.

An internally redundant Safe Mode Electronics Unit (SMEU) (shown in Figure 6.32) is included to enable the Observatory hold position or to slew autonomously to a safe Sun angle in the event of out-of-range onboard parameters. See §6.7.2 for discussion on Safe Mode. Ka-band is not currently part of the SMEU; this will be part of a future trade during preliminary design.

The system design includes three heater controllers to maintain the design temperatures and thermal gradient requirements for key science and spacecraft systems. These controllers are designed with multiple zones, each with 100% redundant heaters and sensors. Figure 6.33 contains a schematic of the temperature control concept.

The *Lynx* avionics are susceptible to galactic cosmic rays and solar particle events at SE-L2. To mitigate resulting negative effects, the avionics design includes components that were specifically selected for a long life in a deep space environment. A more rigorous design, appropriate shielding, and careful parts selection during Phase A is needed (§6.6.2.1).

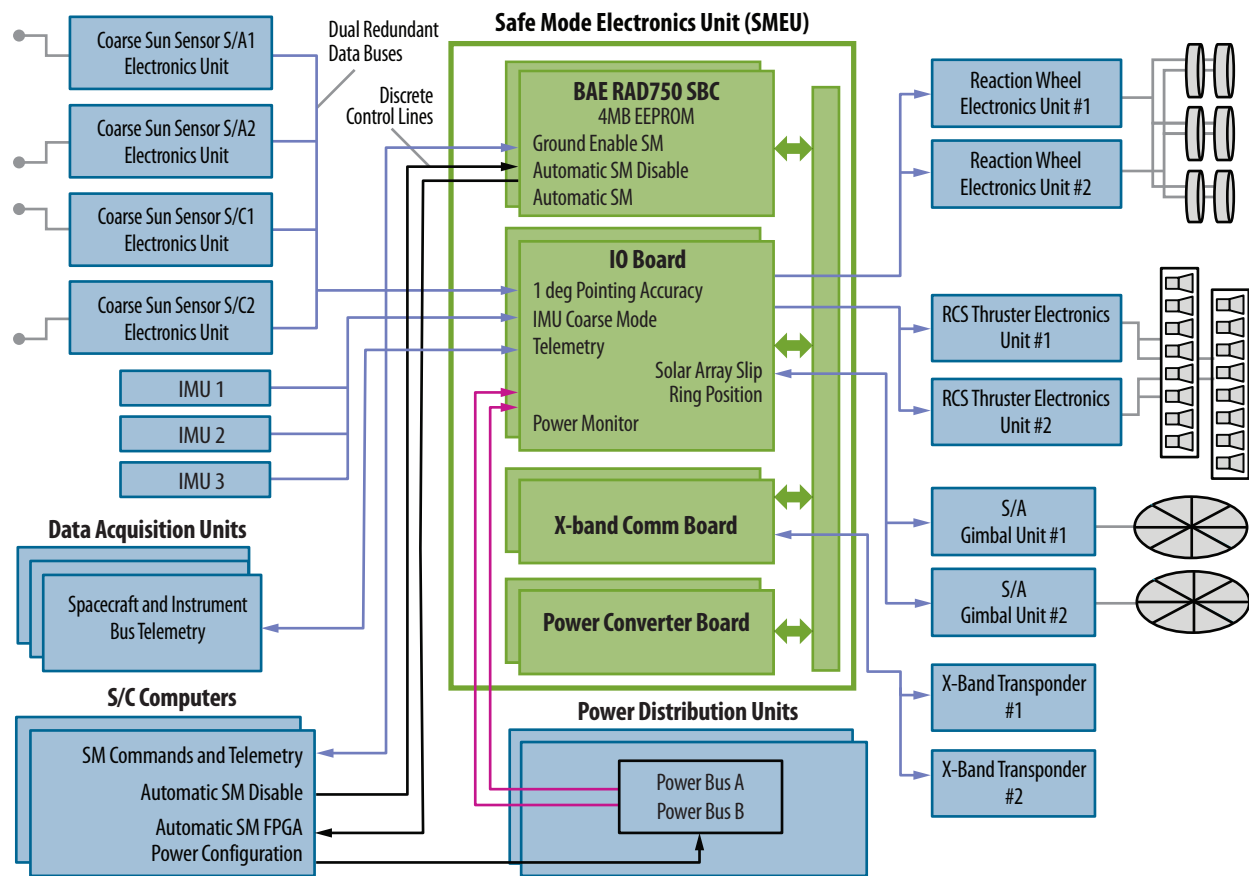


Figure 6.32. The internally redundant SMEU will provides autonomous safing capability.

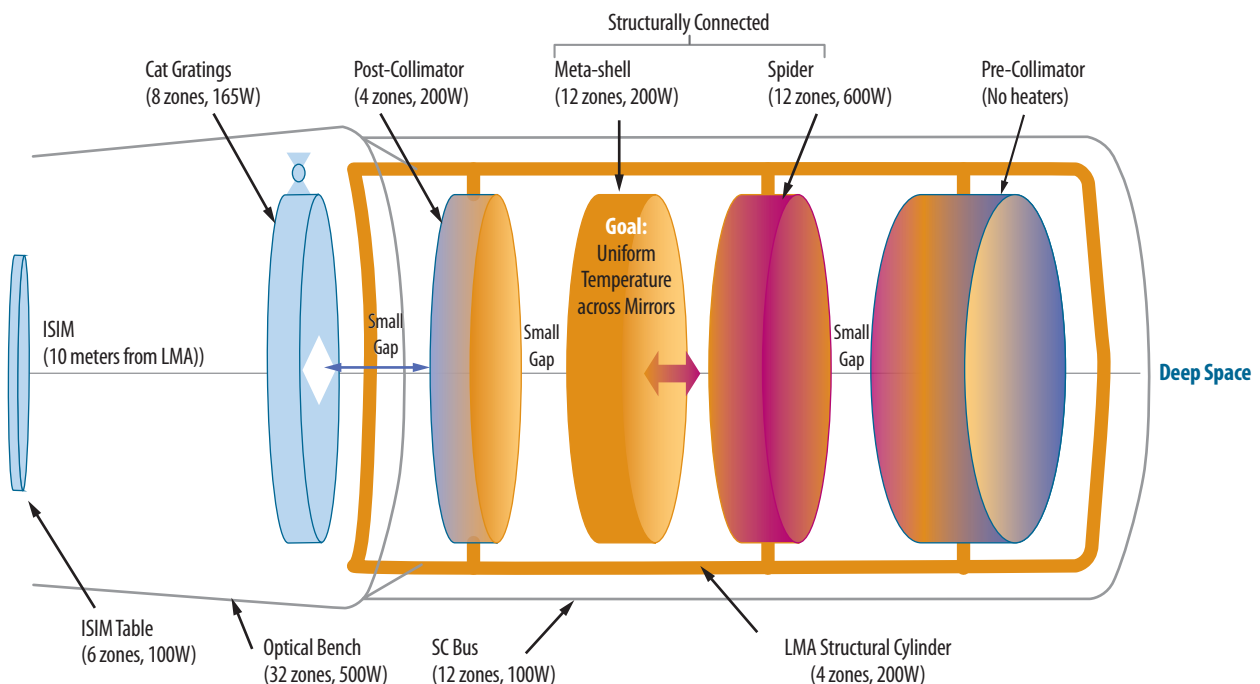


Figure 6.33. Thermal control concept. Multiple thermal zones designed to maintain temperatures and gradients for the mirror, instruments, optical bench and spacecraft. Conservative analysis used to determine number of and size of heater controllers. Power numbers reflect controller capability, not actual heater power required, which is smaller. The colors indicate the relative temperature gradient between elements.

6.4.6 Command and Data Handling

For communications with the ground, *Lynx* will utilize NASA's existing DSN system to provide Telemetry, Tracking, and Command (TT&C), ensuring high-reliability and high-data rate communications for downloading its science and spacecraft health data and uplinking commands. Table 6.19 summarizes the telemetry data rates and volume for the science instruments and spacecraft.

For the DRM, a flight-heritage communication system has been baselined that is similar to that used on the Mars Reconnaissance Orbiter, which supports data volumes up to 270 Gbits/day. It is also assumed that the *Lynx* communication system will utilize the high-heritage Ka-band for data downlink (per Space Communications and Navigation (SCAN) guidance) and X-band for low-rate uplink and backup telemetry. The current *Lynx* concept assumes high-flight heritage, phased-array antennas, avoiding the use of gimbaled antennas and their potential vibrations, providing more stability for the telescope during science operations.

With the guidance from NASA SCAN experts, the *Lynx* engineering team conducted a trade study on future DSN communications and capabilities. Technology for long-distance, space-based laser communications was demonstrated in NASA's 2013 Lunar Laser Communication Demonstration (LLCD), the space terminal that flew on the Lunar Atmosphere and Dust Environment Explorer (LADEE) spacecraft. The LLCD configuration demonstrated an error-free data transmission at a rate of 622 Mbps from lunar orbit. From the science perspective, there are benefits to considering higher data rates. First, the same volume of data could be downlinked in a much shorter time. Feasible data rates could be 5× or more higher than the current baseline. Alternately, larger volumes of data could be downlinked in the same amount of time. A trade study will be carried out during the *Lynx* detailed design phase to assess the state of the technology and applicability to *Lynx*.

Table 6.19. *Lynx* data volumes are modest and easily handled in the 2030s timeframe.

Source	Expected Volume	Data Rate	Comments
Science Data	240 Gbits/day	2.78 Mbps (maximum average)	Based on science objectives and known X-ray fluxes
LXM	< 200 Gbits/day*	200 kbps to 8 Mbps	Minimum rate is background. Maximum rate observations are scheduled for no more than 6 hours and interleaved with low-rate observations
HDXI	< 200 Gbits/day*	600 kbps to 6 Mbps	Minimum rate is background. Maximum rate observations are scheduled for no more than 6 hours and interleaved with low rate observations
Aspect	0.9 Gbits/day	10 kbps	8 stars per second, 4 gyro rates every 31 ms
Grating readout	<160 Gbits/day	600 kbps to 6 Mbps	Minimum rate is background. Maximum rate observations are scheduled for no more than 6 hours and interleaved with low rate observations. Used simultaneously with LXM or HDXI
Housekeeping	17 Gbits/day	200 kbps	Estimate. Flexible depending on mode.
Downlink Frequency	1–3 times/day; 1 hour each	22.2 Mbps	<i>Chandra</i> -like operations
Uplink Frequency	1–3 times/day; 1 hour each	< 1 Mbps	<i>Chandra</i> -like operations

*Only one of the LXM or HDXI takes celestial data at any time.

6.4.7 Mechanisms

Lynx mechanisms for the DRM were chosen to meet all science and mission requirements and to have low development risk. Requirements that the mechanisms must meet include operation in the intended environments, cycles sufficient to complete the 5-year baseline mission (and extendable to a 20-year mission) and to carry out ground processing and verification, reliability, repeatability, accuracy, torque, and motion range. Additionally, all *Lynx* mechanisms have been designed to be either internally redundant or grouped with redundant mechanisms. Most *Lynx* mechanisms have flight heritage, and others are high-TRL with very low development risk. In most cases, a representative off-the-shelf mechanism part number has been identified. As *Lynx* moves into preliminary design, mechanisms will be optimized to increase performance for reduce cost. A summary of mechanisms is provided in Table 6.20.

Table 6.20. *Lynx* mechanisms meet requirements within the current SOA.

System Element	Expected Performance	Mechanism Type/Example Part #	Mechanism TRL
Solar Panel Deployment	Single deployment	Deploys on boom using spring mechanism. Contains deployment and launch locks. Provided by supplier	9
Launch locks for XGA, ISIM, siliconized Kapton thermal sunshade	Single deployment	NEA Model 9106B	9
Forward contamination door/sunshade deployment	Designed for 20 cycles open/close. Single deployment on-orbit	Moog Type 7 Harmonic Drive Rotary Actuators	9
Aft contamination door deployment	Designed for 20 cycles open/close. Single deployment on-orbit	Moog Type 7 Harmonic Drive Rotary Actuators	9
ISIM horizontal translation	750-mm horizontal translation 5- μ m accuracy, 3- μ m stability	PI LS-180 High-Load Stage (or similar)	6+
ISIM Focus	40-mm vertical translation	Moog Linear Actuator (or similar)	6+
HDXI and LXM filter adjustment	Open/Closed positions, lateral repeatability of inserted filter is estimated to be $\pm 6 \mu$ m	Segment Brushless DC Motors	9
XGA deployment	Designed for 10,000 cycles, open/closed positions 200- μ m stability along optical axis and 100- μ m repeatability	Moog Type 7 Harmonic Rotary Actuators	9
XGD Focus	30-mm range with 1.25- μ m step fine focus adjustment	Standa 8MT173V-30 (or similar)	6+

6.5 Launch Vehicle

Lynx is compatible with existing heavy-class launch vehicles, reducing the risk of meeting the constraints (vehicles capabilities in terms of mass, environments, center of gravity location, and dynamic envelope) of future (2030s) similar vehicles.

The *Lynx* Observatory will launch on a heavy-class launch vehicle of identical capability to those currently available (e.g., Delta IV Heavy). The ability to launch on this class vehicle allows launch flexibility, resulting in reduced risk and optimized cost and schedule. The outer diameter of the *Lynx* spacecraft is ~4.5 m in diameter, sufficient to fit into a standard 5-m-class fairing. The overall volume of the *Lynx* Observatory easily fits inside the payload dynamic envelope when the solar panels and sunshade door are retracted. No additional deployments are needed. Similarly, the maximum payload mass requirement is met with adequate margin (Figure 6.34).

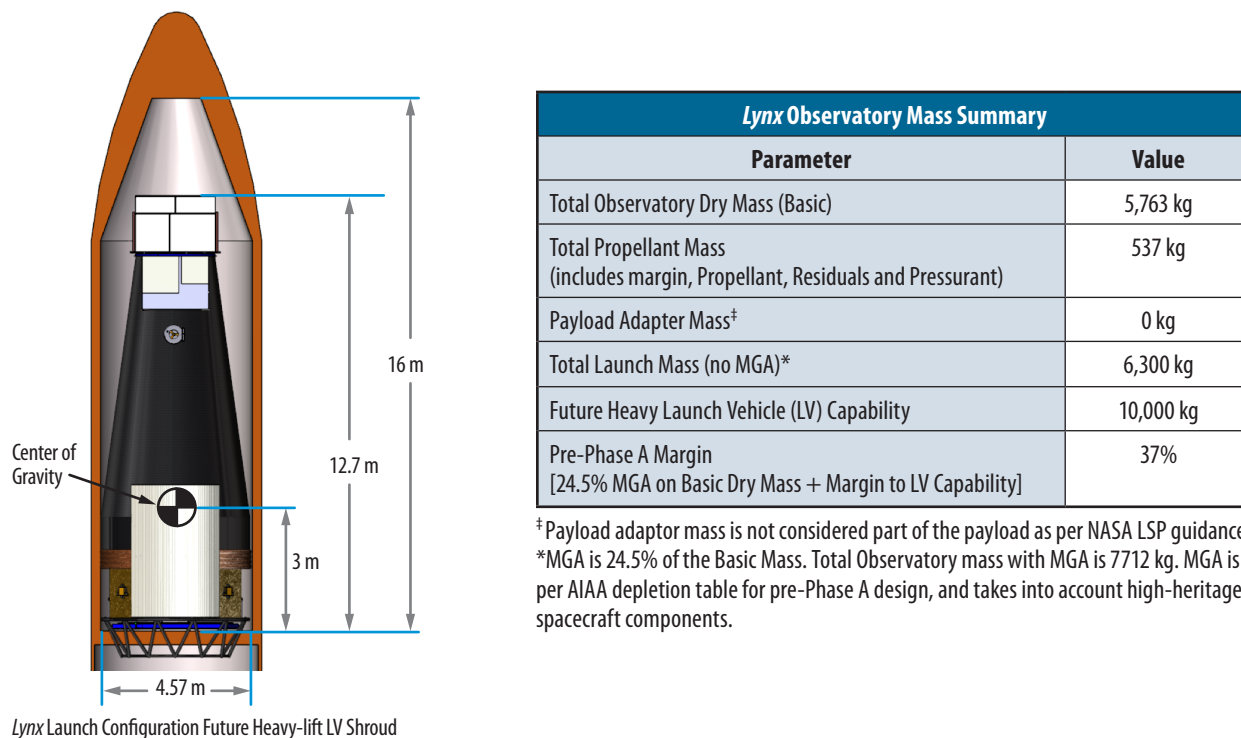


Figure 6.34. *Lynx* Observatory Mass Summary. *Lynx* fits within the payload envelope and can launch on a future Heavy-class vehicle to SE-L2 with sufficient mass growth allowance and launch vehicle margin.

Due to the uncertainty regarding the specific launch vehicle with the payload envelope and lift capability to launch *Lynx* to SE-L2 in the 2030s, NASA's LSP has provided payload envelope, lift capability, and environments for generic vehicle class types (intermediate and heavy class), as well as for the SLS vehicles. Per current LSP guidance, the maximum payload mass to SE-L2 for the intermediate class launch vehicles in the 2030s is 6,500 kg, and for the heavy class launch vehicles is 10,000 kg. The *Lynx* DRM Observatory mass is 7,712 kg, which includes a 24.5% MGA per AIAA recommendations. Based on this information, a heavy-class vehicle meets the requirement to launch *Lynx* to SE-L2 with

an additional launch vehicle margin of 23%, which is sufficient for this stage of mission design and level of high-heritage hardware and systems.

Though the *Lynx* DRM assumes a baseline launch on a heavy class vehicle, a broad trade space regarding the availability and applicability of larger class vehicles such as SLS was explored. The goal of this study was to reduce the risk of launch vehicle availability in the 2030s even further and to provide options that could potentially minimize project cost and optimize schedule (see Appendix B.1.3).

One option worth mentioning is the possibility of launching *Lynx* on the SLS as a single payload with a co-manifested human crew. In this scenario, *Lynx* would be the only payload (other than crew) carried by the SLS, and would maintain its national importance of a Class A flagship mission. This scenario is akin to the space shuttle launching *Hubble*, the *Compton Gamma-Ray Observatory*, and *Chandra* flagship missions.

The current *Lynx* configuration easily meets the 10,000-kg and 7.2-m-diameter co-manifested payload envelope, but not the 8.4-m length limitation. A study was conducted via an industry Cooperative Agreement Notice (CAN) partnership to provide an initial design of an Extendable Optical Bench (EOB) that would allow the *Lynx* launch configuration to fit inside the SLS co-manifested payload envelope. The preliminary design includes three telescoping segments deployed on-orbit via lead screws. The overall concept is shown in Figure 6.35. See also supplemental *DRM Supplemental Design Package* for more details on the design and preliminary analysis.

An SLS co-manifested launch limits launch availability and does not allow for direct insertion to SE-L2 orbit, resulting in an increased total delta-V, propellant load, and other subsequent mass impacts. Cable management, thermal protection designs, and structural stability also need careful consideration. However, because this option could potentially result in significant cost savings to the project, it is worth exploring further at a future date.

The EOB option, in a general sense, provides a solution that would allow *Lynx* to fit into a variety of launch vehicles with shorter payload envelopes. However, this option comes at the added risk of increased number of mechanisms for deployment and additional ground testing and analyses to ensure on-orbit telescope performance is not compromised. As such, the solid OBA and standard heavy-lift vehicle for the 2030s as defined by LSP have been baselined for the *Lynx* DRM.

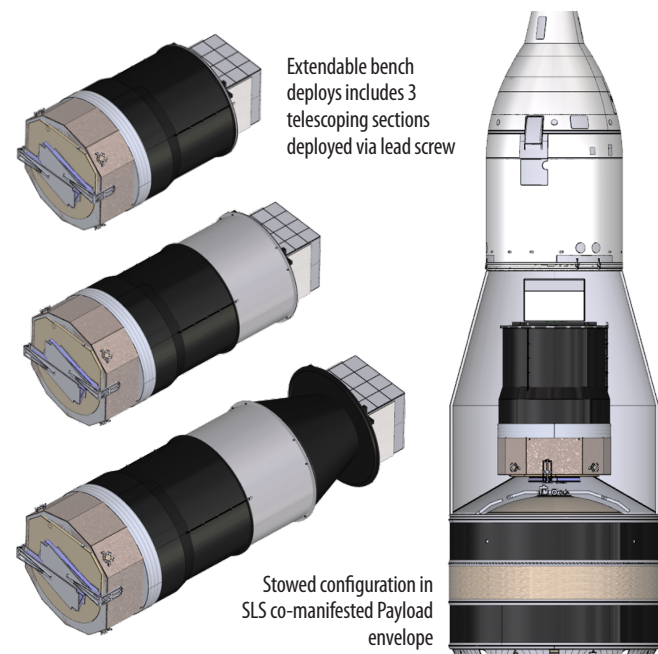


Figure 6.35. EOB design for SLS single-payload co-manifested with a human crew, trade-study option. Preliminary design and analysis shows feasibility, but with increased complexity and risk.

6.6 Systems Engineering and Integration

Lynx will use proven systems engineering principles and processes and apply them using state-of-the-art MBSE tools.

The *Lynx* Observatory will meet its science requirements by developing a robust requirements traceability that emphasizes the full system performance. Using MBSE tools, the *Lynx* team will develop all systems engineering products. MBSE allows for a simulation-driven, end-to-end lifecycle process that supports the development and maintenance of requirements and functional analysis/allocation, system analysis and control, and management. A preliminary model has already been generated by the *Lynx* team working with the University of Alabama in Huntsville (UAH) (Appendix C). Using this model, technical requirements will be developed per the processes outlined in NPR 7123.1, NASA Systems Engineering Processes and Requirements, with implementation details documented in the *Lynx* Systems Engineering Management Plan (SEMP), which will be developed as *Lynx* moves into pre-Phase A.

In pre-Phase A, stakeholder needs, goals, and objectives will be collected; the concepts of operations will be utilized to derive operational requirements; and technical requirements for the *Lynx* system will be derived. These top-level requirements will then be functionally decomposed and allocated through the requirements hierarchy.

The proposed *Lynx* requirements hierarchy, shown in Figure 6.36, takes into account the Work Breakdown Structure (WBS) and Product Breakdown Structure (PBS) to provide clear interfaces and divisions of responsibility between *Lynx* partners and future contractors.

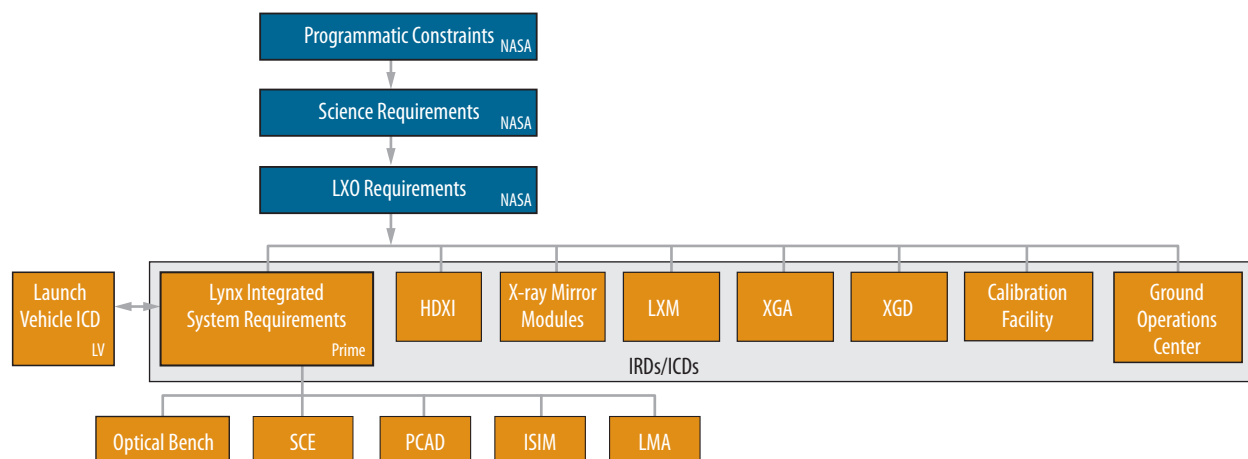


Figure 6.36. Requirements hierarchy tree. Interface Requirement Documents (IRDs) and Interface Control Documents (ICDs) are defined between interfacing elements.

During the study phase, the *Lynx* systems engineering team traced science- and mission-based requirements from the Mission Traceability Matrix to requirement implementation in the conceptual design (FO3) to show that all requirements can be met with margin in at least one feasible concept.

The spacecraft, optical bench, and ISIM element conceptual design shows that requirements can be met with low-risk, high-TRL design solutions. The *Lynx* flight system uses a robust, future-proof system architecture that does not require (but can take advantage of) new technologies to increase reliability and performance margin. This can be implemented on a subsystem level without costly system architecture changes as new capabilities become available. Details of the flight system conceptual design can be found in the *Lynx DRM Supplemental Design Package*.

The systems in the *Lynx* flight design requiring technology development in order to meet requirements are the optics and the instruments, and are detailed in the technology development plans in §7. The *Lynx* ground system concept leverages the existing *Chandra* ground system, using successful flight-proven approaches to meet all ground system requirements, as described in §6.7.4.

The *Lynx* systems-level engineering model and spares philosophy will apply the guidelines in NPR 8705.4 for Risk Class A projects, tailored to meet budgetary constraints. All new technologies such as the science instruments and the LMA will have engineering models or Engineering Development Units (EDUs). During Phase A, a cost-effective and risk-reducing approach will be used to identify the sparing level and specific spare items for each element and subsystem. This could be at the subsystem, box and/or component level, depending on a number of factors such as long-lead procurement times, criticality of the item, risk to the item, and cost and schedule impacts of not having a spare available. After launch, engineering models and unused spares will be configured to simulate on-orbit systems to validate software loads, for example, prior to uploading to *Lynx*. In this way, the investment in spares and engineering models will be leveraged even after launch of the flight system. During this study phase, a percentage was used to cost spares in the parametric cost models (§8.5.2).

The *Lynx* team will perform product Verification and Validation (V&V), ensuring that requirements are met, including those for the flight hardware and software. V&V will be performed at multiple levels of assembly and integration. The approach will be to verify subassemblies to the extent possible prior to integration to a higher-level system and then verify at the system level to ensure that requirements are still met when integrated. This approach will ensure that issues are identified as early as possible and will make locating their root causes easier, thereby saving schedule and cost. This approach will also ensure that possible interface issues are addressed at the integrated system level.

At the *Lynx* Observatory level, the protoflight V&V approach will be used. This is mainly driven by the prohibitive cost impact of a full, observatory-level qualification unit. This is technically acceptable due to the high TRL level of the proposed design solution for the spacecraft, optical bench, and ISIM elements. *Lynx* does not require any new technology in these elements to meet science and mission requirements. The *Lynx* Observatory's lower TRL elements (such as the optics and instruments) will have EDUs that are representative of the flight hardware and will be tested at qualification levels and durations. In addition, these flight units will still be tested at protoflight levels. This rigorous approach will confirm that the final products meet environmental and functional requirements and are able to support science operations.

The V&V methods used for *Lynx* will benefit from the lessons learned from *Chandra*. *Lynx* uses a *Chandra*-like system architecture, which will allow leveraging of the lessons learned from *Chandra*'s verification and Assembly, Integration, and Test (AI&T) to develop a technically rigorous schedule and cost, as well as an efficient verification test flow.

MBSE tools will be used to deliver a technically correct and resource-efficient flow from requirements to verification activities, which will make configuration management, traceability, and verification more integrated as they are performed in the same model. At lower levels of verification, partners and suppliers may use other tools such as relational databases to perform V&V. These can be linked to the *Lynx* Observatory model to ensure an overall integrated V&V picture.

Validation, as separate from verification, will be addressed in two ways by the *Lynx* team. First, by ensuring that requirements fully address end user's needs, goals, objectives, and the intended operational modes and environment; validation can be addressed in verification activities. This is preferable because validation concerns can be addressed prior to flight. Second, during the on-orbit commissioning and calibration phase, the *Lynx* Observatory can be extensively fine-tuned to optimize science return and ensure efficient operations.

6.6.1 System-Level Error Allocations

The *Lynx* design architecture leverages the considerable investment *Chandra* made in detailed error budget development and adapts it. Using lessons learned from *Chandra*, *Lynx* will track error budgets at a higher system level and allocate error to the contributing elements/components across the system. This will provide increased flexibility as the design matures to avoid unnecessary conservatism of any one contributor to the error budget. This, in turn, avoids unnecessary development impacts to cost and schedule while still meeting science requirements at the system level with margin. Reserve has been included to account for any unknown elements that may contribute to the performance.

The *Lynx* team focused on three areas regarding error budget allocations: (1) on-axis image quality, (2) spectroscopic resolving power, and (3) effective area. These TPMs are critical to meeting the *Lynx* science goals. Each error budget provides a first-cut at the error allocations for each element affecting that particular TPM. Reserve usage for each TPM error budget will be tracked and monitored throughout the project.

6.6.1.1 On-Axis Image Quality

The *Lynx* on-axis imaging budget borrows from the *Chandra* budget to identify the main sources of error to imaging performance. This includes the finite optical quality of the LMA, misalignments (static and dynamic) between the X-ray mirrors and the focal plane instruments, and the quality of the aspect solution. The current program links the three main branches of the error budget and includes reserve to realize the 0.5-arcsecond on-axis image quality. This is different from the arrangement used in the legacy program, where the corresponding main sources of image degradation were separately specified (as per MSFC-SPEC-1836).

The current error budget architecture (Figure 6.37) links the main branches of the error budget, allowing for reallocation among these branches to harvest overperformance in one area to ease the allocation on another. This is a key lesson learned from other missions and demonstrates *Lynx*'s conservative approach to design to cost.

The 0.5-arcsecond HPD imaging required for *Lynx* is equivalent to an RMS diameter of 0.416 arcseconds. Figure 6.38 clearly indicates the dominant role LMA imaging quality plays in realizing the *Lynx* objective of 0.5-arcsecond image quality.

Image reconstruction errors (Figure 6.39) and alignment stability errors (Figure 6.40) are derived from detailed budgets from *Chandra* and populated with flight-proven values and analysis of the *Lynx* design. The use of flight-validated performance values in the aspect budget and the reapplication of the alignment tolerance analysis from *Chandra* gives high levels of confidence. Moreover, due to the root-sum-square addition involved in error budgets, small deviations both positive and negative have small influence at the top level. This means that there is little risk to performance from these values and small opportunity, such that the main focus of effort and resources should and will be on the LMA (Figure 6.41).

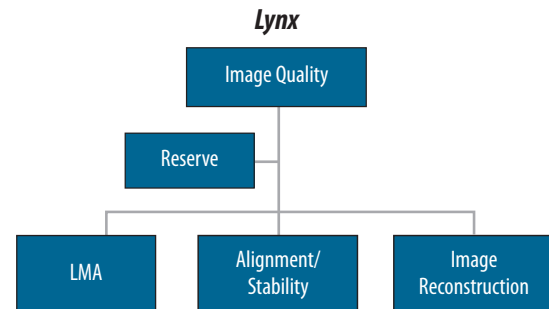


Figure 6.37. High-level error budget architecture for the LMA on-axis imaging. The main elements include the performance of the LMA, the alignment stability between the LMA and the focal plane instruments, and the ability to reconstruct an image. The latter is based on the ground aspect reconstruction of the arrival direction of each photon based on star camera and gyro rate data.

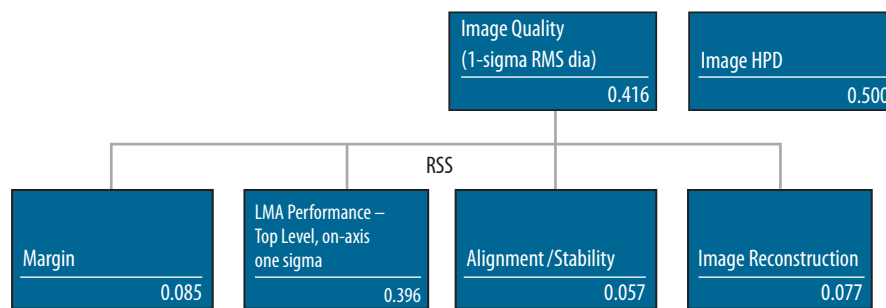


Figure 6.38. High-level error budget architecture for *Lynx* on-axis imaging at 1 keV. The main elements include the performance of the LMA, the alignment stability between the LMA and the focal plane instruments, and the ability to reconstruct an image. The latter is based on the ground aspect reconstruction of the arrival direction of each individual photon, based on star camera and gyro rate data. By linking these three error budgets, we can reallocate error and apply reserve across the three contributors to meet performance requirements with efficient use of cost and schedule resources.

The LMA budget follows lessons learned in the derivation of the *Chandra* imaging budget but also includes specific terms for the Silicon Meta-shell Optics implementation. The left-most branch of the budget contains the scattering terms, which are non-Gaussian and energy-dependent. The geometric branch shown on the right-hand-side is the result of finite tolerances in manufacture, alignment, and environment, which are Gaussian in nature and are energy-independent. The values for the various terms are the result of analysis and simulation using validated predictive tools. Energy-dependent terms are enclosed in the blue-outline boxes.

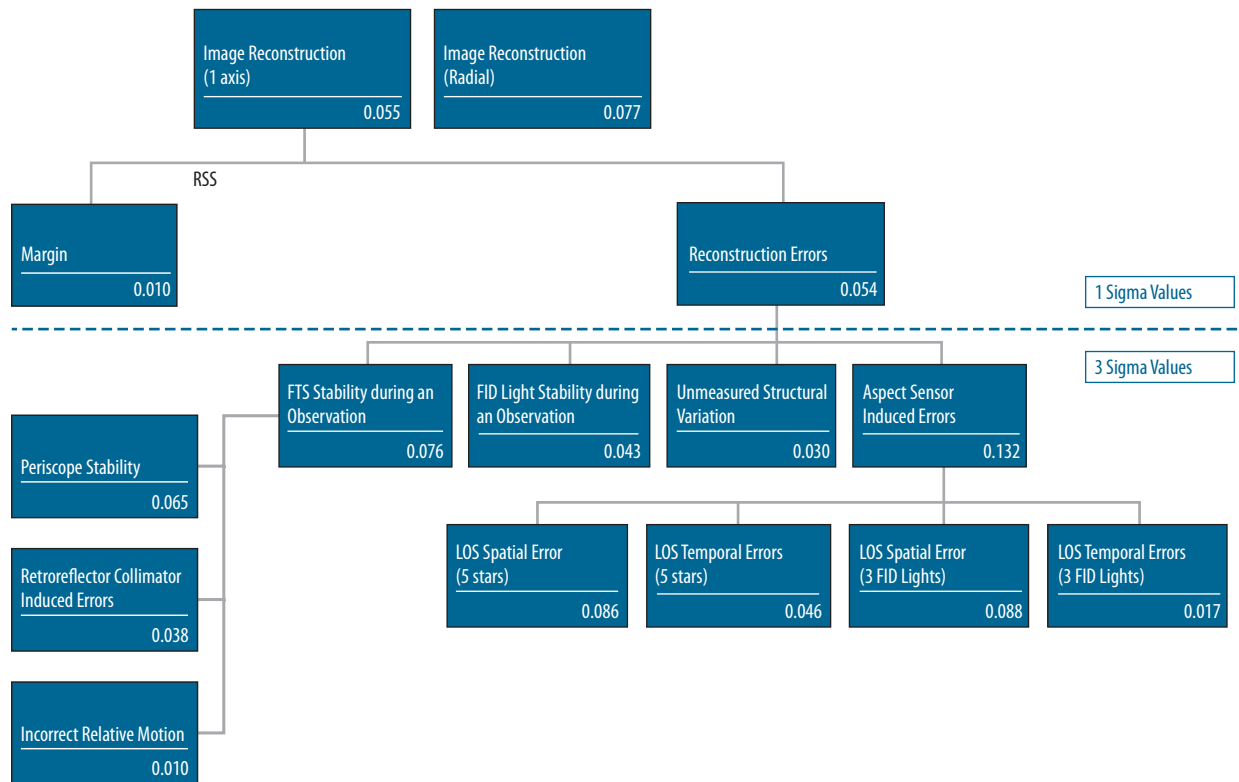


Figure 6.39. Aspect image reconstruction error budget.

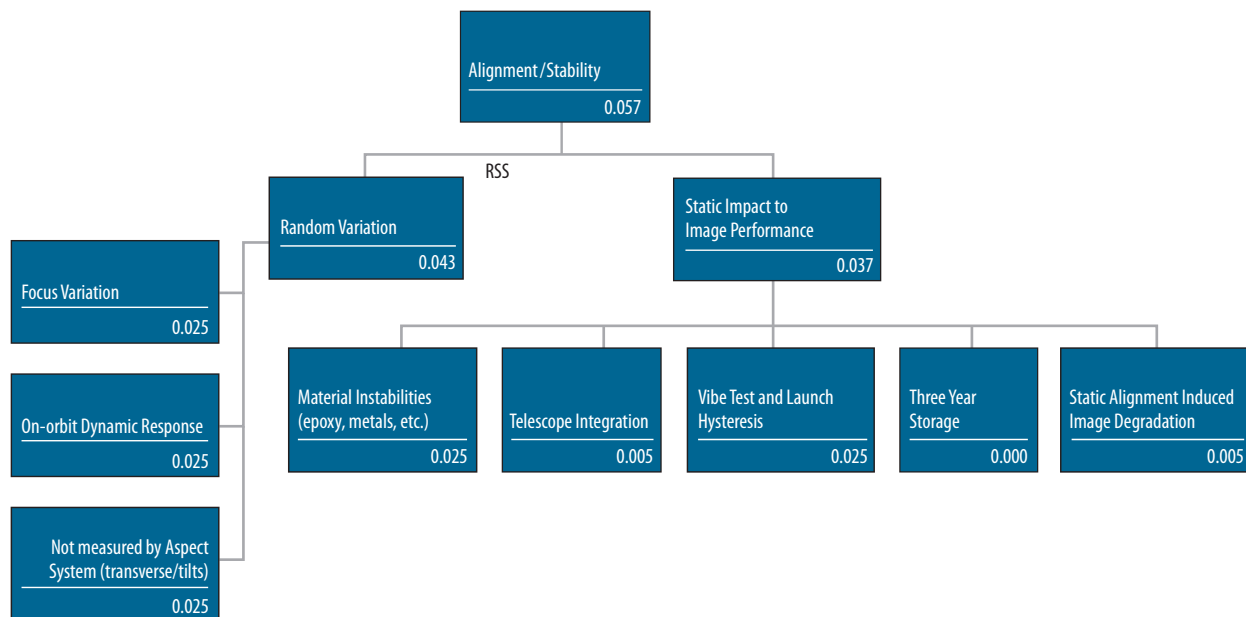


Figure 6.40. Alignment/stability budget for on-axis image quality. Telescope integration includes the degradation of imaging performance due to LMA integration in bench.

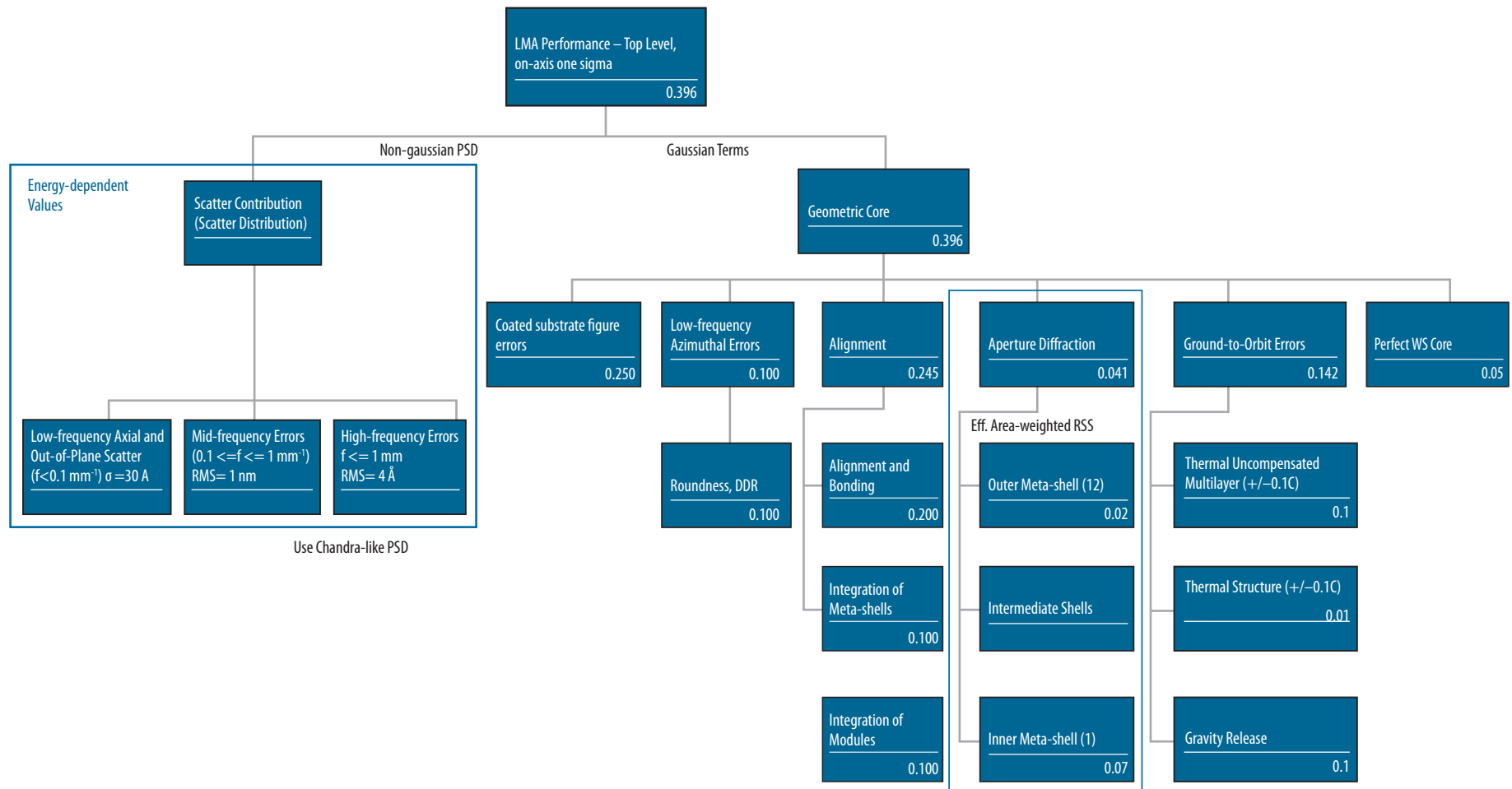
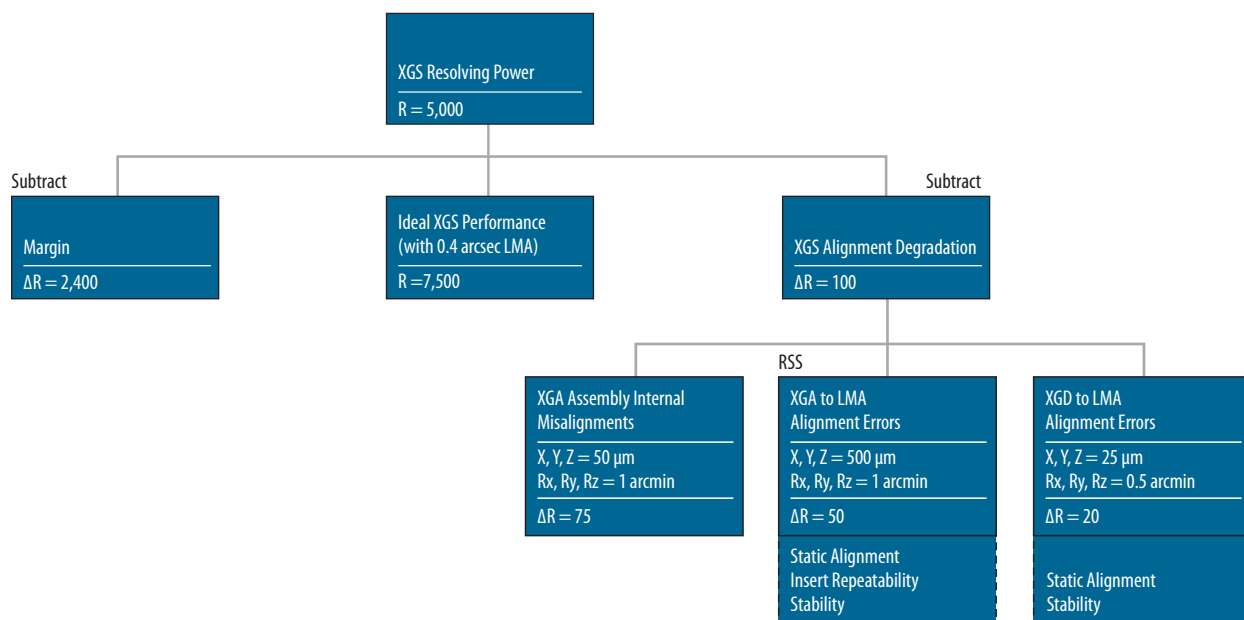


Figure 6.41. LMA top level imaging error budget.

6.6.1.2 Spectral Resolving Power

The *Lynx* XGS performance is characterized by the effective area (A_{eff}) and the spectral resolving power R . Both of these key TPMs are affected by the alignment of the XGA and XGD to the LMA. Integration of the XGA and XGD onto *Lynx* is straightforward, and SOA mechanisms provide more than sufficient tolerances to maintain critical alignments. Since the alignment tolerances required to meet the resolution requirement are tighter than those required to meet the effective area budget, only the resolving power error budget values are shown in Figure 6.42.

Figure 6.42. XGS resolving power R allocation error budget.

The branches of the spectroscopic error budget correspond to the finite tolerances in the assembly and integration of the XGA in the branch labeled “XGA Assembly Internal Misalignments.” Alignment tolerances between the XGA and LMA are detailed in the branch labeled “XGA to LMA Alignment Errors.” These tolerances include static alignment (installation), mechanism repeatability, and stability of the alignment during a measurement. The third branch of the tree focuses on detector alignment effects, including static alignment (installation) or resolution limits for the adjustable Degrees of Freedom (DOFs) and stability.

The error allocations are based on a combination of detailed ray-trace simulations and analytic approximations. The foundation for this analysis is ray-trace work done by the CAT-XGS team at MIT to establish the sensitivity of the CAT gratings to misalignments in the six rigid-body DOFs. The simulations initially assume a perfectly aligned CAT-XGS and include non-ideal effects such as the finite extent of the mirror PSF, astigmatism inherent in the design, and finite sizes of CAT gratings and CCD detectors (which cause deviation from the ideal Rowland torus geometry).

A ray-trace with 200,000 photons for three wavelengths in the XGA band were evaluated and A_{eff} and R were calculated. A_{eff} is the total effective area summed over all dispersed orders that fall on the XGD, and R is the average resolving power, where the resolving power from individual orders is

weighted by the number of photons in that particular order. Using this ray-trace simulation, sensitivities of the six rigid-body deviations from perfect alignment were computed. Figure 6.43 shows an example of the results from a set of simulations, with the top row showing the effects of translations and the bottom row showing the effects of rotations of the grating elements. The coordinate system used is aligned with the global system but centered on the individual grating element. Each figure shows the shift or rotation angle on the x-axis and then plots the spectral resolving power (R) with a solid line; the value for R can be seen on the left y-axis of the figure. Over-plotted is the effective area with dotted lines; the value can be seen on the right y-axis of the plot. Using this method, the sensitivities to facet misalignment within the XGA, the XGA alignment to the LMA, and the XGD to the LMA were determined.

For the XGA assembly internal alignments, small finite alignment tolerances of 50 μm for translations and 1 arcminute for rotations are posited as reasonable tolerances and show negligible impacts to the error budget. XGA to LMA alignment studies indicate that a shift along the x-axis (the optical axis) will not impact performance. Shifts along the other axes will have a negligible impact on A_{eff} but can result in reduced R for shifts larger than 1 or 2 mm.

Alignment requirements are set by R for all rotations. Rotation around the y-axis or z-axis will move some gratings “above” and others “below” the surface of the Rowland torus, dramatically widening the spot of the dispersed rays. Due to the long lever arm, gratings farthest away from the rotation axis have the largest effect. Tolerances for the alignment of the XGA door to LMA of 0.5 mm in translation and 1 arcminute in rotation are easily met and have minimal effect on A_{eff} or R .

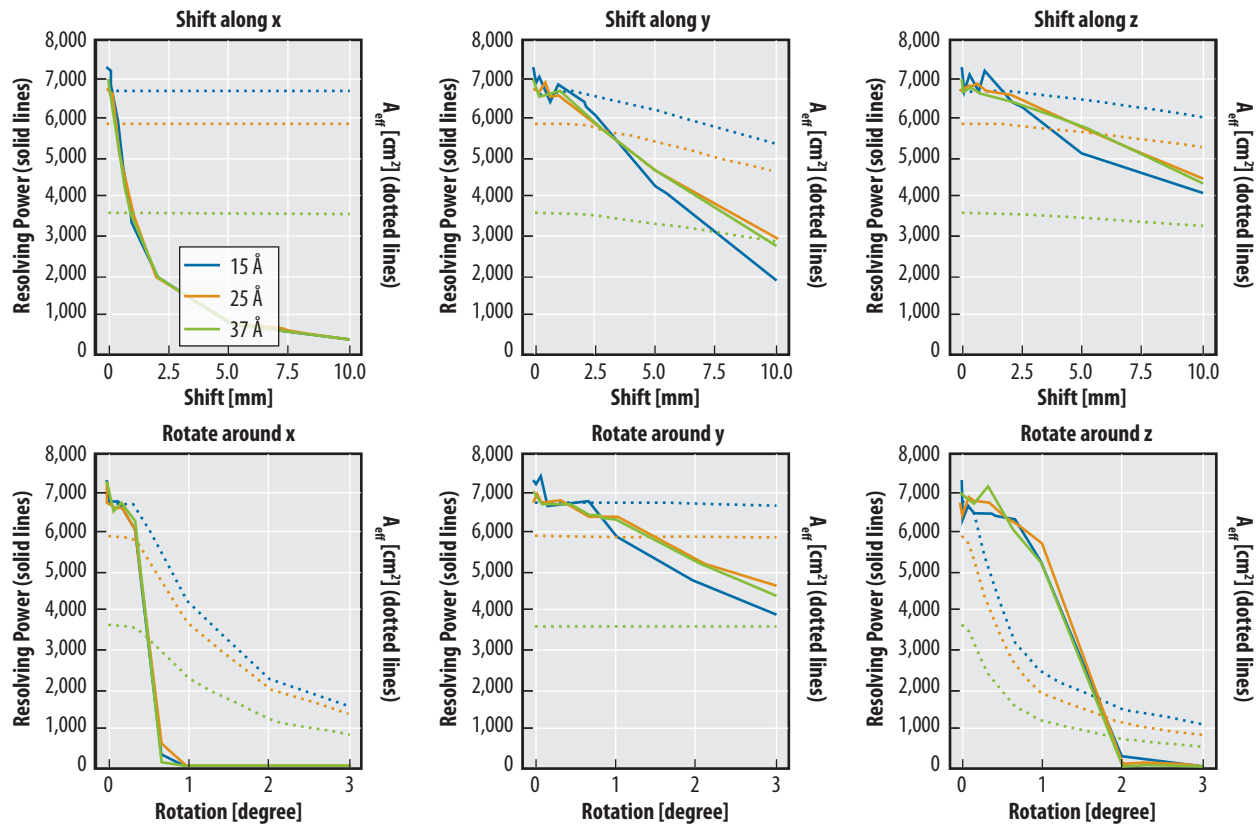


Figure 6.43. Sensitivity of R and A_{eff} to internal XGA tolerances.

The XGD-to-LMA alignment was also studied. A shift along x or a rotation around z will bring the XGD out of focus. Thus, these are the misalignments with the largest impacts. Fortunately, these are also the two DOFs that can be adjusted on-orbit with the planned XGD focusing mechanism. Since focus can be adjusted with a mechanism, the static allocation is just the mechanism resolution, which will be capable of positioning the detector within the depth of field of $25\text{ }\mu\text{m}$.

6.6.1.3 Effective Area

The science requirement for at least 2-m^2 effective mirror area at 1 keV has been decomposed into a high-level error budget shown in Figure 6.44. The dominant terms are obscuration from the support structure and the thermal pre- and post-collimators, and the reflection efficiency of the mirror. To minimize the shadowing, the LMA is designed so that the structural elements of the spider align with elements of the pre- and post-collimators. The total obstructed geometric area is 13.5% , including 2% margin. The error budget will be maintained to manage margin and will become a TPM as the design matures. Contamination also contributes to effective area loss. To maintain the integrity of calibration, particulate contamination is separately controlled to cover no more than 0.005% of the mirror area, which was achieved for the *Chandra* mirrors. During ground handling, the mirror is covered and purged with a positive pressure of clean, dry nitrogen. On-orbit, the thermal control system keeps the mirror at a higher temperature than any surfaces in view to reduce the chance of volatile contaminants condensing on the reflecting surfaces. The grating assembly has been designed to minimize obscuration by aligning its structural elements to the mirror assembly. The mirror has been designed with excess geometric area to allow for the loss of tens of segments or even an entire module, while still preserving margin.

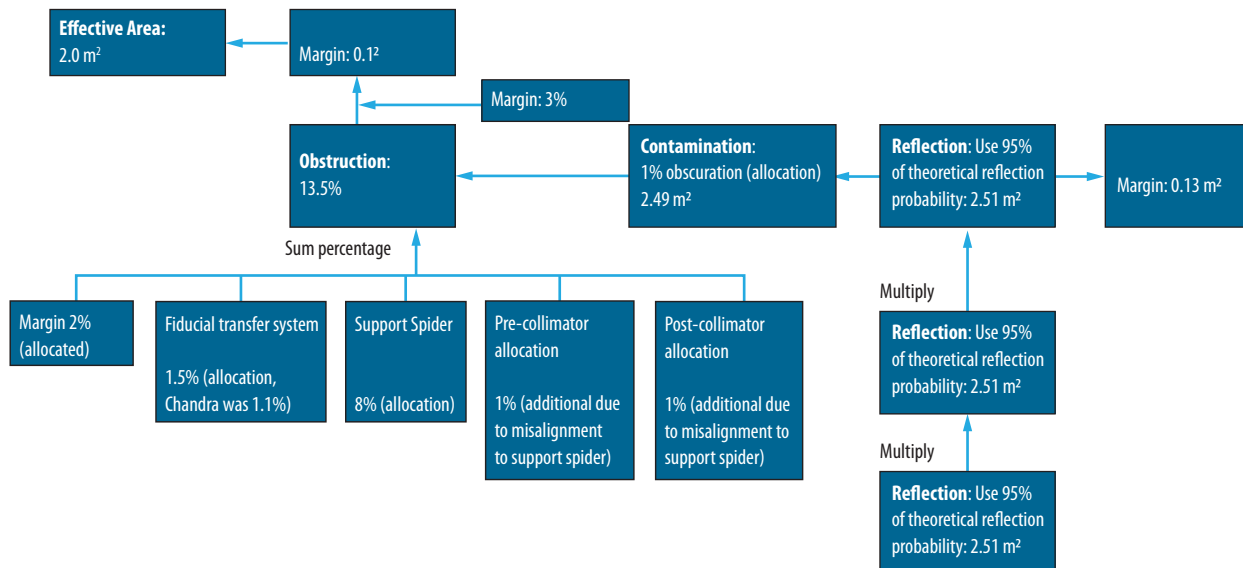


Figure 6.44. High-level block diagram of the error budget elements for the *Lynx* effective area.

6.6.2 Integrated Observatory Performance

The following analyses were completed during the concept study phase to address key performance parameters that directly enable the *Lynx* science mission. Results of these analyses have been incorporated into the *Lynx* conceptual design and are used to show that performance requirements are met with margin.

6.6.2.1 SE-L2 Natural Environment Analyses

The SE-L2 natural environment and the environment of the orbits around that point are relatively benign compared to those of geosynchronous and low-Earth orbits. For this and other reasons, this location will also be home to *JWST*, *WFIRST*, *Spectrum Roentgen Gamma (SRG)*, and *Athena*. *Lynx* will leverage knowledge from these missions regarding predicted (and eventually measured) environmental factors, and will incorporate this knowledge into the detailed design work during Phase A.

The ionizing radiation and meteoroid SE-L2 environments are the primary elements with the potential to influence *Lynx* performance and longevity. Preliminary consideration for each has been given, and mitigation for each is discussed in the relevant subsections that discuss the telescope and spacecraft detail (§6.3). Additional environmental factors have also been considered, such as the thermal properties, orbital attitude disturbance, and control. Additional considerations will be made during Phase A, such as the plasma environment and spacecraft charging.

Ionizing radiation in the form of solar particle events can cause single-event effects and degrade hardware. Galactic cosmic rays can upset avionics and contribute to the total hardware dose, and moderate energy protons (100–300 keV) can scatter down the optical path, creating background events and degrading detector performance. The total ionizing dose over a 20-year mission lifetime was estimated using the Space Environment Information System (SPENVIS). Preliminary analysis by the MSFC Natural Environments Branch of total ionizing dose concludes that there is minimal risk of single-event effects or hardware degradation over a 20-year mission lifetime (including transit and phasing orbits on the way to SE-L2) assuming a modest (2.5-mm-thick) aluminum shielding. For those particles that are scattered down the optical path, the *Lynx* design follows the *Athena* guideline [553] to place strong magnets around the optical path to divert, to the extent practical, focused low-energy protons and electrons away from the X-ray detectors.

In addition, the mass-limited fluxes and impact speed distributions of meteoroids — as defined by NASA’s Meteoroid Environment Office, Meteoroid Engineering Model 3 — on various *Lynx* surfaces indicate minimal risk over the mission lifetime. These surfaces (e.g., radiators, solar panels, thermal blanketing, and similar structures) are sized to allow for predicted degradation. In particular, the modular design of the *Lynx* X-ray mirror elements allows for a small number of damaged mirror segments without measurable degradation to overall *Lynx* performance. Furthermore, it was determined by GSFC’s Mission Design Lab that only a small number of meteoroid particles would potentially penetrate the laminated OBA structure and allow in scattered light over the extended 20-year mission.

6.6.2.2 Telescope Thermoelastic Analysis

A thermoelastic analysis of the *Lynx* telescope system was performed to estimate the order of magnitude of global deformations between the LMA and the focal plane due to predicted thermal gradients. Three of the available predicted gradients were used as input loads to the *Lynx* structural Finite Element Model (FEM), an image of which is shown in Figure 6.45. These gradients represented the steady state thermal gradient when oriented 45°, 90°, and 175° to the Sun. Displacements at the aft end of the OBA and at the center of the LMA spider were predicted for each gradient.

Assumptions for this analysis included:

1. Assuming that the structure is deformed at predicted thermal steady state conditions (as opposed to performing transient thermal analyses) is conservative.
2. The derived CTE based on *JWST*-heritage CTE data is achievable for the specific OBA composite layup design.
3. At the start of the *Lynx* service life, the system will be focused and aligned.

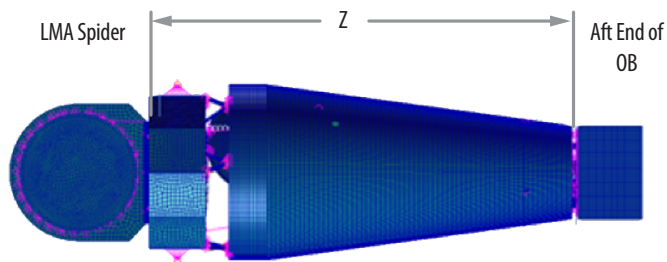


Figure 6.45. FEM used for telescope thermoelastic analysis. Results show an order of magnitude of margin of optical axis motion over error budget allocation.

Focus was expressed as the primary concern; therefore, thermal deformations were predicted in the z-axis (optical axis) direction. The difference between the predicted deformation at pairs of steady state thermal gradients (45° and 90°, 90° and 175°, and 45° and 175°) was considered a conservative estimate of changes in the structure's geometry.

Results indicated an estimated 2.5- μm optical axis relative motion between the center of the LMA spider and the center of the aft end of the OBA. The current error budget allocation for this motion is 25 μm , resulting in an estimated order of magnitude of error budget margin

6.6.2.3 Observatory On-Orbit Dynamic Analysis

A lesson learned from *Chandra* was that while jitter or relative motion between the mirrors and the focal plane was not an issue, resonances of the mirror shells due to Reaction Wheel Assembly (RWA) vibrations was. This issue was discovered during system testing and manifested as an impact to image quality. The solution at that time was to incorporate RWA passive isolators into the design. The *Lynx* design incorporates this lesson by including passive isolation for the RWA as well as for the LXM cryocooler to circumvent the risk of pertinent dynamics negatively affecting Observatory image quality. Detailed design and analysis of the passive isolation system will be conducted as the overall *Lynx* design matures.

A detailed dynamic analysis was performed to determine the relative motion perpendicular to the optical axis between the LMA and a point near the center of the focal plane. The *Lynx* structural FEM was used for this analysis. Existing reaction wheel specification data were used as inputs, and 1% damping was assumed. The predicted maximum relative motion was $<0.004 \mu\text{m}$, which is compared to the jitter error budget of 13 μm . Without the planned RWA passive isolation, three orders of magnitude of margin exist.

Vibrations associated with the LXM cryocooler will result in relative motion between detectors on the ISIM. The predicted motion between the HDXI and the XGD is planned future work. However, with isolation between the cooler and adjacent structure, there is no known reason to think pertinent motions will pose a significant engineering challenge. Detailed design and analysis of the cryocooler isolation systems will be conducted as the overall *Lynx* design matures.

6.6.2.4 Observing Efficiency Assessment

The *Lynx* conceptual design maximizes science observation time and minimizes time spent on non-science operations.

An analysis was performed using the conceptual Observatory design and conservative estimates to show a *Lynx* observing efficiency of 91.5%, including 3.3% of the time observing celestial calibration targets. Details of this analysis are provided in the *Lynx DRM Supplemental Design Package*. This observing efficiency provides a margin of an hour per day compared to the required minimum observing efficiency of 85%. The analysis used an example observing schedule from the *Chandra* project using 720 targets and a non-optimized observing schedule to be conservative. The time for each slew to target was based on the *Lynx* reaction wheel sizing and moments of inertia, and an additional 10 minutes of time was added to each slew maneuver to account for star acquisition and settling of any vibrations. Two 10-minute momentum dump intervals per week and one 10-minute station-keeping maneuver every three weeks were included. Instrument and spacecraft configuration will take place during slews, and communication to DSN will occur at any time including during science observations. Only nominal conditions were used in the study, with no safing actions or solar event shutdowns, as these were not intended for inclusion in the 85% requirement. The observing efficiency analysis and error budget allocation will be updated as the *Lynx* design matures.

6.6.3 Observatory Assembly, Integration, and Test

Many basic optics module and science instrument characteristics will be measured during subassembly, while only system-level ground X-ray calibration of the flight optics and instruments will be carried out at a dedicated calibration facility. Additional X-ray calibration at a continuum of energies using celestial sources and full-aperture illumination will be performed in-flight.

6.6.3.1 Ground Calibration

A key difference with *Chandra* calibration is the hierarchical design of the meta-shell optics planned for *Lynx*. This approach enables the PSF and effective area of individual optics modules to be mapped over a full range of energies and pitch and yaw angles with relatively modest Ground Support Equipment (GSE) and X-ray test facilities (preferably co-located with module production facilities). Visible light metrology is sufficient to verify module-to-module co-alignment within meta-shells and of meta-shells within the LMA. The LMA (protected from contamination) is then transported to a dedicated calibration facility for the final verification of the system at a small subset of X-ray energies and angles, thereby reducing schedule and cost.

After performing an assessment of available X-ray calibration facilities, the *Lynx* team decided to baseline the use of MSFC's X-ray and Cryogenic Facility (XRCF) for on-ground calibration activities of the LMA and scientific instruments. This facility was built in the 1990s for the *Chandra* project, is being considered for use by ESA's *Athena* project, and can accommodate the *Lynx* on-ground calibration campaign. Figure 6.46 shows a diagram of the instrument chamber.

Modifications to the facility are required and are under consideration for the *Athena* calibration campaign scheduled to take place in the FY28–FY29 timeframe. Anticipated XRCF modernization and upgrades include changes to the X-ray source system, X-ray detector system, X-ray data acquisition and control system, contamination control and monitoring system, thermal control system, and cleanroom facilities. The *Lynx* project will leverage these upgrades to reduce overall cost. Specific upgrades for *Lynx* will include but are not necessarily limited to mirror and instrument handling fixtures, a mirror reorientation fixture, focal plane instrument positioning fixtures, a high-speed detector, a metrology system, and other handling equipment. XRCF upgrades and usage are included in the project schedule and cost (\$8).

Ground calibration of the LMA includes verification of effective area and PSF at highly oversampled spatial resolution. The diameter of the X-ray beam entering the XRCF test chamber is 1.46 m, allowing ~20% of the LMA aperture to be illuminated at one time. The plan is for the LMA to be aligned in the test chamber offset from the boresight of the beam and translated and/or rotated about its optical axis (under vacuum) to successively illuminate the entire LMA aperture as shown in Figure 6.47.

Ground calibration of the XGA includes verification of the dispersion relation, effective area in all diffraction orders, and line response function. XGA calibration will require the LMA to ensure that it is properly aligned and that the grating deployment mechanism and the grating focal plane detector meet requirements.

Ground calibration of the HDXI (and XGD) and the LXM in tandem with the LMA is planned (see §8.4). The proposed LXM development schedule follows the approach used by the SXS instrument on *Hitomi* [585], is planned for the Resolve instrument on *XRISM*, and is similar to the approach planned for the *Athena* X-IFU. It is based on the development of an engineering model and a protoflight unit, with selected subsystem flight spares but no complete instrument spare. The engineering model will

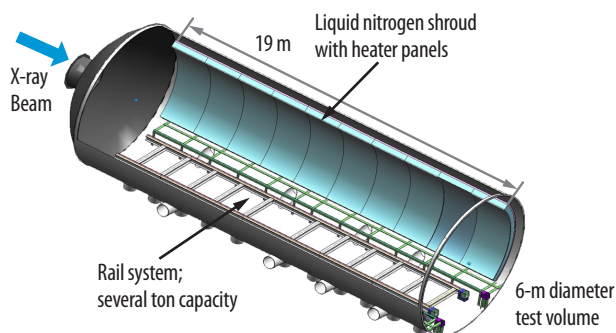


Figure 6.46. XRCF Instrument chamber accommodates *Lynx* on-ground calibration requirements.

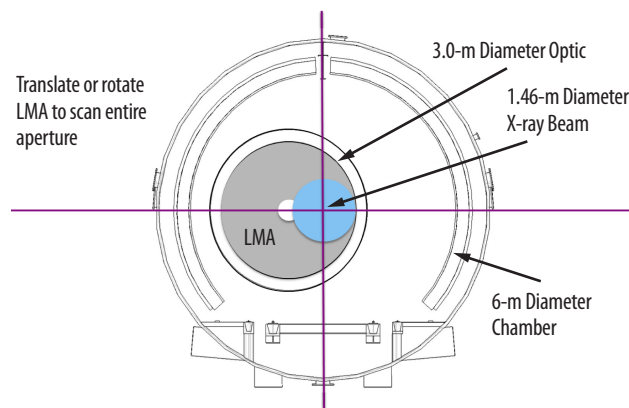


Figure 6.47. Schematic of the XRCF test chamber (outer circle), X-ray beam (blue) and X-ray mirror modules aperture (gray) viewed along the beam boresight. The X-ray mirrors can be translated and/or rotated about its optical axis to illuminate different ~20% portions of the full aperture.

undergo extensive qualification testing beyond the typical level of an EDU in order to space-qualify the design. The engineering model, not the flight unit, will be X-ray tested along with the LMA TRL demonstrator (§7.2.1) at the XRCE.

The X-ray calibration of *Lynx* will require a suite of GSE, including focal plane detectors and flight-like communications within a flight-like thermal environment. The calibration will be in two stages. The first is a six-month setup and rehearsal designed to test all GSE, communications, harnessing, and alignment procedures; validate performance simulations; verify data flow; and develop test schedules, handling procedures, and contamination control procedures. The calibration rehearsal will use engineering models of the optics and all science instruments. The six-month ground calibration of flight units (and LXM engineering model) will immediately follow the rehearsal as shown on the project schedule (§8.4). The rehearsal will be conducted within a 40-hour workweek, while the calibration of the flight equipment will utilize 24/7 operations.

6.6.3.2 Lynx Mirror Assembly Integration & Test

The LMA structure consists of the X-ray mirror module assembly, forward and aft contamination doors, barrel assembly, and structural mounts. The fiducial transfer system components are also integrated at this assembly step. The high-level LMA Integration and Test (I&T) flow is shown in Figure 6.48. LMA I&T begins with the availability of the validated mirror module assembly. The LMA test campaign includes pre-environmental functional testing, Electromagnetic Interference/Electromagnetic Compatibility (EMI/EMC) testing, Thermal Vacuum (TVAC) testing, first-motion testing of mechanisms, and post-environmental testing. All tests can be conducted using existing NASA and/or contractor facilities. Following testing, the LMA is shipped for integration into the XRT. LMA I&T is expected to take six months. An additional two months of risk mitigation has been assumed.

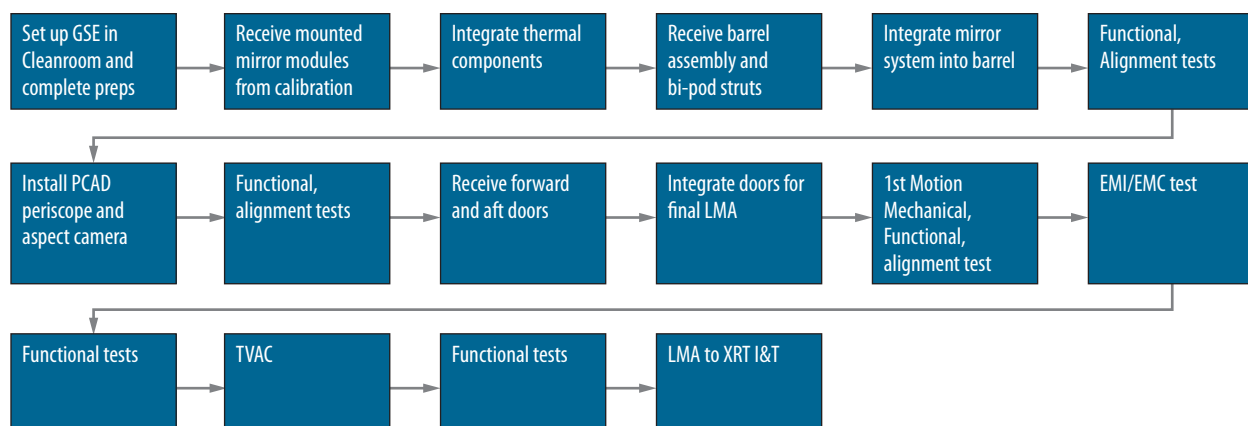


Figure 6.48. LMA I&T flow.

6.6.3.3 Integrated Science Instrument Module I&T

The ISIM assembly includes the LXM and HDXI mounted on the translation table, the XGD mounted on a stationary or “fixed” plate, electronics boxes, harnesses, and radiator panels. The high-level ISIM I&T flow is shown in Figure 6.49. ISIM I&T begins with the mounting of the translation mechanisms to the closeout plate and translation stage. The LXM is then integrated and aligned to the translation stage, followed by the HDXI. Then, the XGD is installed and aligned on the stationary closeout plate, followed by installation of the electronics boxes, harnesses, and thermal components. The test campaign includes pre-environmental functional testing, EMI/EMC testing, TVAC testing, first-motion testing of mechanisms, alignment, and post-environmental functional tests. All tests can be carried out at existing NASA and/or contractor facilities. Following testing, the ISIM is shipped for integration into the XRT. The ISIM I&T is on the *Lynx* critical path and is expected to take 14 months to complete. A critical path margin of two months has been added to this activity per critical path schedule margin guidelines.

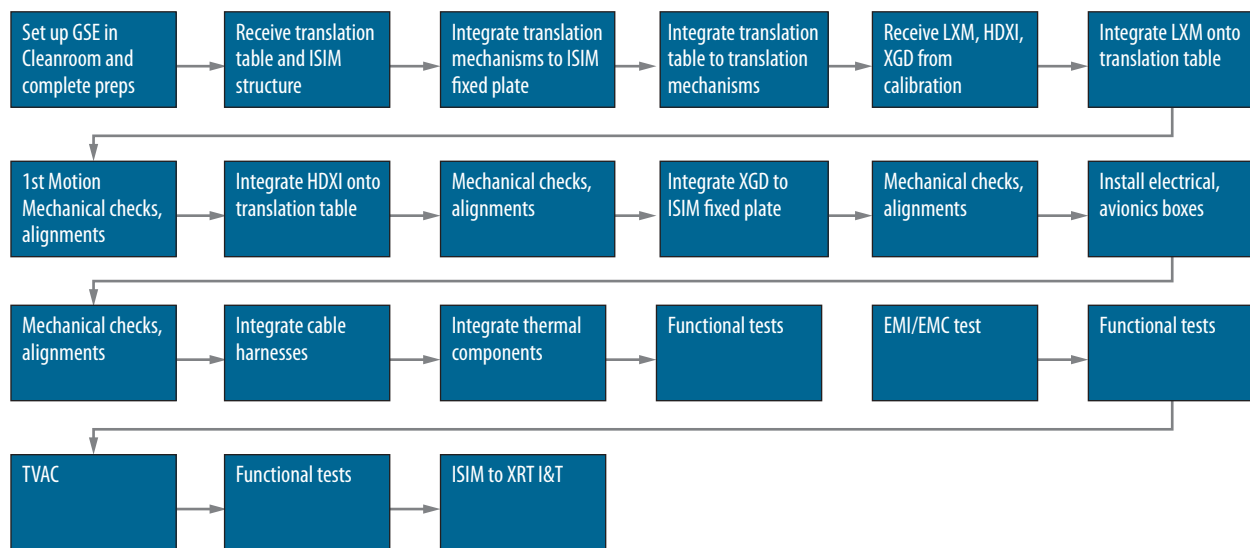


Figure 6.49. ISIM I&T flow.

6.6.3.4 X-ray Telescope I&T

The X-ray Telescope (XRT) assembly includes the XRT, XGA, OBA and electronics, harnesses, and thermal system components. The high-level XRT I&T flow is shown in Figure 6.50. XRT I&T begins with the integration and alignment of the XGA to the LMA. This assembly is then mounted to the OBA, and finally, the ISIM is integrated. The test campaign includes pre-environmental functional testing, single-motion mechanical testing, alignment tests, and PCAD system tests. All tests can be conducted at existing NASA and/or contractor facilities. Following testing, the XRT is shipped for integration into the SCE. The XRT I&T is on the *Lynx* project critical path and is expected to take 18 months to complete. A critical path margin of nine months has been added to this activity per critical path schedule margin guidelines.

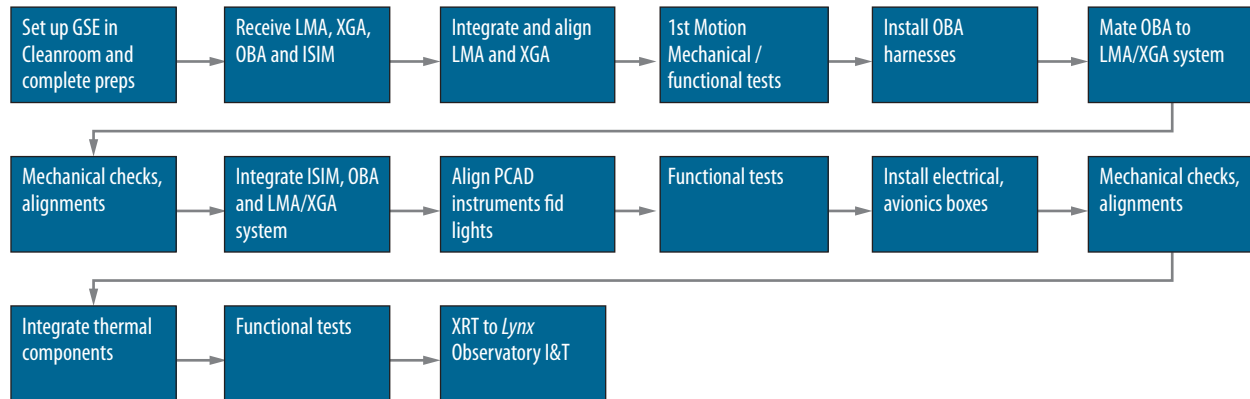


Figure 6.50. XRT I&T flow.

6.6.3.5 Spacecraft Element I&T

The SCE consists of the spacecraft and all of the subsystems, such as power, thermal, C&DH, GN&C, and propulsion. The high-level SCE I&T flow is shown in Figure 6.51. SCE I&T begins with integration of the propulsion system, followed by the GN&C, power system components, thermal components, C&DH system components, harnesses, and MLI. Spacecraft testing includes functional and performance testing, verification of all electrical interfaces, comprehensive performance test (pre- and post-), alignment checks, acoustics, shock and vibe, EMI/EMC, three-point thermal balance, end-to-end data flow, deployment testing of the solar arrays, sunshade and contamination doors, and mechanisms. All of these tests can be conducted at existing NASA and/or contractor facilities. Following testing, the SCE is shipped for integration with the XRT into *Lynx*. SCE I&T is expected to take eight months to complete. No additional margin is included for this activity. The *Lynx* spacecraft is a similar design to *Chandra*, which took seven months for I&T.

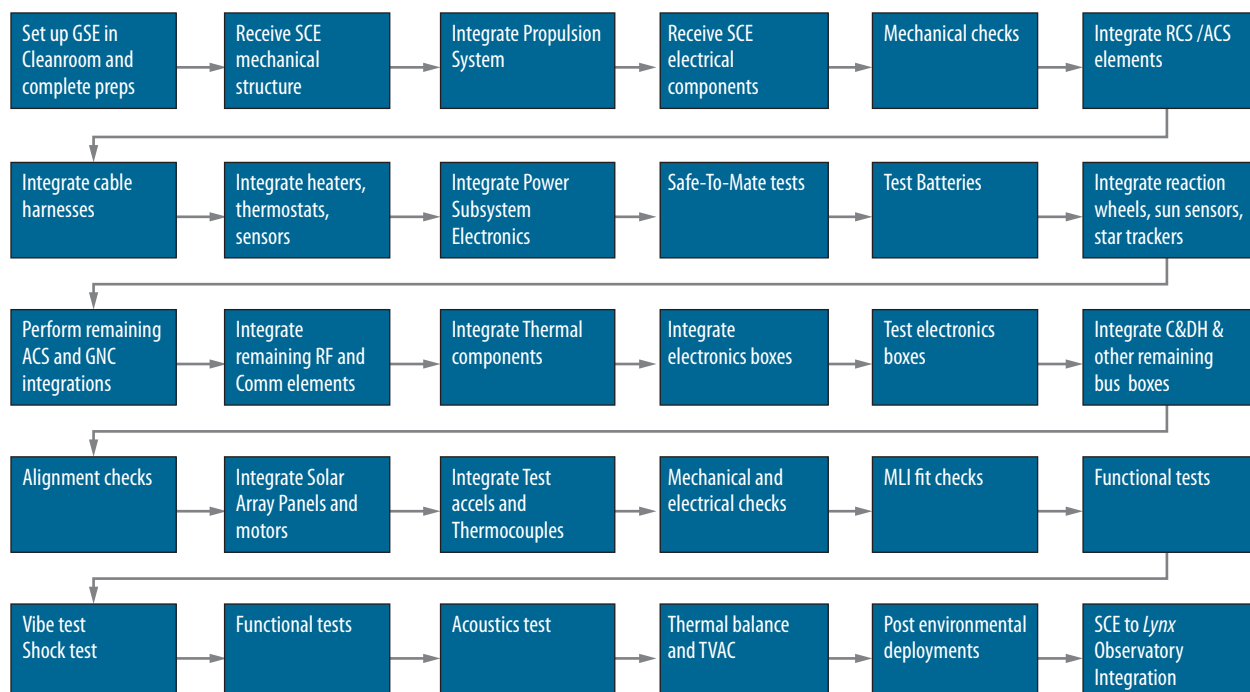


Figure 6.51. SCE I&T flow.

6.6.3.6 Observatory I&T

The *Lynx* Observatory I&T integrates the fully qualified XRT and SCE. The high-level *Lynx* I&T flow is shown in Figure 6.52. *Lynx* Observatory I&T includes ambient functional testing, alignments, leak checks, deployments, full Observatory functionality, and electrical/mechanical compatibility. The test campaign includes pre-and post-functional testing, cryogenic vacuum and thermal balance tests, EMI/EMC tests, and acceptance-level acoustic and vibration testing. Furthermore, data flow to the *Lynx* Science and Operations Center will take place during this phase of I&T. All of these tests can be conducted at existing NASA and/or contractor facilities. Following testing, *Lynx* is shipped to the launch site for the launch vehicle integration and is readied for flight. The *Lynx* Observatory I&T is on the project critical path and is expected to take six months to complete. Critical path margin of one month has been added to this activity per critical path schedule margin guidelines.

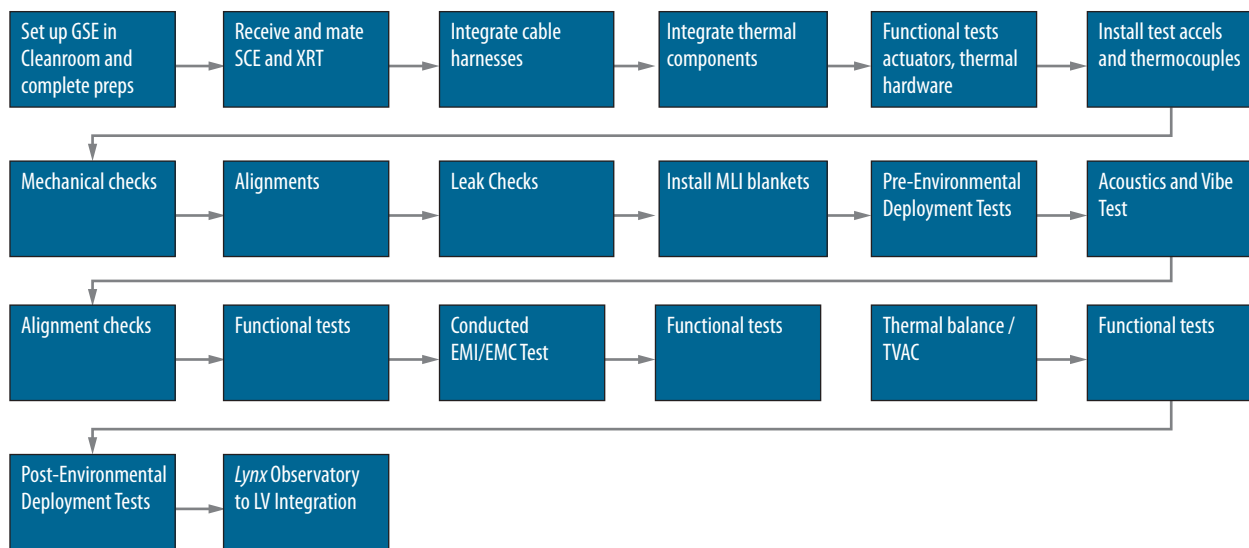


Figure 6.52. *Lynx* Observatory I&T flow.

Key operations during *Lynx* AI&T are performed to verify and validate system performance requirements. Given the commonalities between the *Lynx* and *Chandra* architectures, the AI&T flow for *Lynx* closely resembles the heritage assembly and test philosophy of *Chandra*. The overall AI&T flow is shown in Figure 6.53.

The AI&T activities and flow were developed by the *Lynx* systems engineering team consisting of MSFC and SAO systems engineers along with industry CAN partners with direct experience on the *Chandra* Observatory. This flow outlines the system-level integration sequence for *Lynx*, high-level tests at the end of each assembly sequence, and the assumed durations for each. This information was used as direct input into the late-Phase C/Phase D portions of the *Lynx* project schedule described in §8.4.

The *Lynx* Observatory architecture includes two primary elements: (1) the XRT and (2) the SCE. These elements are further broken down into subelements and assemblies as defined in Table 6.21.

A feasible assumption (based on *Chandra*) for subsystem Design, Development, Test, and Evaluation (DDT&E) is that the mirror modules, XGA, LXM, HDXI, and XGD are all government-furnished and that the prime contractor has DDT&E responsibility for the OBA and ISIM, as well as the entirety of the SCE. Further, it can be assumed that the prime contractor is responsible for integration of the mirror modules into the LMA, integration of the LXM, HDXI, and XGD into the ISIM; and for integrating the LMA, XGA, OBA, and ISIM into the XRT. It is assumed that all subassemblies are delivered to the next level of integration fully qualified to the extent practical. The XRT and SCE will be delivered to *Lynx* Observatory I&T as fully qualified units.

Protoflight-level environmental testing will be performed at the subelement level, and acceptance-level vibration and acoustics testing will be performed at the Observatory level. Interface simulation hardware will be used during tests at lower levels of assembly to provide data for final analysis and verification. Testbeds, mock-ups, and engineering models and test units at the subelement level will be used as pathfinders to provide data and analysis to be used for final verification at the Observatory level. Specifically, engineering models of the X-ray Mirror Modules and scientific instruments will be used for calibration checkout, early testing, schedule risk mitigation for manufacturing, and assembly of these complex components.

Electrical Ground Support Equipment (EGSE) and Mechanical Ground Support Equipment (MGSE) will be developed and qualified to safely handle and align the flight hardware during AI&T, and special transportation equipment will be developed as needed to move flight hardware during assembly and test activities. A standard C-5 cargo plane can be utilized for transporting the large assemblies. Existing test facilities are anticipated to be used during the AI&T campaign for *Lynx*. Specifically, cryogenic vacuum testing can be performed at NASA Johnson Space Center Chamber A or GSFC Chamber 290. *Lynx* will require an ISO-7-class cleanroom facility such as the GSFC's Space Systems Development and Integration Facility (SSDIF) to mitigate contamination, specifically on the X-ray optics. Furthermore, the test and cleanroom facilities used for *Chandra* are still available and operational; however, this in no way presumes contractor preference or selection. Original *Chandra* partners as well as other aerospace contractors have developed new or improved facilities since that time that would be acceptable for this mission.

Table 6.21. *Lynx* Observatory primary elements, subelements, and subassemblies.

Primary Elements	Primary Subelements	Primary Subassemblies
XRT	LMA	X-ray Mirror Modules
		LMA Structures
		PCAD system
	XGA	GAS
	OBA	Magnetic Broom
	ISIM	LXM
		HDXI
		XGD
		ISIM Structures
SCE	Structural System	Secondary structures and mechanisms
	Thermal Control System	MLI, heaters
	Electrical Power System	Solar arrays, batteries
	C&DH System	Flight computer, controllers
	Communication System	Antenna, transponders
	GN&C System	Rxn Wheels, PCAD, Star Trackers, IRUs
	Propulsion System	MPS, RCS/ACS engines, tanks

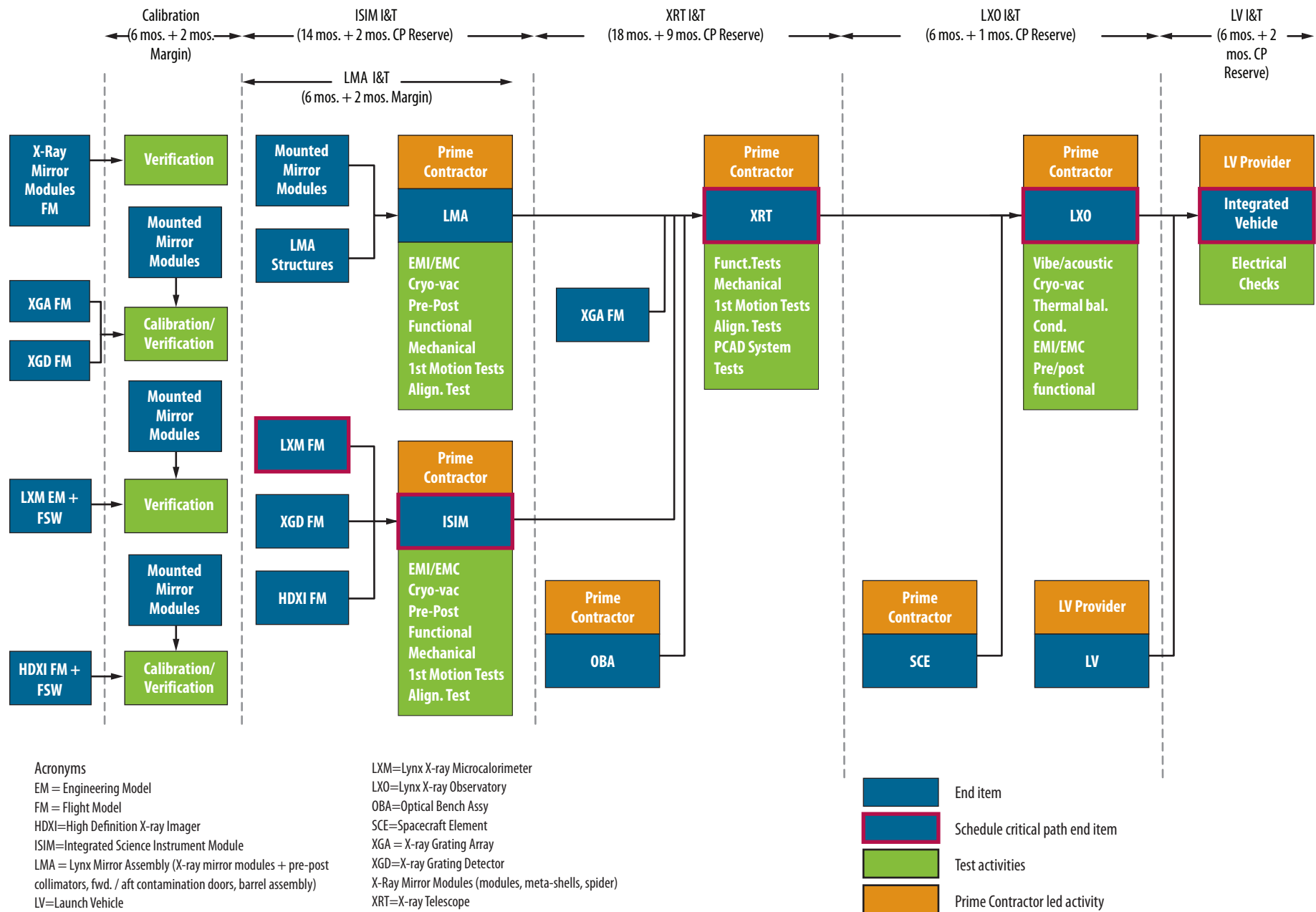


Figure 6.53. Lynx AI&T flow

6.7 Concept of Operations

The *Lynx* Observatory will serve the worldwide astronomical community as an efficient, long-lived scientific observing platform.

The concept of operations describes the fundamental on-orbit and ground support operations necessary to conduct the *Lynx* science program. In the *Lynx* paradigm (Figure 6.54), end users (referred to as general observers) conceive scientific experiments that define celestial targets, instrument configurations and observing modes, and durations of observations. The *Lynx* mission operations infrastructure then turns these definitions into scheduled programs of actions through mission planning and scheduling, commands the Observatory to execute the programs through operations activities, and ensures the resulting data are recovered, processed and validated, and then distributed to the general observers and the broader community in a timely manner. The *Lynx* Science and Operations Center sends commands to the Observatory and receives data from the Observatory through the DSN. The commands include all of the general observers' target and configuration requests, as vetted by mission support, and the spacecraft responds by positioning the proper instruments in the correct arrangements and photon-counting modes, and by slewing to and holding on targets. The process is made efficient by placing *Lynx* in an optimized observing environment capable of a long mission lifetime using flight-proven mission operations befitting a community-driven flagship mission, and maintaining data integrity and fidelity throughout.

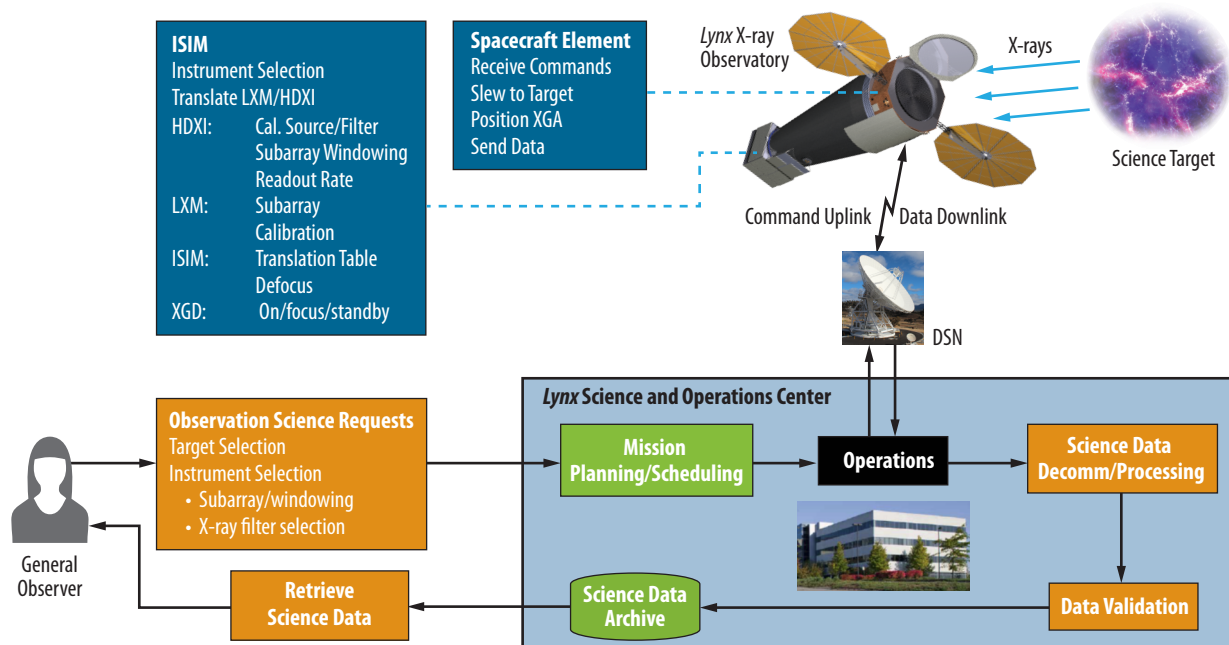


Figure 6.54. Concept of operations showing the cycle from user requests for observations to user receipt of science data. Following review, observation requests are processed by the *Lynx* Science and Operations Center into commands uplinked to the Observatory. Physical data from the Observatory flow through the DSN to the *Lynx* Science and Operations Center (which includes both mission and science operations), and ultimately to the observers, the general scientific community, and the public.

The *Lynx* Observatory is accommodated, with margin, in a standard heavy-lift vehicle for the 2030s. The SE-L2 orbit planned for *Lynx* easily meets the high observing efficiency requirement with a launch-to-orbit timeline sufficient to carry out all necessary performance verification and commissioning tasks. The subsequent science operations phase (§6.7.2) can fulfill the entire range of *Lynx* science objectives with enough flexibility to accommodate rapid response for unanticipated Targets of Opportunity (ToOs). There is sufficient propulsion for orbital maintenance, power, data, and communications capability during the science operations phase. See §6.4 for mission implementation details.

To best support the user community, *Lynx* ground operations (§6.7.4) are modeled after *Chandra*-proven practices and infrastructure. All *Lynx* science instruments are photon-counting detectors that accumulate event-based time, position, and energy data. These data (along with engineering data) are accumulated and temporarily stored on board before being periodically telemetered to the ground, where the data are then archived, processed, and distributed to the scientific community.

Finally, the *Lynx* concept of operations includes plans for the decommissioning and disposal of the Observatory and the preservation of science and engineering data and data products (§6.6.3).

6.7.1 Launch to Orbit — Cruise, Commissioning, and Check-Out

Lynx will launch in the mid-2030s under the current assumption that it will be integrated onto a heavy-class (expendable or recoverable) vehicle that will launch from NASA Kennedy Space Center (KSC). Following a Transfer Trajectory Insertion (TTI) maneuver, *Lynx* will be inserted into the 800,000-km, semi-major axis halo orbit around the SE-L2 libration point. As summarized in Appendix B.1.2, several orbits were analyzed for *Lynx*, including SE-L2, drift-away, Lunar Distant Retrograde Orbit, *Chandra*-type orbit, and Transiting Exoplanet Survey Satellite- (TESS-) like orbit. After careful consideration, the SE-L2 orbit was selected because it provides: (1) no eclipsing, (2) a stable thermal environment, (3) avoidance of trapped radiation belts, (4) high observing efficiency, and (5) moderate fuel and propulsion requirements relative to some of the other orbits considered. The observing efficiency is the percentage of real time *Lynx* will spend on science observations and takes into account the estimated times for slewing, thermal, and vibrational stabilization.

The estimated time to reach SE-L2 is 104 days. During this time, the spacecraft and telescope systems are powered on, allowed to outgas, and undergo system checks and initial calibration. Early orbit operations schedules are being developed for each of the telescope systems, with an integrated element that provides contamination mitigation during the outgassing and checkout phases.

6.7.2 On-Orbit Operations

The on-orbit operational modes are preplanned using a scheduling process that seeks to maximize the time on-target while accommodating all necessary spacecraft operations. The sequence of slews and dwell times are planned to achieve an observing efficiency of at least 85% [579], while staying within budgets for consumables, momentum unloading, and data storage. The mission schedule plan will be used to generate spacecraft and instrument commands, which are then uplinked to the spacecraft and stored. A sufficient number of commands will be loaded to ensure autonomous operations for 72 hours.

On-orbit operational modes can be classified as “Normal Pointing Mode” or “Maneuver Mode” with an additional “Safe Mode.” ToOs are carried out using the Normal Pointing and Maneuver modes.

Normal Pointing Mode—Following on-orbit activation and checkout, *Lynx* will be primarily in Normal Pointing (also called “Science”) Mode conducting an autonomous pre-planned program of celestial observations. In this mode, the telescope’s optical axis is pointed within 10 arcseconds of a commanded celestial position, which is assured by locking on pre-planned stars at specific positions in the aspect star camera. The positions of the stars are constantly monitored and recorded for later downlink, along with the positions of fiducial lights in the focal plane projected onto the star camera image and inertial reference sensor data. All these data are needed to reconstruct the X-ray image on the ground with precise celestial coordinates. The X-ray camera uses its internal computer software to detect and recognize single photons as they arrive and tags them with arrival time, position, and energy (or, equivalently, wavelength).

When the XGA is inserted, the XGS-dispersed spectrum is directed onto the XGD, while the non-dispersed portion can be focused onto either focal plane instrument. Therefore, there are four observing configurations available for science observations:

1. XGS gratings inserted and LXM at the primary focus (XGS+LXM)
2. XGS gratings inserted and HDXI at the primary focus (XGS+HDXI)
3. HDXI as the primary with gratings retracted (HDXI only)
4. LXM as the primary focal plane instrument with gratings retracted (LXM only)

A typical scientific observing scenario may involve the spacecraft dithering the optical axis in a pattern on the focal plane in order to average the response over many pixels. Typical data collection times for *Lynx* are expected to range from ~1 ks up to a few hundred ks per pointing, limited only by angular momentum buildup. There is no practical limit for the total time on a single target via multiple pointings. Slews to new targets require only 1–3 ks.

The Nominal Pointing Mode is transparent to the selection or internal settings of the focal plane instruments. The *Lynx* data subsystem interfaces with each camera to collect CCSDS-standard encoded packets of data as they are assembled by the camera software. Data collection and time registration are synchronized by signals from the precision spacecraft clock. The data packets contain X-ray events, background events that mimic X-rays, and auxiliary configuration, timing, temperature, voltage, and current “housekeeping” data from the instrument. During the observation, the reaction wheel speeds are adjusted based on data from the star camera and gyros to absorb angular momentum generated by disturbance torques and thus keep the pointing direction within limits. At the commanded end time of the observation, the spacecraft computer sends signals to allow the X-ray camera(s) to transition to standby and prepares to enter the Maneuver Mode.

On-orbit calibration observations are performed as part of the Normal Pointing Mode science operations. See §6.7.3 for more details.

Maneuver Mode—In Maneuver Mode, a new target quaternion is loaded from the stored command sequence, and an eigen-axis rotation is computed for slewing the optical axis to the new position. The reaction wheel speeds are changed to generate appropriate torques on the Observatory, keeping the total angular momentum unchanged. The expected slew path is continuously compared to the gyro

rate data to ensure the maneuver is progressing properly. At the end of the maneuver, the star camera is commanded to acquire pre-determined acquisition stars. Deviations of these stars from their expected positions allows a fine update to the pointing direction, whereupon the star camera locks on guide stars used to hold during the observation, and the Observatory transitions to Normal Pointing Mode. The guide stars may include some or all of the acquisition stars. During Maneuver Mode, the ISIM and XGA mechanisms are used to place either the HDXI or the LXM at the mirror aim point, to insert or retract the XGA, and to adjust detector positions along the optical axis to nominal focus locations. Commands are sent to the focal plane instruments to configure for the upcoming observation. Reaction wheel momentum may be unloaded by firing the reaction control propulsion engines during Maneuver Mode.

Safe Mode—Safing actions are initiated autonomously by onboard detection of one or more preset sensor limit violations. Depending on the alarm, the Observatory may continue control by the spacecraft computer and either hold on stars at the current attitude (“Bright Star Hold Mode”) or use coarse and fine Sun sensors to reorient normal to the Sun line (“Normal Sun Mode”) while awaiting ground instructions to affect a recovery. Such alarms do not indicate any spacecraft system failures, and the onboard computer maintains control. In the presence of more significant alarms that might indicate possible hardware failures, the computer may switch to redundant subsystems and electronics, or may switch off the computers and transfer to the SMEU firmware to hold the vehicle in a safe, power-positive orientation (Safe Mode). The spacecraft is designed to be able to survive in Safe Mode indefinitely. Upon receiving telemetry, any anomalies will be recognized automatically by ground software and alarms relayed to mission operations personnel. The anomaly response will ensure that the spacecraft and instruments are safe, and will then develop and implement an appropriate recovery plan to return to Normal Mode observations. A hierarchy of safing actions will be defined.

The phased array antenna allows ground contacts and solid-state recorder data playback to take place in any mode, including Safe Modes.

Rapid Response Capabilities—Stored command loads can be interrupted and updated as needed to accommodate ToOs. In assessing the strategies for *Lynx* response to the ToOs, it is important to note that *Lynx* will fly in an astrophysical landscape shaped by transformative capabilities in the time domain. Detection rate of transient events will increase by orders of magnitude compared to the present. As a long-lived Great Observatory platform, ToO follow-up with *Lynx* will enable extraordinary advances in the astrophysical transient discovery space.

Optimistically, *Lynx* could respond to a ToO trigger within three hours of approval. This is possible for ~10% of triggers, and requires a 24-hour availability of the relevant mission planning and operations teams. Longer response times are possible with an increased probability and require less strain on mission operations. An 8-hour response can be achieved for ~100% of targets, still assuming that the relevant teams are available 24/7. A ToO turnaround response time of faster than 24 hours can be routinely guaranteed without additional strain on the mission operations.

The interruption and re-planning of command loads for a Risk Class A observatory like *Chandra* (and indeed *Lynx*) dominates the ToO response time. A review of procedures developed during two decades of *Chandra* operations suggests the following most optimistic scenario, in which it is possible for *Lynx* to respond within three hours for high-priority transient events (also shown graphically in Figure 6.55). This scenario still maintains the conservative risk posture appropriate for the Risk Class A Observatory:

1. **Community alerts triggered, and relevant *Lynx* team members are notified** — Following submission of the request, an alert mechanism is triggered to notify all relevant persons on the *Lynx* team of the urgent science event. Upon review, the request is approved. Procedures for quick approval of the ToO requests are developed with input from, for example, the *Lynx* User's Committee or its equivalent. The ToO response timeline starts from this point.
2. **Reschedule and review of the new observing schedule** — New schedule and satellite commands are generated on a timescale of minutes. Once the commands are generated, they are distributed to subsystem groups for review. Conducted in parallel, each review typically takes 1.5 hours to complete.
3. **Archiving of the approved schedule, transmitting to the DSN ground station, and DSN uplink** — This step takes 30 minutes. If it is completed during the normally scheduled DSN uplink, the new command load can be immediately sent to the spacecraft. This condition is satisfied for ToO observations approved within a time window from $t_{\text{DSN,start}} - 2$ hours to $t_{\text{DSN,end}} - 2$ hours. Assuming three DSN contacts per day and a 1-hour duration of the contact, the delay related to DSN contacts can be avoided for approximately one-eighth of the triggers.
4. **Satellite slewing and science observation** — Upon receiving a new command load, it takes 45 minutes for *Lynx* to perform a 90° slew, acquire guide stars, and start a new observation. For a smaller fraction of targets, the slew is shorter and the new observation can start sooner.

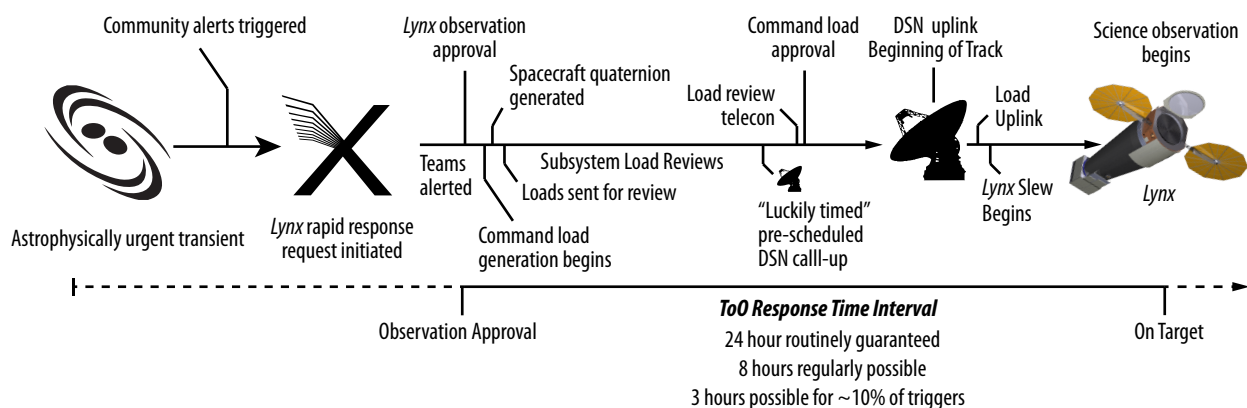


Figure 6.55. A summary of the technical and programmatic steps needed to plan, review, and uplink *Lynx* command loads following a ToO request. In some cases, the response time could be as short as three hours, though 24 is more typical.

6.7.3 On-Orbit Calibration

A set of standard celestial targets will be determined for on-orbit calibration use. These targets will be periodically observed to monitor the LMA, all science instruments, and aspect system performance. Calibration observations are planned, scheduled, and executed as part of Normal Pointing Mode operations (accompanied by Maneuver Mode slews) (see §6.7.2). Calibration measurements during the course of the mission science phase primarily monitor changes in performance characteristics such as detector background, energy resolution, energy gain, and filter throughput; grating line response function; system on- and off-axis PSF and optical alignment; and cross-calibration amongst the three *Lynx* science instruments. Some performance characteristics can be monitored parasitically using science observations without the need for separate calibration measurements. The same amount of calibration time as for *Chandra*, about 1 Ms per year, decreasing later in the mission to about 700 ks per year, has been budgeted for *Lynx*.

In addition, the HDXI and LXM contain in situ calibration sources that are mounted on their filter assemblies. Specifically, the LXM design includes a modulated X-ray source of pulsed X-rays at multiple energies similar to that used on *Athena*'s X-IFU [569] and *Hitomi*'s SXS [576]. The HDXI includes a radioactive ⁵⁵Fe source in its selectable filter mechanism. These onboard calibration sources allow calibration data acquisition during Normal Pointing Mode (see §6.7.2) when the given instrument is not being used as the primary instrument for an observation.

6.7.4 Ground Operations

All science and observatory data will be received, and all commands to *Lynx* will be generated by a co-located team of flight, science, and ground operations personnel. This team will be responsible for the spacecraft health and safety, carrying out all observational programs, monitoring and performing necessary maintenance, and retrieving and transmitting all data for processing, archiving, and distribution.

Several ground operations teams are necessary to plan *Lynx* operations and to process science data collection and distribution:

- The **Flight Operations Team** schedules, plans, generates spacecraft command sequences, uplinks, verifies spacecraft commands, and monitors real time data during communications with *Lynx*. The team performs engineering analysis of subsystems and diagnoses anomalies.
- The **Science Operations Team** is responsible for planning the mission schedule sequence by optimally scheduling targets provided by the *Lynx* user community. That team specifies the science instrument configuration for each observation and conducts on-orbit scientific instrument monitoring and calibration.
- The **Science Planning Team** coordinates with observers and with the staffs of other observatories to carry out coordinated multi-wavelength campaigns and to perform simultaneous observations.
- The **Science Data Team** performs standard data processing (with scientific validation and verification), archiving of data products, and distribution to the *Lynx* community, maintenance and distribution of calibration products and analysis tools, and archival search and retrieval services.

- The **Ground Operations Team** is responsible for supporting and maintaining all ground support hardware and software facilities used for scheduling, commanding, data flow, archiving, and communications. This includes facility infrastructure upkeep, network integrity, and facility security. Redundant critical systems will be provided for at a physically separate site.

A schematic of the *Lynx* data flow is shown in Figure 6.56. Communication to the *Lynx* Observatory from the *Lynx* Science and Operations Center will be through the DSN. One hour of telemetering during one to three daily contacts are envisioned during normal operations. Following data receipt and quality check, housekeeping data will be forwarded to the flight operations team for monitoring and safety checks while all data will be transmitted to the science data team for processing.

By analogy to *Chandra*, and accounting for differences, it is estimated that the ground software system will include 1.2 million logical lines of code. Standard data processing proceeds via automated pipelines, controlled by a parameter file derived from the archive defining observer requirements.

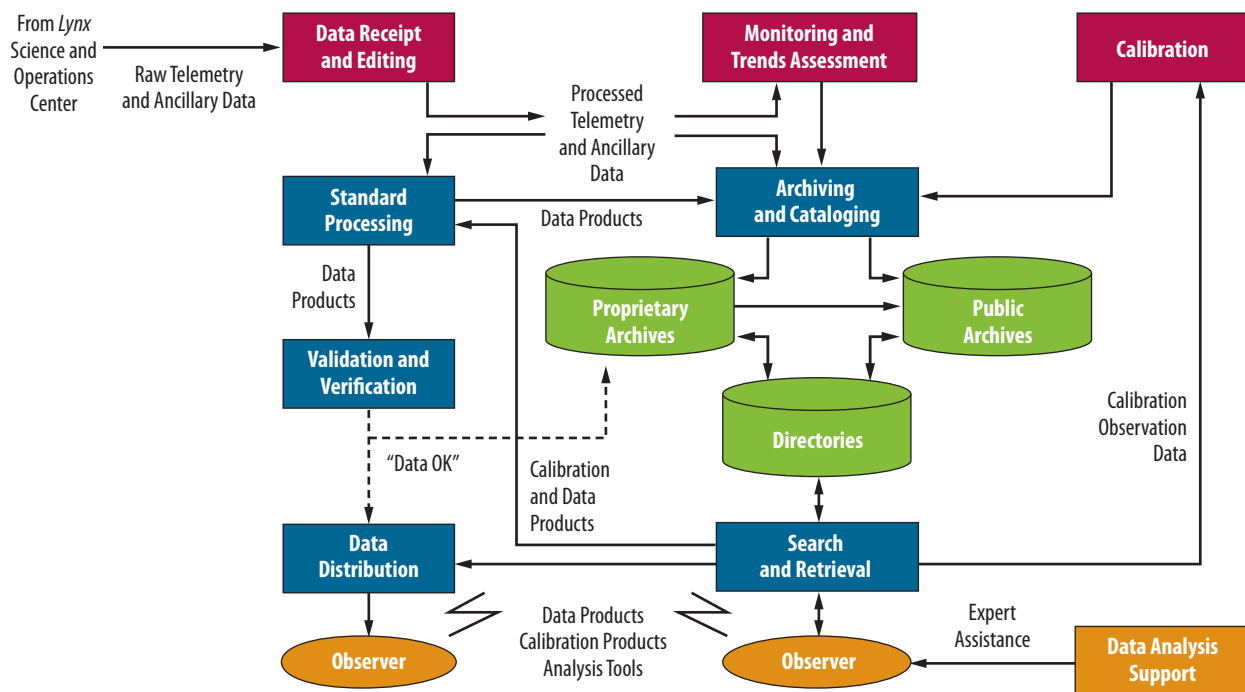


Figure 6.56. Data flow through the *Lynx* Science and Operations Center. Functional operations are performed by the science and the data operations teams, under the cognizance of the director's office.

Level 0 processing decommutates telemetry data. In Level 1 processing, the decommutated telemetry files have all camera events extracted (necessarily including both background and genuine X-ray photons), the aspect solution performed, and the time, celestial position, energy, and a quality flag tagged to each event. All products are archived and made available to the observer. In standard Level 2 processing, analysis tools are applied to generate a higher quality selection of celestial X-ray photon events. The Level 1 and 2 results go through an automated V&V process prior to ingesting into the archive and notifying the observer of their availability. Science-oriented software for data reduction and analysis will

comprise about one-third of the total data system. Processing tools will include the ability to model the mirror PSF as a function of energy and position at both low and high fidelities and the ability to model cosmic, instrumental, and in situ particle-induced backgrounds. ATOMDB [586] or a successor will be integrated with the analysis system to provide spectral line identifications and to model thermal plasmas. Tools will allow model fitting of spectra and of spatial structure. The data archive, data management, ingest, and distribution functions will comprise about one-third of the data system. This includes protection of proprietary data, the pipeline control software, search and retrieval tools, and interfaces to mirror archives. Remaining software will provide for proposal solicitation, management, planning, and peer review infrastructure, as well as science mission planning and scheduling tools.

Operations software will take advantage of Commercial Off-The-Shelf (COTS) systems for data transmission, raw data storage, communications, and assistance with mission planning and scheduling. Operations personnel will modify and configure these systems for *Lynx*-specific characteristics. A command and telemetry database will be developed and maintained. Software will monitor real time data, check for limit violations, and send out appropriate automated notices as needed. Monitoring and trends tools will provide data to subsystems engineers for detailed spacecraft performance assessment.

Table 6.16 from §6.4.6 shows the telemetry rates and data volume from the expected focal plane detectors. With the CCSDS packetization, the instantaneous data rates are allowed to exceed the telemetry downlink capacity so long as the onboard memory storage capacity of 480 Gbits is not exceeded. Only a very few sources will approach the maximum data rates shown in the table. Observations will be scheduled so that the daily average telemetry does not exceed 240 Gbits so that it can be downlinked at the 22.2-Mbps rate in three 1-hour contacts per day.

6.7.5 Serviceability

The science opportunities enabled by *Lynx* are greatly enhanced by its long mission lifetime. *Lynx* has been designed and provisioned to operate for 20 years at SE-L2 without significant reduction in capability, and with sufficient redundancy of key systems. Robotic serviceability will further help to ensure this long lifetime and could extend it further. To the extent practical under this study, the *Lynx* team has considered and incorporated robotic servicing design elements into the Observatory, consistent with guidance provided by the Satellite Servicing Projects Division (SSPD) at GSFC and the congressional mandate for all future observatory-class scientific spacecraft to include servicing.[†]

Lynx Observatory servicing is enabled primarily using “cooperative servicing aids” in the areas of remote survey, Rendezvous and Proximity Operations (RPOs), and capture to enable refueling and refurbishment (Figure 6.57). These servicing aids include standard interfaces and designs that are universally applicable to all new satellite missions, and are described in detail in [587].

Remote Survey — Allows the Observatory to be inspected from a distance in order to diagnose issues. *Lynx* will include retroreflectors installed on the tips of the antennas and solar panels, the OBA, and ISIM to facilitate this.

[†] Public Law 111-267-Oct. 11, 2010, 124 Stat. 2833, Sec. 804. In-Space Servicing [<https://www.congress.gov/>]

RPO — Rendezvous with a servicing satellite is enabled by the inclusion of specifically designed fiducial labels that are placed strategically across the Observatory. Once the servicing satellite is within 100 m of *Lynx*, proximity operations can commence (following capture). Prior to launch, closeout detailed photos using optical and IR will be taken of the Observatory at the launch site, with servicing in mind. Additionally, the forward *Lynx* sunshade door is designed to close in order to mitigate contamination of the optics from robotic servicing vehicle thruster plumes.

Capture — Standardized grapple fixtures will be installed on the forward and aft regions of the Observatory for easy capture by the servicing spacecraft. An external grounding point will be added to mitigate potential electrical differences between *Lynx* and the servicing spacecraft. During the detailed design phase, *Lynx* will consider implementing yet-to-be determined techniques to accommodate on-orbit loads during capture. While captured, refueling is possible with standardized valves designed specifically for robotic refueling [588], and MLI panels can be refurbished.

A more complete trade study will be carried out during pre-Phase A and Phase A and refined further as the *Lynx* design matures. This trade space will likely include (and is not limited to) spacecraft repair/replacements (e.g., thrusters and solar panels), replacing external sensors such as star trackers, repairing external mechanisms, and including test ports for on-orbit diagnostics. Designing for the replacement of the focal plane instruments is not practical based on their requirement to maintain translation and focus tolerances relative to the LMA and/or XGA, their integration into the ISIM translation stage, and in the case of LXM, its large mass. However, this could be revisited during the detailed design phase.

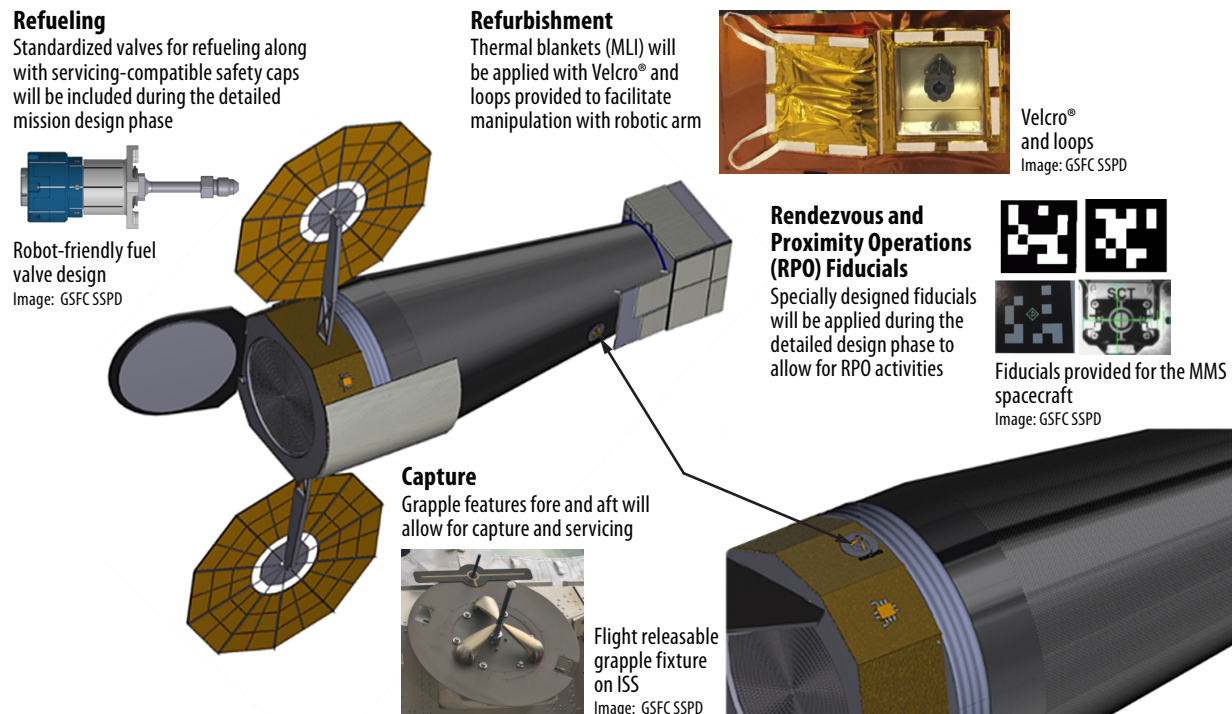
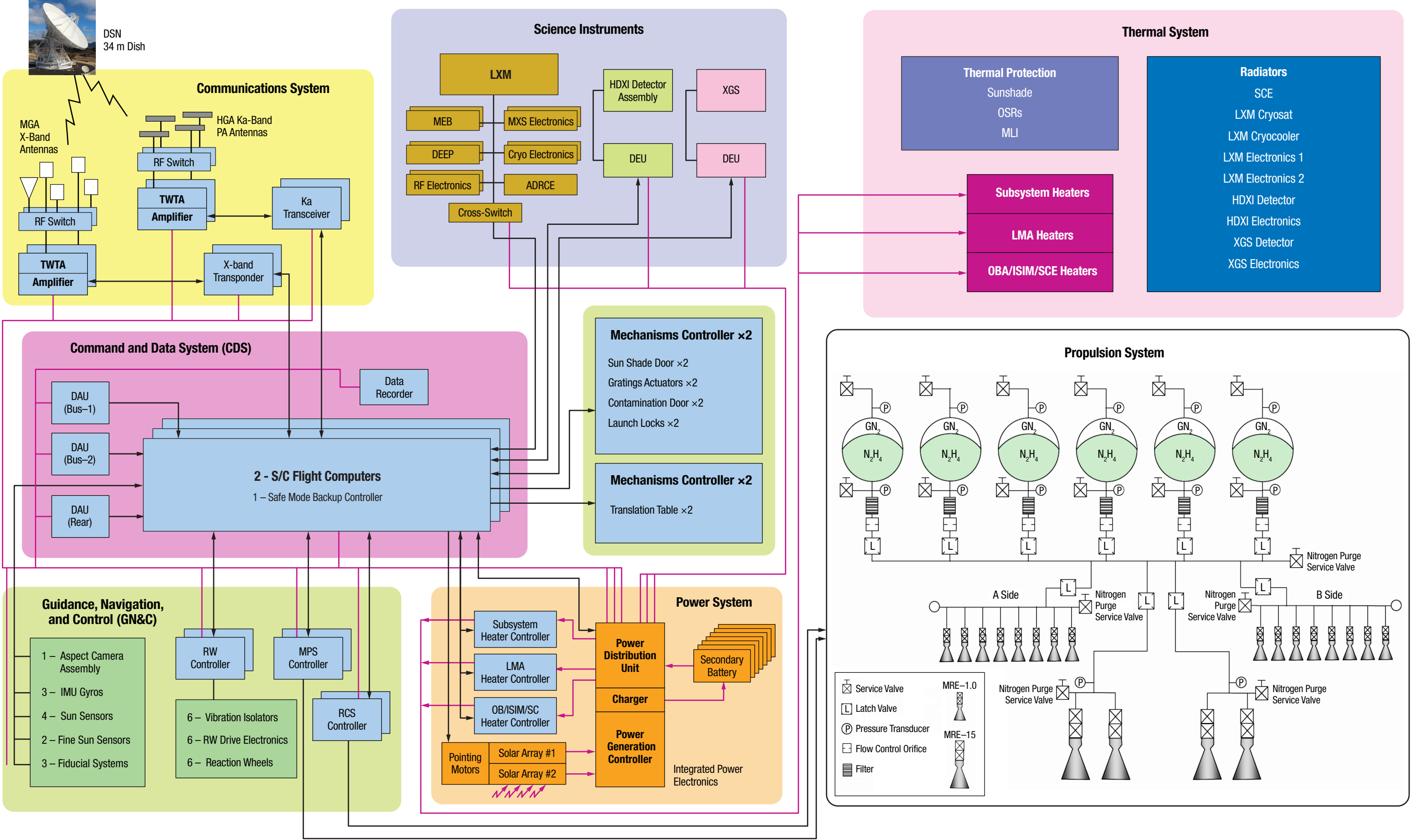


Figure 6.57. Future robotic servicing is enabled by incorporating servicing features into the *Lynx* design. Areas of servicing include remote survey, RPOs, and capture for refueling and MLI refurbishment.

6.7.6 End of Mission

After the 5-year baseline mission (with a potential extension up to 20+ years) of scientific discovery, *Lynx* will enter the end-of-mission operational phase. *Lynx* will comply with all applicable requirements in NASA-STD-8719.14, Process for Limiting Orbital Debris, and planning and compliance will be documented in an End of Mission Plan (EOMP). In the *Lynx* conceptual design, the delta-V budget and propellant load includes a disposal maneuver for end-of-mission. This will nudge *Lynx* out of its SE-L2 operational orbit and into a heliocentric disposal orbit. Although not required by NASA-STD-8719.14, *Lynx* can passivate (depletion of stored energy such as propellant and batteries) the Observatory to reduce future risk. After the operational mission is complete, the legacy of *Lynx* will live on in the archived scientific data, enabling astrophysical discoveries for years to come.

F02. Lynx System Block Diagram



F03. Lynx Mission Trace Matrix										
A. Mission Functional Requirements			B. Mission Design Requirements		C. Spacecraft Requirements		D. Ground System Requirements		E. Operations Requirements	
	Requirement	DRM Design Confirmation	Requirement	DRM Design Confirmation	Requirement	DRM Design Confirmation	Requirement	DRM Design Confirmation	Requirement	DRM Design Confirmation
1	Design for minimum observing efficiency of 85%	Verified by simulation of a realistic target sequence. Study of <i>Lynx</i> Observing Efficiency*	<ul style="list-style-type: none">• DRM requires 2.5 years to complete• Minimize on-orbit transients that reduce observing time• Provide propulsion to reach SE-L2, maintain orbit, and provide momentum management"	<ul style="list-style-type: none">• To meet the <i>Lynx</i> effective collecting area requirement requires nesting large numbers of thin, lightweight, co-aligned, co-axial mirrors in order to optimize the available aperture. 85% efficiency verified by simulation of a realistic target sequence. 6.1.2, 6.4.5, and Study of a <i>Lynx</i> Observing Efficiency*• Design of attitude control system, CDMS, propulsion system, and thermal system minimizes non-science time. Thermal system can control temperatures within science requirements at any allowable pointing attitude and throughout maneuvers.• Propulsion system has adequate propellant load and control authority. Sufficient momentum unloading prop allocation.*	<ul style="list-style-type: none">• Provide for attitude control• Provide ability to maneuver between celestial targets	<ul style="list-style-type: none">• <i>Chandra</i>-proven mission operations and infrastructure will be implemented to ensure efficient, queued observing scheduling; <i>Chandra</i>-like pointing attitude control, stability, and knowledge consistent with subarcsecond imaging. (6.1.1)• The reaction wheel configuration, consisting of 6 wheels, along with the attitude control system thrusters, and MIMUs, provide for 3-axis control. The MIMUs and reaction wheels are used to maneuver to science targets. (6.4.2)	<ul style="list-style-type: none">• Provide efficient mission planning and target sequencing• Derive aspect solution	<ul style="list-style-type: none">• <i>Chandra</i> legacies include adopting an updated, state-of-the-art pointing and aspect determination system conceptually identical to <i>Chandra</i>'s PCAD, and implementing the <i>Chandra</i> operations and mission planning paradigm. (6.1.2)• A PCAD system is integrated with the telescope and spacecraft to provide a highly accurate aspect solution and to control pointing and dithering. (6.2)	<ul style="list-style-type: none">• Acquire 1–20 targets/day• Provide for continuous data collection for 1–100 ks/target	<ul style="list-style-type: none">• The GN&C system maintains knowledge of the spacecraft orientation, controls the maneuvers required to orient desired celestial targets within the telescope FOV, and holds each target attitude for the command duration. (6.4.2)• Assuming a maximum disturbance torque of 0.00037 Nm, the accumulated momentum in 100,000 s of continuous observation is 37 Nm. The momentum capacity for the baseline 6-wheel pyramid is 59.5 Nm, providing >60% margin. This allows continuous target pointing to meet/exceed the requirement.*
2	Design for operation and survival in science orbit	Observatory designed to survive in radiation and thermal environment at SE-L2. Spacecraft systems are designed to provide a stable platform and maintenance of the halo orbit, as well as keep the observatory attitude within mission guidelines for Sun avoidance. Environments* and Thermal Control*	<ul style="list-style-type: none">• Provide solar power with battery storage• Provide propulsion for momentum-unloading maneuvers, station-keeping and EOL disposal• Design S/C surrounding X-ray mirrors to ease thermal management of the mirrors• Leverage hot/cold sides of observatory for thermal management• Design for Risk Class A• Provide for minimal on-orbit servicing• Provide for SE-L2 radiation and particle environment	<ul style="list-style-type: none">• The power system batteries are sized to provide adequate power during launch and ascent, including survival power to the payload, prior to solar array deployment, with 40% margin. Solar arrays are sized to provide the maximum needed observatory power for 20 years.*• Propellant load and propulsion systems were designed to meet the requirements that flowed from the science objectives to the mission and spacecraft, including EOL disposal maneuver.• The spacecraft thermal subsystem is designed to maintain the spacecraft and OBA at an average temperature of 283 K, which allows the LMA to maintain positive thermal control at 293 K. (6.4.4)"• The use of MLI with a hot-side sunshade provides positive thermal control of the telescope, and pointing constraints provide a cold-side location for radiators for the instruments and electronics. (6.4.4)• Spacecraft components are fully redundant, for any credible failure, where required to meet the risk standard.*• Grapple fixture, reflectors are located on the observatory. Sunshade door can close during servicing.*• Charged particles exist as an omnidirectional flux, a portion of which can be concentrated through the LMA directly onto the focal plane. Relatively low (~90 C) sensor operating temperature and shielding on the HDXI enclosure will be used to mitigate the ambient particle flux, and a magnetic diverter will be used to divert the charged particle flux away from the focal plane. Micrometeoroid environment was modeled and has a near-zero percent chance of degrading performance. (6.3.2.2)	<ul style="list-style-type: none">• Distribute needed power; peak <8 kW• Provide for communication with existing ground stations (DSN)• Maintain operating temperatures within required limits• Place instruments at optimum focus	<ul style="list-style-type: none">• Power system is designed to deliver 4430 W to the payload at the end-of-life (20 years), which includes a 40% power margin for the instruments and an overall payload power margin of 30.5%.*• For communications with the ground, <i>Lynx</i> will utilize NASA's existing DSN system to provide telemetry, tracking, and command, ensuring high reliability and high data rate for communications for downloading its science and spacecraft health data and uplinking commands. (6.4.6)• Cooling for the sensor array is through a cold strap connection between the sensor array that conductively coupled to a SiC mosaic plate and the enclosure. The enclosure, along with its thermal load from the rest of the instrument through heat pipes that move along with the translation table. (6.3.2.1)• Strong space flight heritage (high TRL) and flight heritage mechanisms will be employed for focal plane instrument translation and focusing and for grating array insertion and retraction. (6.1.2)	<ul style="list-style-type: none">• Monitor health and safety of observatory• Provide for on-orbit calibration	<ul style="list-style-type: none">• All science and observatory data will be received and all commands to <i>Lynx</i> will be generated by a co-located team of Flight, Science, and Ground operations personnel. The team is responsible for the spacecraft health and safety, carrying out all observational programs, monitoring and performing necessary maintenance, and retrieving and transmitting all data for processing, archiving, and distribution. (6.7.4)• A set of standard celestial targets will be determined for on-orbit calibration use. These targets will be periodically observed to monitor LMA, all science instruments, and aspect system performance. (6.7.3)	<ul style="list-style-type: none">• Maintain 45 degree Sun avoidance• Command instruments for data collection and standby• Restrict roll angle to manage thermal environment• Store commands for up to 72 hours autonomous operation	<ul style="list-style-type: none">• Observations will be checked by the mission planning software to ensure observations remain outside the Sun-avoidance angle, and maneuvers between targets will be designed to avoid even momentary entry into this region.• The avionics equipment located in the <i>Lynx</i> spacecraft is designed to perform the functions of GN&C, thermal control, power switching, data storage, command management, and uplink of commands and downlink of data. (6.2, 6.4.5)• Thermal analysis informed the design such that this requirement is met.*• On board flight computer RAD750 can perform autonomous operations with flight control and operations software uplinks to non-volatile memory.*
3	Design for accommodation of payload in launch vehicle	Payload meets mass, and static and dynamic envelope requirements for generic heavy-class launch vehicle for the 2030s, as defined by LSP. Spacecraft, optical bench, and integrated science instrument module structure are sized to survive the launch environment as specified for Delta IV Heavy. See Section 6.4 and Configuration*	<ul style="list-style-type: none">• Design for NASA-provided LV per LSP recommendations• Design to survive launch: fit w/ in static and dynamic envelope defined by LV; exceed minimum modal frequency requirements for LV	<ul style="list-style-type: none">• Baseline configuration sized to fit within the LSP Future Heavy payload dynamic envelope provided.*• Observatory mass, volume, and dynamic analysis make <i>Lynx</i> compatible with multiple anticipated future heavy-class launch vehicles expected to be available in the 2030 timeframe including, the Space Launch System. (6.1.1)	Battery power until solar array deployment	Energy storage is provided via five 28-V batteries with one additional battery to ensure single fault tolerance. The batteries are sized to provide launch power (743 W) for 156 minutes from launch to the completion of initial checkout and solar array deployment, and for 5 minutes of survival mode. (6.4.3)	Plan initial on-orbit activation and checkout	For 156 minutes following launch, <i>Lynx</i> will rely on batteries to power minimal spacecraft systems, survival heaters for critical telescope elements, and to deploy the solar panels. During travel to SE-L2, the spacecraft and telescope systems are powered up, allowed to outgas, and undergo system checks and initial calibration. (6.7.1)	<ul style="list-style-type: none">• Maintain optics and instruments in low-power mode prior to solar array deployment• Instrument initial V&V	<ul style="list-style-type: none">• Energy storage is provided via five 28-V batteries with one additional battery to ensure single fault tolerance. The batteries are sized to provide launch power (743 W) for 156 minutes from launch to the completion of initial checkout and solar array deployment, and for 5 minutes of survival mode. Power will be provided to all attached architecture elements during initial checkout (2.6 hours) and solar array deployment per power schedule. Full power will remain available during final orbit insertion. (6.4.3.3*)• For 156 minutes following launch, <i>Lynx</i> will rely on batteries to power minimal spacecraft systems, survival heaters for critical telescope elements, and to deploy the solar panels. During travel to SE-L2, the spacecraft and telescope systems are powered up, allowed to outgas, and undergo system checks and initial calibration. (6.7.1) Note that the L2 halo orbit has no eclipse time to interrupt solar panel provided power.

*DRM Supplemental Design Package

F03. Lynx Mission Trace Matrix *continued*

A. Mission Functional Requirements			B. Mission Design Requirements		C. Spacecraft Requirements		D. Ground System Requirements		E. Operations Requirements	
	Requirement	DRM Design Confirmation	Requirement	DRM Design Confirmation	Requirement	DRM Design Confirmation	Requirement	DRM Design Confirmation	Requirement	DRM Design Confirmation
4	Provide data collection that is sufficient for uninterrupted observations by all science instruments	On board computer provides for 1 Tbit of onboard data storage. Comm plan allows for sufficient downlink of data to satisfy maximum expected data rates from instruments, with margin. See Section 6.4.6 and C&DH*	<ul style="list-style-type: none">• Use existing DSN ground station for communications• Use Ka-band for science data downlink (per SCan guidance)• Use X-band for command uplink and engineering up/downlink	<ul style="list-style-type: none">• For communications with the ground, <i>Lynx</i> will utilize NASA's existing DSN system to provide telemetry, tracking, and command, ensuring high reliability and high data rate for communications for downloading its science and spacecraft health data and uplinking commands. (6.4.6)• A flight-heritage communication system will be baselined, similar to that used on the Mars Reconnaissance Orbiter, which supports data volumes up to 270 Gbits/day. The <i>Lynx</i> communication system will utilize the high heritage Ka-band for science data downlink. (6.4.6)• The <i>Lynx</i> C&DH system baselines X-band for low-rate uplink and backup telemetry. (6.4.6)	<ul style="list-style-type: none">• 6 Mbps maximum instantaneous data collection rate• 1 Tbit onboard data storage• Provide for 240 Gb downlink/day• Translate science instruments to/ from primary aim point• Insert/retract XGS	<ul style="list-style-type: none">• Using a standard 10Base-T Ethernet bus supports 10 Mbps rates.• Included in the Avionics equipment is a 1 Tbit mass data storage device, which provides 100% redundancy.• Following a <i>Chandra</i>-like DSN schedule of 3 one hour links per day at 22 Mbps achieves the 240 Gbits per day downlink requirement.• HDXI and LXM, along with their electronics and radiators, are mounted on a moveable platform that is part of the ISIM. The translation table assembly permits either instrument to be placed on-axis. (6.3)• On-board mechanisms will all have strong space flight heritage (high TRL) and flight heritage mechanisms will be employed for focal plane instrument translation and focusing and for grating array insertion and retraction. (6.3)	<ul style="list-style-type: none">• Plan Normal (Science) Mode program• Provide L0 data to the• Operations Center with < 72 hours latency.• Provide for data archival, retrieval, and distribution to public• Plan instrument configuration to avoid excessive data collection	<ul style="list-style-type: none">• <i>Lynx</i> will be primarily in normal pointing mode conducting an autonomous pre-planned program of celestial observation. The telescope optical axis is pointed within 10 arcsec of a commanded celestial position, which is assured by locking on pre-planned stars at specific positions in the aspect of the star camera. (6.7.2)• The 1 Tbit of on board memory stage provides a latency capability which exceeds the 48 hour requirement.*• All <i>Lynx</i> science instruments are photon counting detectors that accumulate event based time, position and energy data that are accumulated and temporarily stored on board before being periodically telemetered to the ground where it is processed, archived, and distributed to the scientific community. (6.7)• The Science Operations Team is responsible for planning the mission schedule sequence by optimally scheduling targets provided by the <i>Lynx</i> user community. That team specifies the science instrument configuration for each observation and carries out on-orbit scientific instrument monitoring and calibration. The Science Data Team performs standard data processing, archiving data products, and distribution to the <i>Lynx</i> community, maintenance, and distribution of calibration products and analysis tools, and archival search and retrieval services. (6.7.4)	Follow Normal (Science) Mode pre-planned observing program	<i>Lynx</i> will be primarily in normal pointing mode conducting an autonomous pre-planned program of celestial observation. The telescope optical axis is pointed within 10 arcsec of a commanded celestial position, which is assured by locking on pre-planned stars at specific positions in the aspect of the star camera. (6.7.2)
5	Design for 5-year mission	All Observatory systems designed for on-orbit life of at least 5 years with margin and not to preclude 20 years. See Section 6.4.1; Propulsion*	<ul style="list-style-type: none">• Provide consumables for up to 20 years contingency• Provide for robust safe modes system	<ul style="list-style-type: none">• Prop load is sized for 20 year mission, including momentum unloading and station-keeping.*• An internally redundant Safe Mode Electronics Unit (SMEU) is included to allow the observatory to autonomously slew to a safe Sun angle in the event of out of range on-board parameters. Safe mode control will include a separate set of control processing electronics that operate with different software. (6.4.5, 6.4.6)						
6	Provide pointing control of the optical axis at desired targets.	Pointing and propulsion systems were designed to meet the requirements that flowed from the science objectives to the mission and spacecraft. The design of the OBA and its attachments to the LMA and ISIM minimize telescope boresight variation. See Section 6.3.6, 6.4.2, and GN&C*	<ul style="list-style-type: none">• Photon counting science instruments to record time, position, and energy for each event• Limited optical bench length variation keeps image in focus, and lateral boresight variation is tracked with a fiducial light system• Stability 0.17 arcsec/sec	<ul style="list-style-type: none">• All <i>Lynx</i> science instruments are photon counting detectors that accumulate event-based time, position and energy data that are accumulated and temporarily stored on board before being periodically telemetered to the ground where it is processed, archived, and distributed to the scientific community. (6.7)• OBA is made of a low CTE material to minimize length variation and potential "hot-dogging" due to maneuvers changing the temperature profile, and the sunshield maintains cold-bias for positive heater control. Bipod struts to LMA are an a thermalized design and temperature-controlled, as is the flexure connection to the ISIM• The pointing control system incorporates hardware that has equivalent or better performance than the <i>Chandra</i> PCAD system, which allows the observatory to meet this requirement.*	<ul style="list-style-type: none">• Pointing attitude to 10 arcseconds absolute• On-board knowledge 4 arcseconds	<ul style="list-style-type: none">• The reaction wheel configuration, consisting of 6 wheels, along with the attitude control system thrusters, and MIMUs, provide for 3 axis control. 3-axis reaction wheel typically provides pointing accuracy of +/- 0.0001 deg (0.36 arcsec).*• Sensor suite includes Inertial Measurement Unit 3x plus High Accuracy Star Tracker for state updates (+/- 0.2 arcsec/axis, 1 sigma).*	<ul style="list-style-type: none">• Post facto image reconstruction consistent with 0.2-arcsecond RMS system accuracy• Absolute celestial location to 1 arcsecond	<ul style="list-style-type: none">• A <i>Chandra</i>-like PCAD system is integrated with the telescope and spacecraft to provide a highly accurate aspect solution and to control pointing and dithering. (6.2)• The GN&C system maintains knowledge of the spacecraft orientation, controls the maneuvers required to orient desired celestial targets within the telescope FOV, and holds each target attitude for the command duration. (6.4.2)	Monitor exact pointing attitude history and spacecraft alignment	The <i>Lynx</i> GN&C system has adopted <i>Chandra</i> heritage PCAD system. To hold the target attitude, the star camera acquires and tracks known guide stars in the target vicinity, the MIMUs monitor rotational and translational drift rates, and reaction wheels are commanded to spin, as needed, to compensate for disturbance torques. (6.3.6, 6.4.2)

*DRM Supplemental Design Package

7 Lynx Technology Development

The *Lynx* X-ray mirror assembly and three science instruments are the critical technologies that will enable the *Lynx* Observatory's revolutionary science. To date, significant development efforts have advanced these technologies to a Technology Readiness Level (TRL) of 3 or higher based on non-advocate estimates. Credible and executable technology development plans are in place to advance all components of these technologies to TRL 5 by the start of Phase A and to TRL 6 by the Preliminary Design Review. These plans have been independently and objectively assessed with respect to risk, cost, and schedule. These *Lynx* technology development plans will ensure that the telescope optics and instrument systems meet the scientific performance and programmatic requirements for the *Lynx* Observatory.

7.1 Four *Lynx*-Enabling Technologies

The *Lynx* Observatory will require the development of four enabling technologies: an X-ray mirror assembly and three science instruments. For purposes of in-depth cost, schedule, and system integration evaluation, the Silicon Meta-shell Optics, the hybrid Complementary Metal-Oxide Semiconductor (CMOS) High-Definition X-ray Imager (HDXI), the Critical-Angle Transmission (CAT) X-ray Grating Spectrometer (XGS), and the *Lynx* X-ray Microcalorimeter (LXM) have been designated as the Design Reference Mission-enabling technologies. (§6) These technologies have matured significantly and are all currently at TRL 3 or higher, with some elements or components at a higher TRL, as assessed by the most recent Physics of the Cosmos (PCOS) Technology Management Board assessment in 2019. In addition, multiple credible technology options are being independently developed for each of these four technologies (or for components of these technologies). Cultivating multiple technology options at this time will significantly diminish risk to the project.

Each technology contains several key elements that require maturation to TRL 6. Complete development plans for each technology (a.k.a., technology roadmaps) have been developed and are included as supplements to this report. The *Lynx* technology maturation plans were developed by expert teams—often with participation across multiple academic, industrial, and government institutions. The technology plans follow the development paths from the current State of the Art (SOA) to TRL 5 by the start of Phase A (Key Decision Point- (KDP-) A: October 1, 2024) and to TRL 6 by Preliminary Design Review (PDR): February 1, 2028). This schedule assumes a launch date of November 2036, technology development funding starting three years prior to KDP-A (FY22), and final architecture selection beginning eight months prior to KDP-A (§8.4). At currently anticipated funding levels, most enabling Design Reference Mission (DRM) technologies are expected to achieve TRL 4 by the start of directed funding, and there are no known fundamental physical challenges to reaching TRL 6 for any *Lynx*-enabling technology.

While this report is focused on the specific technologies selected for the DRM, the *Lynx* team recognizes the risks inherent in developing specialized technologies with characteristics that are beyond the SOA. For this reason, the program is supporting parallel “alternate technology” efforts for the mirror assembly and all three science instruments (or components of instruments) for the purpose of risk reduction. These include two alternate X-ray mirror assembly architectures—called the Full Shell Optics and the Adjustable Segmented Optics—and an alternative feasible XGS technology: the Off-Plane X-ray Grating Spectrometer (OP-XGS). Complete technology development plans for these three alternates are provided as supplements to this document. The HDXI development plan includes two architectures in addition to the hybrid CMOS technology: the monolithic CMOS and the advanced “digital” Charge-Coupled Device (CCD). All three HDXI technologies are included within a single development plan because, while they differ in architecture, they are nearly identical in functionality and require similar Observatory resources and interfaces. The LXM development plan includes alternative technologies for thermal sensor, readout multiplexing, and cryocooler subsystem components.

All the *Lynx* technology development plans present reviews of the SOA; descriptions of the technical elements being developed, tested, and verified; statements of TRL 4, 5, and 6 specific to each technology; assessments of the key milestone elements (with Advancement Degree of Difficulty (AD²) evaluations[†] [626]) needed to advance each technology to successive TRL levels; and estimates of the associated schedules, costs, risks, and risk mitigations. In addition, a special section of the *Journal of Astronomical Telescopes, Instruments, and Systems* (JATIS Vol. 5(2), 2019) dedicated to *Lynx*-enabling technologies provides 20 open-access refereed articles with additional information on *Lynx* technology development plans.

Table 7.1 summarizes the enabling *Lynx* DRM technologies, their SOAs, the specific *Lynx* requirements driving their development, top-level challenges to advance their *Lynx*-specific TRLs, and a synopsis of the milestone(s) for TRL advancement to the next level. The following subsections highlight the most challenging technology development elements for each enabling technology.

The combination of significant relevant heritage and high current SOA ensures that further technology development for all four *Lynx*-enabling technologies is well within the experience base with a high degree of confidence that TRL 6 can be achieved with low schedule and cost risk. All technologies have analytically and experimentally demonstrated critical function and characteristic proof-of-concept while validating model predictions of key parameters.

The *Lynx* team recognizes the complex interrelationship among these four enabling technologies and the need to demonstrate required performance at a system level early in the development schedule. The natural juncture in the *Lynx* project development schedule for such a demonstration matches the X-ray mirror assembly and the X-ray Grating Array (XGA) TRL 6 maturation point in early 2027. A joint TRL 6 demonstration combining a mirror engineering unit—with representative components spanning the full range of the *Lynx* aperture diameters, with a complementary grating array portion of the XGS—is planned at this time in the program schedule. X-ray performance and environmental tests of this engineering model are planned at NASA Marshall Space Flight Center’s (MSFC’s) X-ray and Cryogenic Facility to accommodate the test article’s large size. Ground Support Equipment (GSE) will be used for mirror and grating array X-ray performance.

[†]AD2 is a bottoms-up assessment of the anticipated difficulty over the course of a technology maturation project. AD2 is determined through consideration of cost, schedule, and risk with a resulting value on a scale of increasing difficulty from 1 to 9.

Table 7.1. *Lynx*-enabling technologies requiring technology maturation.

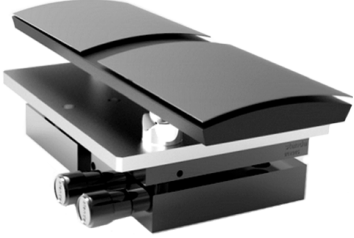
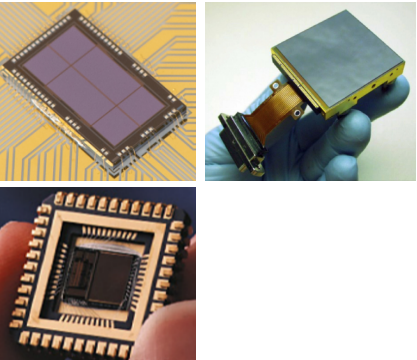
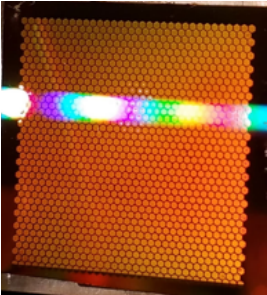
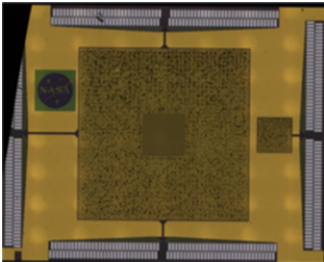
Technology	Function	Development Challenges	Development Path	AD2 - Rationale
Lynx Mirror Assembly (LMA) 	<p>Silicon Meta-shell Optics – Modular design with many thousands of thin, lightweight mirror segments integrated (via modules/meta-shells) into the <i>Lynx</i> Mirror Assembly</p> <p>Current TRL = 3</p>	<ul style="list-style-type: none"> • Demonstrate a reliable fabrication process to mass produce quality mirror segments • Verify processes for assembling the required 611 mirror modules • Demonstrate assembly processes for 12 meta-shells • Demonstrate final assembly, alignment, and testing processes 	<ul style="list-style-type: none"> • Develop alternate mirror technologies in parallel with baseline • Fabrication, alignment, coating, bonding, and qualification of single-mirror segment pairs (TRL 4) • Fully populating and qualifying multiple mirror modules and a single meta-shell (TRL 5) • Assembly and qualification testing of subscale (3 meta-shell) engineering model <i>Lynx</i> Mirror Assembly (TRL 6) 	<ul style="list-style-type: none"> • TRL 4: $AD^2 = 3$ – All required fabrication processes (substrate, coating, bonding, alignment) demonstrated, process refinement for mass production to be developed • TRL 5: $AD^2 = 3$ – Alignment and bonding processes will carry over from TRL 4 development; iterative fabrication assembly process required to ensure throughput and environmental survivability is straightforward • TRL 6: $AD^2 = 3$ – As with TRLs 4 and 5, this is a relatively straightforward (albeit intricate) assembly, fit, and test phase that will likely require iterations; No fundamental barriers are apparent.
High-Definition X-ray Imager (HDXI) 	<p>Imaging spectrometer leveraging pixelated silicon sensor technology heritage from many ground- and space-based applications</p> <p>Current TRL = 3</p>	<ul style="list-style-type: none"> • Provide excellent low-energy X-ray response (high quantum efficiency) and fine spatial resolution at high frame rates • Demonstrate low detector noise, high pixel-to-pixel response uniformity, and reliable readout processing 	<ul style="list-style-type: none"> • Demonstrate required sensor (with Application-Specific Integrated Circuit (ASIC)) noise, resolution, and quantum efficiency at high and low energies in representative multichannel sensor • Demonstrate required performance of integrated sensor/ASIC system of representative size before and after environmental testing • Demonstrate required performance of ¼-size focal plane in relevant environment before and after environmental testing 	<ul style="list-style-type: none"> • TRL 4: $AD^2 = 5$ – Optimization of pixelated silicon sensors and ASICs is standard industry practice, but all science requirements must be demonstrated on a single custom sensor; may require long lead-times • TRL 5: $AD^2 = 2$ – Integrating a sensor/ASIC and associated readout electronics for evaluation to TRL 5 is largely an engineering activity • TRL 6: $AD^2 = 2$ – Combining multiple sensors and ASICs into an engineering model focal plane of pixelated silicon sensors has high heritage from many missions

Table 7.1. Continued

Technology	Function	Development Challenges	Development Path	AD2 - Rationale
X-ray Grating Spectrometer (XGS) Very high resolving power, dispersive, soft X-ray spectrometer optimized for efficiency at astrophysically critical atomic line energies Current TRL = 4 	Provide high-throughput, very high resolving power, dispersive spectroscopy to meet <i>Lynx</i> science goals for bright, point-like sources	<ul style="list-style-type: none"> Fabricate high-efficiency diffraction gratings (thin grating bars but deep device layers with low support structure obscuration) Advance metrology for alignment and mounting to preserve energy resolution (Line Spread Function (LSF)). Develop “chirped” gratings to maintain LSF of large grating facets 	<ul style="list-style-type: none"> Develop alternate grating array technology in parallel with baseline Increase depth and decrease width of grating bars using Deep Reactive-Ion Etching and KOH polishing solution Leverage experience from past mission development as foundation for alignment metrology and assembly Build toward TRL 6 large-scale prototype matched to LMA TRL 6 demonstrator 	<ul style="list-style-type: none"> TRL 5: $AD^2 = 3$ – Fabricating grating membranes with reduced structural obscuration is an incremental development but must pass environmental tests; conception and implementation of metrology infrastructure for mounting and alignment in brassboard is new development. TRL 6: $AD^2 = 3$ – Fabricating larger grating membranes with designed grating bar widths and period chirp will leverage semiconductor and Micro-Electrical Mechanical Systems (MEMS) industry practices – most development is incremental
Lynx X-ray Microcalorimeter (LXM) Large-format fine pixel microcalorimeter with three pixel array types providing a large range of scientific capabilities Current TRL = 3 High-bandwidth microcalorimeter readout Current TRL = 3 Focal Plane Assembly (FPA) and Optical Photon Blocking Filters Current TRL = 4 Cryogenic cooling system Current TRL = 4 	Provide high-spatial resolution energy dispersive imaging capabilities to meet multiple <i>Lynx</i> science goals	<ul style="list-style-type: none"> Reduce slew rates for the thermal multiplexed pixels to adequately match the readout capabilities of the μMUX readout Reduce thermal crosstalk Avoid substantial energy degradation from crosstalk in readout circuitry at relevant mux factors Advance cryocooler and ADR technologies to required TRL within schedule and budget 	<ul style="list-style-type: none"> Develop alternate sensor technology in parallel with baseline Fabricate heat-sinking of arrays with buried wires through multiple approaches to achieve best thermal crosstalk reduction Design readout components and operational parameters (e.g., tone power to amplifiers) to mitigate crosstalk Leverage <i>Athena</i>'s X-ray Integral Field Unit (X-IFU) development for <i>Lynx</i> Focal Plane Array Utilize two independent industry-based cryocooler design and development paths and choose best option 	<ul style="list-style-type: none"> TRL 4: $AD^2 = 3$ – Existing TES-based arrays lack only standard testing; μMUX readout needs optimization for bandwidth required – testing/modeling efforts indicate no fundamental design limits for LXM TRL 5: $AD^2 = 3$ – Arrays require advancement in heatsinking – buried wire technology scale-up straightforward; significant carryover from ongoing development efforts for multiple terrestrial applications expected for readout advancement ($AD^2 = 4$); cryocooler advancement requires funding investment TRL 6: $AD^2 = 2$ – Straightforward engineering advancement of arrays to full size; readout integration into new FPA geometry is $AD^2 = 4$; new FPA is an engineering effort leveraged from <i>Athena</i> ($AD^2 = 3$) – blocking filter sizing and environmental testing not a technical challenge; cryocooler straightforward optimization between structural and thermal performance

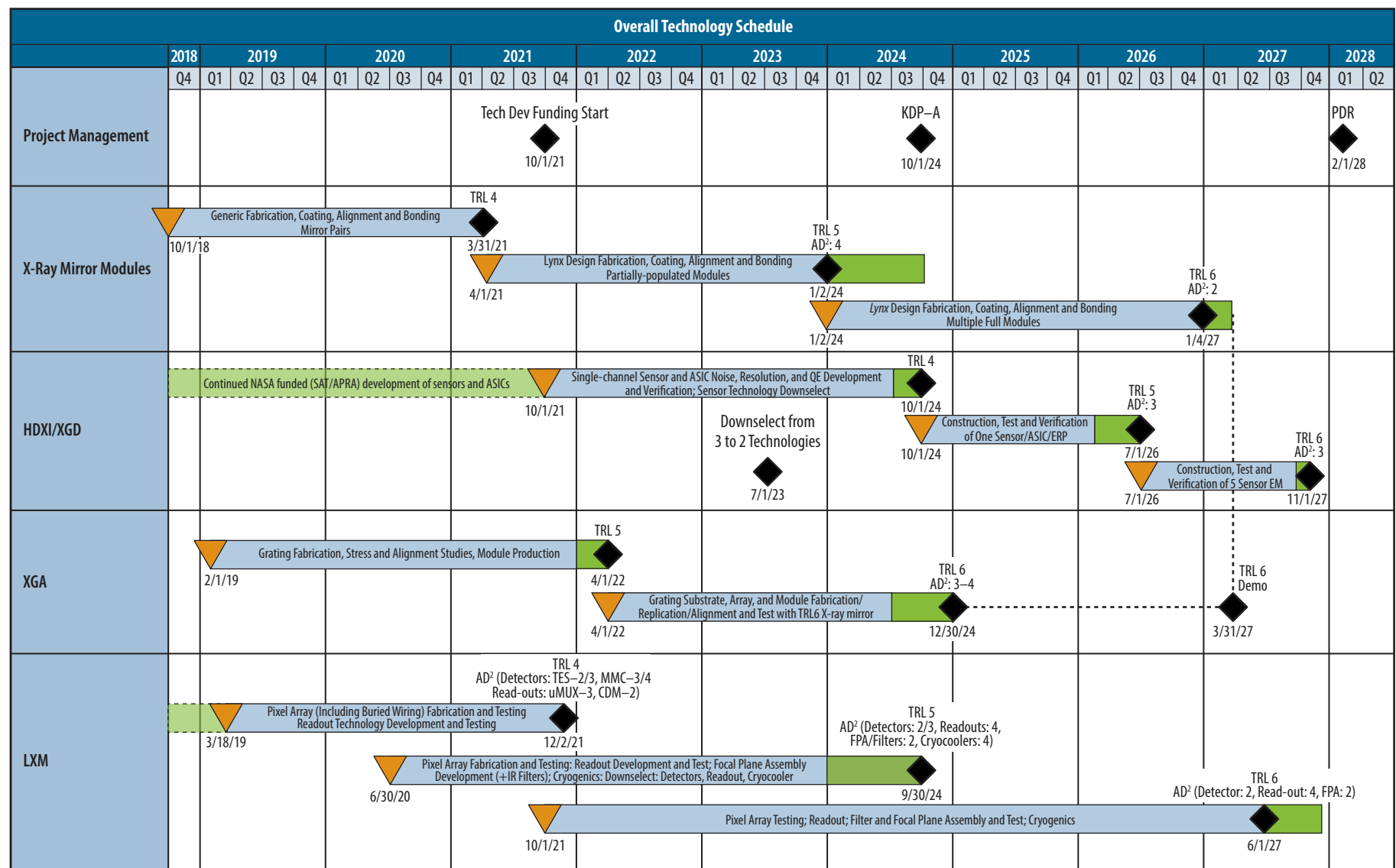


Figure 7.1. Development schedule to mature four *Lynx* enabling technologies to TRL 6 by mission PDR.

Figure 7.1 displays the overall project schedule (including margins) for developing the four DRM technologies to TRL 6 prior to PDR. The schedule is the result of grassroots analyses by the individuals and organizations active in the respective technology development efforts and reflect realistic estimates of workload, procurement lead time, and funding profiles as detailed in the supplemental development plans for each technology. A full project schedule is given in §8.4, and each technology development plan supplement provides schedules detailing individual development milestone tasks.

Most enabling DRM technologies will achieve TRL 4 by the start of directed funding, which is expected to begin in FY22. The exception is the HDXI, whose early technology progress is through iterative cycles of design improvement and fabrication. Anticipated funding allows only a few development cycles to be completed up to and during the pre-Phase A period, leading to a longer development path to TRL 4. In contrast, developing the HDXI to TRL 5 and 6 will be rapidly advanced.

All technologies described in this report are currently funded by NASA and other sources. Grassroots technology development (directed) and Phase A cost estimates are given for each *Lynx* technology in their individual technology development plans. The required funding estimated for the three-year pre-Phase A period for the four enabling technologies is in-family with *Wide Field Infrared Survey Telescope (WFIRST)* estimations, with Phase A funding estimated at a comparable level.

7.2 Optics Development

Lynx X-ray mirrors must enable leaps in sensitivity, spectroscopic throughput, survey speed, and most importantly, imaging performance over past or planned missions. Because of this critical significance, the *Lynx* team performed a comprehensive technology assessment trade study (Appendix B.2.1) of three X-ray optics technologies. The study evaluated each approach's ability to meet *Lynx* science requirements, their capacity for overcoming technical challenges, and the validity of their schedule, cost, and risk estimates. The study recommended the Silicon Meta-shell Optics assembly architecture (§7.2.1) to focus the Observatory DRM while maintaining the Full Shell Optics (§7.2.2) and the Adjustable Segmented Optics (§7.2.3) architectures as feasible alternatives. The study cited Silicon Meta-shell Optics as being the most mature of the three technologies with the shortest path to achieving TRL 5 and 6. Comprehensive technology development plans for all three architectures are provided in the supplemental documentation.

7.2.1 Silicon Meta-shell Optics

The DRM optics design for *Lynx* employs a highly modular approach to building, testing, and qualifying a mirror assembly [589]. In this approach, tens of thousands of similarly dimensioned, ~100- \times -100- \times -0.5-mm, lightweight mirror segments (and nonreflecting stray light baffles) are integrated into mirror modules by attachment (directly or indirectly) via other mirror segments onto module mid-plates. The mirror modules, in turn, are integrated into full-circumference meta-shells of different diameters before finally being integrated to create the *Lynx* X-ray mirror assembly (§6.3.1.1). The technology development

plan follows this hierarchy by first refining four technology elements through repetition: (1) fabrication, (2) coating, (3) alignment, and (4) bonding of single pairs of mirror segments (TRL 4). This is followed by partially to fully populating mirror modules (including environmental qualifying and X-ray testing; TRL 5). A TRL 6 engineering model demonstration of a *Lynx* Mirror Assembly (LMA) will contain numerous modules aligned and mounted within representative meta-shells whose parameters span the full range of the LMA. The full technology development plan to reach TRL 6 by Q4 2026 (well in advance of the start of Phase B) is contained in the *Silicon Meta-shell Optics Technology Roadmap*. The following is a summary of the key technology development elements from that document.

The Next Generation X-ray Optics group at NASA Goddard Space Flight Center (GSFC) has been continually developing the Silicon Meta-shell Optics technology since 2011. This technology combines the direct fabrication grind-and-polish method (proven for *Chandra*'s sub-arcsecond optical performance) with mature production technologies widely used in the semiconductor industry, such as ion beam figuring and CNC machining. Critically, the technology uses a nearly ideal substrate (monocrystalline silicon) to fabricate extremely thin optical components.

The DRM optics design for *Lynx* uses monocrystalline silicon—an inexpensive staple of the semiconductor industry—for its mirror substrate material. Monocrystalline silicon, also known as single-crystal silicon, is a continuous crystal lattice free of grain boundaries. It can be ground, honed, lapped, cut, sliced, diced, and etched and remain free of internal stress. It is lightweight, stiff, and thermally conductive with a low coefficient of thermal expansion. Monocrystalline silicon is the ideal material for *Lynx* mirrors.

At present, numerous monocrystalline silicon mirror substrates have been repeatedly fabricated and (optically) demonstrated to meet figure requirements. A pair of uncoated mirrors aligned and bonded at four locations with silicon supports onto a breadboard silicon plate (as specified in the optical design) has achieved 1.3-arcsecond Half-Power Diameter (HPD) at 4.5 keV (Figure 7.2). Performance was demonstrated by full-illumination X-ray tests at the X-ray beamline at GSFC; simulations show that equivalent performance in the absence of gravity would be close to 0.5-arcsecond HPD. A similar module was independently measured at the PANTER 130-m X-ray beamline for its effective area at several different energies, agreeing within 2% with calculations

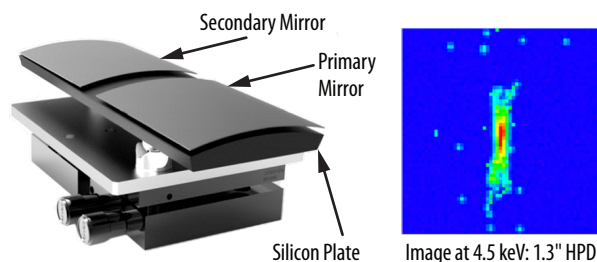


Figure 7.2. A primary and secondary mirror pair aligned and bonded on a breadboard silicon plate. The concave reflecting surface faces down in this photograph, and the four (per mirror) silicon supports are hidden between the reflecting surface and the silicon plate. Right: An X-ray image obtained with a fully-illuminating beam of 4.5-keV (Ti K) X-rays showing a half-power diameter of 1.3 arcseconds. The effective area at several energies were measured at MPES PANTER X-ray beam line from a similar mirror pair and shown to agree with theoretical expectations within 2%.

based on atomic form factors. These demonstrations place the fabrication, alignment, and bonding development of the *Lynx* baseline optics at TRL 3. The PCOS Program assessed the Silicon Meta-shell Optics technology at TRL 3.

Table 7.2 summarizes the approach or strategy used to meet each of the mirror performance requirements derived from the *Lynx* science objectives, with items in square brackets correlating these strategies with specific milestones (M1, M2, etc.) identified in the complete *Silicon Meta-shell Optics Technology Roadmap*, the associated TRL, and the planned completion date.

Table 7.2. *Lynx* requirements on its mirror assembly derived from its science drivers and the strategy of the Silicon Meta-shell Optics technology to meet them.

LMA Requirements Derived from Science Requirements		Silicon Meta-Shell Optics Strategy to Meet LMA Requirements
Point Spread Function (PSF) (on-axis)	Better than 0.5 arcsec	1. Use of a Wolter-Schwarzschild optical prescription optimized for best off-axis response and use of mirror segments short in the axial direction (100 mm) to minimize effects of field curvature. [COMPLETE]
PSF (10 arcmin off-axis)	Better than 1 arcsec	2. Use of modern proven and deterministic polishing technology and metrology techniques to make and fully qualify each mirror segment. [COMPLETE] 3. Use of traditional kinematic support for alignment and minimal constraint for permanent bonding of each mirror element to realize the performance potential of each mirror segment. [M3, TRL 4, Q4/2019]
Effective area	2 m ² at 1 keV	1. Choose monocrystalline silicon to make thin (0.5-mm) mirror segments to efficiently pack the large mirror area into a small volume. [COMPLETE] 2. Coating of the mirror surface with iridium film and possibly other interference coating to enhance or maximize reflectivity. [M2, TRL 4, Q3/2019] 3. Incrementally fabricate and assemble up to 360 m ² of mirror surface area [TRL 5, 6]
Mass	<2,500 kg	1. Use of monocrystalline silicon to make mirror segments that are geometrically thin and lightweight. [COMPLETE] 2. Use of the modular and hierarchical buildup process to minimize the mass of required mechanical structural and support material.

For an advanced optical assembly like the *Lynx* mirrors, performance must ultimately be viewed in the larger context of the Observatory's overall ability to meet scientific goals. Thus, errors affecting performance must be identified in a flowdown of requirements, and realistically allocated bounds must be assigned at the component or finer level. For the hierarchical meta-shell approach, the error allocations apply to the technology development elements (i.e., fabrication of mirror segments, coating, alignment, and bonding) at the mirror module level, and additional allocations are assigned for aligning and bonding into meta-shells and for aligning and attaching the meta-shells into the mirror assembly. A complete error budget (to be summed in quadrature) for the *Lynx* design, in units of angular distance, is given in Table 7.3. To meet *Lynx* requirements, the technology development plan must be executed within these error allocations at each stage of the process.

Table 7.3. Top-level angular resolution error budget guiding Silicon Meta-shell Optics technology development to meet *Lynx* requirements.

Major Steps	Cumulative HPD Req (arcsec, 2 reflections)	Error Sources	Allocation (or Req) (arcsec HPD, 2 reflections)	Technology Status as of Q1 2019 (arcsec HPD, 2 reflections)	Notes
Optical prescription	0.11	Diffraction	0.10	0.10	At 1 keV, weighted average of diffraction limits of all shells.
		Geometric PSF (on-axis)	0.05	0.05	On-axis design PSF is slightly degraded to achieve best possible off-axis PSF.
Fabrication of mirror segments	0.25	Mirror Substrate	0.20	0.40	Each pair of mirror segments must have a PSF better than 0.2-arcsec HPD, based on optical metrology.
		Coating	0.10	0.20	Coating that maximizes X-ray reflectance must not degrade the mirror pair's PSF by more than 0.1 arcsec.
Integration of mirror segments into modules	0.34	Alignment	0.10	0.30	Each pair's image must be located within 0.1 arcsec of the module's overall image.
		Bonding	0.20	0.30	Bonding of a mirror pair must not degrade its PSF by more than 0.2 arcsec.
Integration of modules into meta-shells	0.36	Alignment	0.10	0.10*	Each module's image must be located within 0.1 arcsec of the meta-shell's image.
		Bonding	0.10	0.10*	Bonding must not shift the module's image by more than 0.1 arcsec.
Integration of meta-shells into mirror assembly	0.39	Alignment	0.10	0.10*	Each meta-shell's image must be located within 0.1 arcsec of the overall assembly's image.
		Attachment	0.10	0.10*	Permanent attachment of the meta-shell must not shift its image by more than 0.1 arcsec.
Ground-to-orbit effects	0.43	Launch shift	0.10	0.10*	Launch shift must not degrade PSF by more than 0.1 arcsec.
		Gravity release	0.10	0.14*	Disappearance of gravity must not degrade PSF by more than 0.1 arcsec.
		On-orbit thermal	0.10	0.16*	On-orbit thermal disturbance must not degrade PSF by more than 0.1 arcsec.
Mirror assembly on-orbit performance			0.43	0.70	On-axis PSF of the optics. Add effects of jitter and other effects to get the final Observatory-level PSF.

* Model performance estimates

7.2.1.1 Key Elements and Milestones

Fabrication of Mirror Substrates — Numerous mirror substrates meeting performance requirements have been fabricated in recent months. Thus, the development work beyond the current TRL will refine the fabrication process to achieve higher efficiency at lower cost, as well as to fabricate a sufficient number of mirror segments (>100) for making multiple mirror modules (TRL 4 and 5) and mirrors of varying optical prescription (TRL 6). Ultimately, tens of thousands of flight-quality mirror segments will be needed for *Lynx*.

The fabrication process steps (Figure 7.3) to be refined and made more efficient in the technology development path start with a commercially procured block of monocrystalline silicon measuring $150 \times 150 \times 75$ mm, into which a conical approximation contour is cut with a band saw and then lapped to generate a precision conical surface that is a zeroth- and first-order approximation to an X-ray mirror segment. A thin top layer is then cut from the block. To remove the damage caused by the cutting and lapping process, the silicon shell is etched in a standard industrial process with an HNA solution, a

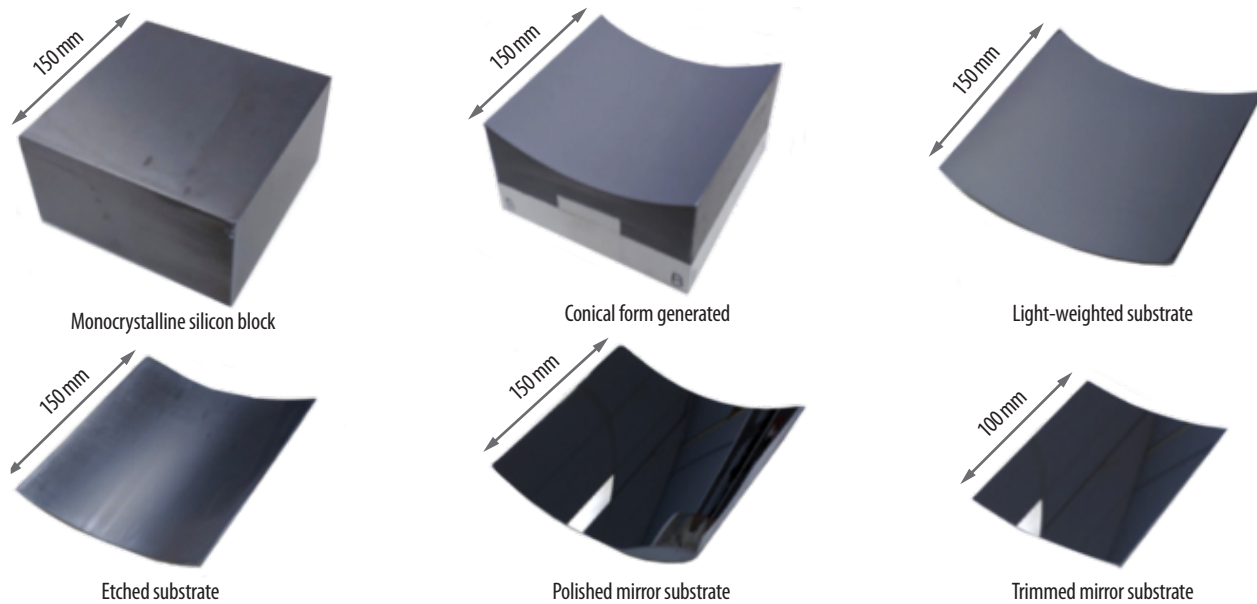


Figure 7.3. Six major steps of fabricating a mirror substrate. The process is highly amenable to automation and mass production methods, leading to high throughput and low cost.

mixture of hydrofluoric, nitric, and acetic acids. Following this etching step, the thin shell is a single crystal, free of any internal stress. The conical substrate is then polished with synthetic silk on a cylindrical tool to achieve required specularity and micro-roughness. This step results in a mirror substrate with a clear aperture of approximately 100×100 mm, and 0.5 mm thickness with roll-off errors near the four edges. The areas near the edges are removed with a dicing saw, resulting in a mirror substrate of the required size. The damage along the cut edges is removed via etching to again restore the pristine monocrystalline nature of the substrate.

The final step in fabricating the mirror substrate is a figuring process using an ion beam. The mirror substrate is first measured on an interferometer to produce a topographical map used to guide the ion beam to preferentially remove material where the surface is high.

The development plan for this technology element is to refine this fabrication process. Using no special equipment other than what is commonly available; the entire fabrication process used to complete one mirror segment currently takes about 15 hours labor time and less than two weeks of calendar time.

By TRL 6, a team of scientists, engineers, quality control personnel, and managers who are fully knowledgeable of the entire *Lynx* mirror production process will be in place. This team will include industry partners and other potential technology transfer recipients. At a minimum, as a first step of a technology transfer process, a list of potential suppliers, contractors, and industrial facilities that are technically ready to implement one or more production lines for making mirror segments, modules, and for integrating and testing those modules will be in hand. This plan includes the development of the mirror testing and qualification processes, including both science performance and environmental testing. Given the mass production nature involved in making the LMA, it is critical that there be three separate, efficient qualification processes: one for the modules, one for the meta-shell, and finally, one for the full mirror assembly. This is reflected in the calibration and assembly, integration, and test plans described in §6.6.3.2.

Mirror Coating— The mirror substrate needs a thin film coating to achieve high reflectance and meet effective area requirements. However, this coating introduces stress that can severely distort the figure of a mirror substrate. Preserving the substrate figure therefore requires a way to cancel or otherwise compensate for this effect to prevent the coating from degrading the mirror pair’s Point Spread Function (PSF) by more than a budgeted 0.1 arcsecond.

The coating stress compensation plan is shown in Figure 7.4. Using the semiconductor industry’s dry oxide growth process, the backside (i.e., the convex non-reflecting side) of the mirror substrate is coated with a layer of Silica (SiO_2). The SiO_2 exerts compressive stress on the substrate, causing it to distort. Then, a thin film of high-reflectivity iridium with an undercoat of chromium serving as a binding layer is sputtered onto the front side.

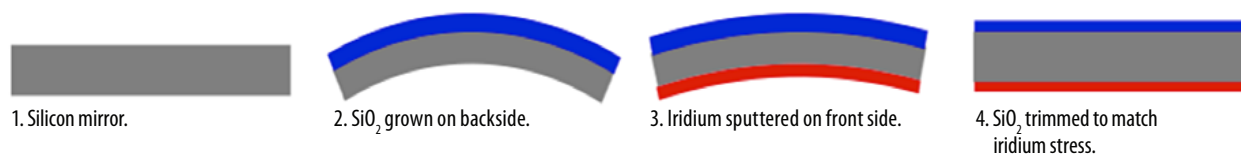


Figure 7.4. Illustration of mirror coating process to enhance X-ray reflectance while preserving the figure quality of silicon substrate: The distortion caused by the stress of the iridium thin film is precisely balanced or compensated for by the stress of the silica on the other side of the mirror substrate.

The compressive stress of the iridium film counteracts the SiO_2 stress and cancels some of the distortion, but significant distortion remains. The final step is to trim the thickness of the SiO_2 layer to achieve precise cancellation of stresses and restore the figure of the substrate. This trimming step is guided by precise figure measurement and finite element analysis.

Two trimming methods for restoring the mirror figure to within the error allotment are being studied. One recently demonstrated method involves the use of hydrofluoric acid chemical etching [590]. Another is through the use of an ion beam, the same as that used for final figuring the silicon substrate. Since ion beam figuring is a dry process, it has the advantage of being cleaner; however, unlike chemical etching, it must be done under vacuum. Both methods are expected to meet stress compensation requirements. In the end, the method with the higher efficiency and lower cost will be used. Refinement through experimentation is expected to be completed by Q3 2019, and mirror segments with the correct physical dimensions (including thickness) and coated with iridium will be built as single-pair modules and tested in Q2–Q4 2020. The condition of the coated surface will be verified with a Zygo surface profiler (or equivalent) to ensure micro-roughness requirements are met, and by X-ray measurement to ensure the effective reflectance requirements are met.

Mirror Alignment— In the Silicon Meta-shell Optics design, each mirror segment will have four supports at optimized locations that necessarily and sufficiently determine the location and orientation of its curved surface (just as three supports are needed for a planar surface). The alignment of the mirror segment is determined by the heights of the four supports. The alignment task is an iteration

of Hartmann measurements using a beam of visible light monitored by a CCD camera (shown in Figure 7.5) and precise grinding of the heights of the supports. The precision required to meet the 0.1-arcsecond budgeted alignment error translates into a support height error of as little as 25 nm in the worst case corresponding to the largest (outermost) radius of curvature. This level of precision is easily achievable with a deterministic grinding material removal process.

As of early 2019, an X-ray mirror capable of being supported at four points and aligned to about 1 arcsecond Root Mean Square (RMS) error has been repeatedly demonstrated. This error is currently dominated by two metrology factors: (1) the size of the light source and (2) the diffraction of the visible light that degrades the ability to locate the centroids of Hartmann maps, thereby degrading the precision of mirror alignment. Solutions to both of these problems have been identified: a smaller pinhole will be used to reduce the light source size from its current 100 μm to 5 μm , and beam-reducing optics will be used to focus the diffraction spot size from about 30 mm down to 5 mm, significantly increasing the centroiding precision. This work is necessary to achieve TRL 4 and is expected to be completed by the end of 2019.

Co-aligning (and bonding) another mirror segment pair on top of the first (for TRL 5 demonstration) is simply a repetition of the same procedure. The only significant difference lies in the optical prescriptions of the mirror segments. This difference only entails the use of different tooling, which is procured commercially and does not present any technical issue. There is the possibility that the diameter of the supports may need to be made larger than that used in demonstrating TRL 4 to ensure that the module can sustain the vibration test environment. If larger diameter supports have to be used, the support grinding process would need to be refined to ensure an accurate top surface. There is no intrinsic technical difficulty, but additional time and effort would be needed to ensure the completion of TRL 5 demonstration.

Mirror Bonding — Mirror segments are bonded onto the four supports using epoxy adhesive. Figure distortion and alignment disturbance caused by epoxy shrinkage must be minimized such that bonding of a mirror pair does not degrade its PSF by more than the budgeted 0.2 arcseconds.

Bonding the mirror segment is a direct extension of the alignment process. Once the four supports have the correct heights as determined by the Hartmann measurements, the mirror segment is fixed with epoxy and vibrations are applied to help the mirror segment settle in its optimal configuration. The epoxy on each support is spread uniformly and compressed, and the mirror segment is permanently bonded once the epoxy is cured. Any local distortion caused by epoxy cure is minimal, as the diameter of the support is only a few times larger than the thickness of the mirror segment. The 0.5-mm-thick mirror segment is very stiff over the length scale of the support diameter.

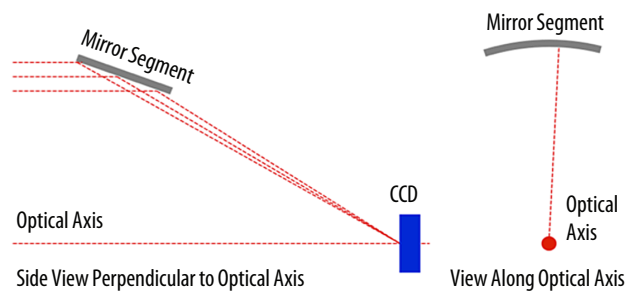


Figure 7.5. Illustration of the Hartmann setup using a beam of visible light to measure the location and orientation of the mirror segment being aligned.

As of early 2019, mirror segments have been repeatedly bonded using different epoxies, and multiple variables have been found that can affect the bonding quality: (1) epoxy type, (2) cure strain of the epoxy, (3) epoxy viscosity, (4) diameter of the supports, and (5) surface geometry of the support in contact with the mirror segment. Finite element analyses have reproduced these effects. Numerous additional experiments will be conducted in combination with finite element analyses to quantify the relationships among these variables and arrive at an optimal specification. This work is expected to be completed by Q2 2020. By Q3 2020, it is expected that single-pair modules capable of consistently meeting *Lynx* PSF and effective area requirements (as well as Field of View (FOV) requirements) will be successfully built and tested.

There remains a risk that epoxy shrinkage during cure may cause larger-than-expected figure distortion within the segment “stack” comprising a mirror module. If this risk materializes, the number of mirror segments bonded to a module may need to be reduced, therefore increasing the number of modules needed. This will effectively reduce strength requirements and enable the use of much smaller amounts of epoxy, leading to less distortion. The net consequence of this is a slight reduction in the effective area of the LMA, as more modules will lead to a slightly lower nesting efficiency.

7.2.1.2 Programmatic Considerations

The four basic elements of the Silicon Meta-shell Optics approach have been empirically demonstrated. Further technical and engineering development in the coming years will ready this technology for implementing the *Lynx* mission.

The main challenge for this optics design is the large numbers of mirror segments that need to be fabricated, coated, aligned, and mounted. This is mitigated by the hierarchical approach that reduces the mirror assembly production into a small number of highly repetitive, mature, and efficient routines. Nearly all future technology development steps for the LMA are incremental improvements upon the current TRL. These new developments are similar enough to existing experience that a single development approach may be taken with a high degree of confidence for success. Current NASA investments in Silicon Meta-shell Optics technology development, followed by directed *Lynx* technology development funding, will bring the mirror assembly to TRL 6, well within the schedule for *Lynx*.

The hierarchical approach for building the *Lynx* mirrors is also highly conducive to developing, refining, and perfecting a set of iterative work procedures that involve building and testing many hardware pieces at many different integration levels, guided by optical, thermal, and structural analyses. Thus, reaching TRL 6 will demonstrate that not only can the LMA be made to meet science performance and spaceflight environment requirements, but also that its production procedures meet the stringent schedule and cost requirements outlined in §8.5.2.1 and can be transferred to industrial partners for large-scale mirror production.

7.2.2 Full Shell Optics

The Full Shell Optics option for *Lynx* [591, 592] is a direct fabrication technology with direct lineage to *Chandra* that combines traditional grinding and polishing with precise metrology to produce finely figured, full-circumference mirrors. The advantages of full shells over segments lie in the simplified alignment requirements, the inherently greater structural integrity, and the lower susceptibility to coating-induced stresses and mounting-induced distortions. The direct fabrication process flow

encompasses substrate procurement and initial preparation, successively finer grinding/machining, polishing and super-polishing steps, and final post-fabrication figure correction using ion beam figuring [593] and/or differential deposition [594] techniques.

The full shell optics solution for *Lynx* is based upon low-density and low-coefficient of thermal expansion materials with high elastic modulus and high yield strength, such as lightweight metal alloys, glass, and fused silica. Detailed *Lynx*-specific optical designs and structural, thermal, and mechanical analyses of mirrors and mirror support structures during manufacture, integration, and flight have been provided in the *Full Shell Optics Technology Roadmap*. These analyses and simulations show that the full shell design can meet all scientific, technical, and programmatic evaluation criteria for *Lynx*.

The Full Shell Optics technology has been assessed at TRL 2 by the 2017 PCOS Technology Management Board. This assessment is based on X-ray testing in 2011 [595] of a directly fabricated fused silica shell. This shell was designed to meet the 10-arcsecond requirement of the Wide Field X-ray Telescope (WFXT) concept [596] and performed within a factor of two of that requirement. Direct fabrication Full Shell Optics is being funded by NASA's Internal Scientist Funding Model (ISFM) program at MSFC to develop processes based on lightweight metal and metal matrix composites substrates [592, 597] and by the Italian Space Agency (ASI) at the Brera Astronomical Observatory (OAB) based on glass and glass-like substrate materials [591, 598].

Performance, Issues and Challenges — To date, only moderate-size, ~0.5-m-diameter, thin full shell X-ray optics have been directly fabricated. Larger diameter thin mirrors are unwieldy and susceptible to large-scale distortions or damage during the manufacturing and handling processes. While there is little or no difficulty meeting reduced outer diameter requirements such as the 1.3-m² configuration (\$10) with full shell technology, potential solutions for large-diameter shell fabrication risks include using alternative substrate materials, thicker substrates, or shell segments of limited azimuth rather than full shells. Another challenge is obtaining measurements of the mirror shell figure throughout the manufacturing process to monitor progress and plan further processing. If metrology cannot be performed in situ, then the production schedule will need to be extended to account for delays due to installation and re-alignment between metrology and fabrication processes.

There are no fundamental physical barriers to achieving TRL 3 and 4 (X-ray test of a modest diameter, breadboard-mounted, coated mirror shell demonstrating ~3 arcseconds or better HPD). Achieving TRL 5 requires multiple two-reflection shells (representing diameters up to 1 m) mounted on a single flight-like support structure and X-ray calibrated. While both mounting and alignment are new developments (e.g., documenting epoxy shrinkage and integrating shrinkage into models), similarity to existing experience is substantial and sufficient to warrant a single development path. Reaching TRL 6 is an extension of the TRL 5 milestone to larger diameter mirror shells. Attaining TRL 6 requires additional (larger) machines that can fabricate mirrors aligned in a vertical orientation. Conceptually, TRL 6 is merely a scaling from TRL 5, but costs are substantial, as are estimated lead times to procure shells and manufacturing hardware.

7.2.3 Adjustable Segmented Optics In development

The Adjustable Segmented X-ray Optics concept is designed to enable the fabrication, alignment, and mounting of lightweight X-ray optics with a figure that can be corrected to the desired precision after assembly. Adjustable X-ray Optics borrow from techniques to remove the blurring effects of atmospheric turbulence in active ground-based optical/Infrared (IR) applications. The technology can potentially ease segment fabrication requirements, thereby reducing segment cost and schedule. In addition to fabrication errors, the addition of addressable actuation is also motivated by the need to correct mounting-induced distortions, reflective coating stresses, and epoxy creep, and by the potential to correct for post-launch environmental (temperature) changes on-orbit.

Actuation is accomplished by the patterning of sputter-deposited Lead Zirconate Titanate (PZT) electrodes and necessary electrical contacts on the backs of individual mirror segment substrates. Applying a low DC voltage across the thickness of the PZT produces a stress in the piezoelectric material that introduces a localized bending of the mirror segment analogous to the bimetallic effect. The resulting “influence function” of the electrode can be well characterized, and algorithms for the overall figure correction of the mirror can be constructed and applied. Applications have been made to 0.4-mm-thick slumped glass (Corning Eagle XGTM), and plans are to use 0.5-mm-thick, single-crystal silicon mirror segments (equivalent to the *Lynx* DRM optics technology) instead.

The technology is currently at TRL 3, as assessed by the 2017 PCOS Technology Management Board. It has been under development jointly by the Smithsonian Astrophysical Observatory (SAO) and Penn State University (PSU), with funding since 2013 through NASA’s Strategic Astrophysics Technology (SAT) and Astrophysics Research and Analysis (APRA) programs. A complete *Adjustable Segmented Optics Technology Roadmap* has been prepared for *Lynx*.

Performance, Issues and Challenges — An Adjustable Segmented Optics-based optical point design that satisfies *Lynx* science requirements has been developed, and a detailed imaging error budget is in development. In parallel, developments have led to both a mirror mounting scheme that satisfies the demands of minimizing induced distortions and an optical alignment metrology and processes that align mirror segment pairs to ~0.35 arcseconds RMS diameter. The mirror point design makes use of a modular approach as previously envisioned for Con-X and the International X-ray Observatory (IXO). The present design, which makes use of preliminary structural plans, includes three radial rows of modules — inner, middle, and outer — with 10 inner modules, 20 middle modules, and 40 outer modules. Each mirror segment is 200 mm long (axially), and segment azimuthal spans range from ~100 mm to ~220 mm.

Current development efforts are restricted to smaller mirror segments (i.e., 100 × 100 mm) to avoid large investments in larger PZT deposition and other processing equipment during the early development phase. The key areas to mature to TRL 4 are the addition of Zinc Oxide (ZnO) transistors to facilitate row-column addressing, the alignment of a mirror pair in a proof-of-concept mounting frame, the testing of this mirror pair in an X-ray beamline, and performance validation through simulations. Demonstrating the required TRL 5 performance will include the fabrication and testing of full-sized mirror segments. This will require either an investment in larger processing equipment or partnering with an industry supplier. Other key maturity elements that need to be demonstrated include the addition of strain gauges to monitor mirror figure and partially populating and environmentally testing at least two modules (including mass simulators as needed). The main hurdle in achieving TRL 6 is building and testing a higher fidelity, full-size, multi-module prototype that meets all *Lynx* requirements.

7.3 Science Instruments Development

There are three enabling technologies that provide the full range of imaging and spectroscopic capabilities needed for *Lynx* and define the science instrument suite: (1) the HDXI (§7.3.1); (2) the XGS (§7.3.2), which consists of an XGA mounted along the optical path just aft of the mirror assembly and a matched focal surface X-ray Grating Detector (XGD); and (3) the LXM (§7.3.4).

For the HDXI (and the similarly capable XGD), the *Lynx* team has identified three sensor technologies (discussed in §7.3.1) with the potential to meet all scientific requirements for *Lynx*.

For the XGS, two grating technologies have been identified as feasible for *Lynx*: (1) the CAT (§7.3.2) gratings and (2) the OP-XGS (§7.3.3). Both technologies are expected to meet *Lynx* diffraction efficiency and spectral resolution requirements, and reach TRL 6 well before PDR. The *Lynx* team conducted a trade study (Append B.5.1) in Q3 2018 to recommend one architecture to focus the design for the *Lynx* DRM. This study found that CAT gratings offer more relaxed alignment tolerances, making it easier to integrate within the Observatory and somewhat lower system mass, whereas off-plane gratings have higher diffraction efficiency, thereby requiring less aperture coverage to meet the effective area requirement and a smaller XGD footprint (and power consumption). Ultimately, the CAT-XGS was recommended for the DRM because of relative insensitivity to contamination, ease of implementing thermal controls, and greater simplicity of alignment.

7.3.1 High-Definition X-ray Imager

The HDXI instrument is an imaging X-ray spectrometer capable of achieving a minimum $22\text{-}\times\text{-}22\text{-arcminute}^2$ FOV while simultaneously achieving a fine angular resolution of 0.33 arcseconds ($\leq 16\text{-}\mu\text{m}$ pixel size) to directly oversample the PSF of the mirrors. The *Lynx* HDXI configuration adopted for the DRM (§6.3.2) has twenty-one $1,024\text{-}\times\text{-}1,024$ -pixel sensors arranged in a $5\text{-}\times\text{-}5$ tiling with the four corners excluded. The HDXI spectrometer must function at high quantum efficiency over the full *Lynx* bandpass from 0.2 to 10 keV. The HDXI instrument design is derived from the highly successful CCD-based X-ray imaging spectrometers built for *Chandra* and XMM-Newton. The challenge to HDXI sensor technology for *Lynx* is providing both excellent low-energy X-ray response and fine spatial resolution in a rapid readout, low-power operational environment. To meet this challenge, HDXI sensors must satisfy demanding requirements on detector noise, pixel-to-pixel response uniformity, and readout processing.

Three promising sensor technologies are being extensively studied and developed for *Lynx*. The first, hybrid CMOS sensors, under development by Teledyne Imaging Systems, use a thick, fully depleted silicon wafer bump-bonded to a Readout Integrated Circuit (ROIC) with multiple high-speed readouts, low power, and on-chip digitization [599]. Another is a monolithic CMOS sensor in development at Sarnoff Research Institute (SRI) [600] that features in-pixel, high-responsivity sense nodes and on-chip digitization for fast, low-noise operation. And third, an advanced, “digital” CCD being developed at the Massachusetts Institute of Technology’s (MIT’s) Lincoln Laboratories combines CMOS-compatible

operating voltages and high-speed, on-chip amplifiers with parallel CMOS signal chains for greatly increased framerate and lower power [601]. Each of these sensor technologies is illustrated in Figure 7.6.

The current performance of these three sensor technologies is compared to the *Lynx* requirements in Table 7.4. As can be seen, reducing read noise in the hybrid CMOS architecture, increasing depletion depth of the monolithic CMOS sensors, and increasing framerate in the digital CCD design are the key advancement requirements for the three sensor technologies, respectively.

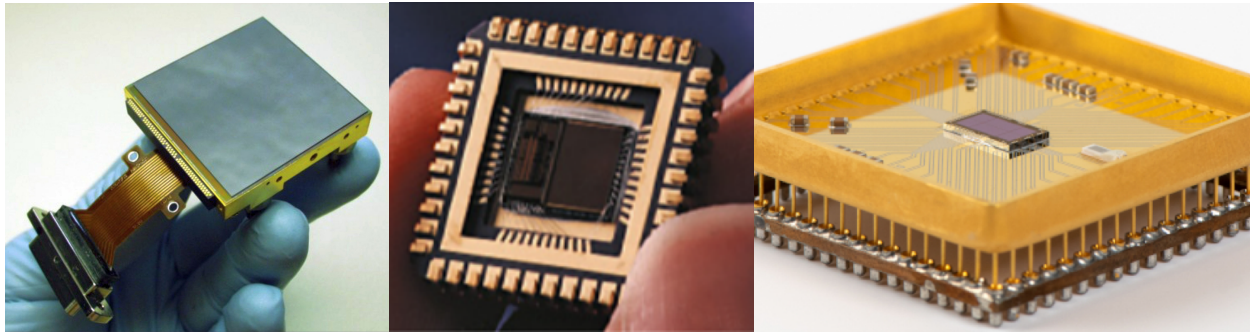


Figure 7.6. Prototypes of three sensor technologies under development for the *Lynx* HDXI. Left to right, these are the Teledyne/PSU hybrid CMOS sensor, the SRI/SAO monolithic CMOS sensor, and the MIT/Lincoln Laboratory's digital CCD.

Table 7.4. HDXI sensor requirements and current performance of a single detector device.

Parameter	Requirement	Current Performance		
		Hybrid CMOS	Monolithic CMOS	DCCD
Pixel size (μm)	$\leq 16 \times 16$	12.5×12.5	16×16	8×8
Spectral resolution (eV, FWHM)				
at 0.5 keV	< 70	78	60 (at 0.183 eV)	Measurement not available
at 6 keV	< 150	156	150	145
Read noise (electrons, RMS)	≤ 4	5.6	2.9	4.2
Single-sensor framerate (frame/s) \times (frame size in Mpix)	$\geq 100 \times 1$	$> 100 \times 1$ breadboard in design	20×1	4.7×0.5
Depletion depth (μm)	100	100	15	75
ASIC status		Developed; simplifying improvements are planned	In development	Breadboard in design

In addition to advancing the X-ray photon-counting imaging sensor technology, the HDXI technology development plan includes maturing readout electronics specific to each sensor architecture. The sensors convert incoming X-ray photons to electrical signals containing information about photon energy and interaction position, while readout electronics extract this information from sensor output signals and digitize it while also providing the timing and bias voltages required by the sensor. Readout electronics are expected to be implemented with Application-Specific Integrated Circuits (ASICs). Optimizing sensor-specific readout and control functions, operating temperatures, and developing flight packaging are the key advancements for the ASIC signal processors.

Specific milestones have been established along the TRL 6 development path for these elements, as documented and described in detail in the complete *HDXI Technology Roadmap*. The *Lynx* HDXI technology development plan is derived from experience with developing sensor technologies and

ASICs for previous missions by the teams at MIT, PSU, and SAO in consultation with experts at Lincoln Laboratory, Teledyne, and SRI and with support from the *Lynx* engineering and technical teams at MSFC and SAO.

These technologies differ primarily in their architecture, but not in their functionality; each has demonstrated proof of concept. At present, each of these technologies individually meets some, but does not simultaneously meet all, of the *Lynx* HDXI requirements, and each is assessed at TRL 3 for *Lynx* by the most recent PCOS Program Annual Technology Report. Each technology requires similar resources from the spacecraft, and all three have similar development paths. The development plan assumes initially funding all three options to minimize risk. During the course of pre-Phase A activities, a downselection to two technologies will precede a final downselection prior to Phase A.

The pixelated readout sensors for the *Lynx* XGS (§7.3.2) will require many of the same capabilities as the HDXI detectors. Therefore, no separate XGS sensor technology development plan is needed.

7.3.1.1 Key Elements and Milestones

The link between the science drivers and the performance requirements for the HDXI was detailed in §6.3.2. Here, those performance requirements are linked to the strategy to reach TRL 4 by the start of Phase A and to reach TRL 5 and 6 by mission PDR, as outlined in Table 7.5. A few additional performance parameters, such as radiation tolerance and temporal resolution, are omitted here for brevity but included in the full *HDXI Technology Roadmap*.

Table 7.5. HDXI technical requirements and the strategies to meet them.

HDXI Parameter	Requirement	HDXI Development Team's Strategy to Meet <i>Lynx</i> Requirements
Quantum Efficiency (excluding optical blocking filter)	≥ 0.85 , 0.5–10 keV >0.1, 0.2–0.5 keV	<ol style="list-style-type: none"> 1. Use of proven silicon wafer processes to develop sensors on high-resistivity material 2. Use of heritage from highly successful <i>Chandra</i>/ACIS and <i>Suzaku</i>/XIS among others 3. Use of demonstrated entrance window (backside) passivation to enhance low-energy spectral resolution and quantum efficiency
Field of view	22 x 22 arcminute (5k x 5k pixels)	<ol style="list-style-type: none"> 1. Employ four-side abutable sensors as demonstrated for <i>WFIRST</i> 2. Leverage ability to closely pack sensors and associated electronics successfully as shown on many other missions
Framerate—full frame	>100 frames s ⁻¹	<ol style="list-style-type: none"> 1. Use highly parallel sensor and readout architectures and high-responsivity output transistors 2. Use current generation Field Programmable Gate Array (FPGA) capabilities to perform event/island detection at these data rates

The sensor technology and associated analog signal processing ASICs are the primary elements of the HDXI that need further development to reach TRL 6 by PDR. Other HDXI electrical elements such as high-speed event recognition processors and large free-standing optical blocking filters require some development, but more importantly, integrated system level testing is required for the complete HDXI system to achieve TRL 6. Thus, the HDXI technology development plan has three major stages: (1) advancing the sensors and ASICs from their present TRL 3 to TRL 4, (2) demonstrating that two sensor/ASIC pairs operating in close proximity meet TRL 5 requirements, and (3) demonstrating that a fully functional, flight-like system of five 1,024-x-1,024-pixel sensor/ASICs with representative event recognition processors (and optical blocking filters) meets all science requirements, operates at required rates, and meets all TRL 6 performance requirements, including appropriate environmental tests. The general technology development strategy for the sensor and readout electronics elements is discussed below.

Two major development efforts are needed to advance the sensor and ASIC technologies to TRL 4. First, several dedicated device fabrication runs (three are planned) must be made to optimize a given sensor. Each such run entails a cycle of design improvement, lithographic mask production, wafer fabrication and test, device packaging, and laboratory characterization. The sensors must demonstrate low-noise performance at representative pixel rate, energy resolution, and quantum efficiency at high and low energies in a representative single-channel sensor before and after exposure to flight ionizing and non-ionizing radiation environments.

Second, and in parallel, several custom ASIC development runs must be made for each sensor technology. As with the sensors, dedicated fabrication runs are required for ASICs. Sensors and ASICs for each of the three technologies will initially be developed in parallel. An external review by subject matter experts and downselection to two sensor/ASIC technologies is planned in Q3 2023. The two ASIC/sensor combinations will then be tested to ensure adequate single- and multi-channel noise performance and radiation tolerance as needed to attain TRL 4 performance.

The risks and challenges to advancing the HDXI technology to TRL 4 are primarily attributable to budget and schedule if all the HDXI requirements cannot be demonstrated on a single architecture over the course of the TRL 4 development process. Funding three sensor technologies in the early stages of the *Lynx* mission is a risk mitigation approach that warrants a high degree of confidence for success based on past experience. A final downselect to a single architecture is planned at the start of Phase A following demonstration of TRL 4 performance.

To demonstrate TRL 5, an integrated system comprising two sensor/ASIC units of representative size operating in close proximity will be constructed and subjected to environmental tests. The two-sensor configuration will simulate multi-sensor focal plane operation, and the environmental testing will include vibration, thermal cycling, and (10-year equivalent) radiation exposure.

Finally, TRL 6 will be demonstrated using an engineering model including a quarter-scale focal plane with five flight-sized sensors and ASICs in a realistic geometry using flight-like sensor-to-ASIC electrical interconnects. This unit will be subjected to full environmental testing.

7.3.1.2 Programmatic Considerations

The HDXI technology development plan outlines significant upfront effort to develop sensors and ASICs optimized for *Lynx*. This process of developing mission-specific pixelated silicon sensors has been successfully executed for numerous astrophysics missions including *Chandra*, *Suzaku*, and *Hubble Space Telescope*, as well as a much larger number of missions outside astrophysics. Lessons learned from these past programs suggest advancement to TRL 4 requires new development that is similar to existing experience but that multiple development approaches should be pursued to provide a high degree of confidence for success. Thus, to reduce risk and ensure performance requirements are met, three separate sensor/ASIC development paths are funded for study early in the HDXI plan. Furthermore, development of large focal planes (as needed for TRL 5 and 6 demonstrations) has considerable heritage in industry, academia, and government laboratories. Achieving TRL 5 and 6 requires only straightforward engineering processes that will be tailored for the development of a configuration representative of the HDXI focal plane for testing across the range of anticipated environmental conditions. Finally, sufficient funded schedule reserve will be in place to mitigate the (low) risks of sensor/ASIC fabrication delays, the need for additional fabrication cycles to meet performance requirements, and additional packaging development effort.

7.3.2 Critical-Angle Transmission X-ray Grating Spectrometer

The *Lynx* XGS will provide high-throughput, high resolving power ($R > 5,000$) spectra over the soft X-ray energy band. The XGS is comprised of the XGA mounted along the optical path just aft of the mirror assembly and the XGD located on the Integrated Science Instrument Module (ISIM) (§6.3.3; readout array performance requirements are similar enough to those of the HDXI that its development path is addressed in §7.3.1.)

The CAT grating design combines the high diffraction efficiency of specular reflection at grazing angles of incidence below the critical angle with the orders-of-magnitude relaxed alignment tolerances of transmission gratings to preserve the exquisite *Lynx* angular resolution in the resulting diffracted spectra leading to high spectral resolving power.

The CAT grating design combines the high diffraction efficiency of specular reflection at grazing angles of incidence below the critical angle with the orders-of-magnitude relaxed alignment tolerances of transmission gratings to preserve the exquisite *Lynx* angular resolution in the resulting diffracted spectra leading to high spectral resolving power.

The CAT grating is a blazed dispersive transmission grating optimized to achieve maximum efficiency in high diffraction orders near the astrophysically important, He-like O VII line energies. CAT grating bars are inclined by an angle less than the critical angle of total external reflection, relative to the incident X-rays, efficiently blazing into diffraction orders near the angle of specular reflection from the grating bar sidewalls (Figure 7.7).

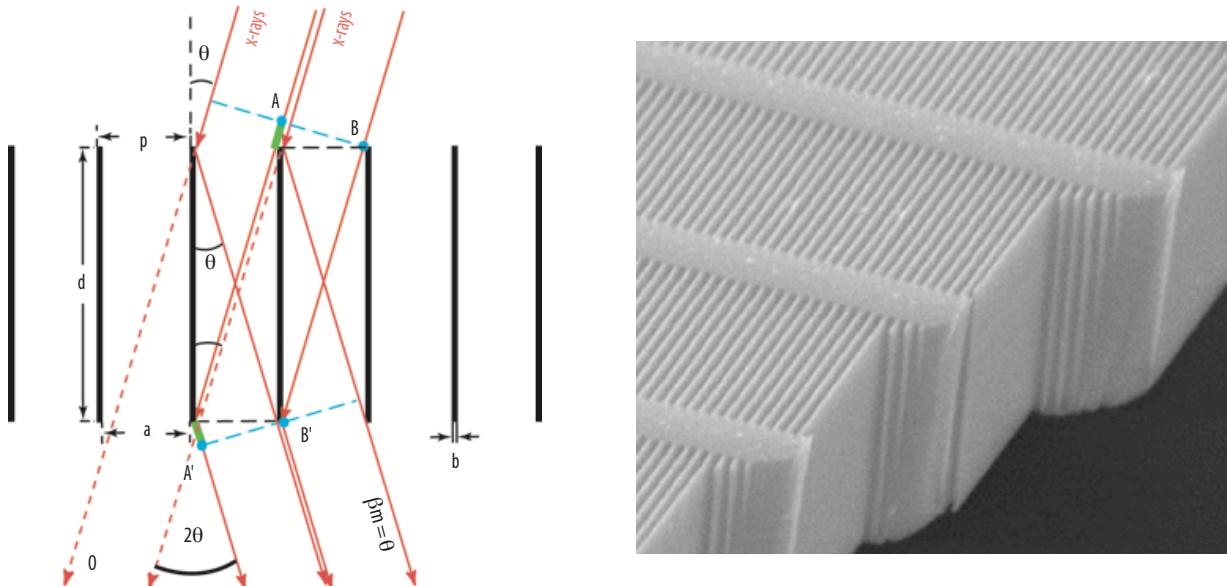


Figure 7.7 (Left) Schematic CAT grating of period p . The m^{th} diffraction order occurs at an angle β_m where the path length difference between AA' and BB' is $m\lambda$. Shown is the case of blazing in the m^{th} order where β_m coincides with the direction of specular reflection from the grating bar sidewalls ($|\beta_m| = |\theta|$). (Right) Scanning electron micrograph of a cleaved free-standing silicon grating membrane with 200-nm period grating bars and 5- μm period cross supports.

CAT gratings are being fabricated at MIT's Space Nanotechnology Laboratory; the same laboratory that produced gratings for *Chandra*, the *Solar and Heliospheric Observatory* (SOHO), the *Imager for Magnetopause-to-Aurora Global Exploration* (IMAGE), the *Geostationary Operational Environmental Satellite* (GOES), *Two Wide-Angle Imaging Neutral-Atom Spectrometers* (TWINS), and the *Solar Dynamics Observatory* (SDO). The full CAT-XGS Technology Roadmap has been developed by the CAT grating team at MIT with support from the *Lynx* engineering and technical teams at MSFC. The *Lynx* design is based on the Rowland torus concept used by the *Chandra* High-Energy Transmission Grating Spectrometer (HETGS; [607]), which was also built by MIT. The initial CAT grating design was conceived in 2005, and the technology has been under development since 2007 principally through NASA's APRA and SAT funding programs. The 2017 PCOS Program Annual Technology Report assessed the CAT-XGS technology at TRL 4.

CAT gratings are fabricated from Silicon-On-Insulator (SOI) wafers. The grating bars (Figure 7.8) and integrated Level 1 (L1) support structures are etched from the 4- to 6- μm -deep device layer side of the wafer, and a stiffer, hexagon-shaped Level 2 (L2) support mesh is etched from the thicker opposing handle layer, with the buried SiO_2 insulator layer between them removed from the open areas (Figure 7.8; center).

The resulting grating membrane (Figure 7.8; right) is bonded to a narrow frame comprising a grating facet. Hundreds or possibly up to 2,000 co-aligned and mounted facets (depending on facet size) are needed to populate a Grating Array Structure (GAS) for *Lynx* that densely tiles a large enough fraction of the mirror aperture to collectively meet the system effective area requirement.

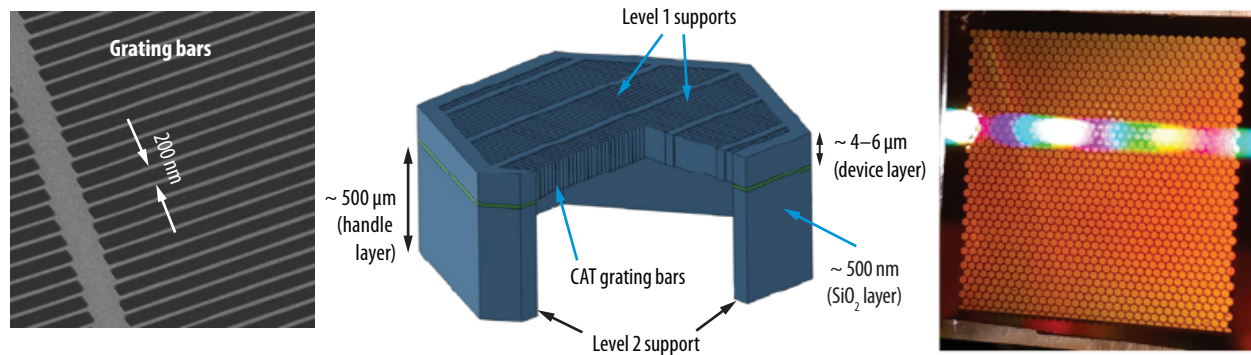


Figure 7.8. (Left) Micrograph of CAT grating bars. (Center) Schematic of CAT grating “unit cell” showing the structural hierarchy (not to scale). (Right) A 32-x-32 mm² CAT grating membrane. Note the honeycomb structure of the unit cell’s hexagonal L2 mesh and the visible light diffraction due to the aligned L1 mesh in the device layer.

Grating membranes of $32 \times 32 \text{ mm}^2$, yet slightly thinner than required for *Lynx*, have been fabricated, and individual platinum-coated facets of $10 \times 30 \text{ mm}^2$ have demonstrated $R > 10,000$ in 18th-order using Al-K α radiation and illumination with an ~ 1 -arcsecond mirror pair (Figure 7.9; [602, 605]). Facets with the same parameters have undergone thermal and vibration testing without any loss in X-ray performance [603]. These particular facets provide $\sim 30\%$ diffraction efficiency [604], which would fall short of the baseline design for *Lynx* by $\sim 20\%$. Nevertheless, all the basic concepts of a CAT grating spectrometer have been demonstrated.

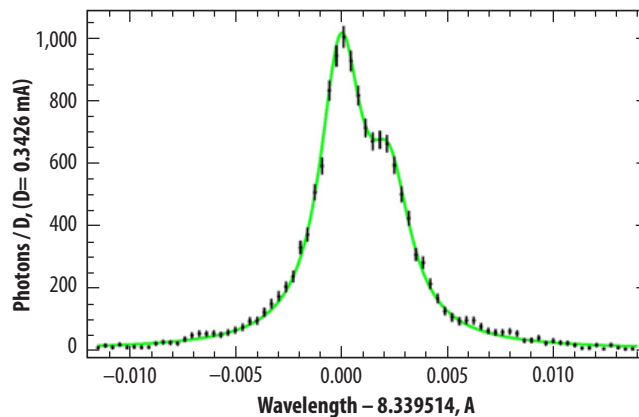


Figure 7.9. Spectrum of Al-K α doublet (1.49 keV) in 18th-order from a single platinum-coated CAT grating measured at the NASA MSFC Stray Light Test Facility demonstrating $R > 10,000$.

The MIT Space Nanotechnology Laboratory is currently producing 200-nm-period CAT gratings with 4- μm depths and 60-nm grating bar widths and facet areas up to $32 \times 32 \text{ mm}^2$. The baseline design for *Lynx* calls for 5.7- μm -deep, 40-nm-wide grating bars with 200-nm period.

The CAT grating array optical design for *Lynx* has been developed using geometric ray-trace simulations [606] based on the DRM design mirror properties, grating sizes, and other grating properties, and optimized for resolving power. The main error terms for resolving power are misalignment and placement of individual grating facets, misalignment and placement of the grating array as a whole, grating facet period distortion, thermal gradients, aberrations in the optical design, deviation of detector surface from ideal placement (static and dynamic), and readout sensor pixelation.

7.3.2.1 Key Elements and Milestones

The key elements of the CAT-XGS design requiring maturation are improving the system effective area and preserving the spectral resolution. While preliminary ray-trace simulations supporting these design elements have been performed, additional work is anticipated in parallel with any future mirror assembly design modifications because the grating array layout is specific to the mirror assembly characteristics.

System Effective Area — Increasing grating depth increases diffraction efficiency, and reducing bar width increases throughput. While etching ultra-high-aspect ratio structures on the nanometer scale is challenging, the required etch depth has already been achieved using tools developed for the semiconductor and Micro-Electrical Mechanical Systems (MEMS) industries. Specifically, grating bars with 200-nm pitch, 6- μm depth, and L1 structures of the needed dimensions have been etched from bulk silicon using Deep Reactive-Ion Etching (DRIE), followed by a short potassium hydroxide polish to create nanometer-smooth grating bar sidewalls. Fabrication of a full grating membrane from an SOI wafer with the required device layer thickness will be part of TRL 5 development (Q4 2019). To further increase geometric throughput, all the support structures (L1, L2, and facet frames) need to be thinned by small amounts without compromising structural, thermal, or mechanical integrity. Larger

grating membranes will increase throughput and system effective area. Grating facets of $60 \times 60 \text{ mm}^2$ are planned for TRL 6 demonstration (Q4 2022). The main challenge for the CAT-XGS fabrication of large-area grating facets with the required performance is process development on SOA fabrication tools from the semiconductor and MEMS industries, as well as development of some custom fabrication steps and optimization of support structures with the goal to maintain launch survival and to minimize membrane distortions due to bonding into facets. The larger the membrane area, the smaller the number of required grating facets, and the lower the ultimate cost of the grating array.

Spectral Resolution — Large grating facets are desired for reducing production schedule and cost and for improving throughput. However, large flat facets cannot continuously match the curved Rowland torus surface (§6.3.3.1). Deviations lead to aberrations that broaden the diffracted Line Spread Function (LSF), thus reducing resolving power below requirements for the largest facet sizes considered. The use of chirped gratings (i.e., imposing a variable grating period over the membrane) promises to recover resolving power. Current developments include patterning methods for 200-nm-period CAT gratings using $4\times$ projection lithography with e-beam written masks, as is standard in the semiconductor industry. Fabricating large membranes with period chirp is scheduled for TRL 6 (Q3 2023).

Mounting and alignment distortions of grating membranes and facets need to be kept low to prevent grating period variations from impacting resolving power. The *Lynx* CAT grating array will consist of a large number of grating facets that must be arrayed on the Rowland torus to within well-defined tolerances. Facet alignment and bonding equipment and facet-to-GAS alignment and mounting equipment (including metrology infrastructure) will need to be designed, procured, and applied to reach TRL 5 brassboard (Q2 2021) and TRL 6 prototype (Q4 2023) demonstrations. The *Lynx* XGS strategy to meet science requirements is shown in Table 7.6.

Table 7.6. XGS requirements derived from *Lynx* science drivers and the strategy of the CAT grating technology to meet them. Values in [] refer to milestones, TRL, and expected completion date as given in the full *CAT-XGS Technology Roadmap*.

Lynx X-ray Grating Spectrometer Requirements Derived from Science Requirements		CAT XGS Strategy to Meet Lynx Requirements
System effective area at OVII lines	$4,000 \text{ cm}^2$	<ol style="list-style-type: none"> 1. Increase diffraction efficiency by fabricating deeper device layer (grating bar depth) [M1, TRL 5, Q4 2019] 2. Increase geometric throughput by decreasing obstruction due to support structures [M2,3, TRL 5, Q2 2020] 3. Fabricate larger grating membranes [M11, TRL 6, Q4 2022] 4. Fabricate thinner grating bars to increase throughput and diffraction efficiency [M9, TRL 6, Q4 2022]
Resolving Power	$R > 5,000$	<ol style="list-style-type: none"> 1. Develop concept and metrology infrastructure for mounting and alignment to preserve LSF [M4, TRL 5, Q3 2020] 2. Develop “chirped” gratings to maintain LSF of large membranes [M12,13, TRL 6, Q3,Q4 2023]

7.3.2.2 Programmatic Considerations

Advancing from the demonstrated SOA to the *Lynx* performance requirements will require several step-wise advancements in grating fabrication, facet assembly, and precision alignment on the integrated grating assembly. However, there are no known physical barriers to achieving the required capabilities (i.e., formulating and applying the processes needed to produce the required number of finished

grating membranes, facets, and array structures are extensions and refinements of current practices). Identified risks are primarily matters of production and manufacturing scale and can be mitigated by design conservatism. For example, the system effective area requirement can ideally be met by reducing support structure obscuration as planned or by increasing the mirror aperture coverage from the current ~65%. The latter incurs greater mass and cost but remains a viable option lowering the overall risk posture. Steady and reasonable investment in technology development through NASA SAT funding, followed by *Lynx* technology development funding, is expected to bring the CAT-XGS to TRL 6 by Q3 2024, well in advance of mission PDR.

7.3.3 Off-Plane Reflective Grating Spectrometer

The reflection grating (also referred to as off-plane gratings or OP-XGS) concept for *Lynx* [608] is an alternative to the DRM grating architecture with a fully-developed *OP-XGS Technology Roadmap*. The reflection grating design utilizes a blazed grating to intercept light exiting the telescope optic to create a high-resolution dispersed spectrum. The light is incident nearly parallel to the grating grooves at grazing incidence. The small graze angles at X-rays allow close stacking of the gratings commensurate with the nesting of the X-ray optics. Large-format ($\sim 100\text{-x-}100\text{-x-}0.5\text{-mm}^3$) gratings are fabricated using standard nanofabrication techniques [609]. The process begins by writing the groove pattern into a resist using an electron beam lithography tool. This pattern is transferred into a substrate to produce a master grating that can then be replicated hundreds to thousands of times using standard techniques such as substrate conformal imprint lithography. Once the gratings are replicated, they are aligned and mounted into modules appropriate to the telescope optic.

The OP-XGS reflection grating technology has been assessed at TRL 4 by the 2017 NASA PCOS Technology Management Board. The concept has been recently demonstrated on the suborbital *Water Recovery X-ray Rocket* (WRXR; [610]) and is slated to fly on the *Off-plane Grating Rocket Experiment* (OGRE; [611]). The latter includes a 12-shell polished silicon optic similar to the *Lynx* baseline design. Experiments using similar gratings [608] have demonstrated diffraction efficiency over 60% (exceeding the *Lynx* estimated requirement of 40%) and resolving power of $R = \sim 8,000$ (*Lynx* requirement is $R = 5,000$). The specific technology described here has been under development at PSU (and formerly at the University of Iowa) since 2011 through funding by NASA's SAT, APRA, and Roman Technology Fellowship (RTF) programs.

Performance, Issues and Challenges — The OP-XGS design requires a smaller fractional occultation of the mirror aperture, allows for a wider working energy range (0.2 to 2 keV), and a smaller focal plane footprint (fewer focal plane sensors) relative to the baseline CAT-XGS. However, the OP-XGS has more restrictive alignment tolerances and a greater mass XGA than the CAT-XGS design. The alignment allocation, including sensitivity to repeated insertions and retractions of the XGA, is captured in the overall error budget. As with the CAT-XGS, the XGS system resolving power is affected by these alignments and by other tolerances within this error budget.

There are two main challenges for the OP-XGS technology development. First, while blazed gratings have been fabricated for high efficiency and radial profiles (needed to diffract the converging telescope beam) have been fabricated for high resolving power, a large-format, radial blazed grating has not been tested to demonstrate both concurrently. At least four methods are under study that can

potentially be used to fabricate gratings of the required geometry. The highest risk for the most viable of these options is a decrease in diffraction efficiency because of increased scattering due to roughness caused by the radial profile not following the crystal structure of the silicon substrate.

The second challenge is achieving alignment per stringent *Lynx* requirements. A full error budget has not yet been validated specific to *Lynx*, but contributions have been identified that include grating-to-grating alignments within a module, module-to-module alignments within the array, array-to-mirror alignments, and mirror + XGA alignment to the focal plane. These alignments, along with factors such as the details of the telescope PSF, pointing knowledge, and detector pixelation will form the error budget for the spectral LSF, which will ultimately determine the performance of the OP-XGS. Concept designs and initial calculations argue that the tightest translational tolerance is on the order of 100 μm (1 σ), while the tightest alignment tolerance is around 5 arcseconds (1 σ). The WRXR grating module demonstrated ~ 10 s of arcseconds (1 σ) angular alignment and translation alignments better than 100 μm (1 σ).

7.3.4 *Lynx* X-ray Microcalorimeter

LXM requires an over 30-fold increase in the number of X-ray absorbers (pixels) compared to *Athena*'s X-ray Integral Field Unit. This is being realized through significant technology investment that has already demonstrated (1) thermal multiplexers (a.k.a., "hydraz") linking 25 pixels to a single temperature sensor; (2) fine-pitch, multilayer, superconducting wiring buried beneath planarized substrates—leveraged from superconducting digital electronics and quantum computing developments—enabling wiring of large-format arrays; and (3) readouts using Superconducting Quantum Interference Devices (SQUIDs) coupled to microwave resonators—using technology pioneered for infrared detectors—for a 10-fold advancement in the number of sensors read out on each signal chain without loss of energy resolution. A full-size, 102,800-pixel, *Lynx* X-ray Microcalorimeter array is under development today with fabrication scheduled for completion in 2019.

The LXM is a broadband, energy-dispersive, high spectral and spatial resolution imaging spectrometer focal plane instrument (§6.3.4). The LXM X-ray absorbers and sensors, operating at 50 mK, precisely determine incident photon energies by measuring the temperature rise from the heat they deposit. The LXM instrument concept builds upon substantial experience in developing microcalorimeter instruments for space, including *Astro-E*, *Astro-E2*, *Hitomi*, the *X-ray Imaging and Spectroscopy Mission* (XRISM) (launching in 2022), and *Athena* (slated for launch in 2031). The major technological differences of LXM from these predecessors are the 30-fold increase in the number of absorbers (10^5 pixels), their much finer pitch (25 to 50 μm), and the improved spectral resolution for a lower energy range subarray (<0.3 eV Full-Width Half-Maximum (FWHM)).

The LXM concept has been advanced by scientists and engineers from several low-temperature X-ray detector groups in the U.S. Key members of this group located at GSFC have substantial experience in developing all the microcalorimeter instruments listed above; most apropos being *Athena's* X-ray Integral Field Unit (X-IFU). Members of this group working on LXM are funded through NASA's APRA, SAT, and ISFM programs.

There are four elements to be matured from the current SOA to TRL 6 for the LXM: (1) the arrays of detectors, (2) the readout electronics, (3) the Focal Plane Assembly (FPA) and optical/IR photon blocking filters, and (4) the cryogenic cooling system. These technology elements were collectively assessed by the 2017 NASA PCOS Technology Management Board for *Lynx* at TRL 3; however, the first element is expected to reach TRL 4 before this year is out, the second element within another year, and the third and fourth elements are already at TRL 4. Parallel development paths are actively being funded for most of these elements, greatly enhancing the potential for rapid advancement while helping reduce technical and schedule risk. Detailed development plans for all baseline and alternative technologies are provided in the complete *LXM Technology Roadmap*.

To meet all the science objectives for *Lynx*, the LXM design consists of three types of pixel arrays with different performance capabilities. These are referred to as the Main Array (MA), Enhanced Main Array (EMA), and Ultra-High-Resolution Array (UHRA). Required performance characteristics for each array are listed in Table 6.11 of §6.3.4.1. The SOA performance of these arrays and of the associated multiplexing readout electronics are compared to the *Lynx* requirements in Table 7.7.

Table 7.7. LXM array and readout electronics derived requirements and current performance.

Parameter	Requirement	Current Performance		
Pixel Array	MA / EMA / UHR	Main Array	Enhanced Main Array	Ultra-Hi-Res Array
Pixel pitch (μm)	50 / 25 / 50	50	25	50
Array size	86,400 / 12,800 / 3,600	37,500	10,000	1,600
Hydra Factor	25 / 25 / 1	25	25	1
Spectral resolution in large-format prototype array (FWHM eV): Comment:	MA: 3 eV up to 7 keV EMA: 2 eV up to 7 keV UHRA: 0.3 eV up to 0.75 keV	Int. NEP _(no X-T) = 2.7 eV Measured FWHM: 3.3 eV @ 1.5 and 6.4 keV No heat-sinking => high cross talk	Int. NEP _(no X-T) = 1.2 eV Measured FWHM: 1.7 eV @ 1.5 keV (No heatsinking => high crosstalk)	Int. NEP _(no X-T) = 0.26 eV Measured FWHM: 0.26 eV @ 3, 6 and 9 eV (Not yet measured at higher energies)
Performance in similar pixel type in other arrays		Measured FWHM in 20-absorber hydras (50 μm , 4.2 μm thick): 3.4 eV @ 5.4 keV	—	Measured FWHM in absorber of 4.2 μm : 0.7 eV at 1.5 keV
Multiplexing Readout				
Electrical multiplexing: Resonators/HEMT	400 / 100 / 667	128 TESs on single HEMT through 128 μMUX SQUID resonators (with 2-MHz bandwidth)		
Resonator bandwidth	1.4 MHz / 5.6 MHz / 0.86 MHz	Resonators of this BW successfully tested	Resonators produced – not yet tested	Resonators of this BW successfully tested
Resonator spacing	10 MHz / 40 MHz / 6 MHz	Most demanding spacing (6 MHz) demonstrated in 128-TES demonstration		

Int. NEP is the integrated Noise Equivalent Power, which is a measure of the achievable energy resolution calculated from the measured signal from X-ray events (responsivity) and the quiescent noise excluding thermal background crosstalk events (no X-T)

A fully wired **microcalorimeter array** prototype using the baseline Transition-Edge Sensor (TES) detector technology has been fabricated with over 55,000 pixels representing all three array types [612]. A full-size LXM microcalorimeter array is under development, with fabrication scheduled to be completed in late 2019. A central component of the MA and the EMA technology is the use of hydras linking multiple X-ray absorbers (pixels), each with a different thermal coupling, to a single TES microcalorimeter. The thermal conductance of each link is tuned so that the TES measures a different characteristic temperature profile for X-ray events absorbed in the different pixels (Figure 7.10). The shape of the pulse is measured to determine the event position.

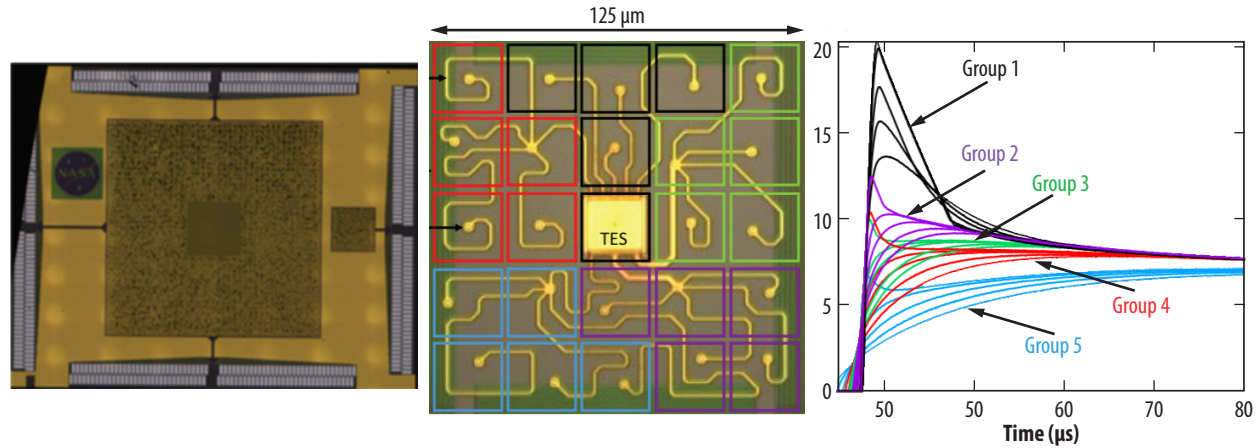


Figure 7.10. (Left) 50,000-pixel two-thirds linear scale LXM prototype detector array. The large square in the middle is the MA surrounding the EMA at its center. The UHRA is to the right. (Center) Single 25-pixel EMA hydra (25-μm pitch) prior to depositing absorbers. Colored squares delineate absorber locations. The TES is the large central square, the small dots are pixel contact stems, and narrow lines are thermal links connecting absorbers to the TES. Note the four “trunks,” each “branching” into four more stems for a total of five pixels for each of five hydra groups (one trunk is the TES itself). (Right) Measured pulse shapes for all 25 pixels color-coded by group corresponding to center panel.

For use as an effective spectrometer, the combination of signals from all pixels in a hydra needs to produce a narrow spectrum, as shown [613] for the MA and EMA in Figure 7.11, ensuring high system energy resolution. The UHRA uses single-pixel detectors to maximize the energy resolution at low photon energies. The energy resolution of the UHRA has also been characterized (Figure 7.11, right panel), but not yet at representative energies because of the difficulty in producing a photon source with a sufficient intensity of 3 eV photons per pulsed laser-diode event.

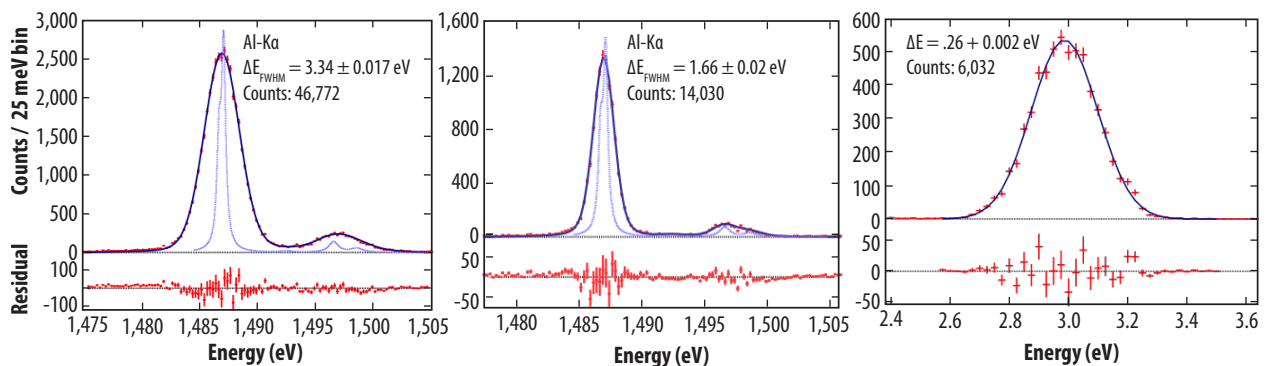


Figure 7.11. X-ray spectra measured by prototype LXM sensor arrays. (Left) Co-added Al-K α for all 25-pixel MA hydras. (Center) Co-added Al-K α for all 25-pixel EMA hydras. (Right) Single-absorber UHRA spectrum of a narrow-line ultraviolet laser diode source at 3 eV.

These first prototype arrays fabricated specifically for LXM incorporate microstrip-buried wiring layers, developed through a collaboration between GSFC and MIT Lincoln Laboratory. They are of suitable pitch and density to read out a full-scale array; however, the prototype does not yet incorporate a heatsink layer required to prevent noise from thermal crosstalk degrading the energy resolution. Improvements estimated for a device with suitable crosstalk heat-sinking are within LXM energy resolution requirements.

Readout electronics based on microwave SQUID multiplexing of up to 128 TESs have demonstrated good performance without energy resolution degradation from the readout [614, 615]. These demonstrations have shown microwave SQUID multiplexing is capable of providing the necessary bandwidth for single-absorber TESs, and components spanning the necessary parameter space to read out the high slew rates of the multi-absorber hydra microcalorimeters have been experimentally proven. The current technology assessment is TRL 3 because the readouts designed for each of the specific LXM pixel types have not yet been tested with LXM microcalorimeters and are likely to require some further iteration [616].

The microcalorimeter array, anti-coincidence detector, and cold readout components are packaged inside a **focal plane assembly (FPA)**. At the instrument base temperature, the FPA provides thermal-mechanical isolation and electromagnetic shielding. The LXM will leverage much of the same technology in the mechanical design, thermal design, magnetic shielding, and design of the anti-coincidence detector as *Athena's* X-IFU FPA [617] and is assessed at TRL 4. The design of the LXM FPA is summarized in [612]. The LXM will use a set of blocking filters mounted within the dewar that transmit the X-rays of interest while attenuating longer wavelengths to prevent performance degradation of the microcalorimeters and cooling chain [618]. Current technologies meeting LXM requirements are at TRL 4. Additional development will leverage highly from *Athena's* X-IFU. Optical/IR blocking filters are at TRL 5.

The cryogenic **cooling system** envisioned for LXM is also assessed at TRL 4. Many cryostats have already been developed for space-based applications, and many cryocoolers that integrate into them are under development in the commercial sector. As the *Lynx* FPA develops, the cryocooler definition will improve, the vibration requirements will be better refined, and designs specific to *Lynx* will reach higher fidelity. Part of the cryogenic system, the Adiabatic Demagnetization Refrigerator (ADR), provides the 50-mK cooling, as has been demonstrated on *Hitomi* by an ADR lifting 0.4 μW from the detector array. To achieve the estimated 6 μW of cooling needed for the LXM, a Continuous ADR (CADR) will be needed. CADRs have been demonstrated at TRL 4 with four cooling stages operating between 4.5 K and 50 mK. For the LXM, a fifth stage operating continuously at 0.6 K must be demonstrated.

7.3.4.1 Key Elements and Milestones

Development paths for each of the four elements to be matured for LXM are outlined below. Table 7.8 lists the strategic approach used to mature these elements to meet the *Lynx* scientific goals.

Table 7.8. *Lynx* requirements on the LXM derived from its science drivers and the strategy of the LXM technology to meet them

Main Array	Requirement	LXM Development Team's Strategy to Meet <i>Lynx</i> Requirements
Energy Range	0.2 to 7 keV	Energy range is set by (1) design of TES transition width, (2) pixel heat capacities, and (3) readout capability. Already shown that (1) and (2) are possible up to 7 keV. Will trade detector energy resolution with readout capability to allow standard energy range >7 keV in normal operating mode and will adjust bath temperature (energy resolution) for mode extending to 15 keV.
Field of view	5 arcmins x 5 arcmins	The use of hydras with 25 pixels attached to each sensor and high-yield buried multilayered superconducting wiring makes this feasible with only a factor of 2 more sensors than <i>Athena's</i> X-IFU. Prototypes with half this FOV area (two-thirds the linear dimension) have already been fabricated with wiring pitch consistent with fabrication of full-size array.
Pixel size	1 arcsec x 1 arcsec	Ion-milling of all-gold absorbers with the required quantum efficiency on 50- μ m pitch has already been demonstrated. Area fill factor will be further optimized but current fill factor already acceptable.
Energy Resolution	3 eV (FWHM)	Have demonstrated 3.3 eV for 1.5 and 6.4 keV X-rays in a 25-pixel hydra, and have shown sensitivity will be <3 eV when suitable heat-sinking incorporated. Will optimize absorber thickness and TES design to optimize resolution and ease of readout.
Enhanced Main Array	Requirement	LXM Development Team's Strategy to Meet <i>Lynx</i> Requirements
Energy Range	0.2 to 7 keV	Strategy same as for main array.
Field of View	1 arcmin \times 1 arcmin	Strategy similar to that of main array. Use 25-pixel hydras attached to each sensor and high-yield buried multilayered superconducting wiring.
Pixel Size	0.5 arcsec \times 0.5 arcsec	Strategy same as for main array.
Energy Resolution	2 eV (FWHM)	Have demonstrated sensitivity in suitable 25-pixel hydras of 1.6 eV at 1.5 keV. Will optimize absorber thickness and TES design to optimize resolution and ease of readout.
Ultra-High-Resolution Array	Requirement	LXM Development Team's Strategy to Meet <i>Lynx</i> Requirements
Energy Range	0.2 to 0.75 keV	Basic strategy similar to main array, but main development and focus is on the engineering of the TES transition properties.
Field of View	1 arcmin \times 1 arcmin	Fully wired full-size arrays utilizing buried superconducting multi-layered wires have already been designed, fabricated and tested. The FOV of this subarray is not a driver of technology development.
Pixel size	1 arcsec \times 1 arcsec	Strategy same as for main array.
Energy Resolution	0.3 eV (FWHM)	This energy resolution has already been demonstrated for low-energy photons and needs to be demonstrated at energies in the bandpass of interest. Transition width will be engineered to optimize energy resolution and energy range to meet simultaneous requirements.
Readout	Requirement	LXM Development Team's Strategy to Meet <i>Lynx</i> Requirements
Flight qualify suitable HEMT amplifiers	HEMTs must adhere to requirements for > 10-years at L2.	Will flight-qualify suitable HEMT amplifiers working together with a suitable HEMT manufacturing company.
Microwave SQUID resonator components.	Readout (μ MUX SQUID resonators) must meet noise, bandwidth, and resonator spacing requirements of each LXM subarray.	Design, fabricate, and test microwave SQUID circuitry with the appropriate noise level resonator bandwidths and resonance frequency spacing for the LXM to demonstrate that subarrays can be read out without significant energy resolution degradation from the readout. Special care will be taken to minimize crosstalk between signals at different resonator frequencies. Parallel technology effort to develop code division multiplexing option until TRL 5 is established by a readout technology.

Table 7.8. *Continued*

FPA	Requirement	LXM Development Team's Strategy to Meet <i>Lynx</i> Requirements
Magnetic shielding	Shielding factor $> 6 \times 10^5$ Ambient field $< 1 \mu\text{T}$	Use identical approach to magnetic shielding as has been developed and proven for the <i>Athena</i> X-IFU
Electrical wiring/ contacts	44 coaxial cables from 283 K to 50 mK	Regular semi-rigid coax cables from room temperature to HEMTs at 4.5 K. Will verify thermal conductance of low thermal conductivity of superconductivity coax cables for use from 4.5 K to 50 mK. Will integrate superconducting bump bonds for connections between TESs and μMUX readout. Will use superconducting microstrip flex under development at GSFC between detectors and readout.
Mechanical mounting	Kinematically mount detector and readout chips. Support low temperature stages with rigid low thermal conductance supports.	Implement application-specific kinematic mounting techniques developed for mounting filters on <i>Hitomi</i> SXS and evolved for the <i>Athena</i> X-IFU. Develop and test low thermal conductivity thrust cones between lowest temperature stages using low thermal conductivity thin fiberglass structures.
Cryogenics	Requirement	LXM Development Team's Strategy to Meet <i>Lynx</i> Requirements
Cooling from 283 K to 4.5 K	50 mW @ 4.5 K High reliability	Use of 4-stage pulse-tube cryocooler specially designed to meet cooling requirements as well as cooling of 3 thermal shields at intermediate temperatures. Parallel option of using 3-stage Turbo Brayton Coolers. Need to develop 4.5-K turbo-alternator.
Cooling from 4.5 K to 50 mK	Cooling: 250 μW @ 0.6 K 6 μW @ 50mK Heat generated: $< 4 \text{ mW (avg.) @ 4.5 K}$	Further develop multistage continuous ADR similar to previous 4-stage ADRs but with additional 5 th stage to provide required cooling at 0.6 K. Heat generated, while cyclical, will be time-averaged through thermal design to provide constant quiescent level of less than 4 mW.

Element 1: Microcalorimeter Arrays — To achieve TRL 4 for the LXM MA, EMA (25 absorber hydras), and UHRA (single-pixel readout), prototype arrays with suitable form factors are needed. A subset of pixels from each subarray type has already demonstrated energy resolution that is close to meeting all LXM requirements (Figure 7.11). It remains to verify that the energy resolution and pixel discrimination properties (for the MA and EMA hydras) are maintained when measurements are performed using suitable Nyquist inductors in the bias circuits. Previous measurements have shown no detrimental effects [619], but these measurements must be reproduced on LXM-compatible hydras to reach TRL 4.

At TRL 5, all three required pixel arrays will be fabricated on a single substrate (as already demonstrated) and tested for quantum efficiency, pixel uniformity, and radiation hardness. Also, at TRL 5, the integration of heatsinking (via a gold thermal ground plane underneath the array, where the substrate has been thinned in the region of the absorbers) suitable to minimize thermal crosstalk across a full-size array will be performance tested. The technical approach to heatsink advancement will be similar to one that has previously been successfully demonstrated at the necessary level. Scale-up of existing buried wiring technology is not expected to be an issue.

At TRL 6, a full-size, flight-like array with a pixel yield of $>95\%$ will be tested to verify that all performance and radiation hardness requirements are met. This test will be conducted with a full-scale demonstration FPA and readout electronics that support the operation of at least 25% of the pixels simultaneously. The AD² to TRL 6 is low because the development needed is only incremental due to the previously successful demonstration of large-scale detector fabrication. Once TRL 5 is established, the detector essentially already exists, and only fabrication yield and sensitivities to the environment need to be verified, which are not expected to be problematic.

There are no known fundamental barriers to straightforward technology advancement using standard engineering practices for the microcalorimeter arrays given the recent breakthroughs made in the development of smaller pixels, fine-pitch wiring, and hydras.

Element 2: Microcalorimeter Readout — To achieve TRL 4, the multiplexing focus will be on developing microwave SQUID circuits for each of the required pixel array types at reduced multiplexing factors to minimize design and fabrication time while still providing important information about the interactions between the sensors and the readout system. Some new development is needed to optimize the designs for the bandwidth required. At TRL 5, the requirement will be ramped up to full bandwidth and energy resolution that meets full requirements. Additionally, radiation hardness will be tested on the TRL 5 test article. At TRL 6, a scalable readout geometry will be developed to read out >25% of the full-scale pixel arrays simultaneously.

At TRL 4, a High-Electron Mobility Transistor (HEMT) amplifier suitable for flight qualification will be designed and fabricated. At TRL 5, a set of flight-like HEMT amplifiers, complete with requisite cabling, will be fabricated and included in the TRL 5 test setup. Upon reaching TRL 5, these flight-like amplifiers will have demonstrated that any energy resolution degradation after a 5-year equivalent radiation dose remains within the allowed range. The HEMT design will require no further development and can be used for TRL 6 system testing.

Room temperature readout electronics for LXM are currently at TRL 3. The progression to TRL 4 will proceed by assembling an appropriate set of room temperature readout electronics using commercial parts as a breadboard model spanning a bandwidth of 4–8 GHz and testing with low-temperature SQUID resonators. This will be carried out using a lesser performing Field Programmable Gate Array (FPGA) than the one envisioned for LXM, but will prove the concept for being able to read out a 1–2 GHz sub-band of the 4–8 GHz bandwidth. To progress to TRL 5, the breadboard components will be upgraded with flight-qualified components (a few components may need to be qualified through a NASA flight qualification process). This will again be a room temperature operation, and will demonstrate isolated readout of relevant pixel types at relevant multiplexing factors at frequencies ranging over the full bandwidth range of the HEMT. TRL 6 will be achieved by fabricating and testing a full-scale readout system, with at least one quarter of the array using flight-qualified parts.

Overall, the advancing the readout to TRL 5 is moderately challenging but has a high degree of confidence of success because of widespread industry needs identical to those of LXM. The scale-up of the low-temperature electronics to TRL 6, with integration into a new FPA geometry, is similarly challenging. The room temperature electronics have a clear and feasible development plan, requiring a straightforward but large engineering support effort.

Element 3: Focal Plane Assembly and Optical/Infrared Blocking Filter Assembly — The *Lynx* FPA design is leveraged from *Athena*'s, and as such, it is currently at TRL 4. Advancing to TRL 5 will require:

1. Design and testing of kinematic mounting approaches for the FPA chip and the anti-coincidence detector, and also the microwave SQUID resonator chips together with Nyquist inductors and bias resistors;
2. Simulations and experiments to determine whether there will be issues related to RF signals interfering with each other among the different microwave SQUID resonator chips; and
3. Verifying the thermal and mechanical properties of the T-300 cone-shaped thrust tubes used for mechanical support of the FPA between different temperature stages, as well as verification of the mechanical properties and the DC- and AC-shielding performance of the magnetic shields.

To progress to TRL 6, a full-scale model FPA attached to a CADR to provide representative temperatures/conditions for FPA operation will be designed, built, and tested. This will include appropriate interconnects and bump bonds. Advancing to TRL 6 represents a large engineering effort but will leverage *Athena's* similar FPA design.

It is likely that connectorized coaxial cables that are suitable in size and thermal conductance for the LXM FPA will be used between each HEMT and the readout at 50 mK. Currently, there are only limited data available on the properties of such interconnects. To progress to TRL 5, measurements must be made to verify that the thermal and mechanical properties are suitable. Superconducting flex (around-the-corner wiring) is needed to carry signals between the detector arrays and the multiplexer chips, and measurements must be made to verify that the thermal, mechanical, and electrical properties are suitable for the LXM. TRL 6 will be verified as a part of the full-scale demonstration model FPA's verification testing.

Optical blocking filters are already at TRL 5. Progressing to TRL 6 requires building a set of filters that are compatible with the FPA and cryostat designs, with appropriate kinematic mounts. Demonstration in the relevant environments will then be performed using a vibration table for mechanical verification.

Element 4: Cryogenic Cooling System — The commercial pulse tube cooler under consideration for LXM is currently at TRL 4, while the Reverse-Brayton (RB) cooler is at TRL 3. In order to advance the RB cooler to TRL 4, only the 4.5-K turboalternator stage remains to be demonstrated. Then, at TRL 5, the RB cooler must demonstrate launch load survivability, and TRL 6 requires integration into the TRL 6 LXM test article and performance verification.

Advancing the pulse tube cooler to TRL 5 involves the design, fabrication, and demonstration of the full cryocooler system performance as proposed for the LXM, meeting all the cryogenic performance requirements. Breadboard electronics will be used with flight-compatible electronics components and verify that the system meets performance requirements and is compatible with expected launch loads. Ultimately, TRL 6 will be achieved when an entire flight-like system is demonstrated with performance testing in pre- and post-launch load environments and with flight-like support electronics.

The LXM cryostat, which houses all components lower than room temperature, is based on design principles used for many previously flown cryostats. The design challenge is primarily a tradeoff between structural and thermal performance and is considered normal engineering work for experienced cryogenic engineers. Previous missions employing long-life dewars operating at this low temperature include the *Infrared Astronomical Satellite (IRAS)*, *Cosmic Background Explorer (COBE)*, the *Infrared Space Observatory (ISO)*, *Suzaku*, *Hitomi*, *Spitzer*, and *Herschel*, among others. In the case of LXM, there will be no liquid helium, which simplifies the design. Nevertheless, the cryostat is considered TRL 5, and to advance to TRL 6, a cryostat design that meets the LXM's thermal and structural requirements is needed, and structural and/or thermal sample tests are needed where suitable data for specific materials used in the design do not currently exist.

The ADR for LXM is already at TRL 4. To raise the 50-mK CADR to TRL 5 requires adding to the system and demonstrating a high-performance magnetic shield, as well as demonstrating that meeting launch load vibrational requirements can be met. To advance to TRL 6, a secondary continuous stage operating at 0.6 K must be added. This is a straightforward addition of another stage and its support and heat switch. This TRL 6 unit will need to demonstrate 6- μ W cooling at 50 mK.

7.3.4.2 Programmatic Considerations

As presented in detail in the *LXM Technology Roadmap*, alternative technologies are being independently funded and investigated for the thermal sensor, readout electronics, and cryocooler elements of the *Lynx* design. This approach helps to mitigate about one-third of the identifiable technical and schedule risks while simultaneously enhancing the potential for bringing new and innovative technological solutions to the program. Formal selection of baseline LXM technologies for these elements will be made soon after TRL 5 performance has been verified (i.e., near the start of Phase A).

The FPA is a special-purpose entity that needs to be integrated and tested with the rest of the instrument. This means the design, fabrication, and testing of the detectors and readout should start early, and these components should be at TRL 6 early. Thus, all the critical technologies needed for LXM will achieve TRL 4 by the start of pre-Phase A, funded through ongoing existing research and development programs, achieve TRL 5 nine months prior to the end of pre-Phase A, and the critical detector and readout technologies will achieve TRL 6 by the end of Phase A through a TRL 6 demonstration unit, with seven months of margin.

Beyond that, the overall LXM development approach is based upon that followed by the Soft X-ray Spectrometer (SXS) instrument on *Hitomi* and is similar to the approach planned for the *Athena* X-IFU. It is based on the development of an engineering model and a protoflight unit, with selected subsystem flight spares but no complete instrument spare. There is no qualification model at the instrument or subsystem level, but the engineering model is planned to undergo extensive qualification testing beyond the typical level of an engineering development unit in order to space-qualify the design. The philosophy behind this approach is to optimize schedule considerations, with time for proper feedback between the engineering and flight model construction, without adding risk.

The LXM's development will benefit greatly from the availability of additional experienced engineers and scientists becoming available during Phase A to complement the LXM development team following the launch and commissioning of *XRISM* and from the ramp-down of *Athena's* X-IFU activities during its Phase B. Furthermore, there are no major infrastructure upgrades needed, as the LXM program will leverage the substantial investment made for developing detectors for the X-IFU.

8 Lynx Design Reference Mission Programmatic

Lynx is a flagship NASA mission designed to execute an ambitious and revolutionary science program while maintaining a low risk posture, and delivering on technical, cost, and schedule commitments to ensure mission success. This approach enables a launch in the mid-2030s at a reasonable cost for a flagship mission, consistent with pre-Phase A concept maturity.

The Design Reference Mission (DRM) programmatic details describe a well-validated and achievable project management approach, as well as schedule and cost formulation representative of a mature mission design, enabling technologies that are rapidly progressing and relatively small-quantity, manageable technology development risks, and a strong use of heritage. In addition to the technology development roadmaps described in §7, the DRM is further enabled by project management practices and approaches that leverage substantial *Chandra* heritage and team experience. The result is a well-developed project organization, detailed WBS, feasible and achievable schedule, mitigatable risks, and credible and validated costing consistent with pre-Phase A formulation practices. The *Lynx* team understands the challenges related to developing and costing flagship class missions [620], and has taken a conservative approach throughout by including substantial margins and reserves to mitigate cost and schedule risks.

8.1 Project Classification and Authority

The *Lynx* DRM delivers on the transformative science program (§1 through §5), consistent with a NASA Flagship mission. *Lynx* is a Category 1 project as defined in NASA Procedural Requirements (NPR) 7120.5, *NASA Space Flight Program and Project Management Requirements*, and is classified as Risk Class A per NPR 8705.4, *Risk Classification for NASA Payloads*. This risk class is assigned due to the criticality of *Lynx* to NASA's strategic plan, very high national significance, and long mission lifetime. The *Lynx* project will be under the decision authority of the NASA Associate Administrator (AA) and the Science Mission Directorate (SMD) AA. The project will be part of the recently established Astrophysics Strategic Missions Program within the NASA SMD Astrophysics Division, and overall project management responsibilities will be assigned to the selected lead NASA Center.

The *Lynx* project will perform Lifecycle Reviews (LCRs) in accordance with the project management processes defined in NPR 7120.5 and with the systems engineering requirements in NPR 7123.1, *NASA Systems Engineering Processes and Requirements*. An independent Standing Review Board (SRB) will conduct the LCRs and make recommendations on the project's ability to proceed through the prescribed Key Decision Points (KDPs) and life-cycle phases.

8.2 Project Organization and Partnerships

The *Lynx* project organization mimics that of successfully implemented heritage flagship missions. The notional project structure for *Lynx* (Figure 8.1) encompasses the roles necessary to deliver and launch the Observatory, provide required levels of technical authority oversight and insight, and ensure overall mission success. While Centers and contractors have not been assigned responsibility for the *Lynx* mission, estimated costs were burdened with rates and fees typical of the Centers and contractors that might ultimately perform the mission. The resulting estimates are therefore useful for budgeting purposes. This organization is consistent with the project Work Breakdown Structure (WBS) and dictionary summarized in §8.5.1. Specific mission roles will be established prior to Phase A following the final architecture decision and Mission Concept Review (MCR). Strategic partnerships will take advantage of the existing resources (hardware and facilities) and workforce developed, over many years, for *Chandra*. These partnerships reduce risk through the implementation of lessons learned and significant stored knowledge of *Chandra* development through flight. Additionally, as a Flagship mission, *Lynx* welcomes continued international participation. An Acquisition Strategy Meeting will be conducted prior to Phase A to finalize decisions on international agreements, procurements, and partnerships.

The *Lynx* project will be staffed by the lead NASA Center (possibly supported by an external science team) to provide overall management and integration of mission elements, as well as lead project scientist functions. Specifically:

- WBS 01, Project Management (PM) functions include the management, integration, and direction of *Lynx* project activities, in compliance with Agency policies and procedures. The PM is responsible for programmatic business activities, control of the programmatic baseline, and resource management through rigorous project planning and control processes. The science payload manager for development of the X-ray mirrors and science instruments (the *Lynx* X-ray Microcalorimeter (LXM), High-Definition X-ray Imager (HDXI), and X-ray Grating Spectrometer (XGS)) will directly report to the PM.
- WBS 02, Systems Engineering (SE) functions include the technical design and performance of the mission. The Mission Systems Engineer (MSE) provides independent technical authority for *Lynx*.
- WBS 03, Safety and Mission Assurance (S&MA) functions include independent overview of S&MA activities and ensuring compliance with S&MA requirements.
- WBS 04, Project Scientist functions include leading the Science Working Group (SWG), ensuring the science content of the project, managing the technology development activities, and serving as the project interface to the *Lynx* science community.
- WBS 05, X-ray Telescope (XRT) management functions include overall Design, Development, Test, and Evaluation (DDT&E) of the telescope and its subsystems, as well as Integration and Test (I&T) and calibration of the telescope. It is assumed that these activities will be contractor-managed.
- WBS 06, Spacecraft Element (SCE) management functions include overall DDT&E of the SCE and its subsystems, as well as I&T of the SCE. It is assumed that these activities will be contractor-managed.
- WBS 07/09, Ground systems and mission operations functions include responsibility for the design, development, integration, test, implementation, and associated physical support equipment of the systems needed for commanding and operating the Observatory. This includes downlinking, processing, archiving, and distributing telemetry with the engineering and scientific data.

- WBS 08, Launch vehicle services functions include interfacing between the project and launch vehicle provider.
- WBS 10, Observatory I&T functions include management of the overall Observatory I&T program. It is assumed that these activities will be contractor managed.
- WBS 11, Outreach functions include responsibility for informing the public on *Lynx*'s benefits to the community.

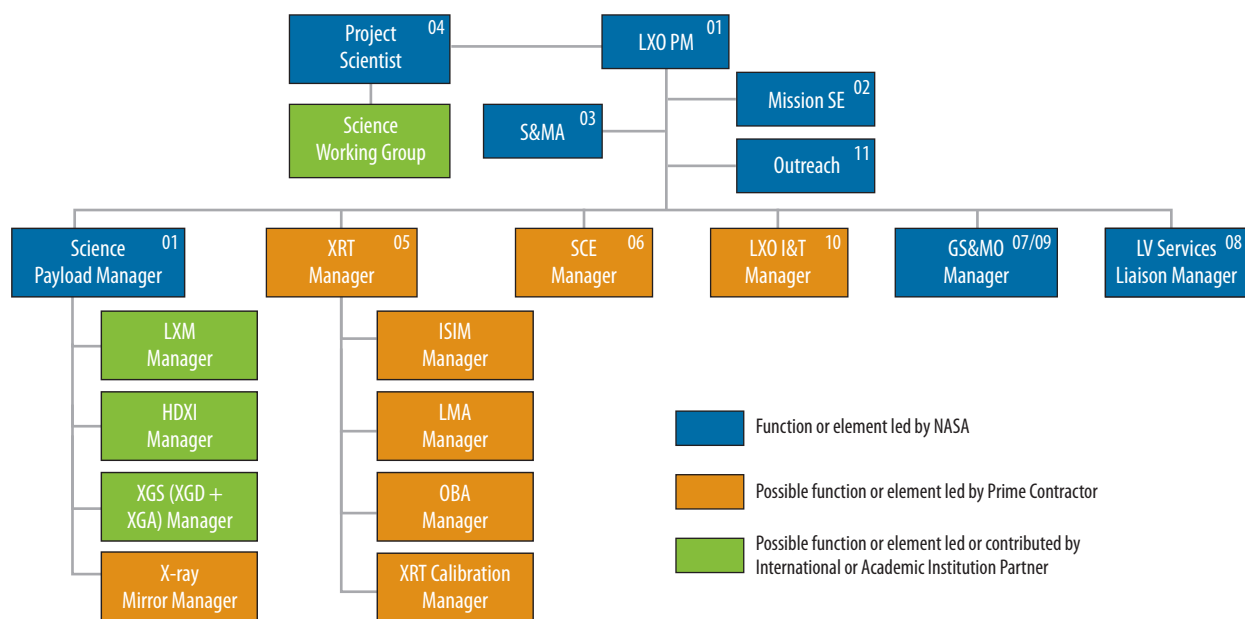


Figure 8.1. Notional *Lynx* project organization is consistent with NASA management practices and considers possible partnerships and prime contractor activities. Final organization will be defined following pre-Phase A procurement decisions and Mission Concept Review.

A prime contract is anticipated to be competitively selected for the DDT&E of the SCE, the XRT (including DDT&E of the Integrated Science Instrument Module (ISIM)), and the *Lynx* Mirror Assembly (LMA). The prime contractor will be responsible for overall integration for the Observatory, including systems I&T. The anticipated prime contract roles defined above are similar to the management approach used for *Chandra*.

The *Lynx* project will benefit from potential international and/or academic partnerships. Along with the intention of having a fully open scientific program similar to *Chandra* and XMM-Newton, and presumably *Athena*, potential areas of contribution could include instruments, building on existing collaborations, or even a distinct contribution to the spacecraft. The possibility of such contributions is being explored and discussions will continue through Phase A.

It is assumed that the science instruments will be provided by an academic institution, NASA or other government agency, or by an international partner, and that the X-ray mirrors will be provided by a contractor. Instrument providers will be selected through a NASA-issued Announcement of Opportunity (AO), and the X-ray mirror provider will be selected through a NASA-issued Request for Proposal (RFP). It is also assumed that a *Lynx* Science and Operations Center (§6.7) will be responsible for developing the ground system and leading Phase E under the direction of the lead NASA Center. The sequencing of the AOs and RFP are discussed in more detail in §8.4.

8.3 Risks and Risk Mitigation

Lynx project risks are well understood and mitigation plans are well defined. For the mirrors, HDXI and XGD sensors, and XGS gratings, multiple feasible (and funded) alternate technologies are available to mitigate technology development risks. Additionally, the LXM leverages strong heritage from similar, in-development flight instruments.

The *Lynx* design meets Risk Class A requirements that are consistent with NPR 8705.4. There are no credible single-point failures in the spacecraft or telescope designs, and the subsystems incorporate multiple redundancies throughout. A Failure Mode and Effects Analysis (FMEA) and Critical Items List (CIL) will be developed as required during project implementation to identify hardware items critical to the performance and safety of the mission, potential failure modes, and any resulting items requiring design improvements or corrective actions necessary to meet redundancy requirements. A summary of specific key redundancies for fault tolerance is provided in Table 6.14.

Level 1 Electrical, Electronic, and Electromechanical (EEE) parts, per the NASA Parts Selection List (NSPL), are included in the cost analysis, as are Engineering Models (EMs), prototypes, and component spares for the optics and instruments as described in §7. A protoflight Verification and Validation (V&V) approach will be used at the *Lynx* Observatory level due to the prohibitive cost impact of a full Observatory-level qualification unit. Lower Technology Readiness Level (TRL) subsystems, such as the optics and instruments, will have engineering development units tested at qualification levels. See §6.6 for more details on the *Lynx* V&V approach.

The *Lynx* team has identified and ranked the top project risks and defined the Likelihood (L) and Consequence (C) of risk occurrence on a scale of 1 to 5, with 1 being the lowest likelihood of occurrence and consequence to the Project and 5 being the highest. The project risk list is shown in Table 8.1, and Figure 8.2 provides 5- \times -5 risk chart for these risks. The risks ratings are per the standard scale for consequence and likelihood, consistent with Goddard Procedural Requirements (GPR) 7120.4D, *Risk Management Reporting*. Project-level risks are defined as those with the potential to change the technical and/or programmatic baseline. In addition to project risks, each major technology under development will also carry risks as defined in the individual technology development roadmaps and summarized in §7. The risks fall under the general categories of technology maturation, manufacturability, and science impact. All of the *Lynx* risks, which are specific to the DRM, have credible mitigation

Table 8.1. Summary of top *Lynx* project risks.

Risk	Title	L	C	T	S	\$
1	X-ray Mirror Module Assembly and Alignment	3	4		X	X
2	LXM Technical Maturation to TRL 6	3	3	X	X	X
3	X-ray Mirror Segment Industrialization	2	3		X	X
4	LXM Fabrication and Assembly	2	3		X	X
5	X-ray Mirror Technical Maturation to TRL 6	3	2	X	X	X
6	HDXI/XGD Detector Technology Maturation to TRL 6	2	2	X	X	X
7	Calibration Facility Availability	1	3		X	X

L = likelihood of risk occurrence; C = consequence of risk occurrence; T = technical risk; S = schedule risk; \$ = cost risk

plans. It is important to note that multiple feasible technologies exist for the mirrors and instruments that might have a different set of opportunities and risks than those listed.

Risk 1 — X-ray Mirror Module Assembly and Alignment:

If the ability to demonstrate and scale up the processes from a laboratory environment to the production levels needed to assemble and align the numerous X-ray mirror modules cannot be achieved while maintaining technical requirements, then the project cost and schedule will be impacted.

Mitigation: For each mirror system design under consideration, a technology development roadmap has been developed that includes early studies of mirror alignment and mounting processes. For the Silicon Meta-Shell Optics specifically, recent developments have shown the feasibility of producing a single aligned high-quality mirror segment pair that meets the necessary mirror figure. Further work is needed to prove full-scale feasibility of the necessary processes with requisite quality control to mount and align the many mirror segments into modules needed for flight. This work will take place during technology development. Starting at TRL 4, multiple partially-populated modules will be demonstrated. By TRL 6/PDR, a high-fidelity, qualification-tested, partially populated EM will be developed and will serve as pathfinder for the technology, as well as the manufacturing and assembly processes. For the Silicon Meta-Shell Optics technology, the EM will consist of three meta-shells (outer, middle, inner) with three fully populated modules in each that serve as a testbed for demonstrating technical and assembly processes. Nine months of DDT&E schedule margin have been added to the Silicon Meta-shell Optics delivery to flight unit calibration/verification. This margin includes three months to delivery of the TRL 6/PDR demonstration unit to cover issues that arise during technology maturation and an additional six months of margin for issues that arise during the manufacturing and assembly process of the flight unit.

Impact: Increased cost and schedule to meet technical requirements.

L × C: 3 × 4

Risk 2 — LXM Technical Maturation to TRL 6: If the LXM is unable to achieve requisite technology maturation and performance to TRL 6, then the mission science and/or technology development cost and schedule will be compromised.

Mitigation: A detailed *LXM Technology Roadmap* that includes cost, schedule, and risk has been developed for the LXM, which is based on extensive experience from previous and planned space-based X-ray microcalorimeters. Technology developments from the *Hitomi* SXS, *Athena* X-ray Integral Field Unit (X-IFU), and *X-Ray Imaging and Spectroscopy Mission (XRISM)* Resolve X-ray microcalorimeter instruments will be leveraged as applicable for the LXM (§6.3.4). Individuals supporting *Athena* X-IFU development also support LXM development from pre-Phase A onward, and those supporting the *XRISM* Resolve instrument will support the LXM from Phase A onward. The large-scale fabrication

Likelihood	5					
	4					
	3		LX0-5	LX0-2	LX0-1	
	2		LX0-6	LX0-3 LX0-4		
	1			LX0-7		
		1	2	3	4	5
		Consequence				

Figure 8.2. *Lynx* risk ranking. No red risks identified; all identified risks can be mitigated.

of detectors is low risk since detectors have already been produced with scale and performance close to requirements, utilizing proven processes with high yield and reliability. For the read-out, the main risk is the number of read-out channels needed and, therefore, how much cooling power is required (and thus spacecraft resources such as power), rather than whether or not it will reach TRL 6. The LXM read-out uses microwave Superconducting Quantum Interference Device (SQUID) resonators that are not difficult to fabricate in comparison to components under development for missions operating at longer wavelength. (For LXM, relatively few resonators per feedline are needed and thus resonance frequency accuracy is not critical). The LXM DRM design requires the read-out of 7,600 sensors—not a major scale-up from the number of sensors in the *Athena* X-IFU—and naturally leads to a focal plane assembly that is 4 inches in diameter at 50 mK (similar to the X-IFU) and with relatively standard optical blocking filter sizes. Several industry studies have been initiated to investigate the LXM cryogenic design to identify the solution space (mass, volume, and complexity versus cost) for this already mature subsystem. Two Cooperative Agreement Notice (CAN) studies were carried out during this study, specifically to investigate the maturity of these systems and to consider their maturity as part of the LXM system. Periodic reviews will be conducted as needed to ensure requisite development milestones are met and that conservative cost and schedule reserves have been applied. As part of the detailed *LXM Technology Roadmap*, a high-fidelity, full-assembly EM will be developed to serve as a pathfinder for Observatory assembly, integration, and test. Six months of DDT&E schedule margin to TRL 6 have been included in the LXM development schedule to cover issues that may arise during technology maturation.

Impact: Reduced science capability or increased cost and schedule for technology development.

L × C: 3 × 3

Risk 3 — X-ray Mirror Segment Industrialization: If the manufacturing process used to fabricate mirror segments cannot be scaled to the required industrial-scale production levels while still meeting the technical requirements, then the project cost and schedule will be impacted.

Mitigation: For each mirror system design under consideration, an early study of manufacturability and production of the mirror elements has been initiated through industry partnerships and as part of overall technology development considerations. For the Silicon Meta-shell Optics specifically, recent developments have shown that producing multiple high-quality segments that meet the necessary mirror figure is feasible within the *Lynx* program cost and schedule. Further work is needed to prove full-scale manufacturing feasibility with requisite quality control to produce the quantity of segments required for flight (§8.5.2.1). An advantage of the Silicon Meta-shell Optics design is the nearly identical sizes and shapes of mirror segments regardless of location within the X-ray mirror assembly, and realization of cost and schedule savings via the utilization of several parallel processes in the manufacturing of these elements. Optimization of the manufacturing process (number of parallel machine lines, polishing lines, coating lines, etc.) will lead to a reduction in cost and schedule once the process steps have been defined and proven to yield segments and modules meeting project requirements. A high fidelity, partially populated EM will be developed as part of the TRL 6/PDR demonstration to serve as pathfinder for the technology and manufacturing processes. For Silicon Meta-shell Optics, an assumed 10% for spares has been included in the cost model to account for quality and other issues during the manufacturing process. Furthermore, via industry partnership, a queuing theory-based

model has been developed for the production time and cost of the LMA to determine the most efficient cost and schedule path through the manufacturing process, including but not limited to identification of gating process(es) and the number of parallel manufacturing lines necessary to prevent pileup [621]. Finally, if schedule and cost challenges arise, mirror pairs can be eliminated from the design for up to a 50% reduction in effective area as discussed in §9. In this case, mass dummies would replace the eliminated mirror pairs, thus saving the time and cost for mirror polishing, coating and ion beam figuring. This option would not decimate the *Lynx* science program, but would necessitate longer exposure times. Nine months of DDT&E schedule margin have been added to the Silicon Meta-shell Optics delivery to flight unit calibration/verification. This margin includes three months to delivery of the TRL 6/PDR demonstration unit to cover issues that arise during technology maturation, and an additional six months of margin for issues that arise during the manufacturing and assembly process of the flight unit.

Impact: Increased cost and schedule to meet technical requirements.

L × C: 2 × 3

Risk 4 — LXM Instrument Fabrication and Assembly: If the LXM and its subsystems and components cannot be fabricated, assembled, tested, and integrated within the projected timescale, then the critical path project schedule margin will be eroded at increased project life-cycle cost.

Mitigation: The DDT&E schedule for the LXM is based on the *LXM Technology Roadmap* and leverages the DDT&E plan from the *Athena* X-IFU, as applicable. A full, high-fidelity LXM EM is planned prior to Critical Design Review (CDR) to serve as a pathfinder for the manufacturing and assembly processes. A team of scientists and engineers at GSFC possess substantial experience in the development of instrumentation of this type. This team developed the detectors, focal plane assembly, filters, Adiabatic Demagnetization Refrigerator (ADRs), etc. for *Astro-E*, *Astro-E2* and *Hitomi*; have applicable experience for I&T, calibration, etc.; and a proven record of having developed space-flight hardware on schedule. This GSFC team is currently focused on delivering similar hardware for the Resolve instrument on *XRISM*, which is scheduled to launch in 2022. The team will likely be available for the full LXM development life cycle. In an almost ideal time-scale, they will be available to complement the separate technology development team currently focused on developing TES detectors and readout for the *Athena* X-IFU at the start of Phase-A. The gradual ramp-down of *Athena* X-IFU activities will likely fit well with the ramp up of LXM detector development work. DDT&E schedule margin of four months plus an additional five months of critical path reserve has been added to the project schedule for LXM delivery to ISIM I&T to account for issues that may arise during the fabrication and assembly process.

Impact: Critical path schedule duration and increased project cost.

L × C: 2 × 3

Risk 5 — X-ray Mirror Technical Maturation to TRL 6: If the X-ray mirrors are unable to achieve requisite technology maturation and performance, then the mission science and/or technology development cost and schedule will be compromised.

Mitigation: Technology development roadmaps (\$7) have been developed for the three different *Lynx*-feasible, actively funded X-ray mirror technologies. Each technology will receive continued funding during pre-Phase A development and a final selection (based on technology maturation and proximity to reaching TRL 5 by the start of Phase A) will be made by the time of the *Lynx* Mission Concept Review (MCR) to ensure that the most mature and capable technology is selected for the mission. Carrying the three technology developments in parallel and making periodic schedule and technology advancement-driven downselect decisions provides risk mitigation among the candidates and optimization of science return. Each of these roadmaps identifies a set of unique risks and mitigation plans. The Silicon Meta-shell Optics technology chosen for the DRM has already validated the basic process of mirror segment fabrication and alignment through X-ray testing. Conservative cost and schedule reserves on the Silicon Meta-shell Optics technology have been applied, and periodic reviews will be carried out as needed to ensure that developmental goals are met. Furthermore, a high-fidelity, partially-populated EM will be developed as part of the TRL 6/PDR demonstration to serve as a pathfinder for the technology and manufacturing processes. Three months of DDT&E schedule margin to TRL 6 has been added to the mirror development schedule to account for issues that may arise during technology maturation.

Impact: Reduced science capability or increased cost and schedule for technology development.

L × C: 3 × 2

Risk 6 — HDXI/X-ray Grating Detector Technology Maturation to TRL 6: If the HDXI and X-ray Grating Detector (XGD) are unable to achieve requisite detector technology maturation and performance, then the mission science and/or technology development cost and schedule will be compromised.

Mitigation: An *HDXI Technology Roadmap* has been developed, and because XGD requirements are met with the same sensors as those for HDXI, the *HDXI Technology Roadmap* is sufficient for both. Though the hybrid CMOS-sensor technology has been selected for the DRM, there are at least two other sensor technologies of similar maturity that can meet *Lynx* requirements. Each of these sensor technologies (hybrid CMOS, advanced Charge-Coupled Device (CCD), and monolithic CMOS) have demonstrated proof-of-concept and are assessed at TRL 3. Each technology will be developed until a predefined downselect milestone in 2023, at which point the two most advanced technologies will proceed with development to TRL 4. These two selected sensor technologies will be funded to achieve TRL 4 by the start of *Lynx* project Phase A. The challenges to developing the HDXI and XGD are primarily confined to achieving TRL 4 performance. Once these fundamental capabilities have been demonstrated, subsequent development efforts focus on the assembly and testing of larger sensor/ASIC arrays and higher fidelity testing with respect to flight conditions. These are considered essentially engineering activities and advancement to TRLs 5 and 6 is expected to be straightforward. A single sensor technology will be selected for TRL 5. Downselect decisions will be based on the cost and schedule to meet remaining TRL milestones and ability to meet *Lynx* performance requirements. Carrying the three technology developments in parallel and making periodic, schedule-driven downselect decisions mitigates risk among the candidates. If none of the advanced technologies makes the requisite progress, the use of existing CCD technology may be utilized, though with reduced capability. Three months of pre-Phase A schedule margin and five months of DDT&E schedule margin to TRL 6 is included in the HDXI and XGD schedules to cover issues associated with technology maturation.

Impact: Reduced science capability or increased cost and schedule for technology development.

L × C: 2 × 2

Risk 7 — Calibration Facility Availability: If NASA Marshall Space Flight Center’s (MSFC’s) X-ray and Cryogenic Facility (XRCF) is chosen as the calibration facility for the *Athena* mission, and if the *Athena* calibration activity is significantly delayed, the *Lynx* schedule will be impacted.

Mitigation: Currently, the *Athena* mission’s notional schedule indicates that the flight unit calibration activities will take place from approximately mid-FY28 to around mid-FY29. The current *Lynx* project schedule has rehearsal and flight unit calibration activities taking place around mid-FY31 to late FY32. To impact the *Lynx* critical path, the *Athena* calibration activity would need to slip by approximately 2.5 years. This issue is currently considered a “watch” item.

Impact: Schedule duration and increased project cost.

L × C: 1 × 3

8.4 Life-cycle Schedule and the Critical Path

The *Lynx* project schedule reflects inputs and development planning from technology, engineering, and industry partner teams. It leverages heritage and analogous AI&T, mission and ground operation, and on-ground calibration planning, and is aligned with NASA project requirements, the WBS, and cost analysis, resulting in a credible path to a launch in the mid-2030s.

The schedule development process included multiple iterations to ensure appropriate completeness and alignment of activities and durations, ultimately resulting in the integrated product shown in Figure 8.3. The project schedule covers all aspects of the Phase A – E portions of the lifecycle. Pre-phase A technology development schedules, outlining milestones, detailed development activities, and associated costs and risks are included in the individual *Lynx* technology development roadmaps and summarized in §7. The technology development schedules include funded margin for achieving each TRL. Pre-Phase A is expected to start October 2021, be 3 years in duration, and end with final technology downselect and architecture decisions. The project lifecycle schedule is detailed in its composition, consistent with the technology development plans and analogous *Chandra* integration activities, and credible for the pre-Phase A stage of development; however, it is still notional. Further development and optimization will take place following final technology and contractor selection during the late pre-Phase A/early Phase A timeframe. Specific analysis to optimize the manufacturing and assembly of the X-ray mirrors to determine the most cost- and schedule-efficient number of parallel manufacturing lines will also take place in the late pre-Phase A/early Phase A timeframe. The approach used for this analysis is described in §8.5.2.1. Additional schedule optimization opportunities include, but are not limited to, AI&T sequencing and on-ground calibration planning with respect to availability of the HDXI and XGD for the duration of the calibration campaign for end-to-end testing.

The schedule for specific elements was determined through various means including, but not limited to:

- Key milestone phasing for the X-ray mirrors and science instruments consistent with costing, technology development (§7), and current DDT&E plans.

- Input from the *Chandra* prime contractor for similar and assumed contracted activities for *Lynx*.
- Input from the *Chandra* science operations team for activities associated with ground systems and mission operations.
- Input from the *Lynx* calibration team, which includes *Chandra* and *Athena* calibration team members, for activities related to X-ray and Cryogenic Facility (XRCF) modernization and on-ground calibration.

The schedule was developed utilizing Government Accountability Office (GAO) *Best Practices for Project Schedules*, consistent with pre-Phase A project maturity. Schedule planning included identification of all milestones and KDPs consistent with NPR 7120.5, as summarized in Table 8.2. Key *Lynx* phase durations, summarized in Table 8.3, were compared to, and validated against, the *Chandra* Actual and *WFIRST* In-Guide Schedules for a 2025 Launch Readiness Date (LRD) where applicable for comparable activities. The *Lynx* schedule is aligned with the WBS and mission cost estimate. Key project-level milestones are indicated along the top row of the schedule. The planned start and delivery dates for all major elements of the project are identified.

All of the *Lynx* technologies for the X-ray mirrors and instruments will receive continued technology development funding during the Pre-Phase A period. A technology review will take place approximately 12 months prior to the start of Phase A to downselect to the individual mirror and instrument technologies most ready to reach TRL 5 by the start of Phase A, TRL 6 by PDR, and meet *Lynx* requirements.

As discussed in §7, there are multiple, actively funded technologies with similar maturity levels currently in development for the optics and science instrument suite, capable of meeting

Table 8.2. Key event dates.

Project Milestone	Approximate Milestone Date
Technology Development / Start of Pre-Phase A	10/2021
Architecture Decision	2/2024
MCR	8/2024
KDP-A / Start of Phase A	10/2024
SRR/MDR	2/2026
KDP-B / Start of Phase B	10/2026
PDR	2/2028
KDP-C / Start of Phase C	4/2028
CDR	11/2029
Start of X-ray Mirror Module, XGD & HDXI Flight Unit Calibration	12/2031
Delivery of LXM Flight Unit to ISIM I&T	6/2032
Delivery of X-ray Mirror Modules to LMA I&T	8/2032
Delivery of LMA to XRT I&T	4/2033
Delivery of ISIM to XRT I&T	10/2033
SIR	6/2035
KDP-D / Start of Phase D	7/2035
ORR	3/2036
LRD	10/2036
KDP-E / Start of Phase E	11/2036
End of Primary Mission	11/2041

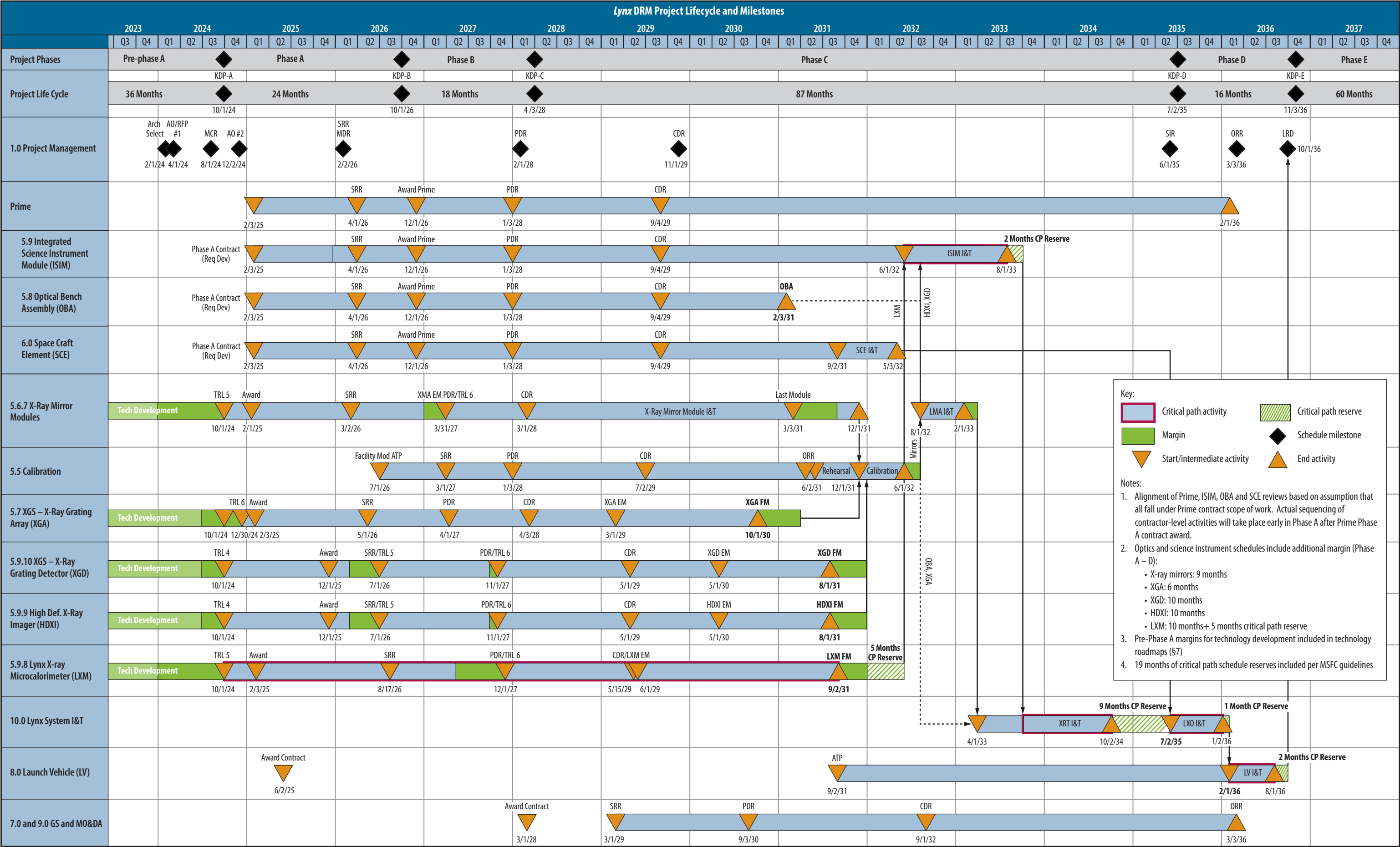


Figure 8.3. Lynx project life-cycle schedule.

mission requirements. These technologies will continue receiving funding through the pre-Phase A period. Carrying these multiple technologies lowers the project risk posture in that downselect decisions will be made in the pre-Phase A timeframe based on the ability of each technology to meet the remaining TRL 5 and TRL 6 maturity and project milestones, and *Lynx* requirements. Final selection of the mirror, XGA and LXM technologies will be made by the architecture selection milestone of February 2024.

As described in the *HDXI Technology Roadmap*, three separate sensor technologies are currently under development for the HDXI and XGD. An intermediate downselect will take place by July 2023, and the final downselect will take place by the start of Phase A, again based on maturation advancement and ability to meet *Lynx* requirements. As noted in the schedule, the selected sensor technologies are expected to be at TRL 4 by the start of Phase A. The challenges to developing the HDXI and XGD are primarily confined to achieving TRL 4 performance. Once these fundamental capabilities have been demonstrated, subsequent development efforts focus on the assembly and testing of larger sensor/ASIC arrays with higher fidelity testing with respect to flight conditions. These are considered essentially engineering activities and advancement to TRL 5 and TRL 6 is expected to be straightforward. Three months of pre-Phase A schedule margin is included in the technology development schedule to cover issues associated with technology maturation. Furthermore, aggressive development efforts are already underway for all three sensor/ASIC architectures and significant advances may reasonably be expected before the pre-Phase A period begins.

It is assumed that a single prime contractor will be responsible for DDT&E of the ISIM, Optical Bench Assembly (OBA), and SCE, as well as I&T of the LMA, the telescope, and the Observatory. Alignment of the ISIM, OBA, and SCE DDT&E milestones reflects this assumption. An RFP will be released after the architecture selection milestone for a prime contractor Phase A contract award by February 2025, enabling the development of system requirements. Detailed schedules and sequencing of any contractor-led elements will be developed after selection. The remaining prime development contract will be awarded in Phase B.

The critical path was calculated based on the longest duration of activities through the project schedule. The *Lynx* critical path runs through the LXM DDT&E, and through ISIM, XRT, Observatory and launch vehicle I&T activities. The X-ray mirror development path through DDT&E only lags the LXM DDT&E path by ~1 month in this schedule. It is recognized that the actual development schedule and critical path analysis will take place in Phase A following decisions on the final architecture and Observatory element providers. Nineteen months of schedule reserves were added to the critical path activities, consistent with guidance from MSFC 7102.1, Table 17-3, *Standard Schedule Margin for Programs/Projects*. In addition to the critical path reserves, margin has been added to the X-ray mirrors and science instrument schedules to account for uncertainties associated with technology development, DDT&E, and key integration activities. Schedule margin has also been added to the on-ground calibration and LMA I&T to account for uncertainties associated with these activities. Critical path and schedule reserves are summarized in Table 8.3.

Table 8.3. Key phase duration table.

Project Phase	Duration (months)	Comments
Pre-Phase A (Technology Development)	36	Pre-Phase A duration based on technology development schedules and assumed funding levels (comparable to <i>WFIRST</i>)
Phase A (Conceptual Design): KDP-A to KDP-B	24	Phase A duration based on technology development schedules and funding (comparable to <i>WFIRST</i> levels).
Phase B (Preliminary Design): KDP-B to KDP-C	18	Phase B duration based on assumed technology development funding and all technologies reaching TRL 6 by PDR
Phase C (Detailed Design): (KDP-C to KDP-D)	87	Phase C includes development of X-ray mirrors (and integration into LMA) and 3 science instruments, mirror and instrument on-ground calibration, ISIM I&T, and XRT I&T. X-ray mirror development assumes multiple parallel manufacturing lines to be optimized during Phase A. LXM schedule comparable to <i>Athena</i> X-IFU. <i>Chandra</i> Phase C duration similar except for no analogous LXM, and <i>Chandra</i> SIM integration took place during Observatory I&T in Phase D. <i>WFIRST</i> Phase C shorter due to less complex design (2 science instruments and no ISIM)
Phase D (I&T): KDP-D to KDP-E	16	Phase D includes integration of XRT and SCE to become the LXO. <i>Chandra</i> Phase D also included integration of SIM during Observatory I&T. <i>Lynx</i> assumes ISIM integration during XRT I&T in Phase C
Phase E (Primary Mission Ops): KDP-E to KDP-F	60	<i>Lynx</i> planned operational lifetime is 5 years, extendable to 20 years with on-board consumables
Start of Phase A to SRR	16	
Start of Phase B to PDR	16	
Start of Phase C to CDR	19	
Start of Phase C to SIR	86	
Start of Phase D to LRD	15	
Phase B to X-ray Mirror Delivery to Calibration	62 (53+9)	<i>Lynx</i> mirror DDT&E includes additional 9 months of schedule margin
Phase B to LXM Delivery to ISIM I&T	68 (53+10+5)	LXM DDT&E includes additional 10 months of schedule margin and 5 months of critical path reserve
Calibration (Flight Unit)	8 (6+2)	On-ground calibration similar to <i>Chandra</i> with exception of additional science instrument (LXM EM); Schedule includes additional 2 months of margin
LMA I&T	8 (6 + 2)	LMA I&T involves integration of the X-ray mirror module assembly, pre- and post-collimators, contamination doors, and other structures into the barrel structure; Schedule includes 2 months of margin
ISIM I&T	16 (14+2)	ISIM I&T is more complex than <i>Chandra</i> SIM actual due to mechanisms and additional instrument; Schedule includes 2 months of critical path reserve
Telescope I&T	27 (18+9)	XRT I&T involves integration of LMA, XGA, OBA, and ISIM; Schedule includes 9 months of critical path reserve
SCE I&T	8	<i>Lynx</i> SCE comparable to <i>Chandra</i> actual; No additional margin included
Observatory I&T	7 (6+1)	<i>Lynx</i> Observatory I&T comparable to <i>Chandra</i> actual; Schedule includes 1 month critical path reserve
Launch Site Activities	8 (6+2)	<i>Lynx</i> LV Integration comparable to <i>Chandra</i> actual; Schedule includes 2 months critical path reserve

Linkages between key elements are shown in Phase C of the schedule, consistent with the AI&T activities described in §6.6.3.

It is assumed that on-ground calibration will take place at the MSFC XRCF as described in §6.6.3.1. Development of a new calibration facility is not required for *Lynx*, but modernization of this *Chandra*-era asset may be required. The XRCF is under consideration as the calibration facility for *Athena*. If selected for *Athena*, facility modernization costs including but not limited to additional X-ray sources, detectors, data acquisition systems, and system-specific GSE, will be encumbered by the *Athena* project.

The *Lynx* schedule and costing are conservative in assuming that XRCF will not be selected by *Athena*, and this work will be encumbered by the *Lynx* project. XRCF modernization activities occur in parallel with Observatory development; major reviews are shown in the schedule. Completion of these activities will coincide with the *Lynx* on-ground calibration during Phase C.

On-ground calibration and environmental testing facilities capable of meeting *Lynx* requirements currently exist and are expected to be available in the 2030s. No new Observatory-level calibration facility construction is needed or included in the schedule or costing.

The development of ground systems, mission operations, and the science data analysis system will occur in parallel with the Observatory development, with major reviews shown in the schedule. The procurement strategy for these systems will be determined at the pre-Phase A Acquisition Strategy Meeting.

It is assumed the selection of the launch vehicle provider will take place in Phase A prior to the project System Requirements Review (SRR) and Mission Definition Review (MDR) to enable close coordination of critical design interfaces between the Observatory elements and the launch vehicle.

The schedule supports an October 2036 launch readiness, with plans for a nominal five years of mission operations. Additional onboard consumables extend the mission life to 20 years.

8.5 Cost

The relatively straightforward *Lynx* Observatory design, technology maturation and evolution, and use of rich *Chandra* heritage and lessons learned enabled the development of a detailed parametric estimate and BOE, as well as multiple independently-developed validation cost estimates that yielded favorable comparisons. The sum total of this effort is a thoroughly and credibly costed pre-formulation stage mission.

The *Lynx* team developed a parametric mission cost estimate for Phase A through the first five years of operation, consistent with *GAO Best Practices for Estimating and Managing Costs* and guidelines and requirements described in the *NASA Cost Estimating Handbook*. The following sections describe the methodologies and summary results of the *Lynx* mission costing effort. Details and results for the entirety of this effort are included in the *Lynx* Costing Book, which is unavailable to the public.

The process for the development of the parametric estimate includes additional levels of rigor, lending to its credibility. This includes the use of:

- Multiple parametric models for all elements
- In-family comparisons at the subsystem level
- Subject Matter Expert (SME) inputs at the component level for all elements
- A transparent and clearly defined BOE and estimating process
- Multiple independently conducted cost estimates and/or assessments using different approaches

The parametric estimate includes 30% reserves on the Phase B–D cost (excluding launch vehicle and fee) and 10% fee on the assumed contractor portions. The estimate is aligned with the WBS, project schedule, Master Equipment List (MEL), and Power Equipment List (PEL), and includes funded schedule reserves to cover development risks discussed in §8.3 and §8.4. The launch vehicle cost was a pass-through per NASA Headquarters (HQ) guidance. The estimate incorporates high *Chandra* architecture heritage, robust and high-TRL spacecraft components and design, and a detailed and credible path forward for all DRM technologies (\$6 and \$7).

The validation estimates range from –11% to +28% of the parametric estimate, and the 40% confidence level (CL) results from the uncertainty analyses were within 1% of the parametric estimate. These independently conducted validation estimates provide credibility of the *Lynx* parametric estimate. (Figure 8.4).

The mission parametric estimate was validated through several separately conducted means to strengthen its credibility. The validation approaches include a *Chandra* analogous estimate, grassroots estimate, a non-advocate Independent Cost Estimate (ICE) with uncertainty analysis and an independent, contracted Cost and Technical Evaluation (CATE) with uncertainty analysis. The parametric estimates for the LMA, HDXI/XGD, and SCE were separately validated with in-family comparisons to historic missions.

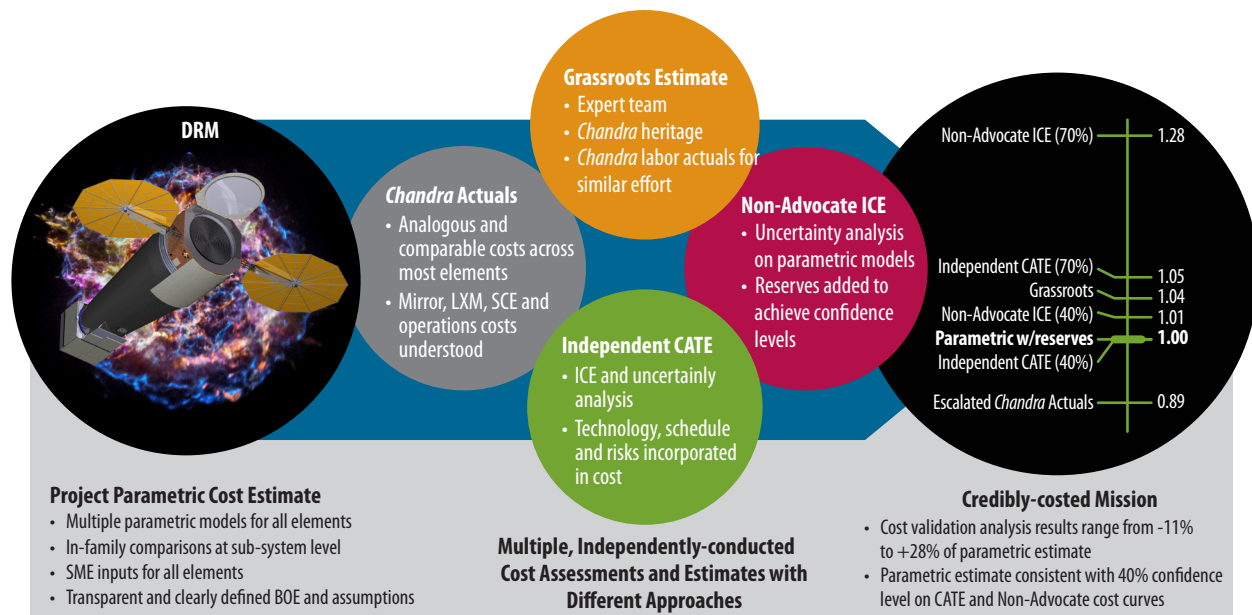


Figure 8.4. The *Lynx* parametric estimate is normalized to 1 and compared with multiple independently conducted cost analyses including a comparison to escalated *Chandra* actuals, grassroots estimate, non-advocate ICE with uncertainty analysis, and an independent CATE with uncertainty analysis. These validation estimate results are within a band of –11 to +28% of the *Lynx* parametric estimate. The 40% CL on the uncertainty analysis cost curves are within 1% of the parametric estimate. These results validate the credibility of the *Lynx* mission cost estimate.

The total *Lynx* DRM parametric mission cost is in the range of \$4.8B at a 40% CL to \$6.0B at a 70% CL in Fiscal Year 2020 Dollars (FY\$20) and \$6.5B at a 40% CL to \$8.2B at a 70% CL in Real Year Dollars (\$RY).

Analysis of the trade space on the science return per dollar indicates that the *Lynx* DRM produces the most scientifically and technically capable architecture that meets the science goals. Details of this analysis are discussed in §9.

8.5.1 Work Breakdown Structure

The *Lynx* Observatory WBS is structured similarly to the *Chandra* WBS and is consistent with guidance provided in the *NASA WBS Handbook* (NASA/SP-2016-3404). The structure allowed for development of an analogous cost comparison to *Chandra*, discussed in §8.5.3.1. The WBS is defined to Level 3 for all elements and to Level 6 for the XRT and SCE due to the in-depth knowledge and details of these systems. A summary of the key WBS elements associated with the DRM and their definitions is provided in Table 8.4. The fully expanded version of the WBS is provided in Appendix E.

The WBS provides the organizational scheme for the overall project, the structure for the cost model, and serves as the genesis of the Product Breakdown Structure (PBS) for all delivered hardware elements.

8.5.2 Cost Estimation Methodology

The primary cost estimate for *Lynx* was developed using parametric modeling, consistent with pre-formulation design maturity. Parametric cost estimation and analysis for the *Lynx* spacecraft, mirror, instruments, and mission utilized the industry-standard Project Cost Estimating Capability (PCEC), SEER®-H (Space Guidance), PRICE® TruePlanning® Space Missions, and PRICE®-H models. The NASA Instrument Cost Model (NICM) was used as a validation model for the instrument estimates. The launch vehicle cost was a pass-through as directed by NASA HQ and based on guidance from the Launch Services Program Office. The estimate for the LXM, discussed in more detail below, was developed by GSFC using PRICE®-H and was a pass-through for the *Lynx* mission estimate. The parametric cost models use Cost-Estimating Relationships (CERs) derived from the analysis of historical data with similar space programs and projects. These models have tailorable inputs allowing specific modifications to closely match the development approach for the *Lynx* optics and scientific instruments. The ability to tailor inputs is critical for these technologies given the uniqueness of Flagship missions in general [620] and the paucity of specific X-ray mission analogies in the historical databases from which the CERs are drawn.

PCEC is a publicly available parametric model developed and maintained by MSFC's Engineering Cost Office that is used to estimate the cost of spacecraft, launch vehicles, and human space flight systems. PCEC contains over 43 planetary and Earth-orbiting spacecraft missions and provides estimates at the subsystem level, which are all documented within the Cost Analysis and Data Requirements (CADRe) database.

Table 8.4. Summary WBS and definitions.

WBS	Elements
Lynx X-ray Observatory Project	
01	Project Management – This element includes the management, business and administrative planning, organizing, directing, coordinating, controlling, approval processes used to accomplish overall project objectives not associated with specific hardware or software elements as well as review planning, project reserves, project planning and control and configuration management, and science payload management.
02	Systems Engineering – This element includes the technical and management efforts of directing and controlling the mission-level engineering efforts for this project, system requirements development, verification, integrated test planning, and system and mission analysis including system architecture development, and technical oversight
03	Safety and Mission Assurance – This element includes the overall efforts of directing and controlling the safety and mission assurance elements of the project, including verification of practices and procedures, safety and mission assurance management, reliability analysis, quality assurance, and mission safety.
04	Science and Technology – This element includes managing and directing the science investigation aspects, science support for Phases A–D as well as leading, managing, and performing the technology demonstration elements of the project. Included is the technology development effort to TRL 6 for the X-ray mirror modules (04.03), LXM (04.04), HDXI (04.05) and the XGS (04.06) which includes the XGA and XGD subassemblies.
05	X-ray Telescope (XRT) – This element includes management (05.01), systems engineering (05.02), product assurance (05.03), integration and testing of the XRT and its subsystems (05.04), on-ground calibration (05.05) and calibration facility modernization (05.12). This element also includes the DDT&E of the X-ray mirror modules and its integration into the LMA with its associated structural and thermal elements, DDT&E of the LXM, HDXI and the XGS (XGA+XGD), DDT&E of the ISIM and its sub-assemblies, integration of the LXM, HDXI and XGD into the ISIM, and DDT&E of the OBA. The completed XRT is delivered to the Observatory I&T in WBS 10.
05.06	Lynx Mirror Assembly (LMA)
05.06.07	X-ray Mirror Modules
05.07	X-ray Grating Spectrometer (XGS) – X-ray Grating Array (XGA)
05.08	Optical Bench Assembly (OBA)
05.09	Integrated Science Instrument Module (ISIM)
05.09.08	Lynx X-ray Microcalorimeter (LXM)
05.09.09	High Definition X-ray Imager (HDXI)
05.09.10	X-ray Grating Spectrometer (XGS) – X-ray Grating Detector (XGD)
06	Spacecraft Element (SCE) – This element includes management (06.01), system engineering (06.02), product assurance (06.03), and I&T (06.04) and DDT&E of the spacecraft element and its subsystems: FSW (06.05), GSE (06.06), Structures (06.07), TCS (06.08), EPS (06.09), C&DH (06.10), Communications (06.11), GN&C (06.12) and Propulsion (06.13). The completed SCE is delivered to the Observatory I&T in WBS 10.
07	Mission Operations – This element covers the totality of Mission Operations and Science Activity (and all associated support) during Phase E, commencing at the end of on-orbit checkout and running through the end of the primary science mission. This element includes tracking, commanding, receiving/processing telemetry, analyses of system status, trajectory analysis, orbit determination, maneuver analysis, and disposal of remaining end-of-mission resources. It also includes all aspects of science operations, mission planning and target scheduling, data analysis, archiving, scientific investigations and reporting.
08	Launch Vehicle Services – This element includes the launch vehicle as well as management and implementation of activities required to place the observatory directly into its operational environment. This element includes activities to support integration and testing of the observatory into the launch vehicle.
09	Ground Systems – This element covers the total development of the Mission Operations Systems (MOS) and Ground Data Systems (GDS), representing the Phase A–D effort to design, develop, integrate, test, and verify the software and hardware to support MOS/ GDS activities on the ground. It includes development of all MOS and GDS-required testbeds, support equipment, and facilities, and development and implementation of procedures, documentation, and training required to conduct mission and science operations.
10	Systems Integration and Test – This element includes management and implementation of activities to perform observatory-level integration and testing. The element includes hardware, software, procedures, and unique GSE and facilities required to perform the integration and testing of the XRT to the SCE as well as I&T at the observatory level. This element also includes sustaining engineering support for telescope and observatory subsystems through on-orbit checkout.
11	Public Outreach – This element includes all aspects of public outreach for the project including but not limited to press releases, media support, videos, models, website development to inform the public of the benefits of the project.

PCEC was selected for the overall mission level and spacecraft estimate because of its following benefits:

- Aligns with standard NASA WBS structure and fully captures NASA efforts under WBS 1, 2, 3, 5, and 10 elements
- Provides full access to the data and analysis used to develop the CERs and related statistics
- Contains data that are normalized to minimize subjective inputs
- Incorporates the Space Operations Cost Model (SOCM) to estimate Mission Operations and Data Analysis functions for Phases B

Chandra and other flagship mission costs provide calibration factors. *Chandra* actuals, SEER-H®, and PRICE® TruePlanning® provides validation for the PCEC mission and spacecraft estimates.

SEER® and PRICE® are commercial cost models that employ large databases as tools for spacecraft and instrument cost estimation. SEER-H® was selected for the HDXI, XGS (XGA+XGD), and LMA estimates because it uses historical data that allows for a more accurate assessment of costs related to detectors and mirror segments. PRICE® TruePlanning® and NICM estimates, and *Chandra* actuals, provide validation for the LMA, instruments, and spacecraft. Furthermore, the SEER® risk analysis capability provides a coefficient of variation ranging from 0.3 to 0.5, consistent with Air Force guidance for space systems as input distribution for the PCEC mission model.

The GSFC Instrument Design Lab (IDL) developed a cost estimate for LXM using the PRICE-H® tool. While this instrument incorporates heritage and design elements from past and planned X-ray missions, it does not have any direct analogies or historical analogies that provide an easy comparison. The GSFC estimate was developed with input from SMEs for the detector technology and manufacturing, X-ray calibration sources, and Flight Software (FSW) testbed and associated hardware development. This estimate was incorporated as a pass-through in the *Lynx* PCEC mission cost model.

The approach to parametric costing of the LMA was given special consideration, as the LMA assembly does not have applicable analogous historical comparisons (§8.5.3.1). The manufacturing of the LMA's many mirror segments (§6.3.1) is of particular importance, and unlike *Chandra*, can take advantage of a highly parallelized manufacturing scheme.

8.5.2.1 LMA Manufacturing Approach and Cost Considerations

The LMA consists of the X-ray mirror modules, integrated with the pre-and post-collimators, contamination doors, and barrel structure. The unique feature of the LMA and key to the *Lynx* science program is the X-ray mirror module assembly. Understanding and preparing for the manufacturing of the mirror modules and the many mirror segments that populate them is a surmountable challenge with a solution that builds upon substantial laboratory work already accomplished. The *Lynx* team recognizes that a fully vetted LMA manufacturing and assembly process must be demonstrated early in the project to demonstrate mission viability.

Industrialization of the manufacturing process and mirror assembly are the subject of two of the top project risks, as discussed in §8.3. Current studies are ongoing and will continue through Phase A to prove out the manufacturability and assembly of the mirrors as part of TRL advancement. The X-ray mirror module TRL 6 demonstration, which includes nine fully populated modules assembled within three meta-shells, will also serve as a test bed for the manufacturing and assembly processes.

The mirror module assembly consists of 611 modules, populated with a total of 37,492 mirror segments that are mounted to a common structural element called the “spider.” A single ring (of a given diameter) consists of multiple identical modules to create a meta-shell. There are 12 meta-shells that form the LMA, enabling *Lynx* to meet its effective area requirement. Each mirror segment has the same thickness (0.5 mm) and roughly the same dimensions (100 mm × 100 mm). Within the modules for a given meta-shell, the radius of curvature of the mirror segments does not change significantly. This modular design allows for parallel manufacturing (by meta-shell), and this is reflected in the *Lynx* parametric cost analysis.

Inputs and Assumptions for Parametric Costing — The parametric costing utilizes an understanding of the LMA fabrication and assembly process, obtained with the detailed input and review by the Silicon Meta-shell Optics team through multiple technical interchange and face-to-face discussions, throughout the course of this study.

The parametric cost model includes all elements required for fabrication and assembly of the LMA. At a high level, there are essentially six cost areas; three are independent of the manufacturing process: (1) the materials for the mirror elements, or consumables, (2) the labor hours to assemble the meta-shells into the LMA, and (3) the *Lynx* specific tooling such as lapping and polishing tools. The elements of cost that depend on the detailed design of the manufacturing process are (4) machine (server) costs, (5) facility costs such as rent, utilities, maintenance, and (6) level-of-effort costs such as management, systems engineering, procurement, quality assurance, and record keeping.

Details for the process and elements are applied during the selection of cost model parameters. Some of the key SEER-H® model inputs include:

- The use of a learning curve to take advantage of the large quantity of similar (but individually produced) mirror segments and mirror modules
- A decrease in the “Percent New Design” at the meta-shell level to account for the benefits of a largely repeatable production process:
 - “Make” was used for the first meta-shell (80% new design)
 - “Major Modification” was used for the second meta-shell (65% new design)
 - “Average Modification” was used for the remaining meta-shells (15% new design)
- The staggering of the development start for the second and third meta-shells to benefit from the development of first meta-shell
- The use of “Minor Design Changes” after the development of second meta-shell
- Concurrent development and production timeline to take advantage of the use of 12 production lines for the meta-shells
- A model hierarchy that reflects each meta-shell as a separate subsystem

The Silicon Meta-shell Optics team also provided guidance on input parameters for prototype definition and spares at the mirror module level consistent with the *Lynx* sparing philosophy. Mass inputs were per the Silicon Meta-shell Optics team-provided MEL.

In parallel, the GSFC team developed a detailed grassroots estimate (Table 8.11, (WBS 05.06.07) and *Lynx Cost Book*). This estimate includes costs for unique tooling such as for lapping and polishing, capital equipment for mirror fabrication and coating, and labor to produce the mirror assembly.

The estimate includes assumptions for process steps and time to complete based on laboratory experience to date, and based on the project schedule (Figure 8.3), estimates the number of machines and parts processed per machine per week to manufacture the 611 mirror modules and assemble the 12 meta-shells. This estimate takes into account the industrialization of the repeatable manufacturing and assembly process, which is key to the cost effectiveness of the Silicon meta-shell design.

The X-ray mirror module parametric estimate was within 4% of the GSFC grassroots estimate and found to be “in-family” with historical x-ray telescope assemblies (Figure 8.7).

Manufacturing Process and Optimization — Based on laboratory work already accomplished to produce and align segment pairs, the Silicon Meta-shell Optics team has developed a detailed flow for the steps required to manufacture the X-ray mirror modules, which are the dominant component in the LMA (Table 8.5). This analysis establishes, by measurement, the time required for each step in the process; identifies capital equipment for mirror fabrication and coating, along with unique tooling for lapping, polishing and the like; sizes and scopes the needed facilities; and estimates the labor necessary to produce the mirror assembly. At this relatively early point in the program, the *Lynx* team has conservatively assumed 12 parallel manufacturing lines, or one per meta-shell, to shorten the overall manufacturing time enabling the work to fit within the overall *Lynx* project schedule (Figure 8.3) by taking advantage of the modular nature of the mirror assembly.

Table 8.5. List of LMA process steps and associated time to complete each step.

	Step	Name	Calendar Time (h)
Element Fabrication	1	CNC Grinding	4
	2	Lapping (buffing and measurement on FizCam)	8
	3	Slicing	3
	4	Coarse edge treatment	1
	5	Etch	1
	6	Polishing (FizCam)	20
	7	Smoothing (FizCam)	4
	8	CNC Grinding	4
	9	Trimming	2
	10	Final Etching	3
	11	FizCam measurement, IBF	3
Coating	12	Cleaning and oxidizing the backside	10
	13	Sputter Ir coating	10
	14	Anneal	10
	15	FizCam measurement, IBF	3
Align and Bond	16	Measure height and locations of 8 spacers	0.5
	17	Fabricate 8 spacers	4
	18	Attach spacers and cure	2
	19	Measure radial heights of 8 spacers and trim to tolerance	3
	20	Align mirror by fine-grinding guided by Hartmann	4
	21	Bond mirror and cure, return to Step 16 to complete module	10

A CAN study was initiated to develop an analytic method for optimizing the LMA manufacturing process. This approach is based on industrial engineering methodology, and the first assessment of the LMA manufacturing process has been reported in the literature [621], indicating that the baseline approach is feasible.

The CAN study derives a method that identifies the optimal number of machines (servers) required for each process step in order to minimize idle, or down time, over the entire manufacturing process. Servers for a single production line include all manufacturing and metrology machines needed to carry out the mirror fabrication, coating, alignment, and bonding. There are 21 identified steps in the manufacturing process (Table 8.5) [622]. Assuming one production line per meta-shell means that there are $12 \times 21 = 252$ server sets to be procured. To be conservative, the full quantity of 252 servers was assumed for the parametric and grassroots cost estimates. Equipment for the servers is a mix of commercially available interferometers, grinders, slicers, etchers, ion-beam figuring machines, cleaners, coaters, ovens and the like, along with hardware unique for *Lynx* such as lapping, trimming, and polishing tools, and machines. Required equipment has been identified and costed based on prices for the commercially available items and costs for developing *Lynx* unique tools during the laboratory demonstration work. For example, individual lapping and polishing tools range in cost from \$10K to \$125K. The grassroots estimate for equipment is ~40% of the total estimated cost. By far the dominant labor effort is that required to fabricate, align, and bond a mirror segment. Based on laboratory experience to date as summarized in Table 8.4, and including ~10% margin, the number of labor hours to produce a mirror segment, which includes direct labor, overhead, and quality assurance, is conservatively estimated at 61 hours. Summed over the full number of segments, the total labor equates to ~1,150 person years, which equates to roughly 288 equivalent persons per year, for a 4-year effort. This effort (plus 6 months of funded schedule margin) is supported by the project schedule (Figure 8.3). While this labor force to produce the mirror segments is considerable, the estimate is conservative and based on non-optimized processes. Labor costs have been estimated using a mix of levels and capabilities and a range of associated rates leading to a labor cost estimated at ~55% of the total grassroots cost.

The simple approach of procuring a complete set of servers for each meta-shell does not account for the fact that each step in the process will be completed at a different rate or that the number of modules and mirror segments in each of the 12 meta-shells differ, indicating that further optimization is possible. Table 8.5 shows that the rate-limiting step is polishing, which is twice as long as the next longest step. Since all of the steps after polishing take less time, there is idle time for those servers. Removing this idle time by optimizing the use of the servers would result in significant cost savings to the project. Adding more servers for the polishing step (or other steps among the most time-consuming) would reduce the time required to flow through those “bottle-neck” stages. This optimization process indicates that the parametric and grassroots estimates are somewhat conservative and that further trades involving the numbers of lines, servers, and related labor costs has the potential to reduce costs. A very preliminary, first pass suggests that a reduction in number of servers of order 30% is possible [621], but a much more thorough analysis will be performed during pre-Phase A to assess pros and cons of 12 completely separate lines (as baselined at this point) versus a more integrated flow and more cost-effective use of servers and resources.

8.5.2.2 Parametric Cost Ground Rules and Assumptions

The ground rules and assumptions (GR&A) for the *Lynx* mission level parametric cost estimate process are summarized in Table 8.6.

Table 8.6. General GR&A for *Lynx* cost estimate.

Parameter	Value
Baseline cost	\$FY20 per NASA inflation tables
Phased mission cost	\$RY per NASA inflation tables
Fee	10% applied to Spacecraft, ISIM, OBA, and LMA (X-ray mirror modules + associated structures); no fee for science instruments (assumed NASA or university-developed)
Reserves	30% on Phases B–D, excluding launch services and fee
Design approach	Protoflight
Mission risk class	A
Parts class	Unmanned space class S1; redundancies provided in MEL (Appendix D)
Flight unit quantity	1
Spares	10% for all subsystems
Phase A estimate	5% of DDT&E + Flight Unit total
Public outreach estimate	1% of XRT (WBS 05) + SCE (WBS 06) totals

Specific cost model inputs for LMA, HDXI, XGS (XGA+XGD) and the spacecraft are provided in Table 8.7. The integrated mission cost estimate was modeled using PCEC, with the mirror, instrument, and spacecraft models, and the SOCM operations model as inputs. The LV was not modeled, as the estimate was provided as a pass-through. As described in §8.5.2, the LXM cost was modeled by GSFC using PRICE-H®, and treated as a pass-through as well.

Table 8.7. Parametric cost model input parameters.

Parameter	SEER-H® (Space Guidance)	PRICE® (Space Missions)	PCEC
Operating Environment	LMA, HDXI, XGS (XGA+XGD), SCE: Space unmanned, science, command and control, Earth-orbiting (SE-L2)	LMA, HDXI, XGS (XGA+XGD), SCE: Space unmanned, Earth-orbiting (SE-L2)	SCE, Mission: Earth-orbiting (SE-L2)1
Platform	LMA, HDXI, XGS (XGA+XGD), SCE: Space unmanned	LMA, HDXI, XGS (XGA+XGD), SCE: Space unmanned	N/A
Standard	LMA, HDXI, XGS (XGA+XGD), SCE: Science, command & control	LMA, HDXI, XGS (XGA+XGD): Payload, Class A mission SCE: Class A mission	SCE, Mission: Robotic spacecraft
Acquisition Category	LMA, HDXI, XGS (XGA+XGD), SCE: Based on component and production plan; varies for individual components from “make” to “space procure to print”	LMA, HDXI, XGS (XGA+XGD), SCE: Based on component and production plan; varies for individual components from “new” to “minimum modification”	SCE, Mission: Based on subsystem heritage factor, parts rating (flagship mission), operating environment
Level	LMA, HDXI, XGS (XGA+XGD), SCE: Component	LMA, HDXI, XGS (XGA+XGD), SCE: Component	SCE: Subsystem Mission: NASA and contractor
Structures Complexity	LMA, XGS (XGA+XGD), HDXI, SCE: Primary/secondary structures knowledge base defaults, nominal complexity LMA-specific: Optics knowledge base, high to very high complexities, learning curve applied for subsequent modules	LMA, XGS (XGA+XGD), HDXI, SCE: Defaults based on environment, subsystem and function LMA-specific: Optics subsystem, high to very high complexities, learning curve applied for subsequent modules	SCE: Defaults based on environment and subsystem Mission: N/A

Table 8.7. Continued

Parameter	SEER-H® (Space Guidance)	PRICE® (Space Missions)	PCEC
Mechanisms Complexity	LMA, XGS (XGA+XGD), HDXI, SCE: Component-specific knowledge bases, defaults and unmanned space operations	LMA, XGS (XGA+XGD), HDXI, SCE: Defaults based on environment, subsystem and function	SCE: Defaults based on environment, subsystem, and function Mission: N/A
Multiples of Same Component	LMA, XGS (XGA+XGD), HDXI, SCE: Multiple at next higher level of assembly	LMA, XGS (XGA+XGD), HDXI, SCE: Multiple at next higher level of assembly	SCE: Multiple at next higher level of assembly Mission: N/A
Electronics Complexity	LMA, XGS (XGA+XGD), HDXI, SCE: Component-specific knowledge bases, defaults, and unmanned space operations XGD-specific: Detector electronics unit (DEU) electronics box—conductive cooling knowledge base defaults—modification minor (15% new)	LMA, XGS (XGA+XGD), HDXI, SCE: Price complexity calibration XGD-specific: Electronics box—20% new	SCE: Defaults based on environment, subsystem, and function Mission: N/A
Thermal Components	LMA: Thermal control knowledge base—passive; spider heaters active; make XGA: N/A HDXI, XGD: Component-specific knowledge base defaults SCE: Component specific knowledge base defaults	LMA, XGS (XGA+XGD), HDXI, SCE: Price default complexity	SCE: Defaults based on environment, subsystem, and function Mission: N/A
Power	Per power schedule (Table 6.16)	Per power schedule (Table 6.16)	Per power schedule (Table 6.16)
Communication	LMA, XGS (XGA+XGD), HDXI: N/A SCE: Component knowledge base, Std. RF X Band and Ka Band TWTA for SE-L2 (1200W Ka Band Transponder)	LMA, XGS (XGA+XGD), HDXI: N/A SCE: Component knowledge base, Std. RF X Band & Ka Band TWTA for SE-L2 (1200W Ka Band Transponder)	LMA, XGS (XGA+XGD), HDXI: N/A SCE: earth-orbiting, Std. RF X Band and Ka Band TWTA for SE-L2 (1,200 W Ka Band Transponder)
Propulsion	LMA, XGS (XGA+XGD), HDXI: N/A SCE: Weight-based, component-based	LMA, XGS (XGA+XGD), HDXI: N/A SCE: Weight-based, component-based	LMA, XGS (XGA+XGD), HDXI: N/A SCE: MPS—86N, 4 thrusters; RCS—5N, 16 thrusters
Quantities ²	LMA: 10% prototype for structural items except for spider and meta-shell structures #1, #6, and #12 (50% to capture quantity for the EM), 4% prototype for mirror segments and modules, 10% spares XGA: 10% prototype for structural items and spares HDXI, XGD, SCE: 65% prototype (10% wrap ETUs, 1 EDU (55% flight-quality unit), 10% spares	LMA: 10% prototype for structural items except for spider and meta-shell structures #1, #6, and #12 (50% to capture quantity for the EM), 4% prototype for mirror segments and modules, 10% spares XGA: 10% prototype for structural items and spares HDXI, XGD, SCE: 65% prototype (10% wrap ETUs, 1 EDU (55% flight-quality unit), 10% spares	SCE: 65% prototype (10% wrap ETUs, 1 EDU (55% flight-quality unit), 10% spares

Notes: 1. Earth-orbiting environment selected for PCEC mission cost model based on Wilkinson Microwave Anisotropy Probe (WMAP) mission, a U.S. system at SE-L2, and classified as near-Earth orbiting. This choice of Earth operating environment is supported by similarities in the mission design and operation requirements for Lynx at SE-L2 and Chandra at High Earth Orbit (HEO). 2. Spares, prototype, Engineering Test Unit (ETU), and Engineering Development Unit (EDU) factors based on development philosophy described in §6.6.

8.5.2.3 Parametric Cost Basis of Estimate

The parametric basis of estimate (BOE) summarized in Table 8.8 provides a basis for the cost estimate by WBS element, and summarizes key parametric model assumptions.

Table 8.8. BOE for parametric estimate by project WBS.

WBS	WBS Title
01	Project Management
Basis of the Estimate: PCEC used for this WBS element. This estimate used a CER in the PCEC tool that utilizes data on Lead Organizations, flight systems organizations, heritage and parts ratings, and from similar projects. Reserves at 30% to Phase B–D costs.	
02	Systems Engineering
Basis of the Estimate: PCEC used for this WBS element. The CER provided estimates for the Government and Contractor SE cost per month at the Project-, Payload-, and Spacecraft-level based on data from mission destination and flight system power for similar projects.	
03	Safety and Mission Assurance
Basis of the Estimate: PCEC used for this WBS element. The CER provided estimates for the Government and Contractor S&MA cost per month at the Project-, Payload-, and Spacecraft-level based on data from mission destinations, lead organizations, and flight system power for similar projects.	
04	Science and Technology
Basis of the Estimate: PCEC used for this WBS element. The CER provided estimates for the Government and Contractor Science and Technology cost based on the Astrophysics science category factor, applied to the sum of WBS 1–3, 5–7, and 9–11.	
05	X-ray Telescope (XRT)
Basis of the Estimate: PCEC used to estimate the structural and mechanical portions of the XRT subsystem. However, the level of detail provided in the MELs made PRICE® and SEER® more suitable tools to estimate the LMA (05.06), the X-ray mirrors (05.06.07), the XGA (05.07) and the ISIM instruments (LXM: 05.09.08, HDXI: 05.09.09 and XGD: 05.09.10). PRICE® does not estimate X-ray optics and sensors well, so SEER® was used for instruments with these components. Also, SEER® provides an embedded Monte Carlo generation capability that provides input distribution into the PCEC model. Although the instrument's mass and power are well outside the dataset in NICM, NICM was used to provide an additional point of comparison as PCEC does not estimate instruments. Note: The GSFC-provided PRICE® estimate for the LXM was a pass-through.	
06	Spacecraft Element (SCE)
Basis of the Estimate: PCEC used to estimate the spacecraft costs because of the level of the data provided. PCEC also allowed the other estimates to be throughput with Monte Carlo input data and Monte Carlo analysis to be performed on the overall estimate. Used a 10% fee and 30% reserves. Flight Software costs are included in the GN&C, Communications, and C&DH Estimates in the mission level estimate. A proto-flight design approach is used, 65% prototype, flight unit of 1, and 10% spares to all subsystems. These percentages are similar/typical of Pre-Phase A efforts.	
07	Mission Operations
Basis of the Estimate: PCEC used for this WBS element. Utilized the near earth CER based on the daily data volume, mission type, tracking network, management mode, science team role, science team size, and quantity and type of instruments.	
08	Launch Vehicle Services
Basis of the Estimate: Throughput from NASA HQ following direction from the Launch Service Program (LSP).	
09	Ground Systems
Basis of the Estimate: PCEC used for this WBS element. Used Mission Operations (MO) and Data Analysis (DA) Phase B–D and near-Earth CER based on the flight system dry mass, mission type, tracking network, management mode, science team role, science team size, and quantity and type of instruments.	
10	Systems Integration and Test
Basis of the Estimate: PCEC used for this WBS element. This CER calculates a monthly cost during I&T based on the mission duration, payload organization, flight system power, total payload mass, and number of payload elements. The monthly charge per phase is determined based on the database average for this type of mission.	
11	Public Outreach
Basis of Estimate: Used 1% of Phase B–D costs. Historically, public outreach has been 1–2% of the project payload and flight system cost.	

8.5.3 Cost Validation

Multiple cost validation exercises conducted separately from the parametric analysis provided additional peer reviews, sensitivity analyses, and independent crosschecks—further strengthening the credibility of the *Lynx* parametric estimate.

The primary cost estimate for the *Lynx* mission is the parametric estimate, which is consistent with pre-Phase A for concept formulation. The credibility of this estimate is strengthened by the SME inputs on the component level for every Observatory element. Further validation of the parametric estimate includes a detailed comparison to *Chandra*, a grassroots assessment developed by a team of highly qualified experts on both *Lynx* and *Chandra*, development of a non-advocate ICE with uncertainty analysis, and development of an independent, contracted cost and technical evaluation (CATE) with uncertainty analysis. In-family comparisons to the LMA, HDXI and XGD assembly, and spacecraft provides additional validation of the parametric estimate for these elements. The approaches to each of these validation methodologies are outlined below.

8.5.3.1 *Chandra* Analogy

The huge gains in capability that *Lynx* provides do not directly translate to a huge cost increase over inflated (\$FY20) *Chandra* actuals due to extensive, existing knowledge-base and lessons learned from past X-ray missions, existing spacecraft hardware, and recent advancements in X-ray mirror and science instrument maturity. As a result, the *Lynx* parametric mission cost estimate is within 11% of the escalated (\$FY20) *Chandra* actual cost.

Given the strong heritage from the *Chandra* mission and availability of actual costs, *Lynx* parametric cost estimates were compared with *Chandra* actuals normalized to \$FY20. Detailed comparisons were performed at the subsystem level for the spacecraft, at the instrument and mirror levels for the telescope, operations, and at the mission level.

Lynx mission formulation and technology development have directly benefitted from having a science community and a contractor base with extensive and applicable experience from working on *Chandra* and other recent X-ray missions. Even though personnel and contractors will change, an exceptionally solid mission concept and cost basis for *Lynx* are developed with inputs and lessons learned from the current personnel base. The *Lynx* DRM uses an over-arching observatory and ground system architecture similar to that of *Chandra*, enabling *Lynx* to take advantage of lessons learned while also taking different approaches as necessary.

The analogous and comparable *Chandra* elements leveraged on *Lynx*, which include the spacecraft, the HDXI and XGS assembly, and operations are summarized in Table 8.9. Items less amenable to direct leveraging from *Chandra* are the X-ray mirrors (and LMA) and the LXM. However, as discussed below, these costs are well understood. For the spacecraft, almost all *Lynx* performance requirements are the same as those on *Chandra*, primarily due to having the same angular resolution requirement. Observatory-wide error budgets for mass, power, thermal, and end-to-end performance, discussed in

§6.6.1, demonstrate that the requirements are well understood and achievable. The *Lynx* design utilizes current high-heritage spacecraft components, analogous to those on *Chandra*. While *Lynx* will ultimately use SOA elements, no new specific technology developments are required.

The mission cost estimate reflects the overall utilization of *Chandra* heritage. The *Lynx* PCEC parametric modeling includes heritage factors with settings of “major modification” (3 on a 1–10 scale) for all spacecraft subsystems and flight systems except structures, and a setting of “new but standard process” for structures. Parameters for mission type, mission destination, and operating environment, which influence the communication and mission operations cost estimates, are set to the same normalization as WMAP, which operated at Sun-Earth L2 (Table 8.7, note 1). Inclusion of these heritage factors lowers the parametric cost estimate.

Table 8.9. Summary comparison of key *Chandra* and *Lynx* spacecraft, telescope elements, and operations.

Observatory Element	<i>Lynx</i> vs. <i>Chandra</i> Requirements	Comments
Spacecraft		
Propulsion	Comparable except <i>Lynx</i> requires more fuel to maintain L2 orbit	Momentum management is similar. <i>Lynx</i> does not require internal spacecraft engines to reach final orbit.
GN&C	Comparable	<i>Lynx</i> requirements are similar for pointing accuracy and control, aspect determination, slew speed, and frequency.
Power	Analogous <i>Lynx</i> ~3x <i>Chandra</i>	<i>Lynx</i> uses different solar panels and battery technology. However, the power design philosophy is similar and high TRL hardware already exists.
Thermal	Comparable	Thermal requirements are similar for the OBA and LMA, but due to aging of <i>Chandra</i> Multi-Layer Insulation (MLI), an additional offset layer and small sunshade is included for <i>Lynx</i> .
Avionics and Flight Software	Comparable	Thermal control, power switching and management, data storage, command management, and uplink and downlink communications require <i>Lynx</i> -specific flight software, but the design philosophy is similar.
C&DH	Comparable except <i>Lynx</i> data storage and downlink rates are nearly 100x <i>Chandra</i>	Frequency of DSN contacts for uplink and downlink is similar to <i>Chandra</i> . Increased requirements for data storage and downlink rate can be met with already existing high TRL hardware.
Telescope		
Mirror Assembly	Comparable requirements, but implementation involves a very different approach	<i>Lynx</i> mirror fabrication and assembly is very different from <i>Chandra</i> . <i>Lynx</i> Mirrors are segmented and made of a different material. <i>Lynx</i> requires the integration of ~37,500 segments to form the LMA. Demonstrated laboratory production of multiple mirror segments, along with plans for mass production, plus modularity of the assembly provide a sound basis for the cost estimate.
HDXI	Analogous	Similar to primary imager on <i>Chandra</i> in terms of functionality and spacecraft resource requirements, even though <i>Lynx</i> HDXI will use SOA technologies.
XGS	Comparable	Grating array structure and mechanisms for <i>Lynx</i> designed similar to <i>Chandra</i> grating array. Detector system is also similar in terms of required spacecraft resources. <i>Lynx</i> grating array is much larger than <i>Chandra</i> gratings and uses a different design.
LXM	Not Analogous	LXM is a unique instrument that leverages heritage and design from JAXA and ESA missions. There is no <i>Chandra</i> analogy. LXM costs are well understood given high heritage with other similar instruments (<i>Hitomi</i> SXS, <i>XRISM</i> Resolve and <i>Athena</i> X-IFU).
Operations	Comparable	Nearly all of the hardware and software requirements and algorithms are available for designing ground operations and science systems. Software heritage is substantial.

Spacecraft Comparisons — Table 8.10 provides a look at two *Chandra* spacecraft subsystems also specified on *Lynx* for which current costing information is readily available.

Table 8.10. Cost comparison between inflated *Lynx* actuals and current vendor estimates for two spacecraft subassemblies.

Subsystem	<i>Chandra</i> Actual Cost	<i>Chandra</i> Cost (\$FY20)	Current Vendor Estimate
Reaction Wheels (6 flt.+1 spare) plus drive electronics and isolation system	\$1.95M	\$3.82M	\$1.0–\$2.0M Range due to uncertain cost for quality control
Aspect camera assembly	\$28.5M (1 optic with flip mirror and 2 readouts)	\$55.9M	\$30M–\$35M (2 complete camera assemblies)

Although not necessarily representative for all spacecraft subsystems, these two examples show that costs have not escalated as quickly as predicted by NASA inflation factors. This assessment is directly relevant to the overall spacecraft cost comparisons since most *Lynx* spacecraft subsystems requirements are met by those used on *Chandra*, so hardware with demonstrated performance is already available.

Labor costs comprise the largest cost element at the full systems level for the spacecraft, with the subsystem hardware costs being a significant, albeit lower, contributor. The data above suggest that the hardware costs for various *Lynx* spacecraft subsystems are likely to be somewhat lower than the inflated *Chandra* actuals, while the labor required should not differ substantially from *Chandra*. These considerations provide additional support for the parametric estimates for the spacecraft being at a level comparable to the inflated *Chandra* actuals.

Telescope Comparisons — The *Lynx* telescope elements are based on technologies currently at TRL 3 or higher. The LMA and science instrument requirements, their current state of development, and their technology development plans to achieve TRL 6 are presented in §6 and §7. Although further technology development is required, the development plans for the payload elements are well understood, leading to credible parametric estimates for each as described in this section and in the *Lynx Cost Book*. The required pre-Phase A and Phase A technology development funding has been identified and is at a level consistent with existing NASA funded development opportunities and that of other similar programs.

***Lynx* Mirror Assembly** — The X-ray mirrors are the dominant component of the LMA, and are akin to the mirror elements within the *Chandra* High Resolution Mirror Assembly (HRMA). The *Lynx* X-ray mirrors have a collecting area ~30x the HRMA, comparable on-axis angular resolution, and a sub-arcsecond point spread function over a FOV 20x the corresponding FOV for *Chandra*. The sub-arcsecond angular resolution over the much larger FOV for *Lynx* results from making small changes to the mirror prescription from the *Chandra* Wolter-1 to the *Lynx* Wolter-Schwarzschild, along with the use of substantially shorter mirror segments on *Lynx*, with no accompanying cost drivers. The tighter nesting of the thinner *Lynx* mirror segments results in a 3-m diameter, which is 2.5x larger than the HRMA. The focal length and focal plane plate scales are identical for *Lynx* and *Chandra*. The LMA is described in detail in §6.3.1.

Design and capability differences between the *Lynx* LMA and *Chandra* HRMA do not translate directly into large differences in cost primarily due to readily available mirror segment Silicon material and cost efficiencies borne out of the repetitive manufacturing processes for the LMA segments and modules (§8.5.2). The estimated cost of the LMA is within 6% of the escalated (\$FY20) HRMA actual cost.

A key factor for the basis of the *Lynx* mirror costs, in addition to the ready availability of high-quality monocrystalline silicon, is the demonstrated laboratory performance of the machinery needed to polish, shape, and smooth the *Lynx* segments, along with the metrology to measure and confirm their performance. This situation can be contrasted with *Chandra* for which all of the equipment had to be developed almost from scratch.

In contrast to HRMA, the LMA is modular, lending itself to a “mass production, assembly line” approach. This systematized manufacturing approach is the essential factor constraining the *Lynx* mirror costs (§8.5.2). While the approximately 37,500 mirror segments represent a large increase relative to *Chandra*’s eight mirror elements, the process is quickly transformed from the specialized, “one-at-a-time” *Chandra* approach to a relatively straightforward manufacturing process for *Lynx*. For *Lynx*, handling and shaping small segments (even very thin ones) is substantially easier than dealing with large, heavy *Chandra* elements. *Chandra* polishing required many months for each element, while *Lynx* segments can be done in a few days, with many segments being fabricated, aligned, and assembled simultaneously. The time, labor, and equipment costs for fabricating these mirrors are well understood and have been applied to project the *Lynx* mirror costs (§8.5.2).

The planned assembly line process for *Lynx* keeps the production time for the total ensemble of segments comparable to the polishing time for the *Chandra* elements; the projected costs are comparable in \$FY20. In addition, a few pairs of segments have already been aligned at close to the precision required for *Lynx*; demonstration of flight-like alignment is included as part of the technology development plan to achieve TRL 6. While *Chandra* had only eight elements, mounting and aligning them was very challenging. For *Lynx*, dealing with and assembling many more small, light-weight segments is also challenging, but is expected to evolve into a “routine” process for which the required time and associated costs are already approximately known.

Ultimately, the modularity of the *Lynx* mirrors provides a “safety valve” against schedule slip, cost growth, and/or depletion of mass margins, as mirror pairs can be eliminated from the design for up to a 50% reduction in effective area (§9). In this case, mass dummies would replace the eliminated mirror pairs, thus saving the time and cost for mirror polishing, coating, and ion beam figuring. While this option would necessitate longer exposure times, a reduced area would not decimate the science program. This ability to react to challenges to cost and schedule during DDT&E provides overall project flexibility and reduces cost and schedule risk. This modular approach also supports having reasonable numbers of spare segments at the 10% level, allowing replacement of broken or non-performing pieces during the manufacturing or assembly process or in a worst-case scenario, simple deletion of a module or a shell. Note that while *Chandra* had spare blanks for each element, none of these were polished, thereby making any potential replacement a more time-consuming and expensive proposition. In terms of modularity and spares, the approach to the *Lynx* mirrors is far more robust and cost-effective than what was available for the *Chandra* HRMA.

Lynx Science Instruments— Though the *Lynx* and *Chandra* science instruments use different technologies, meaningful comparisons can be made. The *Lynx* HDXI and XGD are designed to use similar technologies and both have substantial similarities to the *Chandra* Advanced CCD Imaging Spectrometer (ACIS). However, the *Lynx* detectors provide significant increases in capability through higher quantum efficiency at lower energies, active pixel sensing, faster readout, and radiation hardness (§6.3.2). These *Lynx* detectors do not require technology breakthroughs, just advancements over the current state of the art to couple with the LMA to provide leaps forward in sensitivity (100×) and FOV (20×), with high-angular resolution imaging and survey capabilities relative to *Chandra*. Similar considerations apply to the XGA, which will have on the order of 100× the throughput and 10× the resolving power of the *Chandra* gratings, enabling tremendous advances for spectroscopy of point-like sources such as stars and active galactic nuclei (§6.3.3). *Lynx* costs for each of these instruments are projected to be ~30% higher on average than the inflated *Chandra* costs for ACIS and the High Energy Transmission Gratings (HETG). These estimates are conservative when taking into account ongoing advances in the semi-conductor industry, which have resulted in cost growth rates for sensors, electronics, and similar hardware that are lower than the standard inflation rate applied to escalate the *Chandra* actuals.

The one instrument on-board *Lynx* that does not have a direct analogue from *Chandra* is the LXM. The LXM cost estimate, however, does take into account other heritage and leveraged design elements from planned missions while allocating substantial funding for this new capability. Coupled with the capabilities of the LMA, the LXM provides breakthroughs for high-resolution spectroscopy of extended sources such as clusters of galaxies, galactic halos, and supernova remnants, to name a few (§2.2, §3.3). There have been great advances in the technology development for this type of instrument, both in the laboratory and through flight development for a series of Japanese missions. Those missions include *Hitomi*, where the performance capabilities of the SXS instrument were demonstrated before the premature loss of the mission, and *XRISM*, currently under construction. The LXM also benefits substantially from investments by NASA and ESA in the *Athena* X-IFU, which is a similar detector albeit with fewer pixels, less demanding spatial resolution, and no extra-high spectral resolution subarray as is planned for the LXM. Through the use of thermal and electronic multiplexing, the LXM has a comparable number of readout channels to *Athena* and thereby comparable cooling requirements (§6.3.4).

The LXM design leverages successes and developments related to *Hitomi*'s SXS and *Athena*'s X-IFU instruments. Vibration isolation necessary to avoid performance degradation related to the cryocooler relies on heritage from *Hitomi*. The LXM also includes an assembly with a modulated X-ray source capable of providing pulsed X-ray lines at multiple energies and is similar to that used on *Hitomi* for in-flight calibration. Infrared/optical blocking filters that are necessary to block long-wavelength photons from reaching the microcalorimeter array are also included and based on the *Hitomi* and *Athena* designs. The ADR baselined for the LXM and its control electronics are adapted from those used on *Hitomi*, with additional stages of similar design being added to provide further cooling power. The burst disc, filter wheel, pump-out port, by-pass valve, dewar door mechanism, and event signal processor electronics and software are based upon those developed for and used on *Hitomi*. Since the baseline sensor technology uses Transiting Exoplanet Survey Satellites (TESS), there are many advances being made for *Athena* that will be leveraged for the LXM, such as the focal plane assembly that houses the sensor array, the cold read-out, and the anticoincidence detector for reducing background events.

Operations Comparisons—The direct transfer of *Chandra* experience to *Lynx* also applies to the development and operation of the ground system, starting with a baseline to co-locate the science and operations centers and form an integrated team for all relevant activities. Even with the change from High-Earth Orbit (HEO) to an L2 orbit, *Lynx* requirements are similar to those of *Chandra*. The HEO has to deal with regular passages through trapped radiation zones, while the L2 has an added requirement for station keeping. Nearly all of the hardware and software requirements and algorithms are already available for scoping the ground operations and science systems and for guiding their development, testing, and utilization. Software heritage is substantial, although *Lynx* anticipates new coding for a mission in the 2030s and beyond, utilizing more powerful hardware and software platforms available in that timeframe. Understanding the operations scope, and taking advantage of less expensive computer hardware and cost reductions from evolved *Chandra* operations, reduces cost and risk for *Lynx* relative to *Chandra*. This is especially the case for the first several years where the *Chandra* learning curve was still quite steep. One area where *Lynx* requires capabilities that are more sophisticated is the analysis of the detailed, high-resolution spectra obtained with the XGS and LXM. Overall, the combined ground system development and actual *Lynx* operations are comparable to the *Chandra* inflated costs, even after folding in an increased level of funding for *Lynx* science grants compared with *Chandra* levels. The parametric estimate for *Lynx* ground system development and operations is based on the Space Operations Cost Model (SOCM) that uses *Lynx* baselines for mission destination, operating environment, length of development, number of instruments, center or PI-led effort, single or multi-operations center, length of mission, size of science team, and several other parameters.

In comparing *Lynx* to *Chandra*, the spacecraft plus two out of the three *Lynx* instruments are not substantially different from evolutions of the *Chandra* equivalents and do not require significant breakthroughs or new inventions. Mission operations are particularly well understood, with plans and cost estimates derived from *Chandra* experience. The ability to produce a *Lynx* mirror at a cost similar to *Chandra*'s can be tracked to tangible technological advances, along with a mirror design amenable to mass production. The LXM is quickly gaining technology maturity from laboratory efforts and from other X-ray missions (*Hitomi*, *XRISM*, *Athena*), and can be viewed as a well-understood evolution of the *Athena* X-IFU (in which *Lynx* instrument leads are already involved). Given the achievements in key technology areas and the development plans to achieve TRL 6 for the LMA and the science instruments over the next several years, *Lynx* costs in \$FY20 only modestly exceed the *Chandra* costs inflated to \$FY20.

8.5.3.2 Grassroots Estimate

The detailed grassroots estimate for project Phases A–E is within 4% of the parametric estimate.

The *Lynx* team developed a DRM grassroots estimate to validate the parametric estimate. The grassroots estimate was developed for each Level 2 WBS code, and in some cases, down to the WBS 3 level. A skilled and diverse team of experts including *Chandra* project and prime contractor team members and *Lynx* science, engineering, and technology team members provided estimate inputs for the individual WBS elements. The estimates consist of a mix of *Chandra*-analogous estimates, scaled *Chandra* actuals for prime contract activities, and true grassroots based on development planning.

For the prime contractor portions of the grassroots estimate, an analysis of actual *Chandra* prime and subcontractor labor hours was performed via an industry CAN partnership. The prime contractor efforts for *Lynx* approximate the same scope for *Chandra* and include contract management; mission assurance; telescope and science instrument module subcontract management; observatory systems engineering and Assembly, Integration, and Test (AI&T); spacecraft DDT&E; and observatory commissioning. Actual *Chandra* labor hours were collected by WBS; scaling factors ranging from 1.0 to 1.5 were applied based on knowledge of the design, scope of work, and schedule durations of both the *Chandra* and *Lynx* projects. An hourly labor rate was derived by averaging the actual *Chandra* average contractor rate (inflated to \$FY20) and an average Department of Labor rate for aerospace industry workers. The derived average fully wrapped contractor labor rate was used for the prime portions of the grassroots estimate. Material costs were estimated at 50% of labor costs for those WBS codes involving development of flight hardware and GSE.

The grassroots estimate was developed for Phase A–E (first 5 years of operation) and aligned with the *Lynx* DRM project schedule. The Phase A estimate was based on ~150 civil servants and support contractors for WBS 1, 2, 3, and 4, which is similar to the number of personnel that supported the *Chandra* project in Phase A. An average fully loaded labor rate in \$FY20 for MSFC personnel was applied to that level of support. Additionally, it was assumed that support from the Prime contractor for a Phase A requirements development contract would be 30 personnel at the derived average fully wrapped contractor rate. The Phase A estimate includes the technology development cost estimates (\$7), and Phase A estimate for WBS 9. Phase A (and pre-Phase A) funding estimates include project office support for management, oversight, risk mitigation, and requirements development associated with technology development efforts. The technology development estimates for Phase A are consistent with the rapidly advancing technology maturation and funding projected during the pre-Phase A period.

The launch vehicle is included in the total grassroots estimate, and uses the same LSP-provided pass-through as for the project parametric estimate. Fee and 30% reserves were applied only to those contracted portions not based off *Chandra* actuals. It was assumed that the estimates based on *Chandra* actuals represent the final cost with 100% of the reserves consumed.

Table 8.11 summarizes the grassroots BOE by WBS. This high-level summary is supported by an extended BOE that is part of the *Lynx Cost Book*. This extended BOE includes details such as a breakdown of assumed labor rates, materials, and equipment. In some cases, Rough Order Magnitude (ROM) cost estimates were provided by the vendor. A summary of personnel who prepared each grassroots WBS estimate and their qualifications is include in Appendix E.

Table 8.11. *Lynx* BOE for grassroots estimate.

WBS	WBS Title
01	Project Management
Basis of Estimate: Task-based estimate developed from project milestones and deliverables and captures the annual average number of personnel based on <i>Chandra</i> project actuals per the project manager. FTE fully loaded cost from the MSFC average rate table for Science Office personnel escalated to FY\$20 was used with additional funding for supplies and travel to calculate total cost for this WBS. Includes project management, project planning and control analysts, project coordinators, scheduler support, configuration and data management support, contract support, supplies, and travel costs.	
02	Systems Engineering
Basis of Estimate: Task-based estimate developed from project milestones and deliverables, and captures the annual average number of personnel based on <i>Chandra</i> project actuals per the project manager. FTE fully loaded cost from the MSFC average rate table for Science Office personnel escalated to FY\$20 was used with additional funding for supplies and travel to calculate total cost for this WBS. Includes Chief Engineer (oversight; NASA-provided Independent Technical Authority (ITA), systems engineering, requirements development & verification, materials support and independent review of analytical integration and requirements, ICDs, and verification products provided by the Prime Contractor.	
03	Safety & Mission Assurance
Basis of Estimate: Task-based estimate developed from project milestones and deliverables, and captures the annual average number of personnel based on <i>Chandra</i> project actuals per the project manager. FTE fully loaded cost from the MSFC average rate table for Science Office personnel escalated to FY\$20 was used with additional funding for supplies and travel to calculate total cost for this WBS. Includes Safety and Mission Assurance support for payload development and testing, reliability analysis, quality assurance and mission safety. Chief Safety Officer oversight is NASA-provided Independent Technical Authority.	
04	Science & Technology
Basis of Estimate: Includes science and technology management, science support (project Phases A–D) and <i>Lynx</i> optics and instrument technology development (Phase A). Estimate is based on 3% of WBS 1, 2, 3, 5, 6, 7, 9, 10 and 11. Same % was used in parametric. Includes the Phase A estimates for technology development for the DRM technologies as per the technology development plans (S7).	
05	X-ray Telescope (XRT)
05.01 – 05.04	Telescope management, systems engineering, product assurance, I&T (Prime Contract)
Basis of Estimate: This WBS includes the DDT&E efforts associated with the XRT including the management, systems engineering, product assurance integration and test, GSE, the structure, thermal control system, and integration of the LMA, OBA, ISIM, and fiducial transfer components of the Pointing Control and Aspect Determination system. This element also includes Prime Contractor management, product assurance, and systems engineering activities. The telescope contractor portion of this estimate is based on a review of actual <i>Chandra</i> WBS level 4 labor hours, rolled up to level 2 and an applied weighted complexity factor of 1.2 based on review of lower level details. The weighted factor was derived by comparison of the <i>Chandra</i> and <i>Lynx</i> designs, complexities and mass differences, and scaled time spans based on project schedules. Overall, the <i>Lynx</i> XRT is more complex than <i>Chandra</i> due to the number of interfaces, overall size, and tight alignment tolerance. The estimate includes the LMA and XRT AI&T including the flight OBA and doors, mechanisms, telescope control electronics and cabling, and thermal hardware. The size of the GSE will drive more manufacturing, materials, and assembly.	
05.05	Telescope Calibration
Basis of Estimate: The <i>Lynx</i> ground calibration activities are assumed to be carried out at the MSFC XRCF as was done for <i>Chandra</i> in the 1990s. The calibration schedule and planned procedures are based on <i>Chandra</i> experience adjusted to better incorporate on-orbit calibration plans that are expected to considerably reduce ground calibration activities. This effort includes the calibration rehearsal activities to practice handling and calibration procedures using EM models for the LMA, XGA, LXM, HDXI and XGD, as well as the calibration of the flight mirrors and grating array to the flight grating and HDXI and XGD detectors. The high-fidelity LXM EM will be used for ground calibration. This estimate includes both MSFC Full-Time Equivalent/Work Year Equivalent (FTE/WYE) and Prime Contractor WYE efforts to perform the <i>Lynx</i> ground calibration campaign. The MSFC portion of this estimate is a bottom-up pricing out of FTE/WYE specific tasks. The cost is based on average fully loaded rates for MSFC Science Office and XRCF personnel. The Prime portions of this estimate are based on actual <i>Chandra</i> hours with a scaling factor of 1.3 to account for the additional size and complexity of the <i>Lynx</i> system and the addition of the LXM instrument. The effort for the rehearsal and flight calibration activities will take ~2 additional months vs. that for <i>Chandra</i> . The Prime contractor portion also includes efforts to provide mirror module assembly-to-XRCF interface hardware necessary for X-ray calibration.	

Table 8.11. Continued

WBS	WBS Title
05.06	Lynx Mirror Assembly
<p>Basis of Estimate: This WBS includes the DDT&E efforts associated with the LMA including the management, systems engineering, integration and test, GSE, the structure, thermal control system, and integration of the X-ray mirror module assembly, barrel, and pre-and post-collimators.</p> <p>The telescope contractor portion of this estimate is based on a review of actual <i>Chandra</i> WBS level 4 labor hours, rolled up to level 2 and an applied weighted complexity factor of 1.2 based on review of lower level details. The weighted factor was derived by comparison of the <i>Chandra</i> and <i>Lynx</i> designs, complexities and mass differences, and scaled time spans based on project schedules. This WBS compares to the HRMA Flight and GSE hardware and integration with similar complexity but with a diameter of 3× time larger than <i>Chandra</i>. All handling operations and gravity offloading need to reflect the constraints due to critical alignments (0.1 arcsec). A high-fidelity verification test article similar to the VETA-II on <i>Chandra</i> is also included for qualification testing. Actuator and electronics verification test sets and GSE fixtures are included. LMA shipping and purge GSE is included.</p>	
05.06.07	X-ray Mirror Modules
<p>Basis of Estimate: The X-ray mirror module estimate is based on work completed by the GSFC Silicon Meta-shell Optics team and technology status as of September 2018. The estimate includes equipment and labor costs of mirror segment fabrication, mirror segment coating, integration of segments into modules, module testing, integration of modules into meta-shells, and integration of meta-shells into the final X-ray mirror module assembly. The estimate includes facility costs for integration of the mirror module assembly into the LMA. The cost model reflects the number of labor hours based on a fully loaded rates for junior workers (technicians, project support etc.), and senior workers (engineers, scientists, etc.), as well as major equipment costs and small consumable items needed. For GSE, past purchasing prices inflated to FY\$20 and/or recent quotations solicited from vendors were used. 30% has been added to cover the price to account for upkeep and servicing contracts that are an essential part of operations. The estimate also includes an additional 10% to cover the procurement work associated with the equipment. For consumables, the estimate is based on usage experience, in combination with experience with many recent purchases. Labor hours are based on fabrication, coating, alignment, and bonding of mirror segments. This estimate does not include the development of the TRL 6 engineering model (included in WBS 4 estimate for Phase A activities).</p>	
05.07	X-ray Grating Array (XGA)
<p>Basis of Estimate: The XGA estimate is for the CAT XGA, and is based on the <i>Chandra</i> HETG experience with grating fabrication and testing, and recent costing for the proposed X-ray Arcus Midex mission. Costs consist of labor (estimated FTE effort and duration for each milestone), new tools and equipment, consumables (boules, wafers, chemicals, etc.), costs for MIT Lincoln Labs to develop their processes and run batches through their fab, and services and fees (use of outside tools, machining costs, deposition services, etc.). Estimates for development includes: Build up fabrication and characterization infrastructure, establish documentation protocols, perform fabrication test runs, refine and optimize fabrication process steps, acquire custom SOI wafers, build assembly and alignment infrastructure, refine and optimize frame design, and long-lead time orders, personnel ramp-up (hiring and training) for the fabrication and characterization ("production"). Two scenarios are considered: Large gratings (2/wafer, ~ 800) and small gratings (7/wafer, ~ 2,050). We estimate that an XGA populated with large gratings is cheaper by ~ \$4.5M, mostly due to labor savings from the smaller number of gratings to be characterized and handled. For the purpose of this estimate, the smaller gratings are assumed.</p> <p>This estimate does not include the engineering model delivered post-CDR that will consist of a flight like grating array structure, several qualification-tested grating facets and mass dummies (part of WBS 4 estimate). This EM will be used to space qualify the design.</p>	
05.08	Optical Bench Assembly (OBA)
<p>Basis of Estimate: This WBS includes the DDT&E efforts associated with the OBA including the management, systems engineering, integration and test, GSE, the structure, thermal control system, and magnetic broom.</p> <p>The telescope contractor portion of this estimate is based on a review of actual <i>Chandra</i> WBS level 4 labor hours, rolled up to level 2 and an applied weighted complexity factor of 1.5 based on review of lower level details. The weighted factor was derived by comparison of the <i>Chandra</i> and <i>Lynx</i> designs, complexities and mass differences, and scaled time spans based on project schedules. Specifically, for this WBS, the differences are based on the increased optical bench diameter, increased size impacts on the GSE, and the thermal heater system and blanketing areas. Key alignment datums for ISIM and LMA will be engineered into the OBA for reference during XRT assembly. GSE fixtures will be manufactured to support assembly of the large composite structures and fittings, and rotation fixture to support final integration steps prior to XRT integration. GSE handling equipment will also serve as shipping supports.</p>	
05.09	Integrated Science Instrument. Module (ISIM)
<p>Basis of Estimate: This WBS includes the DDT&E efforts associated with the ISIM including the management, systems engineering, integration and test, GSE, the structure, electronics system, thermal control system, and translation table mechanisms, as well as integration of the Government-furnished science instruments (LXM, HDXI. and XGD), as well as overall I&T for the ISIM.</p> <p>This estimate is based on analogy using <i>Chandra</i> Prime Contractor actual labor hours to design and build the ISIM, integrate the instruments, perform mechanism life tests and SIM environmental testing. The ISIM for <i>Lynx</i> is estimated to be more complex by a factor 1.5 over the <i>Chandra</i> ISIM due to 3 instruments to be installed, co-aligned and maintained (versus 2 for <i>Chandra</i>), accommodation of the LXM (a state-of-the-art cryogenic instrument) and its cryocoolers and a much more complex dynamics environment than <i>Chandra</i> (which had no coolers).</p>	

Table 8.11. *Continued*

WBS	WBS Title
05.09.08	<i>Lynx</i> Microcalorimeter (LXM)
	<p>Basis of Estimate: The LXM BOE is based upon two rounds of costing carried out by the GSFC Cost Estimating, Modeling & Analysis Office following an Instrument Design Laboratory that was also carried out at GSFC, and is based upon a MEL that was produced during this laboratory in June 2017, and updated in June 2018. The estimate is based upon a combination of sources for the various subsystems in an attempt to provide the best possible estimate, which is different for the various different components. Where possible, the costs were based on the costs of nearly identical heritage components of the Soft X-ray Spectrometer instrument on Astro-H, inflated to \$FY20. Detailed new grassroots estimates were made for the detector focal plane assembly, the majority of the adiabatic demagnetization refrigerator, and also the main detector read-out electronics. These were done by GSFC SMEs, and checked by the GSFC Costing Office to ensure all costs such as design, review, integration, and testing costs had been included. For the cryocooler, quotations were acquired from the two companies considered most able to provide cryocoolers meeting the LXM 4.5 K cooling and micro-vibration requirements, and with the most advanced TRL. For these quotations, the development costs for Pre-Phase A and Phase A costs were kept separate from the main instrument costs and are included in the roadmap separately. These quotations include the cost of all models of cryocoolers needed for the project and are included in the <i>Lynx Cost Book</i>. The highest quotation was used to be conservative. Parametric estimates obtained using PRICE-H® were used for some of the items for which grass-roots estimates were not available, such as for the cryostat other than the cryocooler, the cost of GSE, environmental testing, spares and the cost of selected environmental test units. For the LXM, an EM and a proto-flight unit will be developed, with selected subsystem flight spares but no complete instrument spare. The EM will undergo extensive qualification testing beyond the typical level of an EDU in order to space-qualify the design.</p>
05.09.09	High Definition. X-ray Imager (HDXI)
	<p>Basis of Estimate: This estimate is based on actual costs for the <i>Chandra</i> ACIS instrument, which to a zeroth-order approximation is a reasonable comparison to the <i>Lynx</i> HDXI. Although the <i>Lynx</i> HDXI is more capable than ACIS, 30 years of technical progress provides the extra capability at the same real cost. The estimate is derived from 533M financial reports during the Phase B–D development period (January 1993 through August 1999), escalated to FY\$20. The estimate includes project management, systems engineering and integration, reliability and QA, DDT&E activities, detector assembly, detector electronics assembly, digital processor assembly, instrument integration and verification, GSE, CCD fabrication, fabrication facility and support, instrument flight software, flight operations and data analysis, science support and mission management, Lincoln Laboratory engineering and ACIS (2-chip) calibration support.</p> <p>The GSFC IDL developed a separate grassroots/parametric-based estimate for the HDXI in February 2018. This estimate included DDT&E costs for the instrument based on the IDL design and CBE mass of 80.4kg, flight software, GSE, testing, flight spares and ETU. The total point design estimate was within 3% of the grassroots estimate.</p>
05.09.10	X-ray Grating Detector (XGD)
	<p>Basis of Estimate: The estimate for the <i>Lynx</i> XGD is based on similarity with the ACIS/HDXI, but scaled down to reflect the simpler layout and fewer sensors. Both instruments on <i>Lynx</i> are assumed to utilize the same sensor technology and follow a similar development path. Because <i>Lynx</i> is considering HDXI and XGD as separate instruments, developed by separate teams, most of the development and test costs will be incurred separately for each. ACIS included both an imaging array (4 CCDs) and a grating readout array (6 CCDs). The total raw detector cost was about 15% of the total ACIS instrument cost. Therefore, assuming only a grating readout on ACIS, the cost would have been about 10% (60% of 15%) less. A separate estimate for the XGD was obtained that assumed the use of an existing and commercially available CCD technology. This cost was within 9% of the grassroots ACIS/HDXI estimate.</p>
05.12	<i>Lynx</i> Calibration Facility
	<p>Basis of Estimate: This effort includes calibration facility-related work necessary to perform the rehearsal and flight calibration activities described in WBS 05.05. This includes facilities upgrades and modernization, GSE, DDT&E, labor, (e.g., technical, facility management, scientific, and IT support) and material costs. This effort is considered comparable to the estimates recently developed by MSFC XRCF staff in anticipation of calibration of <i>Athena</i>, currently in development by ESA, and anticipated to go through calibration in the FY28–FY29 timeframe. Anticipated calibration facility modernization and upgrades to the 1990s-era XRCF include changes to the X-ray source system, X-ray detector system, X-ray data and acquisition control system, contamination control and monitoring system, thermal control system and cleanroom facilities. GSE for <i>Lynx</i> calibration includes mirror and instrument handling fixtures, mirror reorientation fixture, focal plane instrument positioning fixtures, high-speed detector, metrology system, and other handling equipment.</p> <p>This estimate includes both MSFC FTE/WYE and Prime Contractor WYE efforts to upgrade the existing XRCF facilities, develop test GSE requirements, define interfaces, and perform test planning and procedure development. The MSFC portion of this estimate is a bottom-up pricing out of FTE/WYE specific tasks. The cost is based on average fully loaded rates for MSFC Science Office and XRCF personnel. The Prime portion of this estimate is based on actual <i>Chandra</i> hours with a scaling factor of 1.0. The facility efforts are expected to be of lower scope as the facility and interface definitions already exist, some <i>Chandra</i> GSE can be re-used, so there is less new hardware. This new hardware is more complex, due to the size and tighter alignment tolerances for <i>Lynx</i>. Net assessment is that the overall effort will be the same.</p>

Table 8.11. Continued

WBS	WBS Title
06	Spacecraft Element
<p>Basis of Estimate: Estimate is based on analogy using <i>Chandra</i> Prime Contractor labor actuals for this WBS element with modifications applied for assessed differences between the <i>Chandra</i> and <i>Lynx</i> spacecraft bus designs. Like <i>Chandra</i>, the Prime Contractor will have the responsibility for DDT&E activities associated with the spacecraft bus. Sub-elements include Management, Systems Engineering, Product Assurance, Integration and Test, and Ground Support Equipment, as well as all of the Spacecraft Bus subsystems (FSW, Structures, Thermal Control, EPS, C&DH, Communications, GN&C and Propulsion).</p> <p>For this element, the Prime contractor effort was scaled at 1.5 over the <i>Chandra</i> effort based on increased mass and power requirements for <i>Lynx</i>.</p>	
06.05	Flight Software
<p>Basis of Estimate: In addition to the analogous <i>Chandra</i> estimate, a separate grassroots estimate for FSW was developed by the MSFC software engineering branch using the Constructive Cost Model (CoCoMo). Two estimates were generated: one using customized parameters based MSFC software team experience and the other using Class A software defaults. Only C&DH software was included in this exercise (no instrument software). 104,739 software lines of code (SLOC) was estimated by the GSFC Mission Design Lab (MDL) for the <i>Lynx</i> spacecraft.</p> <p>It is assumed that this element is include the in Prime contractor's scope already. This grassroots estimate is provided for information and does not contribute to the total.</p>	
07	Mission Operations
<p>Basis of Estimate: The <i>Lynx</i> cost model for Mission Operations in Phases E–F was developed by analogy using the actual costs for the corresponding <i>Chandra</i> WBS elements with modifications applied for assessed differences between the <i>Chandra</i> and <i>Lynx</i> requirements, while also taking into account efficiencies developed over the course of the <i>Chandra</i> operations to date, which are directly applicable to <i>Lynx</i>. The detailed assessment included review of <i>Chandra</i> MO actuals for phase E–F, identification of any differences with the <i>Lynx</i> hardware and operations, development of a <i>Lynx</i> cost model populated with <i>Chandra</i> labor and Other Direct Costs (ODC), and revisions made to the above for noted differences. This element also includes grants for the <i>Lynx</i> general observer program.</p>	
08	Launch Vehicle Services
<p>Basis of Estimate: This cost is based on direction from NASA HQ and from LSP and includes the Full Mission costs for launch services for a composite heavy-class LV based on today's prices escalated out to the <i>Lynx</i> 2035 LRD. Included in this cost is the standard launch provider services defined in the NASA Launch Services (NLS) II contract terms and conditions, as well as additional mission unique services necessary to meet the mission requirements as defined by the spacecraft project (e.g., additional doors, special cleaning, additional analyses cycles, etc.). Integrated Services covers payload processing at the launch site and LSP's support-service contractor costs that will eventually be directly charged to the individual mission work performed. Finally, this element includes the station needed for downrange station telemetry coverage. The stations used during the mission are dependent on the mission-unique trajectory to meet the spacecraft requirements.</p> <p>Per LSP, actual heavy-class vehicles that will exist in 2030s are unknown, so this cost includes a large degree of uncertainty.</p>	
09	Ground Systems
<p>Basis of Estimate: The <i>Lynx</i> cost model for Ground Systems in Phases A–D was developed by analogy using the actual costs for the corresponding <i>Chandra</i> WBS elements with modifications applied for assessed differences between the <i>Chandra</i> and <i>Lynx</i> requirements. The detailed assessment included review of <i>Chandra</i> Ground Systems actuals for Phase A–D, identification of any differences with the <i>Lynx</i> hardware and operations, development of a <i>Lynx</i> cost model populated with <i>Chandra</i> labor and ODC, and revisions made to the above for noted differences.</p>	
10	Systems Integration and Test
<p>Basis of Estimate: Estimate is based on analogy using <i>Chandra</i> Prime Contractor labor actuals for this WBS element with modifications applied for assessed differences between the <i>Chandra</i> and <i>Lynx</i> Observatory I&T efforts. This WBS includes I&T management and systems engineering, GSE, facilities and all work necessary to integrate the XRT with the SCE and perform system-level testing. The scaling factor for I&T management is assumed to be 0.8 for <i>Lynx</i> due to the shortened schedule for this activity. The factor for GSE is assumed to be 1.5 for <i>Lynx</i> due to increased complexity associated with a heavier spacecraft and telescope. The factor for I&T execution is assumed to be 1.0 due to similar effort and testing. The average overall scaling factor is 1.05 for <i>Lynx</i>.</p>	
11	Public Outreach
<p>Basis of Estimate: This element provides the resources to carry out a mission-related public outreach and communication for the project. The same resources as for <i>Chandra</i> are assumed for <i>Lynx</i> in the model. This provides for website and social media support, graphics and video generation, outreach to the public, and press and image releases at ~2/month.</p>	

8.5.3.3 Independent Cost Estimate (ICE) and Uncertainty Analysis

The MSFC Engineering Cost Office performed a non-advocate, independent cost estimate and uncertainty analysis of the *Lynx* parametric estimate and concluded that "...the independent risk assessment results are consistent with historical NASA mission cost growth behavior." The 40% CL on the non-advocate cost curve is within 1% of the *Lynx* parametric estimate.

At the request of NASA HQ, the MSFC Engineering Cost Office developed a non-advocate ICE and performed an uncertainty analysis to validate and determine the CL in the parametric estimate. The ICE addressed the uncertainty in the estimating methods, input parameters, design complexity, and fee. The analysis was performed in FY\$20 and \$RY, using NASA escalation factors for Phases B–E, exclusive of launch vehicle costs and reserves, to derive the cost basis for the assessment.

Input and model uncertainties were calculated for estimates performed using the PCEC tool. Input uncertainty was modeled using a triangular distribution, and model uncertainty was calculated using prediction intervals. Estimates performed for the LMA and science instruments using the SEER® and PRICE® models were assumed to be at a 25% CL. Coefficients of variation (CV), a rough measure of uncertainty, were in the 40% to 50% range. This resulted in conservatism in the range of results. The calculated overall CV of 35% on the derived cost basis is consistent with Air Force guidance for new space systems. Higher CVs for the mirror assembly and instruments reflect the amount of new design and technology development for these elements.

A Monte Carlo simulation on the input models provided a cost curve with CLs ranging from 10%–90% as shown in Figure 8.5. Reserve amounts to achieve corresponding confidence levels were calculated based on the delta between the derived cost basis (parametric estimate for Phases B–E exclusive of launch vehicle and reserves) and the cost at the 50% and 70% CLs on the resulting cost curve. Based on this analysis, the *Lynx* parametric estimate with 30% reserves on B–D costs (exclusive of launch vehicle) has a 38% CL on the independent cost curve. An analysis of 132 historic NASA projects [623] concludes that typically, project estimates with reserves, have ~15% CL. Thus, the *Lynx* parametric estimate with 30% reserves on Phases B–D (less launch vehicle) represents a substantially better reserve posture than historical NASA projects.

The resulting analysis yielded a cost range from \$4.9B at a 40% CL to \$6.2B at 70% CL in \$FY20, and \$6.7B at 40% CL to \$8.5B at 70% CL in \$RY, using NASA escalation factors.

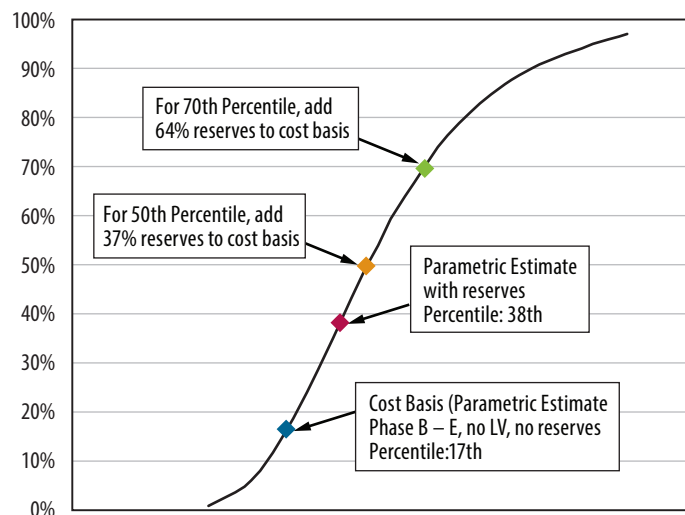


Figure 8.5. The *Lynx* parametric cost estimate with 30% reserves on Phase B–D (exclusive of LV) represents a 38% CL. To achieve a 50% CL, 37% reserves need to be applied to the cost basis. For 70% CL, 64% reserves need to be added to the cost basis.

8.5.3.4 Independent Cost Analysis and Technical Evaluation

The independently developed cost analysis and technical evaluation (CATE) validated the *Lynx* parametric cost estimate and found it, "...reasonable, credible, reproducible, and consistent with the DRM parameters." The 40% CL on the CATE cost curve is within 1% of the *Lynx* parametric estimate.

To further validate the cost estimate and ensure incorporation of cost and schedule risks, the *Lynx* team procured the services of MCR Solutions, LLC to develop an independent risk-based life-cycle project cost estimate and schedule forecast. For this assessment, MCR developed a detailed, independent parametric cost estimate (MCR ICE), analyzed the project schedule (§8.4) with respect to development durations for similar missions, analyzed the *Lynx* Technology Development section (§7), and assessed the DRM architecture (§6) to determine critical missing or underestimated development costs and schedule risks. These analyses were used as inputs into Monte Carlo-based analyses to produce the cumulative distribution functions for the total project and key lower level elements of the WBS that resulted in a total cost probability distribution for the predicted life-cycle cost and schedule realism. The resulting "S-curves" for total project cost and schedule provide an assessment of the project parametric cost estimate and execution plan.

MCR Cost and Schedule Estimating Methodology — The *Lynx* team provided source information to MCR for the CATE analysis including the detailed project parametric costing BOE, project schedule, WBS, technology development roadmaps, DRM MEL and PEL, engineering analyses, and technical papers [624], as well as the non-advocate ICE (§8.5.3.3), and grassroots estimate (§8.5.3.2) for comparison. The CATE methodology for development of the MCR ICE followed the GAO and NASA best practices approaches for cost estimation. The CATE utilized some of the same NASA parametric cost estimating models used in the project parametric estimate, as shown in Table 8.12. Crosscheck models indicated in the table were used for validation of the ICE. PCEC emulated an Earth-orbiting robotic environment and SEER-H® used the unmanned space platform.

Table 8.12. Assignment of primary and secondary models and methods for CATE estimate.

Cost Element (WBS)	Primary and Cross-Check Models and Methods
1.0 Project Management 2.0 Systems Engineering 3.0 Safety & Mission Assurance 4.0 Science & Technology	PCEC and SEER-H®
5.0 X-ray Telescope (XRT)	PCEC at higher WBS-level; except where noted below; SEER-H® for lower-level detail of WBS 5.06, 5.07, 5.09; 10% fee on most instruments. See Section 5 for details on fee.
5.06 LMA	PCEC for primary; SEER-H® for crosscheck.
5.07 X-Ray Grating Assembly (XGA)	Detailed model for primary using SEER-H® and TRL maturity based on MCR paper; PCEC for crosscheck.
5.09 Integrated Science Instrument Module (ISIM)	SEER-H® and PCEC as a crosscheck.
5.09.08 <i>Lynx</i> X-Ray Microcalorimeter (LXM)	Detailed model for primary using SEER-H® and TRL maturity with NICM as a crosscheck.
5.09.09 High-Definition X-Ray Imager (HDXI)	Detailed model using SEER-H® and TRL maturity with NICM as a crosscheck.
5.09.10 X-Ray Grating Detector (XGD)	Detailed model using SEER-H® and TRL maturity with NICM as a crosscheck.

Table 8.12. *Continued*

Cost Element (WBS)	Primary and Cross-Check Models and Methods
5.05 XRT Calibration	Throughput from Northrop Grumman, analogy estimate based on <i>Chandra</i> 1990 design.
5.12 <i>Lynx</i> Calibration Facility	Throughput from Northrop Grumman, analogy estimate based on <i>Chandra</i> 1990 design.
6.0 Spacecraft Element (SCE)	PCEC and SEER-H®, including flight software.
7.0 Mission Operations	PCEC, SOCM, and <i>Chandra</i> analogy.
8.0 Launch Vehicle Services	PCEC and SEER-H® plus throughput for LSP (launch vehicle).
9.0 Ground Systems	PCEC using MO and DA Phase B–D CER; Project grassroots estimate used as roots crosscheck.
10.0 Systems Integration & Test	PCEC and SEER-H®
11.0 Public Outreach	Calculated as a percentage of project costs and PCEC
Schedule	Project-provided schedule; MS Project; @Risk; basis of cost reserve

The MCR CATE used the same inputs and ground rules and assumptions established for the project parametric estimate, specifically:

- Project-provided WBS
- Model input mass, as provided by the MEL, including design redundancy and contingencies
- Achievement of TRL 6 for all instruments by PDR
- Contractor fee was included in selected elements consistent with project parametric estimate; fee was not applied to:
 - WBS 1–4, project management, systems engineering, S&MA, science and technology
 - WBS 5.07, 5.09.08, 5.09.09, and 5.9.10, Instruments
 - WBS 5.05 and 5.12, Telescope Calibration
 - WBS 7 and 9, Operations
 - WBS 8, Launch Vehicle Services
 - WBS 11, Public Outreach
- The total cost estimate was apportioned among project phases, as follows:
 - Pre-Phase A costs were not included in the estimate
 - Phase A: estimated as 5% of the total phase B–D cost
 - Phase B–D: parametric models and select throughput values
 - Phase E: parametric model based on 5-year operating life
- Flight software was estimated by PCEC from engineering data proposing 140 Kilo Source Lines of Code (KSLOC) with 60% reused, adjusted to 96.845 Equivalent Source Lines of Code (ESLOC)
- Throughput estimate values were the derived from the project-provided Grassroots estimate for:
 - WBS 5.5, XRT Calibration
 - WBS 5.12, *Lynx* Calibration Facility Modernization
 - WBS 8.0, Launch Vehicle

As a first step in evaluating the estimate credibility, both the project parametric cost estimate and the non-advocate ICE were evaluated against the MCR CATE estimate range, e.g., at the low to high boundaries before assignment of cost reserve and confidence assessment. At level 2 of the WBS, values were noted to be “within family.”

Crosschecks were made for validation at lower WBS levels using more than one cost method (model, throughput or an analogue source) and at higher WBS levels, comparing cost and schedule with *Chandra* and other relevant projects.

Schedule Analysis—MCR analyzed the *Lynx* project schedule (§8.4) using a Monte Carlo schedule risk assessment. The project schedule was based on an analogy to *Chandra*, other-project actual cost experience, and MSFC policy. It was supplemented with historical schedule estimates (in months) derived from credible other scientific projects. These detailed schedule estimates at lower-level WBS elements are consistent with an optimized project execution schedule and fit into the generally-accepted time-cost trade curve [625] shown in Figure 8.6, where dollars and months are optimized during project planning. Project execution uncertainty incorporates variations in time and cost from the fundamental plan resulting in explainable variances. All *Lynx* cost/time solutions fall within expected limits.

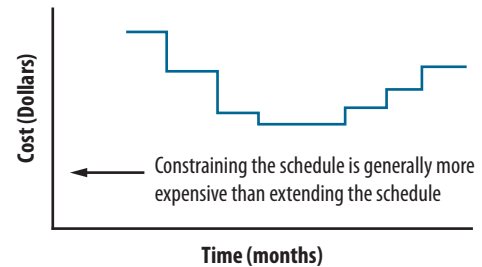


Figure 8.6. Bathtub concept illustrating juxtaposition of optimum cost/time solutions and changes when there is schedule acceleration or delay. This is a nominal-shaped bathtub curve generated by a commercial cost model illustrating cost sensitivity to schedule.

MCR determined that the project schedule demonstrates an estimate confidence greater than 50% for launch readiness based on a task duration range of –5% to +20% for all tasks both with and without planned schedule margin.

The analysis indicates that the current plan with the programmed schedule margin and schedule visibility tasks has a high confidence of meeting launch vehicle integration. While the plan as configured consumes some of the planned schedule margin, it provides adequate reserves accounting for the “unknown-unknown” risks, resulting in a high confidence credible plan.

Uncertainty Analysis—An important purpose of cost and schedule risk is to determine the total likely project cost and reserves that will assure an adequate budget and funding confidence level for successful project execution of *Lynx*. As with the non-advocate ICE, several models with different correlation factors were applied for sub-elements to establish reserve amounts:

- **PCEC:** elements modeled using an assumed triangular risk distribution; mode uncertainty calculated using prediction intervals. The estimate intervals were established by the MEL parameters and TRL analysis as:
 - Lower (L) bound: design weights without contingency
 - Most Likely (L) value: design weights with contingency
 - Higher (H) bound: design weights with contingency plus TRL adjustment to development cost

- **SEER-H[®]**: elements modeled using an assumed triangular risk distribution; mode uncertainty calculated using prediction intervals. The model provided output values for the lower, most likely, and high bounds of the estimate.
- **NICM**: used to crosscheck the instruments and validate “in family” only. Due to the limited number of X-ray instrument data points, spectrometers and particle instruments were used as analogies.
- **@Risk[®]**: lower-level uncertainties combined to determine the top-level correction.

A primary consideration in calculating cost and schedule risk was the project requirement of starting development at low TRLs and assuming a cost and schedule to achieve TRL 5 at the start of Phase A and TRL 6 by PDR. Adjustments to PCEC and SEER-H[®] non-recurring cost estimates were based on MCR’s NASA database of TRL development cost factors, as discussed above.

Other risk considerations included flight software development and instrument development. Operational risks (failure on-orbit) were not considered in this estimate.

The resulting analysis yielded a cost range of \$4.8B at 40% CL to \$5.1B at 70% CL in \$FY20, and \$5.7B at a 40% CL to \$6.1B at a 70% CL in \$RY.

8.5.3.5 In-Family Comparisons

The overall *Lynx* mission parametric cost model is modular and built with multiple, detailed subsystem cost models used for individual elements, as described above. Use of multiple cost models provides validation of the individual subsystem estimates, and thus veracity of the overall mission estimates. The modularity of the mission cost estimate lends itself to further validation with element-level, in-family comparisons to similar elements on historical missions. There is general scarcity of available, comparable, X-ray mission-level cost data that allows for in-family comparisons; however, data exists for comparisons of the LMA (Figure 8.7), HDXI and XGD assembly (Figure 8.8), and spacecraft (Figure 8.9). The *Lynx Cost Book* includes these comparisons with actual costs.

Validation missions used to compare the LMA to historical X-ray telescope optical assemblies was selected from X-ray telescope missions with available cost and technical data. Foreign missions were excluded due to data unavailability.

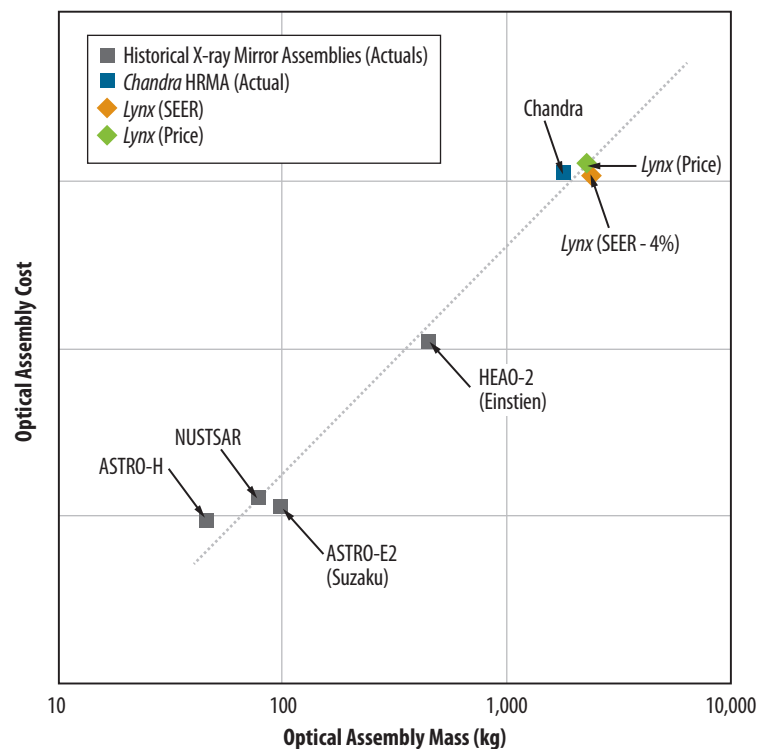


Figure 8.7. LMA in-family comparison to historical, U.S.-developed X-ray telescope optical assemblies.

Historical cost data for the in-family comparison of the HDXI and XGD assembly was selected from spectrometer instruments with total B–D cost data in NICM, excluding spectrometers, spectrographs, photometers, and radiometers designed for wavelengths longer than infrared.

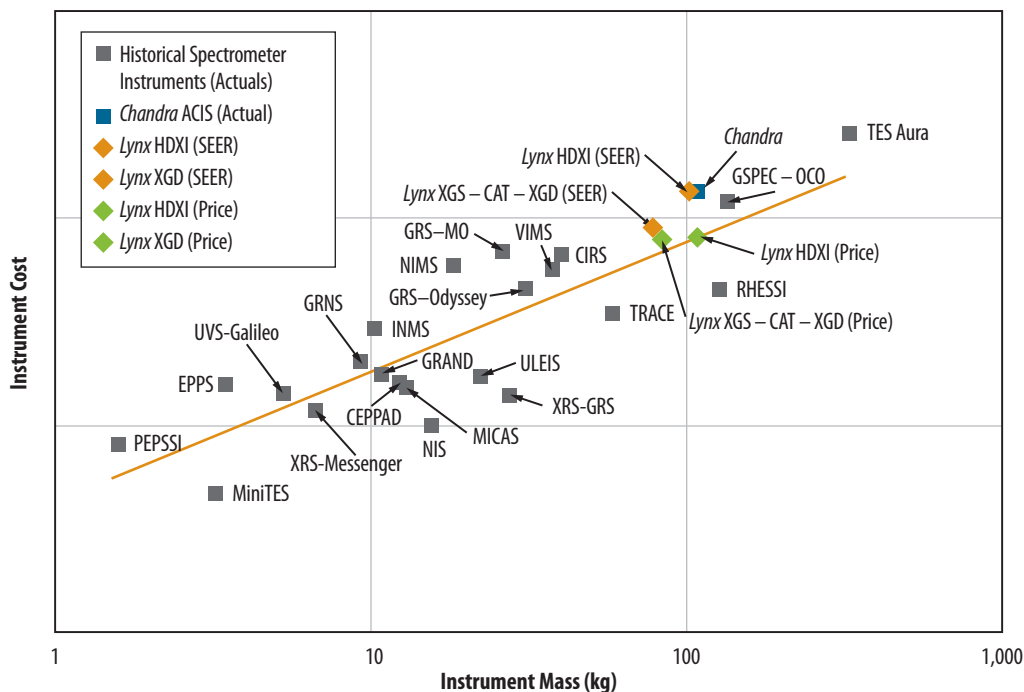


Figure 8.8. HDXI and XGD assembly in-family comparison to comparable spectrometer instruments.

Historical cost data for in-family comparison of the *Lynx* spacecraft element was selected from similar unmanned NASA missions with available cost data.

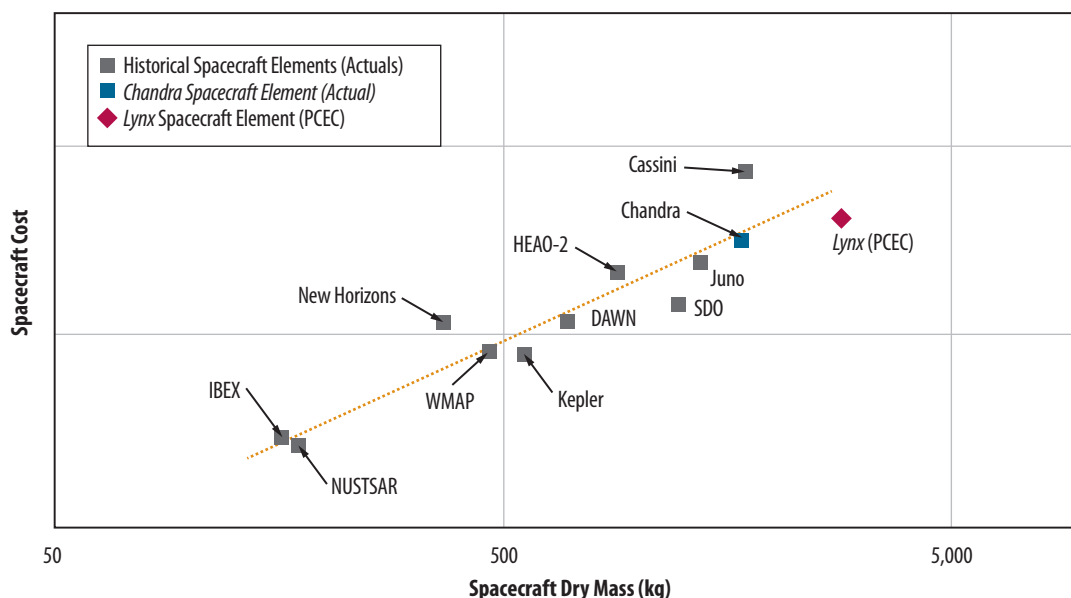


Figure 8.9. *Lynx* spacecraft element in-family comparison to comparable NASA project spacecraft.

The *Lynx* parametric estimate was developed with a thorough understanding of the Observatory architecture, design considerations and programmatic construct. Multiple, detailed cost models were developed for the primary elements of the telescope and spacecraft, with special attention on the development of the cost models for the X-ray mirrors and instruments given the absence of comparable X-ray technologies and missions in available cost data sets. These models were used to estimate the overall *Lynx* mission cost. Several validation analyses were undertaken by the *Lynx* team to provide credibility of the parametric mission estimate. These included a comparison to escalated (\$FY20) *Chandra* actual costs, development of an independently conducted grassroots estimate, an independent non-advocate ICE with uncertainty analysis, and an independently conducted, contracted CATE with ICE and uncertainty analysis. As summarized in Table 8.13, the *Lynx* mission parametric estimate was within a –11% to +28% range of the validation results, and the 40% CL on the cost curves developed as part of the non-advocate ICE and CATE were consistent to within 1% of the *Lynx* mission cost, all resulting in a thoroughly and credibly-costed mission for pre-Phase A formulation.

Table 8.13. Comparison summary of cost validation results to parametric estimate.

Validation Cost Estimate	Delta from Mission Parametric Estimate (%)
<i>Chandra</i> comparison	–11%
Independent CATE (40% CL)	0%
Non-adv. cost analysis (40% CL)	+1%
Grassroots	+4%
Independent CATE (70% CL)	+5%
Non-adv. cost analysis (70% CL)	+28%

8.5.4 Cost Contributions

The *Lynx* team welcomes international participation in the *Lynx* project. Potential areas of contribution could include instruments, building on existing collaborations related to *Athena* and others that offer a distinct contribution to the spacecraft, and calibration support. Specific cost contributions will be sought out and defined more formally during pre-Phase A.



LYNX CONFIGURATION STUDIES

9 Lynx Observatory Configuration Trade Space

The *Lynx* Design Reference Mission Observatory configuration is designed to provide the maximum science-per-dollar. To confirm this, the *Lynx* team conducted a high-level trade study of multiple Observatory configurations. Smaller configurations do not lead to significant cost reductions and result in substantial science losses. Larger configurations have increased capability but are sub-optimal in the science-per-dollar sense.

The nature of the *Lynx* Observatory trade space is multifaceted because it is designed to carry out a broad, Great Observatory-class science program. The *Lynx* team considered multiple configurations to assess the Observatory science capability as a function of cost. This analysis shows that the *Lynx* Design Reference Mission (DRM) is the optimal configuration in terms of science-per-dollar, while fully achieving the identified mission objectives (§6.1.1).

9.1. Trade Configurations

Sampling the broad *Lynx* trade space required a detailed design and costing for two designs that acted as anchor points for this trade. Significant effort was spent detailing all aspects of the DRM (§6) and a second, less capable configuration, dubbed the “1.3-m² Configuration” (which is its mirror effective area at 1 keV). This reduced configuration also has a less capable *Lynx* X-ray Microcalorimeter (LXM) and reduced X-ray Grating Spectrometer (XGS) effective area. The design and cost analyses for this 1.3-m² Configuration are presented in §10. The costs for all other configurations listed in Table 9.1 were obtained by taking appropriate deltas and scaling from the two anchor points.

The Observatory configurations that were considered included combinations of reduced *Lynx* Mirror Assembly (LMA) effective area at 1 keV, while preserving the shape of the effective area curve across the bandpass, and science instrument capability. In all cases, the High Definition X-ray Imager (HDXI), matching the angular resolution and field of view (FOV) provided by the *Lynx* mirrors, was considered essential. However the *Lynx* team considered reductions in capability for XGS and LXM, as well as complete removal. The *Lynx* team also considered a poorer angular resolution of 2 arcseconds (compared to 0.5 arcsecond for the DRM).

Table 9.1. The *Lynx* team studied a variety of configurations. The two anchor points are called out in the table. The 1.3m² Configuration should not be considered a preferred option to the DRM, as it is merely an anchoring point to provide reference for the multiple configurations that were considered. Checkmarks indicate the configurations studied. Bold checkmarks indicate the two “anchor point” configurations with full mission design and cost analyses.

Effective Area (Diameter and Focal Length)	Instrument Configuration				
	Nominal LXM and HDXI, scaled XGS	Nominal HDXI, reduced LXM, scaled XGS	Nominal HDXI and LXM, no XGS	Nominal HDXI, scaled XGS, no LXM	Nominal HDXI, no LXM and no XGS (imaging only)
2.1 m ² [d=3 m, f=10 m]	✓ – DRM		✓	✓	✓
1.3 m ² [d=2.3 m, f=10 m]		✓ – 1.3-m ² Configuration	✓	✓	✓
0.8 m ² [d=1.8 m, f=10 m]	✓		✓	✓	✓
3.0 m ² [d=3.6 m, f=12 m]	✓				
4.1 m ² [d=4.2 m, f=14 m]	✓				
2.1 m ² , 2 arcsecs PSF	✓				

The configurations with a reduced mirror effective were assessed by removing both outer and inner meta-shells from the DRM LMA design while maintaining a focal length of 10 m. A shorter focal length results in unacceptable reductions of the effective area above ~ 4 keV, and so these options are not viable. For configurations with larger effective area, a simplified approach was applied to the optical design. The DRM optical design already populates the input telescope aperture with nearly maximally packed mirror segments. Therefore, any substantial increase of the effective area must come from increasing the diameter of the mirror system. In addition, for the DRM design, the grazing angle for the outer mirror shells is close to the maximum for reflecting 1 keV photons. Therefore, any increase of the telescope diameter must be accompanied by a corresponding increase of the focal length. A transformation of the LMA along these lines, maintaining a uniform increase of the effective area across the band, results in the number of mirror segments and assembly mass scaling as $\sim D^2$. Scalings informed by the *Lynx* parametric cost model and historical trends were applied to estimate the cost for these larger configurations (§9.3.2).

9.2. Impact on Science

The science capability loss and gain is assessed via the estimated effect of the Observatory configuration changes on the notional observing plan (§5, Table 5.1) for the science pillars. The notional *Lynx* observing plan is a diverse collection of generally multi-object and multi-purpose programs, and it serves as a fair representation of the community-driven science program for *Lynx* in the 2030s. This approach allows science “scores” to be assigned for each element of the program, followed by estimates of how the science value of that element scales with available exposure time.

The process of assigning scores requires an assessment of the relative importance of the science that *Lynx* will be able to do in addition to its pillars — the “Observatory/Discovery” portion of the program. Examples of such science are given in §4. More importantly, *Lynx* must provide opportunities for observations that address today’s “unknown unknowns” — questions as of yet unasked. The ensemble of *Lynx* observations, as well as the discoveries across astrophysics, will drive these questions. As such, equal total weights, $w = 0.5$, were assigned by the *Lynx* team for both the Pillars and the Observatory/Discovery portions of the program.

History shows that for major astrophysical missions such as *Hubble*, *Chandra*, *Spitzer*, and *Compton*, unanticipated discoveries are at least as important as the execution of their original science goals. This study accounts for this by assigning equal weight to both the *Lynx* science pillars and the Observatory/Discovery portions of the program.

Next, the science of the three pillars was separated into sub-themes, followed by programs, and then, within some of the science programs, into specific classes of observations. A uniform division of the science scores was used at each level of this hierarchy. More specifically, each pillar was assigned a weight of $w = 0.5/3 = 0.167$, the three sub-themes of the second pillar were assigned $w = 0.167/3 = 0.0556$ and so on down to the lowest level of single-type observations, typically performed with a single science instrument. This hierarchy and the scores are documented in Table 9.2.

The scores assigned to individual programs enable an estimate of the science impact of removing science instruments from the Observatory, because some of the programs become completely unfeasible in this case. For these configuration changes, those programs’ science scores were removed from the overall total. For completeness, the impact of removing the instruments was also estimated for the Observatory/Discovery portion of the program. This was done under the assumption that the pillars portion of the program is a fair representation of the mix of target types, instrument choices, and observation modes for the Observatory/Discovery portion. Several methods (such as using each instrument’s total exposure time, the number of targets, computing the fractional exposure time, aggregated science score) lead to a similar conclusion: the HDXI, LXM, and XGS instruments will contribute approximately 30%, 50%, and 20% to the Observatory/Discovery program, respectively. These percentages are consistent with the *Lynx* team assessment of historical trends of imaging versus spectroscopic observations on major NASA missions and provide a reasonable initial assumption.

Table 9.2. *Lynx* notional observing plan with weights.

Science Theme	Weight	Sub-theme	Program	Weight	Typical Observations	Weight	Instrument	Science with 30% less area	Science with 50% less area
The Dawn of Black Holes	0.167	Black hole dawn	1.1 Origin of supermassive black holes seeds*	0.083	Surveys over 1 deg ² to depth $fx = 1.6^{-19}$ [0.5–2 keV] plus a deeper survey over 400 arcmin ² to $fx = 7\text{--}20$ erg/s/cm ²	0.083	HDXI	0.700	0.500
		From dawn to noon	1.2 Growth of supermassive black holes from cosmic dawn through cosmic noon to the present, relations between AGN and environments, triggering and quenching AGNs, relationship to star formation activity	0.083	Survey down to $fx = 2^{-18}$ over up to 2 deg ²		HDXI	0.850	0.700
The Invisible Drivers of Galaxy and Structure Formation	0.167	State of diffuse baryons $z = 0$	2.1 State of diffuse baryons in galactic halos—direct imaging*	0.028	Survey of ~15 low-redshift isolated (spiral galaxies), pushing 10% thermodynamic (gas density) measurements to 0.5 r500 for $M \sim 3^{12}$ and to r200 for $M \sim 1^{13}$	0.028	HDXI	0.850	0.700
			2.2 State of diffuse baryons in galactic halos—absorption line spectroscopy*	0.028	Observe ~80 AGN sightlines ($fagn \sim 1^{-11}$) to detect ~60 absorption line systems in the foreground galaxy halos, detection limits for absorption lines are EW ~3 mÅ and down to 1 mÅ for $r > r200$, same Milky Way Halo	0.028	XGS	0.700	0.500
		High- z probes	2.3 State of gas and feedback measurements in high-redshift galaxy clusters and groups	0.028	Gas temperature, density, and metallicity profiles in ~30 clusters and groups at $z > 2$, 6 Msec LXM observations	0.028	LXM/main array	0.850	0.700
			2.4 Characterization of the first galaxy groups at $z = 3\text{--}4$	0.028	HDXI observations of ~10 high- z galaxy groups	0.028	HDXI	0.850	0.700
		Feedback	2.5 Spectroscopic survey of AGN to determine energetics of the AGN feedback	0.011	Soft-band spectroscopy with $R > 1,000$ down to 0.2 keV to measure density-sensitive spectral features, 3 Msec XGS, LSM / ultra-high resolution array	0.011	XGS, LXM/ultra-high resolution subarray	0.850	0.700
			2.6 Characterize the supply side of AGN energy feedback	0.011	Measure thermodynamic state of diffuse gas near the Bondi radius of SMBHs in nearby elliptical galaxies	0.011	LXM/enhanced spatial resolution subarray	0.850	0.700
			2.7 Measure the energetics and effects of AGN feedback on galactic scales*	0.011	Observe AGN-inflated bubbles in the ISM of low-redshift elliptical galaxies	0.006	LXM/enhanced spatial resolution subarray	0.850	0.700
					Spectro-imaging of extended narrow emission line in nearby spiral galaxies	0.006	LXM/enhanced spatial resolution subarray	0.850	0.700
			2.8 Understand the energetics and mechanics of the supernovae-driven galactic winds*	0.011	Observe galaxy winds in ~20 objects, with the ability to characterize velocities <100 km/s on arcsec scales, 2.5 Msec LSM / ultra-high spectral resolution array	0.011	LXM/enhanced spatial resolution subarray	0.700	0.500
			2.9 Galaxy cluster-scale feedback	0.011	LXM observations of nearby galaxy clusters to constrain plasma physics effects in the cluster cores	0.011	LXM/main array	0.850	0.700
The Energetic Side of Stellar Evolution and Stellar Ecosystems	0.167	3.1 Stellar coronal physics, impact of stellar activity on planet habitability, accretion on young stars		0.042 c	Spectroscopic survey of 80 stars within 10 p	0.021	XGS	0.875	0.650
					Transit spectroscopy of planets around dwarf stars down to super-earth regime	0.021	XGS, LXM/ultra-high resolution subarray	0.875	0.700
		3.2 Young forming regions		0.042	Surveys to detect entire mass distribution of stars in active star forming regions to $d = 5$ kpc			0.870	0.700
		3.3 Endpoints of stellar evolution: SNRs*		0.042	Targeted observations of the youngest SNRs in the Milky Way, up to ~50 objects	0.021	LXM/main array	0.800	0.750
					Statistics and typing of SNRs in different environments in nearby galaxies	0.021	LXM/main array	0.700	0.500
		3.4 Endpoints of stellar evolution: X-ray binary populations		0.042	Survey of X-ray binary populations and ISM in nearby galaxies 2 Msec LXM		HDXI, LXM	0.850	0.700
Observatory/Discovery Program	0.500					0.500	50% LXM, 30% HDXI, 20% XGS	0.840	0.700

For simplicity, the assumption was that the science capability loss associated with removing science instruments could not be recouped by added exposure time for the remaining instruments. Moreover, the team verified that even with reasonable prescriptions for a redistribution, the DRM configuration still clearly yields the greatest ratio of science to cost (Table 9.3).

Table 9.3. Relative science capability and cost of different mission configurations.

Configuration description	Capability	Relative cost	Science/\$
DRM	1.00	1.00	1.00
DRM, no LXM	0.60	0.87	0.69
DRM, no XGS	0.84	0.94	0.90
DRM, imaging only	0.43	0.80	0.54
1.3 m ² effective area	0.77	0.95	0.81
1.3 m ² , imaging Only	0.34	0.75	0.45
1.3 m ² - no XGS	0.63	0.88	0.71
1.3 m ² - no LXM	0.46	0.81	0.57
4.2 m mirror diameter	1.36	1.48	0.92
3.6 m mirror diameter	1.18	1.24	0.95
2 arcsec angular resolution	0.20	0.97	0.21
0.8 m ² effective area	0.50	0.92	0.55
0.8 m ² , no XGS	0.41	0.85	0.48
0.8 m ² , no LXM	0.29	0.78	0.37
0.8 m, imaging only	0.21	0.66	0.32

Changes in the mirror effective area for most of the *Lynx* programs are equivalent to changes in the exposure time, with decreased area equating to decreased exposure time. For relatively small changes, the science value of individual programs changes approximately as the inverse of statistical uncertainties, effectively scaling as $\sim A^{0.5}$ as the mirror area decreases. This trend continues to $\sim 50\%$ of the nominal area, at which point a big loss of value occurs in the sense that the program can no longer address the corresponding pillar goals. The $A^{0.5}$ trend is not universal, however. For deep surveys of high- z Supermassive Black Hole (SMBH) seeds, absorption line spectroscopy of the Circumgalactic Medium (CGM), measurements of galaxy wind feedback, Supernova Remnant (SNR) observations, and spectroscopic survey of stars, the goals are centered around covering a maximally wide parameter space or observing diversity of properties in a large sample of objects, resulting in a $\sim A$ trend. The science value of the Observatory/Discovery portion is assumed to scale as $A^{0.5}$, reflecting the predominant scaling in the pillars portion of the program. The t_{exp} scalings in the Table 9.2 for these programs reflect the assessment of the science value changes in these situations.

9.2.1. Science Threshold

Throughout this trade study, it was critical to identify the crucial observational capabilities necessary to accomplish the science pillars, maintain ample time for Observatory/Discovery program, and avoid compromising the ability to transform astrophysics in the 2030s and beyond. Because of the complex nature of this task, the *Lynx* team undertook several approaches. The *Lynx* team wanted to be as objective as possible while recognizing that assigning simple numerical scores or rankings might not be adequate for this task.

The science capability threshold is defined as the point at which *Lynx* would lose its ability to execute one or more of its science pillars or to carry out Observatory/Discovery science. These scenarios were deemed unacceptable for a Flagship-class mission for the 2030s. However, configurations both above and below this threshold were considered to allow for a better understanding of how the costs scaled with mission capability.

Maintaining a posture that is appropriate for a Flagship mission and above an acceptable science threshold requires three essential *Lynx* capabilities: (1) large effective area, (2) high-spectral resolution over the entire bandpass, and (3) high-spatial resolution over a large field of view.

Reductions in the mirror effective area larger than 50% of the DRM configuration would result in a configuration below the science threshold. Similarly, the loss of either the LXM or XGS would place the mission below the science threshold. In reviewing the configurations that remove one or both of these instruments, the result is that the amount of science lost per dollar saved does not support removing either instrument.

In addition to maintaining the DRM science instruments, preserving the high-angular resolution is central for the execution of the *Lynx* science and is essential for a 2030s observatory-class X-ray mission. One of the configurations in the trade space (2-arcsecond angular resolution) formally demonstrated the devastating impact of such angular resolution degradation on the *Lynx* science. For this configuration, the notional observing plan was reviewed and programs that could still be carried out with a 2-arcsecond Point Spread Function (PSF) were identified. Primarily, these programs are a subset of the grating spectroscopy programs that do not require high spatial resolution. The total weight of these programs is only 0.2. None of the science pillars can be executed at this level of spatial resolution, although there are still interesting options in the Observatory/Discovery portion of the program. The overall assessment was that a 2-arcsecond configuration is well below the science threshold for a flagship mission.

9.3. Cost Changes

9.3.1. Summary of the 1.3-m² Configuration Costs

Compared to the DRM, the 1.3-m² configuration features a smaller diameter mirror assembly that is accommodated by a smaller-diameter spacecraft and Optical Bench Assembly (OBA) (\$10.1.5). With this configuration, the *Lynx* team explored the cost impact of small changes in the instrument design, such as reducing the LXM FOV from the DRM 5 arcminutes down to 4 arcminutes. This smaller diameter mirror assembly also resulted in a reduced X-ray Grating Array (XGA) effective area (and physical diameter).

The cost changes associated with minimal changes in the science instrument configurations are small (\$10.4.3). There is a small reduction of cost in the spacecraft, mostly due to a mass reduction in the primary structures. The cost of the OBA is reduced due to the smaller diameter; however, the mass reduction is small since the thickness of the OBA had to be increased to accommodate the new observatory center of gravity (\$10.2.2). However, these savings are almost entirely offset by the introduction of an additional launch adaptor required to mate this reduced diameter to the standard ~5-m fairing. The total cost of the spacecraft and the OBA for the 1.3-m² configuration is within 1% of that for the DRM. The smaller mirror effective area results in a 19% reduction of the mirror assembly cost, and it is this component that drives a 5% reduction of the estimated mission cost compared to the DRM.

The fact that a 38% reduction in the mirror effective area only results in a 19% reduction of the mirror assembly cost reflects the modular design of the LMA, its highly parallelize-able assembly process, and the mass-production nature of manufacturing and assembling the required number of mirror segments (\$8.5.2.1).

9.3.2. Mirror Cost Scaling

The key point for comparing the cost estimates for the different mirror assembly configurations is that they have nearly-identical upfront costs associated with technology development, manufacturing readiness, and in the design and engineering of the mirror structure and related subsystems (e.g., thermal). Each configuration requires nearly identical numbers of mirror prototypes, and therefore has the same cost for prototype production and testing. The main difference between configurations is the number of mirror segments and mirror modules produced and assembled into meta-shells. These differences play a role only during the mass-production phase, and therefore the cost reduction is modest.

In the *Lynx* parametric cost models, a “learning curve” setting is used to represent the acquired experience and hence reduced costs of the module production as multiple modules and meta-shells are built (\$8.5.2). Moreover, historical data on the X-ray mirror costs are used to estimate the impact of the learning curve and mass production. The X-ray mirrors for the *NuSTAR* and *SRG-ARTX-C* telescopes are good examples. In both cases, the mirror systems consisted of multiple modules, and a large number of reflecting elements within each module. In these cases, the average cost of the subsequent modules was 11% of that of the first module produced. For *Chandra*, where the mirror manufacturing process was not set up for mass production, the cost of the first set of mirrors was ~2× that of each of the three subsequent sets (\$8.5.3.1).

The parametric model cost difference for the *Lynx* DRM and 1.3-m² configurations is captured by a model that assumes that the cost of the first produced meta-shell is more than the cost of the subsequent meta-shells due to the applied learning curve (§8.5.2.1). The percentage difference in cost for producing subsequent meta-shells is ~10% of the cost of the first meta-shell. This scaling is consistent with historical X-ray mirror manufacturing experience and is used to estimate the mirror costs for the larger and smaller effective area configurations. The results are summarized in Table 9.4.

Table 9.4. Summary of mirror configurations assessed for *Lynx* and their scaled cost compared to the DRM.

Mirror Assembly Diameter (Configuration)	Configuration				
	1.8-m (0.8-m ²)	2.3-m (1.3-m ²)	3.0-m (DRM – 2.1-m ²)	3.6-m (3.0-m ²)	4.2-m (4.1-m ²)
Number of meta-shells	5	7	12	17	24
Relative parametric model cost	—	0.81	1.0	—	—
Relative cost from simple scaling	0.67	0.76	1.0	1.26	1.55

Impact of the coarser angular resolution on cost — The potential cost reductions associated with a coarser angular resolution (2 arcsecond) are assessed and the manufacturing process envisioned for the Silicon Meta-shell Optics technology has been reviewed (§7). No steps in the fabrication, alignment, and mounting process were identified that could be eliminated or significantly shortened because of more relaxed angular resolution requirements. Potential savings might appear during the technology development phase, if the required TRL levels are reached faster because of more relaxed requirements. Coarser spatial resolution allows one to use a larger pixel size in the HDXI detector, which can also accelerate the pace of its technology development, but will only modestly reduce the cost of the flight unit. XGS and LXM technology development costs would not be impacted, though there would be an impact to the science (i.e., resolving power and spatial resolution, respectively). To be conservative in the mission configuration tradeoff analysis, the cost reduction for a 2-arcsecond configuration was assumed to be \$100M.

9.3.3. Instrument Suite Costs

The costs reductions associated with changes in the science instrument suite were estimated for the DRM configuration by using the parametric estimates for the costs of the instrument plus the cost of any components uniquely associated with that instrument, such as mechanisms. Relevant spacecraft systems, such as power and thermal, were also appropriately scaled. As a result, the cost reductions associated with removing the LXM instrument include the ISIM translation mechanism and substantially reduced power and a simplified thermal system. The costs of the XGS instrument include the XGA insertion mechanisms and a reduced footprint of the ISIM. Table 9.5 shows the costs reductions associated with three possible instrument suite changes, as a percentage of the total DRM cost estimate.

Table 9.5. Potential cost savings from *Lynx* instrument changes.

	No LXM	No XGS	No LXM and XGS (HDXI only)
Cost Reduction	–13.3%	–6.5%	–19.9%

Identical absolute cost reductions for instrument removals were applied to smaller and larger mission configurations, which is a sufficient assumption for the purposes of this analysis.

9.3.4. Larger Mission Cost Scaling

Configurations larger than the DRM were assessed by assuming that all cost growth is associated with the increased diameter and focal length of the X-ray mirror modules and of the spacecraft and OBA. The cost of the science instruments is assumed to not change, even though, in reality, these costs would increase because physically larger detector planes would be needed to cover the same area on the sky and larger grating arrays would be required to cover the same fraction of the input aperture. Higher costs of science instruments for configurations larger than the DRM only strengthen the conclusions regarding these options.

The mirror cost scaling is shown in Table 9.4. The mass of the mirror and the OBA increase as the diameter times the focal length or by D^2 . The larger configurations also require a larger diameter spacecraft. The spacecraft and OBA masses increase approximately in proportion to the mass of the mirror assembly. The associated cost growth is $\sim \text{mass}^{1.1}$ as established by historical data on the costs of NASA science mission spacecraft (§8.5.3.5, Figure 8.8). This simple scaling captures the increased demands on the spacecraft structures, power and thermal systems, larger solar pressure torque and moments of inertia, larger Δv for station keeping, etc. It is recognized that this scaling is approximate, but the largest configuration considered is only 40% larger than the DRM. Therefore, the accuracy should be sufficient for this high-level study.

Observatory configurations larger than the *Lynx* DRM cannot fit into heavy-class launch vehicles fairings and exceed their maximum payload mass capacity. Therefore, these configurations would require super-heavy class launch vehicles such as the SLS. The NASA Launch Services Program (LSP) guidance available at the time of this study recommends a cost delta of +\$100M associated with the super-heavy class launchers. A higher cost difference would only strengthen the conclusions provided here. Note that the 0.8-m² configuration may be launched with a medium-class launch vehicle, so the corresponding cost reductions were assumed. Again, if such configurations required a heavy-class launcher, this would only further increase the cost.

9.4. Results

The Observatory configuration “science-per-dollar” is the primary metric for assessing the optimized configuration for *Lynx*. Figure 9.1 plots the relative science capability per unit cost (or “science-per-dollar”) versus the relative science capability, normalized to 1.0 for the DRM on both axes and provided in Table 9.3. Larger circles show the two anchor points in the trade space with full mission design and cost analyses. Open circles show those configurations where scaling was used for the cost of the mirror and spacecraft to extrapolate beyond the range covered by the anchor points.

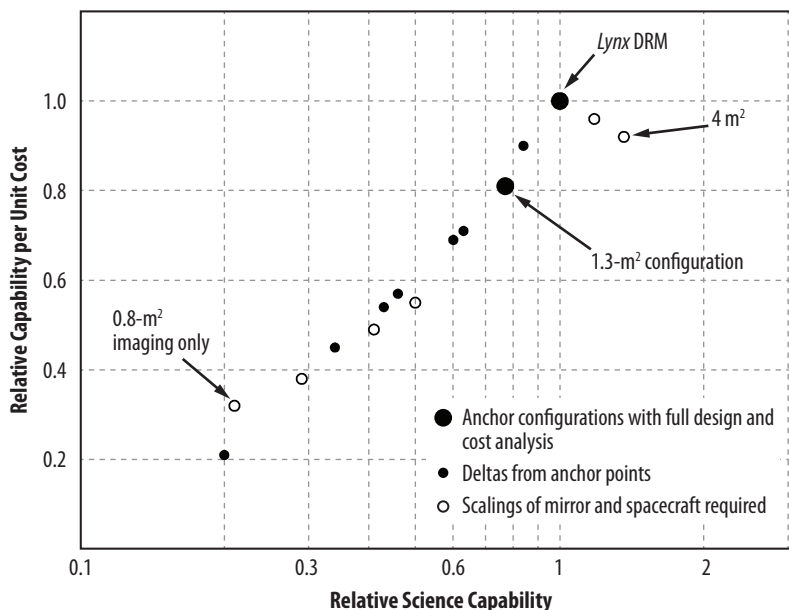


Figure 9.1. *Lynx* Observatory configurations trade, illustrating the optimal *Lynx* DRM configuration providing the maximum “science per dollar”.

The DRM configuration is optimal and maximizes the “science-per-dollar.” Approaching the DRM from the less capable missions on its left, the mission cost grows slowly for increasingly more capable configurations. The primary reason for the relatively slow cost growth in this regime is efficient amortization of upfront costs associated with the development of the 0.5-arcsecond-capable Observatory (telescope and spacecraft) and upfront costs related to production of the first sets of X-ray optics. The mass-production nature of the X-ray mirror manufacturing results in a slow increase of the mirror cost with assembly diameter. These two factors led to a significant increase in science capability-per-dollar shown by the rather steep slope approaching the DRM.

The larger configurations must endure increased spacecraft costs related to the increased mirror assembly diameter and focal length. There is an added cost associated with the need for a more capable launch vehicle; and there is a slower growth in science capabilities. To fully capitalize on the extra effective area for the larger configurations, *Lynx* would need angular resolution better than 0.5 arcsecond, with the next natural science break point estimated by the *Lynx* team to be at a PSF level of ~ 0.1 arcsecond HPD. An X-ray observatory with such angular resolution would be capable, e.g., of detecting individual X-ray binaries in the $z=10$ galaxies and resolving well inside the Bondi radius of supermassive black holes in nearby galaxies. However, achieving the 0.1-arcsecond PSF would require a new set of breakthroughs in both the X-ray mirror and detector technologies that go well beyond the expected state of the art for the next decade. The *Lynx* DRM, with its 0.5-arcsecond angular resolution, is already orders of magnitude more capable than any other X-ray telescope existing or planned, and is capable of executing the *Lynx* science pillars while providing significant time for an Observatory/Discovery science program.

A final comment is in order regarding mission configurations with effective area somewhat smaller than the 2.1-m^2 provided by the DRM. *Lynx* science can tolerate moderate reductions of this type. However, as argued above, substantial cost savings are not projected from reducing the mirror effective area. Instead, a possibility of meeting basic science requirements with a smaller mirror assembly should be viewed as an option to improve cost and schedule margin for manufacturing the LMA.

The Observatory configuration trade study shows that the *Lynx* DRM configuration maximizes the science-per-dollar metric. Smaller configurations lead to only modest cost reductions and result in increasingly larger and eventually unacceptable science losses. Larger configurations have increased capability but lack the higher angular resolution to maximize their science return. Their substantially higher cost and likely longer schedule are inconsistent with the NASA Astrophysics budget and the Decadal timeframe.

10 Lynx 1.3-M² Configuration

The 1.3-m² configuration detailed design, schedule, cost, and assessed science return provides a trade-space anchoring point used to confirm that the *Lynx* Design Reference Mission (DRM) provides an optimal architecture that maximizes the science return for the cost.

The Observatory configuration trade study described in §9 is strengthened by the detailed knowledge provided by the in-depth study of a reduced-capability configuration. The configuration studied has a mirror effective area of 1.3-m² at 1 keV, and reduced X-ray Grating Spectrometer (XGS) and *Lynx* X-ray Microcalorimeter (LXM) capabilities. This configuration was chosen as one of two anchor points (in addition to the DRM) in the configuration trade space.

The 1.3-m² configuration offers a significantly reduced mirror effective area at the expense of increasing the on-orbit time needed to achieve the science pillars to nearly the full 5-year mission lifetime. This configuration is just above the *Lynx* science threshold, which is defined as the point at which the program is no longer able to address the goals defined by the science pillars. Reductions in the mirror effective area larger than 50% of the DRM configuration result in a configuration that is below the science threshold. As mentioned in §9, the loss of any of the science instruments would place the mission below the science threshold.

The reduced effective area for this configuration is accomplished by reducing the number of meta-shells from 12 to 7, thereby reducing the grating array effective area and increasing the time needed for the highest resolution spectroscopy (the system angular resolution is not affected because the focal length is not diminished in this configuration). The High-Definition X-Ray Imager (HDXI) remains unchanged, as there were no credible cost savings in reducing the HDXI Field of View (FOV) or other HDXI science performance capabilities. Importantly, the requirements to maintain high-angular resolution across the 22 × 22 arcminute FOV were not relaxed, as this capability was deemed essential across nearly all *Lynx* science objectives. However, this configuration does have modest reductions in LXM Main Array (MA) FOV from 5 × 5 arcminutes to 4 × 4 arcminutes. This impacts the spatially resolved spectroscopy of the largest apparent-size objects such as nearby supernova remnants, clusters of galaxies, and diffuse or extended galactic sources.

The *Lynx* Mirror Assembly (LMA) effective area for this configuration is ~2/3 that of the DRM configuration. This decrease allows for a smaller diameter spacecraft bus and Optical Bench Assembly (OBA), but essentially leaves unchanged the Integrated Science Instrument Module (ISIM) (Figure 10.1). The focal length was not changed, resulting in a slightly larger depth-of-field and correspondingly relaxed

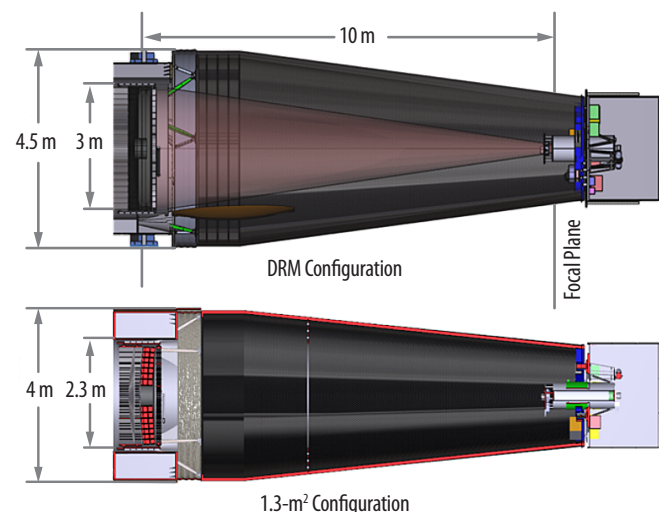


Figure 10.1. (Top) *Lynx* DRM observatory configuration and (Bottom) 1.3-m² configuration with critical dimensions shown.

focus and alignment tolerances. All DRM technologies (i.e., Silicon Meta-shell Optics, Hybrid Complementary Metal-Oxide Semiconductor (CMOS) HDXI, Critical-Angle Gratings (CAT-XGS), LXM relevant technologies) are also assumed for this configuration.

The prime goal for this choice was to provide a detailed analysis for a representative configuration significantly smaller than the DRM and to enable approximate analyses for even smaller configurations for the Observatory configuration trade study described in §9. A detailed design analysis was completed, and a project schedule and cost were generated for this configuration such that the science impact as a function of cost and risk could be assessed and compared directly to the DRM.

The primary characteristics of this configuration in comparison to the DRM are summarized in Table 10.1. Detailed analysis of every major subsystem for the 1.3-m² Configuration, summarized in the sections below, indicates minimal savings of mass and power, and ultimately of cost (§10.4.3). The amount of science lost due to reduced capability for this configuration is not offset by acceptable savings in cost, schedule, and risk as detailed in (§9.3.1, Figure 9.1).

10.1 Telescope Design Details Overview

The telescope elements (i.e., the LMA and science instruments) for the 1.3-m² Configuration in comparison to the DRM are discussed in the following sections. The impact to the science is discussed in §9.

10.1.1 Lynx Mirror Assembly — Reduced Effective Area

The reduced *Lynx* configuration has an effective area of 1.3-m² at 1 keV, decreased from 2.1-m² for the DRM Configuration by removing the outer three and inner two meta-shells. This roughly 1/3 reduction in the effective area of the DRM LMA is taken approximately uniformly across the full *Lynx* bandpass (Figure 10.2, Left). The resulting outer diameter of the 1.3-m² Configuration LMA is 2.3-m, compared to 3-m for the DRM (Figure 10.2, Right).

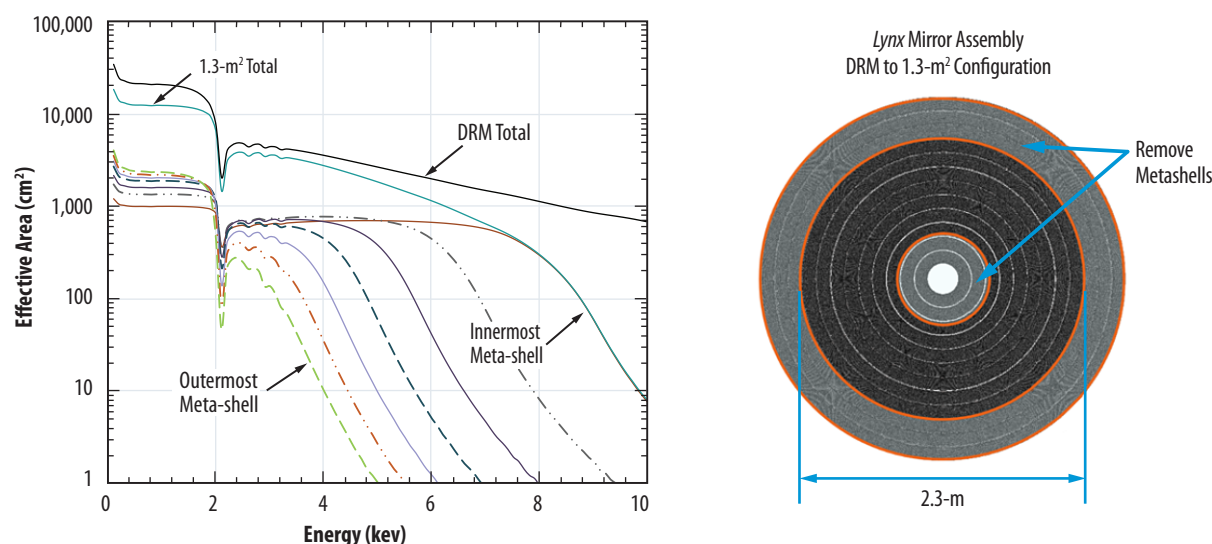


Figure 10.2. (Left) Plot of the LMA effective area for the 1.3-m² Configuration as a function of meta-shell, compared to the total LMA effective area for the DRM. (Right) The 1.3-m² Configuration (shown in dark gray) has five fewer meta-shells than the DRM does, resulting from removing the three outer and two inner DRM meta-shells.

From an Observatory architecture standpoint, this reduction in LMA size necessitates a smaller diameter spacecraft, contamination doors, sunshade, and OBA. The resulting mass savings is minimal, resulting in a mass savings of less than 10% (609 kg) over the DRM (Table 10.1).

Table 10.1. Requirements and *Lynx* Observatory total mass and power estimates based on detailed design and analysis of major observatory elements that include the payload and spacecraft systems.

Requirement	1.3-m ² Configuration	DRM
LMA Effective Area at 1 keV	1.3-m ²	2.1-m ²
XGA Effective Area	~3,000 cm ²	~4,400 cm ² (4,000 cm ² Required)
LXM Main Array FOV	4 × 4 arcminutes	5 × 5 arcminutes
Characteristic	1.3-m ² Configuration	DRM
Total Mass (with Margin)	7,103 kg	7,712 kg
Power (with Margin)		
Launch	720 W	743 W
Survival	2,552 W	2,552 W
Science Mode	7,356 W	7,420 W

10.1.2 High Definition X-ray Imager — No Reductions

A study was carried out by the *Lynx* team to determine a possible reduced configuration HDXI that fit within the context of this reduced-capability configuration. HDXI is described in detail in §6.3.2. Capabilities that were considered for reduction included lower readout rate, the use of fewer but larger sensors, reduced high-energy Quantum Efficiency (QE), reduced FOV, removal of the filter wheel assembly, elimination of windowing capability, and the use of larger pixels for reduced spatial resolution. The team concluded that there were no HDXI capability reductions that would result in an appreciable cost, schedule, or risk savings, and still be consistent with the *Lynx* science goals.

10.1.3 X-Ray Grating Spectrometer — Reduced Effective Area

The XGS consists of a retractable X-ray Grating Array (XGA) located immediately behind the LMA and an X-ray Grating Detector (XGD) assembly located on the ISIM (§6.3.3). The 1.3-m² Configuration has a smaller diameter XGA that is consistent with the reduced LMA effective area as shown in Figure 10.3, but requires that the Resolving Power, $R = 5,000$, remain unchanged. By keeping the focal length the same as that of the DRM, this is easily achieved.

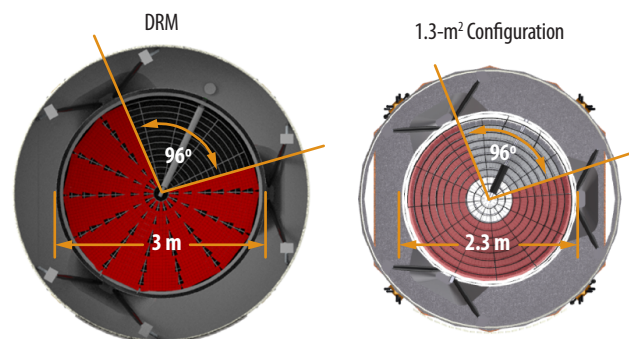


Figure 10.3. The XGA effective area was reduced by approximately the same amount as the LMA across the *Lynx* bandpass.

The XGA effective area was reduced by approximately the same amount as the LMA across the *Lynx* bandpass. This effective area is shown in Figure 10.4 and is compared to that of the DRM. Conservative estimates have been made for both cases.

As for the DRM, the 1.3-m² Configuration assumes that the HDXI technology will be used for the XGD. The length of the XGD assembly on the ISIM is driven by the longest wavelength photons (Figure 10.5) and on the required resolving power. Because the bandpass remains unchanged between configurations, the XGD 1.3-m² Configuration requires the same number of sensors as the DRM.

10.1.4 LXM—Reduced Field of View

The LXM DRM focal plane array consists of three different styles of pixels in three different arrays and are described in §6.3.4. For the 1.3-m² Configuration, the *Lynx* LXM team considered multiple reduction options that included eliminating either the Enhanced Main Array (EMA) or the Ultra-High Resolution Array (UHRA), switching from the baseline readout to a slightly more complex, but higher TRL readout multiplexing scheme, and reducing the FOV of the Main Array.

Extensive discussions within the *Lynx* team on the loss to the *Lynx* science goals related to the elimination of the EMA or UHRA concluded that these were not viable options, especially given the relatively minimal cost savings (§10.4.3) and development risk mitigation. To assess the cost of using the higher TRL readout electronics, a cost exercise was carried out at Goddard Space Flight Center (GSFC). The results indicated a higher cost for these electronics than what was baselined for the DRM, suggesting that the baselined electronics be selected for the 1.3-m² Configuration as well. Reducing the FOV of the MA is a viable and acceptable option, so the *Lynx* team assessed the trades associated with this reduction.

The MA for the DRM Configuration consists of 1-arcsecond pixels over a 5-arcminute FOV, with a 0.2 to 7-keV energy range. The 1.3-m² Configuration MA is designed to maintain the same pixel size and energy resolution as the DRM LXM, but with a reduced MA FOV of 4 arcminutes. The result is a small cost reduction in detector fabrication and readout electronics. The impact to the DRM cryo-cooler, one of the driving cost elements for the LXM, is small, as the reduction in heat load is minimal.

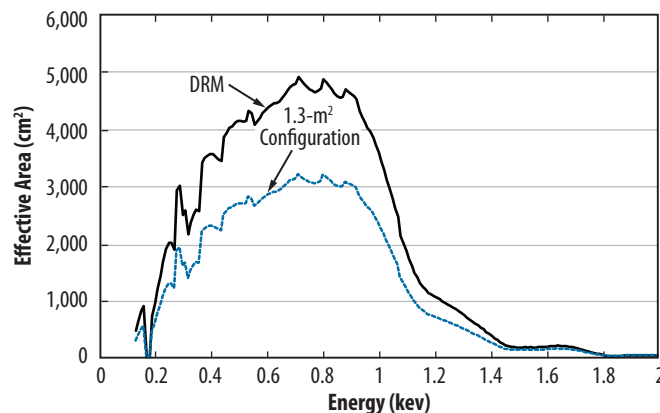


Figure 10.4. The DRM effective area is the black curve and the blue dashed curve is the 1.3-m² Configuration effective area. The analysis neglects drops at certain wavelengths due to XGD chip gaps.

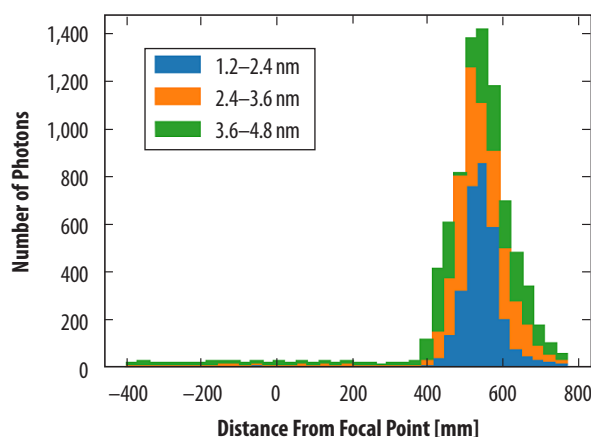


Figure 10.5. Number of photons as a function of the distance from the *Lynx* focal plane.

10.1.5 Optical Bench + Pointing Control and Aspect Determination

The primary impact to the OBA (§6.3.6) is that the 1.3- m^2 Configuration design has a smaller diameter that is consistent with the reduced LMA. Interfaces (use of bipods) between the LMA and the OBA, and between the OBA and the spacecraft, remain unchanged from the DRM.

Reducing the OBA diameter near the LMA requires the thickness of the optical bench to be increased over that of the DRM. Since the Observatory is launched inverted, with the ISIM at the top of the stack, the optical bench thickness had to be increased to meet the stiffness requirements for launch. This mass increase is reflected in the overall Observatory mass given in Table 10.1.

The Pointing Control and Aspect Determination (PCAD) system (also described in §6.3.6) for the 1.3- m^2 Configuration is the same as the DRM. Since the focal length did not change, the aspect system did not change between configurations.

10.2 Spacecraft Design Details

The 1.3- m^2 Configuration spacecraft elements were designed to accommodate the reduced LMA diameter. Changes from the DRM were primarily in the areas of mechanical, structural, thermal, and power. Most elements required no changes from that of the DRM design. Table 10.2 summarizes the impact to each spacecraft element. Detailed analyses are found in the *1.3- m^2 Configuration Supplemental Design Package*.

Only those elements that changed due to the reduced LMA are discussed below.

Table 10.2. Subsystem elements that were changed from that of the DRM are listed.

Subsystem	1.3- m^2 Configuration
Observatory Architecture	Smaller spacecraft diameter, OBA, LMA, XGA, and inclusion of payload adaptor
Structures	Increased OBA thickness
Avionics	Updated heater controllers for reduced LMA
Power and Thermal	Updated to include reduced heaters on the smaller LMA and XGA
Mechanisms	No Change
Environments	No Change
GN&C	No Change
Propulsion	No change
Dynamics	No analysis – Forward Work

10.2.1 Configuration

The large reductions in mirror assembly size and science capabilities resulted in a modest reduction in the spacecraft mass. The mass savings are primarily from reducing the spacecraft inner and outer diameters to accommodate the new LMA size. The smaller spacecraft diameter requires an additional adaptor to mate the Observatory to a standard fairing size (Figure 10.6). This additional mass must be included with the mass of the Observatory, and is bookkept in the MEL for this configuration.

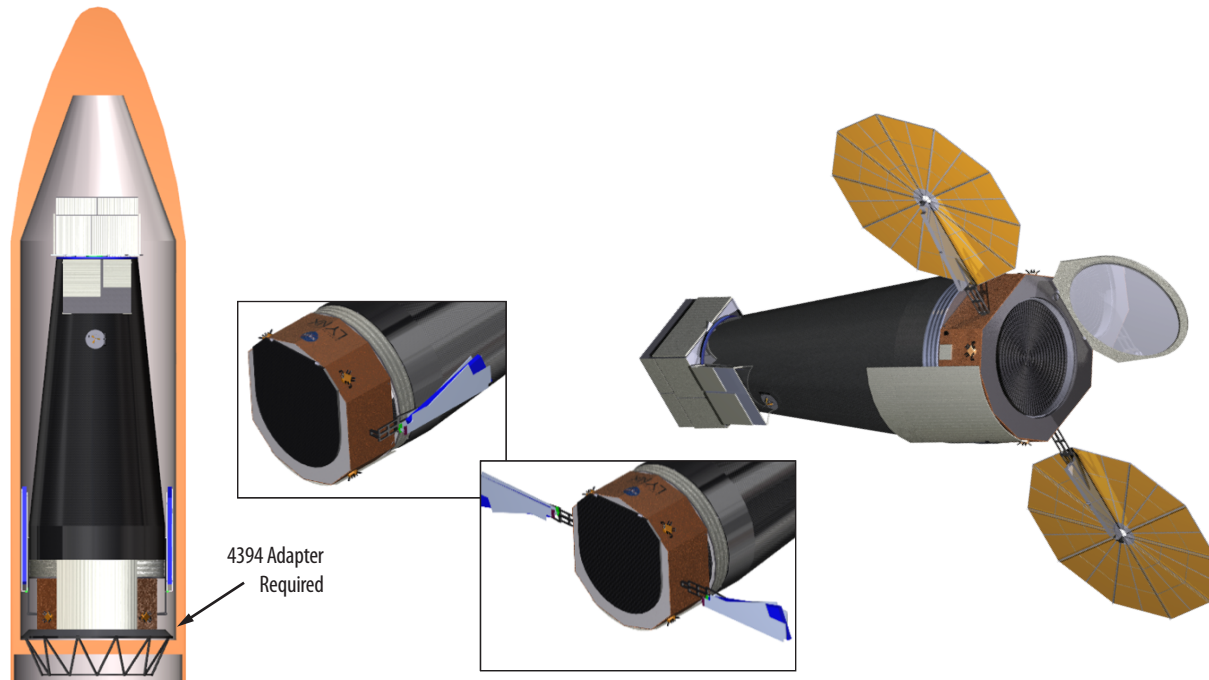


Figure 10.6. (Left) 1.3-m² configuration of *Lynx* inside of a future heavy-class launch vehicle. An adaptor plate is required to mate the Observatory to a standard 5-m fairing. (Top-Right) Solar panels are retracted for launch and (Mid-Right) partially and (Bottom-Right) fully deployed.

10.2.2 Structures

A detailed structural analysis was performed on the 1.3-m² Configuration, taking into account the new mass and Center of Gravity. All primary structures met or exceeded requirements as defined in NASA-STD-5001B for strength and stability, once the thickness of the OBA was increased. The first lateral-constrained normal mode of 9.45 Hz satisfies the Delta IV heavy requirement of 8Hz with an additional 15% margin. Analysis indicates that launch locks are required on the LMA barrel to spacecraft (three locations), on the forward contamination door to LMA barrel (six locations), aft-contamination door to subsystem support ring (six locations), XGA frame to OBA (six locations), and on the ISIM to OBA (four locations).

10.2.3 Avionics and Thermal Control

The 1.3-m² Configuration resulted in minimal changes to the avionics. The primary modification from the DRM was an update to the heater controllers. The heater controllers were updated to account for the reduced LMA, XGA, OBA, and spacecraft size. The number of heaters and temperature sensors were reduced and the heater cabling and the sensor wiring were recalculated. The result was a minimal reduction in heater controller and cabling mass and reduced heater control enclosures for the LMA, XGA, OBA, and spacecraft. Heater controller power was reduced by 32 W.

10.2.4 Power

The primary reduction in power for the 1.3-m² Configuration of the *Lynx* Observatory was due to the reduction in heaters for the smaller LMA, XGA, OBA, and spacecraft. Table 10.3 summarizes the power requirements for the non-science phases.

The total reduction for the launch phase is 23 W for the 1.3-m² Configuration, with minimal savings across the board. Power savings up to a few hundred watts (predicted to be ~2/3 the power required to heat the DRM LMA) are expected for when the Observatory is on orbit and operating in science mode. Currently, the analysis for the 1.3-m² Configuration assumes a conservative estimate for power for the LMA, which is similar to that of the DRM. These power savings are not expected to result in a significant cost savings for this configuration.

Table 10.3. Breakdown of the power requirements for the 1.3-m² configuration of *Lynx*, for all phases except for on-orbit science mode operation.

Source	Launch (0 – 156 min)	Checkout (156 min – 21 days)	Cruise (21 – 104 days)	Safe Hold	Survival (5 min) Battery Power Only
Subsystems					
Avionics	533	1,411	1,411	673	546
GN&C	0	283	283	283	283
Propulsion	0	510	510	510	510
Mechanisms	0	0	0	0	0
Thermal	174	174	174	178	154
Totals (Subsystems)	707	2,377	2,377	1,643	1,492
Payload					
Microcalorimeter	13	14	434	434	14
HDXI	0	249	249	7	7
XGS	0	190	190	7	7
Mirror Heater	0	700	700	1339	593
Optical Bench Heaters	0	403	403	438	438
Totals (Payload)	13	1,556	1,976	2,225	1,059
Total Spacecraft - 1.3 m² configuration	720	3,933	4,353	3,868	2,552
Total Spacecraft - DRM	743	3,991	4,411	3,875	2,552

10.3 Mission Design Details

Given that the 1.3-m² configuration must be able to carry out *Lynx* science pillar goals, no significant changes in the Mission Design were required. The target orbit of SE-L2, transfer trajectory, ascent profile, delta-V budget and timeline, and launch vehicle class (heavy-class) are identical to those for the *Lynx* DRM.

10.4 Programmatics

Like the DRM, the 1.3-m² configuration is required to be a Category 1 project, Risk Class A, suitable for a Flagship mission. The project organization and leadership, and Agency Governance Model do not change as described in §8.1.

A risk assessment, project schedule, and cost have been established for this configuration and findings are summarized in the following sections.

10.4.1 Risk Assessment

The top project risks for the 1.3-m² Configuration, shown in Table 10.4, are the same as those discussed in §8.3 and listed in Table 8.1. None of these risks requires modification.

Table 10.4. Summary of top *Lynx* 1.3-m² configuration Program risks. Risks (2), (3), and (4) Likelihood and Consequence have been changed from that of the DRM to reflect the reduced capability of this configuration.

Risk	Title	L	C	T	S	\$
1	X-ray Mirror Module Assembly and Alignment	3	4		X	X
2	LXM Technical Maturation to TRL 6	3	3	X	X	X
3	X-ray Mirror Segment Industrialization	2	3		X	X
4	LXM Fabrication and Assembly	2	3		X	X
5	X-ray Mirror Technical Maturation to TRL 6	3	2	X	X	X
6	HDXI/XGD Detector Technology Maturation to TRL 6	2	2	X	X	X
7	Calibration Facility Availability	1	3		X	X

L = likelihood of risk occurrence; C = consequence of risk occurrence; T = technical risk; S = schedule risk; \$ = cost risk

Risk 1 — X-ray mirror module assembly and alignment: Because the manufacturing schedule has been reconsidered to account for the reduced number of mirror segments, modules, and meta-shells, the same risk as for the DRM exists. If the schedule is extended due to inability to industrialize the process, there will be cost and schedule impacts. The reduced manufacturing schedule decreases the likelihood that mirror assembly will be on the project critical path.

Risk 2 — LXM technical maturation to TRL 6: The only change to the LXM is that the 1.3-m² Configuration has a slightly smaller MA, which has no impact on the technology maturation to TRL 6.

Risk 3 — X-ray mirror segment industrialization: The potential to increase schedule margin before mirror delivery with fewer mirror segments to fabricate would decrease the likelihood of this risk, but not significantly. The *Lynx* team deemed that this was not a significant enough impact to demote the likelihood from a 2 to a 1.

Risk 4 — LXM instrument fabrication and assembly: The only change to the LXM is that the 1.3-m² Configuration has a slightly smaller MA, which has little impact on the fabrication and assembly. There would be fewer pixels to calibrate, but not a significant enough impact to lower the current risk rating.

Risk 5 — X-ray mirror technical maturation to TRL 6: Because the angular resolution requirement for the 1.3-m² Configuration is the same as that of the DRM, the technical maturation is unaffected.

Risk 6 — HDXI/X-ray Grating Detector technology maturation to TRL 6: The XGS resolving power requirement and relative effective area drives the maturation for the gratings. The resolving power for the 1.3-m² Configuration is the same as that of the DRM. The effective area coverage is a reduction that is equivalent to the percentage reduction of the LMA, and so is effectively unchanged.

Risk 7 — Calibration facility availability: Because the mirror production schedule has been reduced by nine months, there is a slight increased risk that the calibration for *Lynx* would overlap that of *Athena*, if *Athena* were to be calibrated in the MSFC X-ray and Cryogenic Facility (XRCF). The *Lynx* team did not feel that this risk increase was significant enough to warrant changing the risk score.

10.4.2 Lifecycle Schedule and the Critical Path

The life-cycle schedule for the 1.3-m² Configuration is shown in Figure 10.7. The primary difference between this schedule and that of the DRM is a reduction in fabrication time for the mirror modules and the XGS gratings. The reduction in the number of required X-ray mirror modules in this configuration results in a ~9-month reduction in the mirror module schedule, allowing for an earlier start to calibration efforts. Final calibration still requires the availability of the flight model HDXI and XGD, whose development schedules are unchanged in this configuration. Therefore, the total duration for flight calibration efforts increases by ~6 months. As with the DRM, the calibrated HDXI and XGD are needed for ISIM I&T following calibration. With the DRM, the ISIM I&T begins with the availability of the LXM, followed ~2 months later with the availability of the HDXI and XGD following calibration. In the 1.3m² Configuration, the HDXI and XGD are available ~1 month before the LXM. The ISIM I&T effort is unchanged in the 1.3m² Configuration, therefore, the 1 month earlier start in this critical path activity results in **only a ~1 month earlier LRD of September 1, 2036**. The XGA fabrication reduction is ~4 months, with has no impact to the critical path.

10.4.3 Cost

The total *Lynx* 1.3-m² Configuration Phase A–E (first 5 years of operation) cost with fee is around ~\$0.3B less than the cost of the DRM.

As with the DRM estimate, the parametric estimate for the 1.3-m² Configuration includes project level reserves of 30% on the Phase B–D costs less fee and Launch Services Program (LSP)-provided launch vehicle pass-through cost for a heavy-class vehicle. The estimate range is considered credible for the pre-formulation stage of the study given high *Chandra* architecture heritage, robust and high TRL spacecraft components and design, a detailed and credible path forward for all of the DRM technologies, and detailed and thorough parametric estimates for the mirror assembly, LXM, and XGA, which were developed in the same manner as for the DRM and updated to reflect the design changes for this configuration. The parametric estimate for this configuration serves as the primary estimate. The lower estimate (at a 40% Confidence Level (CL)) compares favorably to the *Chandra* mission actual cost of \$4.3B, escalated to \$FY20, and is in line with an independent cost estimate and high CLs. Detailed cost information is included in the *1.3-m² Supplemental Design Package*.

The parametric cost estimate for the 1.3-m² Configuration utilized the same cost models and methodologies as for the DRM that are described in §8.5.2.

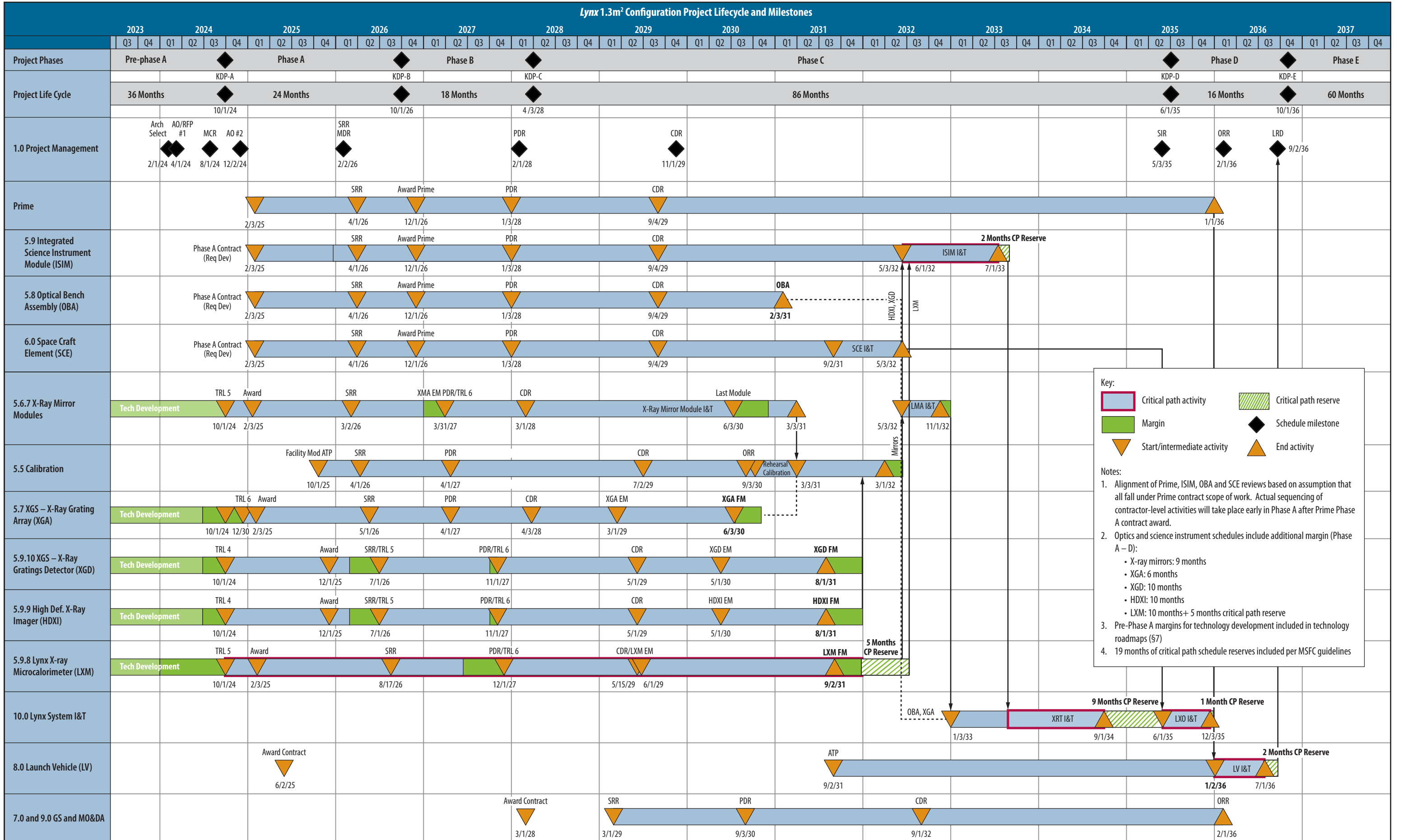


Figure 10.7. *Lynx* 1.3-m² configuration project life-cycle schedule

10.4.4 Work Breakdown Structure

As with the DRM Configuration, the 1.3 m² Configuration estimate was based on the project Work Breakdown Structure (WBS) structure as described in §8.5.1. There were no changes in the WBS for the 1.3-m² Configuration.

10.4.5 Cost Estimation Methodology

The cost estimation methodology for the 1.3-m² Configuration followed that of the DRM Configuration estimate methodology, as described in §8.5.2. Specific parametric model inputs for the LMA and XGA were different for the 1.3-m² Configuration in order to account for the reduced number of meta-shells for the LMA. An updated cost model for the LXM was developed by GSFC and used as throughput into the overall *Lynx* mission cost model for this configuration. The LXM cost model accounted for the reduced LXM focal plane array. These changes are summarized below. All other costing Ground Rules and Assumptions (GR&A) and methodologies are unchanged from the DRM estimate.

LMA parametric model input changes:

- Removed five meta-shells (three outer and two inner) from the LMA cost model.
- Changed mass of thermal pre-collimator, spider, post-collimator, forward and aft contamination doors, and mirror barrel structure per the MEL for the 1.3-m² Configuration. The MEL is provided in the *1.3-m² Supplemental Design Package*.
- The LMA EM unit assumes the use of different meta-shells from those for the DRM.
- LMA new first meta-shell (innermost) acquisition category changed from “Average Modification” (15% new design) to “Make” (80% new design).
- LMA new second meta-shell acquisition category changed from “Average Modification” to “Major Modification” (65% new design). “Average Modification” was used for the remaining meta-shells (15% new design).
- XGA parametric model input changes:
- XGA reduced in size consistent with the reduced LMA.
- LXM parametric model input changes:
- The number of thermal readouts (§6.3.4.1) reduced in proportion to MA (~factor of 2).
- Reduction in electronics assemblies scaled roughly by number of electronic readouts (§6.3.4.1) and reduction of MA.

10.4.6 Cost Validation

The *Lynx* 1.3-m² Configuration cost estimate was validated with a side-by-side comparison by WBS of the analogous *Chandra* costs as described in §8.5.3.1 for the DRM Configuration. A grassroots estimate was not developed for the 1.3-m² Configuration. The *Chandra* analogous estimate agreed to within a few percent of the parametric estimate and provides a high confidence in the reasonableness of the estimate. In addition, as with the DRM, the *Lynx* parametric estimates for the 1.3-m² Configuration LMA, science instruments, and spacecraft element were compared to historical observatory missions. The parametric estimates for these assemblies are within family. This historical comparison further reinforced the reasonableness of the *Lynx* estimate.

10.4.7 Independent Cost Assessment

Per request of NASA Headquarters, the MSFC Engineering Cost Office developed a non-advocate Independent Cost Estimate (ICE) and performed an uncertainty analysis to validate and determine the CL in the 1.3-m² Configuration parametric cost estimate. As with the DRM independent assessment, the ICE addressed the uncertainty in the estimating methods, input parameters, design complexity, and fee. The analysis was performed in \$FY20 and \$RY, using NASA escalation factors, for Phases B–E, exclusive of launch vehicle costs and reserves, to derive the cost basis for the assessment. All assumptions used in the DRM assessment described in §8.5.2 remained the same for the 1.3-m² Configuration, and all other details for the analysis methodology remain unchanged as described in §8.5.2.

A Monte Carlo simulation on the input models provided a cost curve with CLs ranging from 10% to 90% as shown in Figure 10.8. Reserve amounts to achieve corresponding CLs were calculated based on the delta between the derived cost basis (parametric estimate for Phases B–E exclusive of launch vehicle and reserves) and the cost at the 50% and 70% CLs on the resulting cost curve. Based on this analysis, the *Lynx* parametric estimate with 30% reserves on B–D costs (exclusive of launch vehicle and fee) has a 39% CL on the independent cost curve. As with the DRM, and as described in §8.5.3.3, the parametric estimate for the 1.3-m² Configuration with reserves represents a substantially better reserve posture than historical NASA projects.

The resulting analysis yielded a cost range of \$4.6B at a CL of 40% to \$5.8B at a CL of 70% in \$FY20, and \$6.3B at a CL of 40% to \$7.9B at a CL of 70% in \$RY. The 40% CL in \$FY20 on the non-advocate cost curve is within 1% of the *Lynx* parametric estimate for the 1.3-m² Configuration.

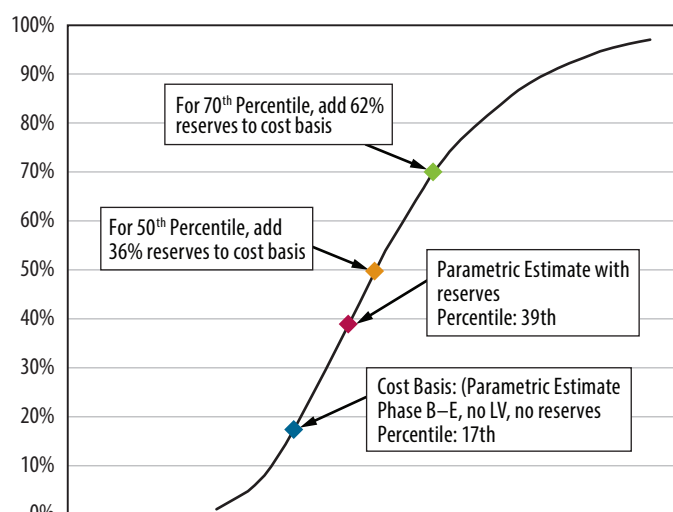


Figure 10.8. The *Lynx* parametric cost estimate with 30% reserves represents a 39% CL. To achieve a 50% CL, 36% reserves need to be applied to the cost basis. For 70% CL, 62% reserves need to be added to the cost basis.